TECHNISCHE UNIVERSITÄT MÜNCHEN

Lehrstuhl für Humanbiologie

The role of Notch signaling in development and tumorigenesis

Pawel Karol Mazur

Vollständiger Abdruck der von der Fakultät Wissenschaftszentrum Weihenstephan für Ernährung, Landnutzung und Umwelt der Technischen Universität München zur Erlangung des akademischen Grades eines

Doktors der Naturwissenschaften

genehmigten Dissertation.

Vorsitzender: Univ.-Prof. Dr. M. Klingenspor

Prüfer der Dissertation:
1. Univ.-Prof. Dr. M. Schemann
2. Univ.-Prof. Dr. R. M. Schmid (schriftliche Beurteilung)
3. Univ.-Prof. Dr. M. Hrabé de Angelis

Die Dissertation wurde am 10.02.2010 bei der Technischen Universität München eingereicht und durch die Fakultät Wissenschaftszentrum Weihenstephan für Ernährung, Landnutzung und Umwelt am 21.10.2010 angenommen.

Summary

In this thesis, the role of the Notch signaling pathway in pancreas and liver development as well as in pancreas and skin tumorigenesis was investigated using chemically and genetically engineered mouse models. The obtained results underscore the high importance of Notch signaling in tissue maturation, homeostasis and disease.

Pancreas development is thought to depend strongly on proper Notch pathway regulation. However, the current study provides proof that Notch1 and Notch2 receptor ablation only moderately disturbs this process. In contrast, ablation of the Notch signaling effector Rbpj dramatically impairs exocrine cell expansion and leads to premature differentiation of progenitor into endocrine cells. This study identifies elements of Notch pathway crucial for pancreas development and may have a significant influence for regenerative medicine.

In addition, the Notch pathway was found to be critical for pancreas recovery after acute pancreatitis. The presented results indicate that Notch signaling is essential for pancreatic exocrine cell regeneration after acute inflammation through modulation of the β-catenin pathway. These results provide a better understanding of the molecular pathways involved in the acute pancreatitis – a disease that displays serious complications and high mortality.

Also, during liver maturation Notch signaling was found to be crucial. In here, evidence is provided for an essential role of the Notch2 receptor in intrahepatic bile duct formation. This finding is especially important since the presented liver specific Notch2 ablated mice recapitulated features of the human Alagille Syndrome (AGS). This multisystem disorder is characterized by developmental abnormalities of the heart, eye, skeleton, and liver. The results reveal molecular mechanisms that may contribute to AGS formation.

Finally, the thesis marks the prominence of the Notch pathway in tumorigenesis and cancerous cell fate decisions. This study elucidates the role of Notch in two highly malignant (pancreatic cancer) and frequent (skin cancer) neoplasias. Skin tumors, with an incidence rate in Europe of over 1 million per year, are the most common human neoplasias and pancreatic ductal adenocarcinoma (PDAC), although less prevalent, has the highest, exceeding 95%, mortality rate among all cancers. The utilized mouse models reveal the cell-context dependent and double-edged Notch signaling effects.

In the study of skin tumor mouse models, the role of Notch1 but not Notch2 as a tumor suppressor was confirmed. Tumor suppressing mechanisms of Notch1 in the epidermis involved modulation of β-catenin and p21 signaling. Also Notch1 but not Notch2 deletion alters hair follicles development suggesting an essential role of Notch1 in skin homeostasis. Additionally, this study revealed a previously unrecognized expression of the pancreatic transcription factor Pdx1 in the skin.

In contrast to cutaneous neoplasias, investigations of the PDAC mouse model identifies Notch2 as pro-oncogenic in the early development of the disease. Its pancreas specific deletion in the established oncogenic $Kras^{G12D}$-induced tumor mouse model leads to prolonged survival with a block in preneoplastic lesion progression and late appearing anaplastic PDAC. Pancreatic Notch2 activates Myc signaling and Notch2 deletion leads to epithelial-to-mesenchymal transition, while Notch1 has no major role in PDAC initiation and progression.

Understanding the molecular biology of cancer is essential to develop new therapies. The presented results provide insights of Notch signaling functions and may open new routes for cancer treatment.

Zusammenfassung

In dieser Doktorarbeit wurde der Beitrag des Notch Signalweges für die Entwicklung von Pankreas und Leber sowie für die Tumorentstehung in Pankreas und Haut untersucht. Hierfür wurden genetisch und chemisch veränderte Mausmodelle verwendet. Die vorliegenden Ergebnisse verdeutlichen, wie wichtig Notch in den untersuchten Geweben für die Entwicklung, Homöostase und Krankheitsentstehung ist.
Bislang wurde angenommen, dass die Entwicklung des Pankreas stark von einem regulierten Notch Signalweg abhängig ist. Allerdings zeigen die hier vorliegenden Ergebnisse, dass die Deletion von Notch1 und Notch2 diesen Prozess nur wenig beeinflusst. Dagegen bewirkte die Inhibierung des Notch Effektors Rbpj ein dramatisch beeinträchtigtes Wachstum exokriner Zellen und eine verfrühte Differenzierung von Progenitor- in endokrine Zellen. Diese Studie konnte wichtige Elemente des Notch Signalweges während der Pankreasentwicklung identifizieren und könnte dadurch einen entscheidenden Beitrag zur regenerativen Medizin leisten.
Des Weiteren wurde die Rolle des Notch Signalweges in der Regeneration des Pankreas nach akuter Pankreatitis untersucht. Die vorliegenden Ergebnisse zeigen, dass Notch essentiell für die Regeneration exokriner Zellen nach akuter Entzündung ist, indem es den β-catenin Signalweg moduliert. Dadurch konnte ein besseres Verständnis für die molekularen Grundlagen der akuten Pankreatitis geschaffen werden – einer Krankheit, die durch ernste Komplikationen und eine hohe Mortalitätsrate gekennzeichnet ist.
Auch an der Entwicklung der Leber ist Notch wesentlich beteiligt. Die vorliegenden Ergebnisse zeigen, dass der Notch2 Rezeptor kritisch für die physiologische Bildung intrahepatischer Gallengänge ist. Die untersuchten Mäuse mit einer Leber-spezifischen Inhibierung von Notch2 weisen die gleichen Symptome auf wie Patienten, die am Alagille Syndrom (AGS) leiden. Diese multisystemische Erkrankung ist durch Entwicklungsstörungen in Herz, Auge, Skelett und Leber gekennzeichnet. So konnte ein wichtiger Beitrag zur Aufklärung der molekularen Ursachen des AGS geleistet werden.
Schließlich wurde in dieser Arbeit die Bedeutung von Notch für zwei der bösartigsten (Pankreaskarzinom) und häufigsten (Hautkrebs) Neoplasien deutlich. Hautkrebs hat eine europaweite Inzidenz von mehr als 1 Mio. Menschen pro Jahr. Das duktale Adenokarzinom des Pankreas (PDAC) weist dagegen die höchste Mortalitätsrate aller Karzinome auf. Die dazu untersuchten Mausmodelle verdeutlichen, dass die Effekte des Notch Signalweges Zellkontext-abhängig sehr unterschiedlich sind.
Während der Tumorentstehung in der Haut fungiert nur Notch1 aber nicht Notch2 durch die Regulierung von β-catenin und p21 als Tumorsuppressor. Auch die Entwicklung der Haarfollikel wird nur durch die Inhibierung von Notch1 beeinträchtigt, so dass auf dessen essentielle Beteiligung in der Homöostase der Haut geschlossen werden kann. Zusätzlich wurde durch diese Studie eine bislang unbekannte Expression des Transkriptionsfaktors Pdx1 in der Haut gefunden. Dagegen zeigte die Pankreas-spezifische Deletion von Notch2 in einem etablierten Tumormodel mit onkogen aktiviertem $Kras^{G12D}$, dass Notch2 im Pankreas die Tumorbildung durch Aktivierung des Myc-Signalweges fördert. Seine Inhibierung bewirkte ein verlängertes Überleben der Mäuse, blockierte die Progression präneoplastischer Läsionen und führte zu sehr spät auftretenden anaplastischem PDAC sowie epithelial-mesenchymaler Transition. Notch1 dagegen hat auf diesen Prozess keinen entscheidenden Einfluss.
Die molekularen Ursachen der Tumorentstehung zu verstehen ist essentiell um neue Therapien entwickeln zu können. Die in der vorliegenden Arbeit präsentierten Ergebnisse ermöglichen einen tieferen Einblick in die Rolle des Notch Signalweges und könnten dadurch neue Wege für die Behandlung von Krebs aufzeigen.

This doctoral dissertation was supervised and approved by the Thesis Advisory Committee as a partial fulfillment of the International Max Planck Research School requirements.

Thesis Advisory Committee members:

Prof. Dr. Reinhard Faessler
Prof. Dr. Michael Schemann
Prof. Dr. Roland M. Schmid
Prof. Dr. Hermann Wagner
Dr. Elke Burgermeister
PD Dr. Jens Siveke
PD Dr. Rudolf Rupec

Moim Rodzicom

To my Parents

TABLE OF CONTENTS

LIST OF PUBLICATIONS

This thesis is based on the following original papers and manuscripts, which are presented in subsequent chapters and are enclosed in appendixes:

1. Presented in Chapter 2.

Pawel K. Mazur, Henrik Einwächter, Bence Sipos, Marcel Lee, Hassan Nakhai, Horst Hameister, Roland Rad, Nathalie Conte, Allan Bradley, Ursula Zimber-Strobl, Lothar J. Strobl, Freddy Radtke, Günter Klöppel, Roland M. Schmid, Jens T. Siveke.
Notch2 is required for PanIN progression and development of pancreatic ductal adenocarcinoma
Proc Natl Acad Sci USA. 2010 Jul 27;107(30):13438-43.

2. Presented in Chapter 3:

Pawel K. Mazur, Hassan Nakhei, Bence Sipos, Ursula Zimber-Strobl, Lothar Strobl, Freddy Radtke, Roland M. Schmid, Jens T. Siveke.
Identification of Pdx1 expression in the skin discloses different roles of Notch1 and Notch2 in Kras^{G12D}-induced skin carcinogenesis.
PLoS One. 2010 Oct 22;5(10):e13578.

3. Presented in Chapter 4:

Jens T. Siveke, Clara Lubeseder-Martellato, Marcel Lee, **Pawel K. Mazur**, Hassan Nakhai, Freddy Radtke, Roland M. Schmid.
Notch signaling is required for exocrine regeneration after acute pancreatitis
Gastroenterology. 2008 Feb;134(2):544-55.

4. Presented in Chapter 5:

Hassan Nakhai, Jens T. Siveke, Bettina Klein, Lidia Mendoza-Torres, **Pawel K. Mazur**, Hana Algül, Freddy Radtke, Lothar J. Strobl, Ursula Zimber-Strobl, Roland M. Schmid.
Conditional ablation of Notch signaling in pancreatic development.
Development. 2008 Aug;135(16):2757-65.

5. Presented in Chapter 6:

Fabian Geisler, Florian Nagl, **Pawel K. Mazur**, Marcel Lee, Ursula Zimber-Strobl, Lothar J. Strobl, Freddy Radtke, Roland M. Schmid, Jens T. Siveke.
Liver-specific inactivation of Notch2, but not Notch1, compromises intrahepatic bile duct development in mice.
Hepatology. 2008 Aug;48(2):607-16.

Chapter 1: Introduction

One crucial factor for the development of multicellular life is the ability to form complex biological patterns. Pattern formation is established by molecular mechanisms of the cell-cell signaling that allow cells to influence each other's fate decisions. One key mechanism in controlling cell-cell communication is the Notch signaling pathway.

I. The Notch signaling pathway

The Notch signaling pathway exhibits unique characteristics. First, it appears only between cells upon close contact since both Notch receptors and ligands are cell-bound. Second, the receptor in order to trigger signaling has to be proteolytically cleaved. Third, Notch signaling is a highly conserved pathway. Finally, the signaling occurs between adjacent cells to direct them to adopt different cell fates. These cell-fate decisions can be categorized, based on cellular outcome, into three distinct models (Fig. 1.1D). The best-known process, called lateral inhibition, in which a population of equivalent cells share developmental potential but only some achieve that fate. Cells that adopt the fate activate Notch in neighbor cells in order to prevent them form acquiring the same fate. This process is involved in morphogenesis (tooth, lung, hair), boundary formation (wing, somites, limb), cell specification (CNS, pancreas) and apoptosis (in cultured neural crest cells). The other process that requires Notch is important for boundary formation where Notch signaling induces rather than selects new cell fates. The last function of Notch is sequential cell fate assignation (lineage decision) dependent on asymmetrical inherence of Notch or its regulators (see Fig. 1.1D), (for reviews see Artavanis-Tsakonas et al., 1999, Greenwald, 1998, Kopan and Turner, 1996, Kopan and Ilagan, 2009)

The Notch history

The first disfunction in *Notch* was identified and studied in the fruit fly, *Drosophila melanogaster* by Dexter in 1914. In fact the name 'Notch' derives from the characteristic notched wing found in flies with haploinsufficency of the *Notch* gene. Homozygous mutations result in lethal phenotypes due to neurogenic aberrations, where cells destined to become epidermis switch fate and give rise to neural tissue (Poulson, 1937, Wright, 1970). Further studies revealed that Notch is involved in many other developmental processes in *Drosophila*, such as bristle formation (Heitzler and Simpson, 1991), maintenance of muscle founder cells (Bate et al., 1993), midgut progenitor cells and regulation of cell-fate decisions in stem cells progeny (Fre et al., 2005). The latter function is conserved and found in mammals as well (van Es et al., 2005, Ohlstein and Spradling, 2006). Our understanding of Notch signaling was increased thanks to studies of the nematode *Caenorhabditis elegans* (reviewed by Kimble and Simpson, 1997), where Notch also plays important roles in cell specification. *C. elegans* unlike *Drosophila* has two Notch homologues, LIN-12 and GLP-1. Intriguingly, they are more diverged than any other pair of Notch receptors in any other organisms, suggesting a very early gene duplication event in the nematode. However, both can substitute each other when expressed in the appropriate tissue (Fitzgerald et

al., 1993). GLP-1 regulates blastomere specification in the early *C.elegans* embryo (Bowerman et al., 1992, Hutter and Schnabel, 1994) whereas LIN-12 is important for gonad development in later stages of growth (Greenwald et al., 1983). Notch receptors have been identified in all vertebrate species. In mammals, four Notch receptors and five ligands have been identified (Fig. 1.1A), (Gordon et al., 2008). Their function in normal physiology and disease will be briefly discussed below.

The Notch receptors

The Notch receptor family encodes large single-pass transmembrane proteins that share some common characteristic features. The extracellular part of the receptors contains a large number of tandemly-arranged extracellular EGF repeats and a family-specific LNR (Lin Notch Repeat) region (Wharton et al., 1985), (Fig. 1.1A and B). Proper folding of the EGF-like repeats has been shown to be Ca^{2+}-dependent (Rand et al., 2000), (Fig. 1.1C) and further influenced by Notch glycosylation (see review Haines and Irvine, 2003). EGF repeats are responsible for ligand binding. The precise role of the LNRs, on the other hand, has not yet been confirmed. Those three juxtamembrane repeats are implicated in modulation of Notch extracellular- and intracellular-part interaction (Yochem et al., 1988). Four main regions can be distinguished in the intracellular domain of Notch: the RAM, ankyrin, TAD and PEST (Fig. 1.1A and B). The region directly inside the membrane is referred to as the RAM domain. Its main function seems to be mediating direct interaction with the transcription factor RBPJκ (CBP or CLS in vertebrates, Su(H) in *Drosophila*, Lag-1 in *C. elegans,* function explored below), (Tamura et al., 1995). The seven ankyrin repeats are flanked by a nuclear localization signal (NLS) that is among the most conserved regions of each Notch receptor. The ankyrin region is crucial for the proper assembly of the effector - transcription complex of Notch-RBPJκ-MAM (review by Lubman et al., 2004). The C-terminus contains the OPA-domain that is rich in glutamine residues and has been shown to function as a transcriptional activation domain (TAD), (Kurooka et al., 1998). Finally, the PEST sequence is the last element of Notch and mediates ubiquitination, thus protein stability.

The Notch protein is in fact a heterodimer, because during the posttranslational modification it is cleaved (S1-cleveage). The extracellular part is non-covalently associated with the membrane-tethered intracellular domain. Such a division corresponds with functional divergence. Generally, the extracellular Notch is responsible for ligand binding whereas the intracellular is important for signal transduction. The intracellular domain of Notch (NIC) functions as a constitutively-active receptor (gain-of-function).

Effects of Notch ablation

The function of the mammalian Notch receptors has been studied using genetically engineered gene knockouts in mice. These experiments provided proof how important Notch signaling is for development (see also Chapter 5, 6).

Notch1 null mutations are embryonically lethal (embryos die prior to embryonic day E11.5) and affect proper segmentation by disrupting somite organization (Fig. 2A). Increased apoptosis can also be detected, but is not considered to be the main cause of developmental arrest (Swiatek et al., 1994, Conlon et al., 1995,

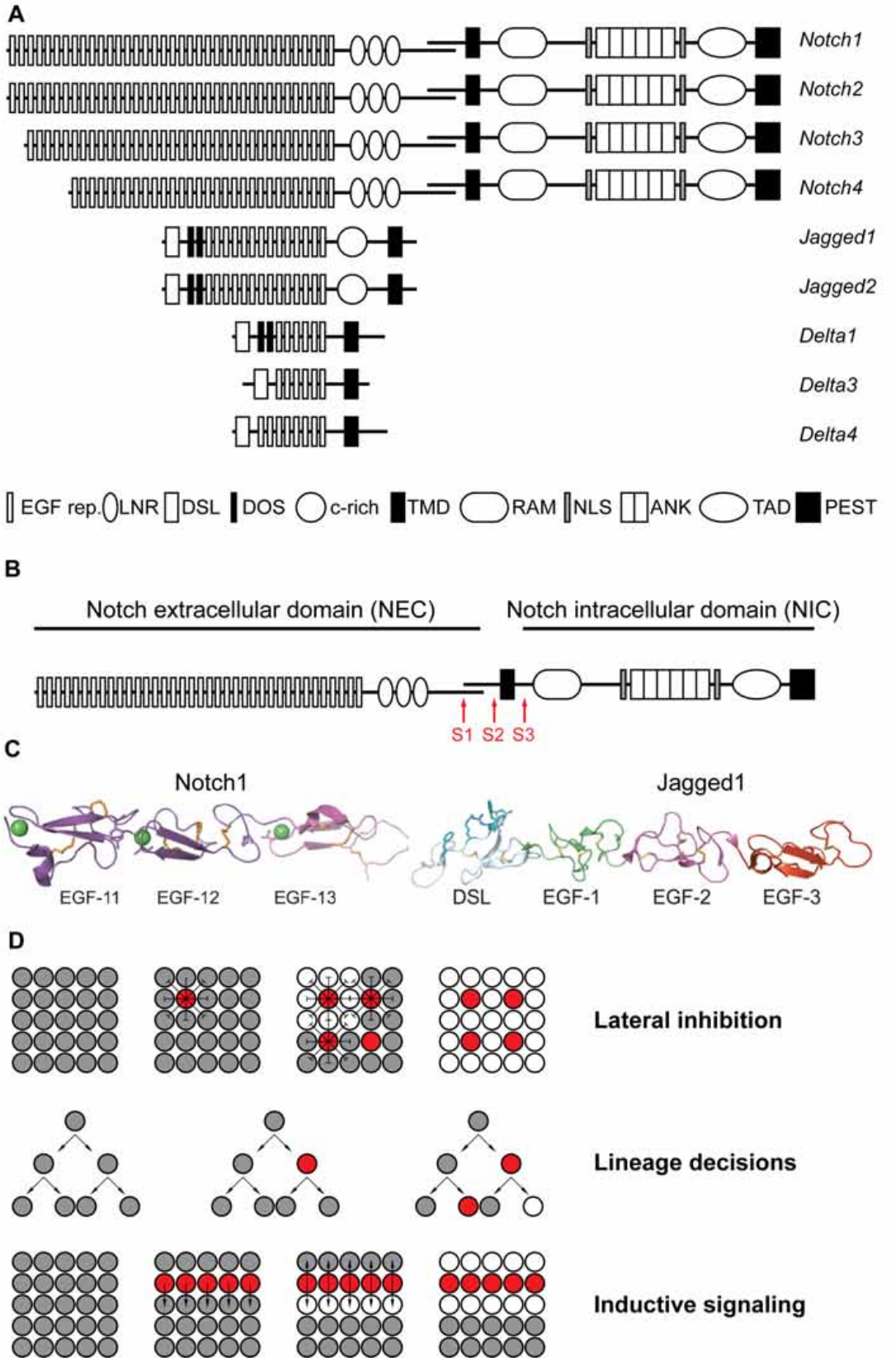

Figure 1.1. The Notch signaling pathway anatomy and function. (A and B) Schematic representation of the domains organization in Notch receptors and ligands (B) S1, S2, S3 indicate the crucial proteolytic sites. NIC is the constitutively active form of Notch. (C) Structure of EGF repeats in Notch1 and Jagged1. (D) Models of Notch regulatory functions (Gordon et al., 2008).

de la Pompa et al., 1997). In further studies a knock-in mouse with defective Notch1-clevage was generated showing similar phenotypes to *null* mutants (Huppert et al., 2000).

Notch2-deficient mice also die at E11.5 (Fig. 1.2B). However, no obvious developmental retardation has been identified except for abnormal levels of apoptotic cells (Hamada et al., 1999). Of note, only the ankyrin repeat region was removed in those mice with the entire extracellular domain still expressed as a fusion protein with β-galactosidase. Another group targeted *Notch2* with use of a hypomorphic allele rather than a true null allele (McCright et al., 2001). The mutation resulted in perinatal lethality due to kidney dysfunction. Mutants exhibited defective differentiation and patterning of the glomeruli (capillaries in the kidneys) and vascular defects of the eye.

Notch3 ablated mice have no apparent phenotype, are viable and fertile (Krebs et al., 2003). This is surprising, given the strong expression for Notch3 during embryogenesis, and suggests a possible redundancy by some of the other Notch receptors. Adult *Notch3-knockout* mice exhibited marked arterial defects including deficiency of maturated vascular smooth muscle cells (Fig. 1.2C), (Domenga et al., 2004).

Notch4 disrupted animals are also viable and fertile (Fig. 1.2D). However, the *Notch4* mutation displays synergy with the *Notch1* mutation. Embryos with deleted *Notch4* and *Notch1* genes display a more severe phenotype than only Notch1 ablated embryos. Both *Notch1* mutant and double Notch1 and Notch4 mutant embryos have severe defects in angiogenic vascular morphogenesis and remodelling (Krebs et al., 2000).

The Notch ligands

There are two types of Notch ligands, Delta and Jagged. The ligands are type I transmembrane proteins containing an N-terminal DSL domain and several EGF-like repeats in the extracellular part plus a short intracellular domain (Fig. 1.1A and C). Both genetic and biochemical analysis *in vivo* and in cell cultures reveal that several regions of Notch EGF repeats are able to bind ligands. However it is not established exactly which ligands activate which receptor (see review Nye and Kopan, 1995 and D'Souza et al., 2008). In mammals, the ligands are expressed in almost all embryonic tissues and their expression patterns partly overlap spatiotemporally. The apparent simplicity of Notch signaling raises the question, if different ligands could induce distinct signaling responses. In addition, a growing number of noncanonical ligands have been shown to activate Notch. Intriguingly, ligands not only activate Notch signaling in the neighbor cell, but they are also able to affect Notch signaling within the same cell (cis-interaction). In contrast to canonical trans-interaction, cis-interaction is inhibiting Notch signaling, however, the biological sense of this binding is unknown (excellent review by D'Souza et al., 2008).

Effects of Notch ligands ablation

The ligand-induced Notch signaling pathway regulates many cellular processes like morphogenesis, differentiation, apoptosis, proliferation etc. Thereby, it is not surprising that disruption in the Notch ligands is associated with many hereditary diseases such as Alagille's syndrome (Chapter 6) and Spondylocostal

dysostosis. The Notch ligands have been studied most extensively using gene knockout technology in mice. Major findings are briefly described below.

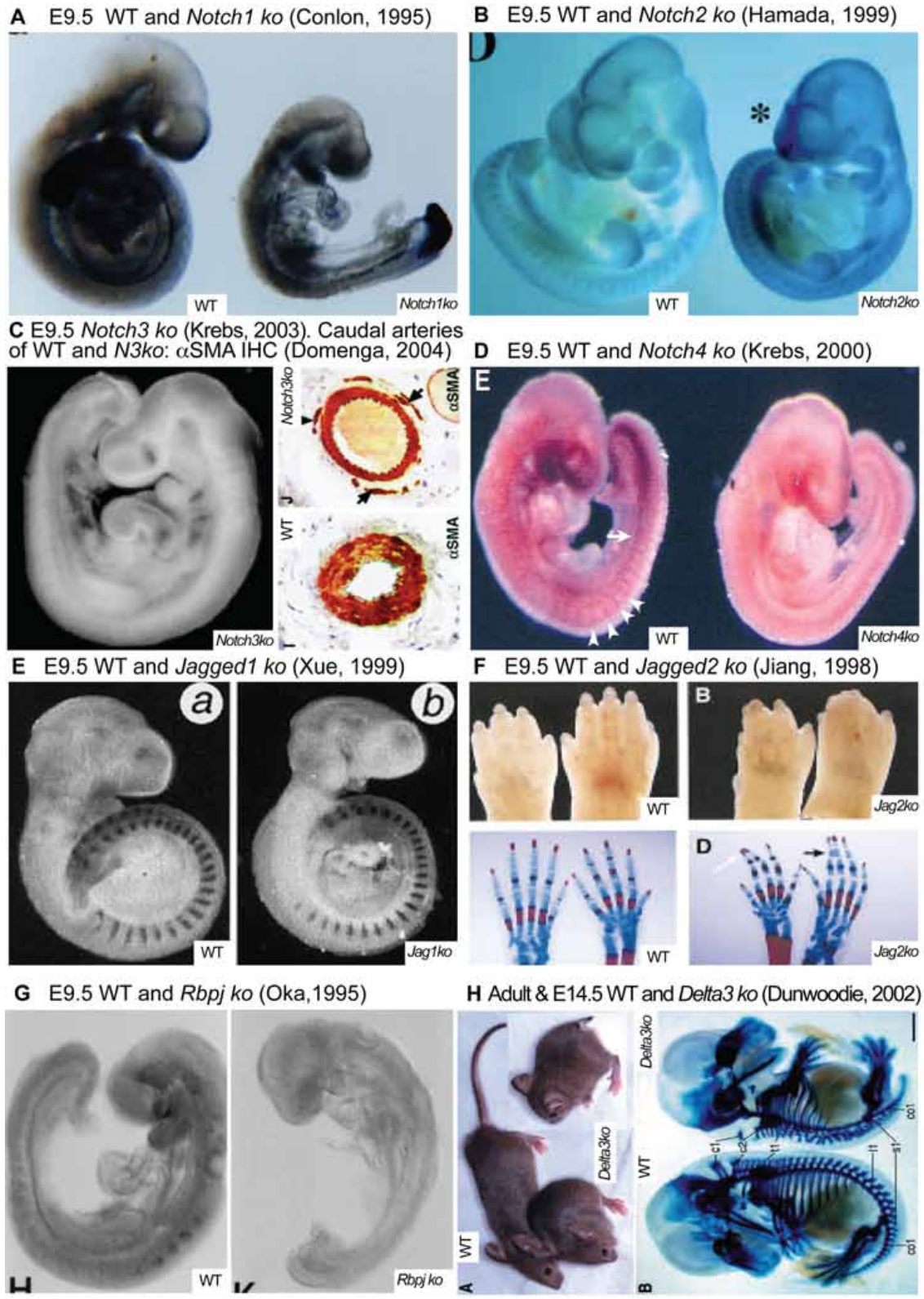

Figure 1.2. Phenotypes of mice with deleted elements of the Notch pathway (detailed description in text).

Jagged1 is essential for remodeling embryonic vasculature and homozygous mice die prior to E11.5 from severe hemorrhage due to defective formation of the vascular system (Fig. 1.2E). Heterozygous mice exhibit an eye phenotype similar to that in Alagille's, but do not exhibit other features of this disease (Xue et al., 1999). Jagged1 displays a genetic link to Notch2 in that double heterozygote *Jagged1*$^{+/-}$*;Notch2*$^{+/-}$ mutants show more severe phenotypes than the single mutants (McCright et al., 2001).
Jagged2 mutant mice die at birth, with severe craniofacial and limb malformations. The craniofacial malformations manifest as cleft palate and fusion of the tongue with the palatal shelves, which prevents the pups from breathing. The mutant mice also exhibit syndactyly (finger fusion) of the limbs (Jiang et al., 1998), (see Fig. 1.2F).
Delta1 deficient mice show severe segmentation defects and fail to maintain the integrity of the somites (Hrabe de Angelis et al., 1997). This phenotype is reminiscent of that of Notch1 mutants.
Delta3 knockout mice survive and are vital but have a shortened body (40% reduced) and a short tail (Fig. 1.2H). Homozygous null embryos show a delayed, irregular somite formation, leading to severe axial skeletal malformations consisting of highly disorganized vertebrae and costal defects. Moreover, mice exhibit defects in the neuroepithelium (Dunwoodie et al., 2002)
Delta4 ligand alone is required in a dosage-sensitive manner for normal arterial patterning in development. Homozygous deletion is lethal and only some heterozygous mice are vital. This incompletely penetrant haploinsufficiency depends on the genetic background of the mice. *Dll4* heterozygous embryos, have reduced caliber of the dorsal aorta but some are able to survive, despite the poor vitelline (yolk-sac - embryo) circulation (Duarte et al., 2004).

Mechanism of Notch signaling
Notch is translated as a single polypeptide and during posttranslational modification it is proteolytically cleaved at a site named S1 by furin-like enzyme in trans-Golgi vesicles. That creates two non-covalently associated parts, extracellular and membrane-tethered intracellular. Ligand binding triggers two rapid consecutive proteolytic events at sites designated as S2 and S3. The first catalyzed by a metalloprotease of the ADAM (TACE/Kuzbanian) family (Mumm and Kopan, 2000) releases the extracellular part of Notch. The second (S3) cleavage is processed by γ-secretase in the presenilin protein complex (review by Fortini, 2002). The latter is analogous to the processing of the amyloid precursor protein (APP), which is associated with Alzheimer's disease. Presenilin/γ-secretase abrogation renders impossible the Notch signaling. As a result of two proteolytic reactions the intracellular part of the Notch receptor (NIC) is released into the cytoplasm and then translocates, driven by the NLSs to the nucleus (Fig. 1.3A). The mechanism decribed above is referred to as RIP (Regulated Intramembrane Proteolysis) and it is shared by some other proteins, like mentioned APP and SREBPs (sterol regulatory element-binding proteins) (reviewed by Hass et al., 2009). The transcriptional regulator RBPJκ (gene name *Rbpj*) is a constitutive repressor of Notch target genes. It was first isolated from mouse pre-B cells and was initially believed to be involved in VDJ-recombination. However, this was not the case and later it was correctly identified as the

vertebrate homologue of *Drosophila Supressor of Hairless* (*Su(H)*) part of Notch signaling. *Rbpj* mutations cease canonical Notch signaling and are lethal for the embryo (Fig. 1.2G).

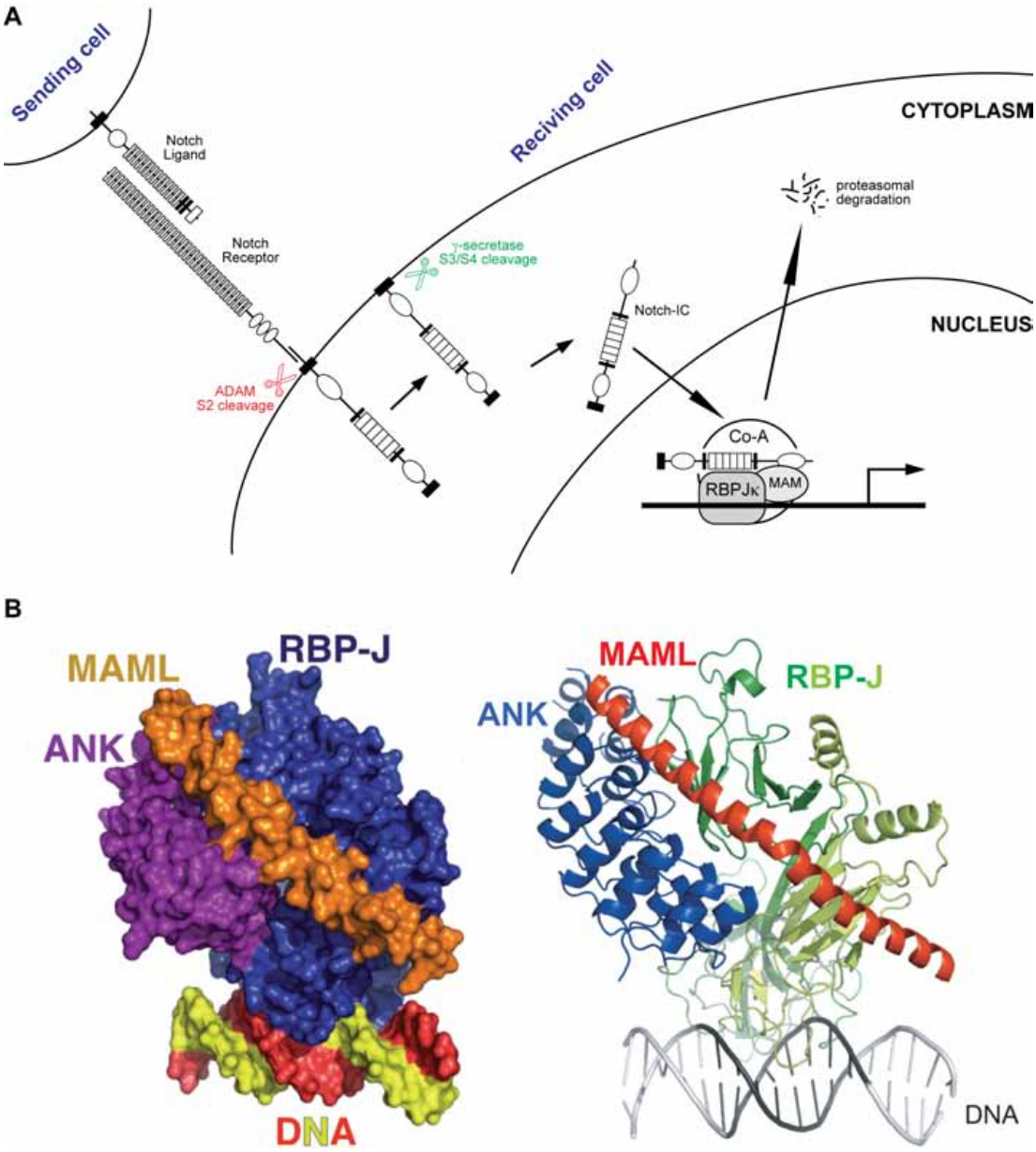

Figure 1.3. The canonical Notch signaling pathway.
(A) Notch activation leads to a cascade of proteolytic events resulting in Notch-IC translocation to the nucleus and Notch-IC/RBPJκ dependent target gene expression.
(B) Surface and ribbon diagrams representing the structure of the human complex of the ANK domain of Notch1, RbpJκ and the N-terminal region of MAM1 bound to an 18 base-pair DNA sequence from the *hes1* promoter (PDB code 2F8X). The structures illustrate the cooperative binding of MAM to a composite surface that is created at the interface between the Notch ANK domain and RBPJκ.

RBPJκ recruits co-repressors such as SMRT, N-coR, SHARP and others of which some are associated with histone deacetylase complexes. Upon entering the nucleus NIC displaces the co-repressors and interacts with Rbpj and together with Mastermind (MAM) co-activators are recruited including histone acetylases (HATs) and other tissue specific factors (Fig. 1.3B). The Notch induced transcriptional activation is abolished by NIC phosphorylation (by CDK8) followed by proteasome degradation lead by nuclear ubiquitin ligase FBW7 (SEL10 or CDC4). The transcriptional regulator RBPJκ (gene name *Rbpj*) is a constitutive repressor of Notch target genes. It was first isolated from mouse pre-B cells and was initially believed to be involved in VDJ-recombination. However, this was not the case and later it was correctly identified as the vertebrate homologue of *Drosophila Supressor of Hairless* (*Su(H)*) part of Notch signaling. *Rbpj* mutations cease canonical Notch signaling and are lethal for the embryo (Fig. 1.2G). RBPJκ recruits co-repressors such as SMRT, N-coR, SHARP and others of which some are associated with histone deacetylase complexes. Upon entering the nucleus NIC displaces the co-repressors and interacts with Rbpj and together with Mastermind (MAM) co-activators are recruited including histone acetylases (HATs) and other tissue specific factors (Fig. 1.3B). The Notch induced transcriptional activation is abolished by NIC phosphorylation (by CDK8) followed by proteasome degradation lead by nuclear ubiquitin ligase FBW7 (SEL10 or CDC4).
The molecular mechanism of Notch signaling has many advantages i.e. the effector identifies the target genes in the absence of a signal therefore allowing rapid changes in levels of pathway activity. In addition the Notch pathway is regulated at multiple levels beginning at receptor and ligand modification and trafficking to degradation and auto regulation (extensively reviewed by Kopan and Ilagan, 2009).

Notch target genes

Surprisingly, only few target genes of Notch have been identified, considering the number of developmental processes regulated by Notch. The most extensively studied and best understood targets are *Hairy* and *Enhancer of split* (*E(spl)*) in *Drosophila* and the related genes *Hes* and *Hey* in mammals. Besides the activation of target genes via *Rbpj*, referred to as canonical pathway (Fig. 1.3), additional non-canonical functions have been characterized (eg. regulation of actin cytoskeleton, interactions with Wnt signaling or *Rbpj*-independent activation of target genes), (see Lai, 2004).
In the mouse genome seven *Hes* (*Hes1-7*) and three *Hey* (*Hey1, 2, L*) genes have been identified. However, only *Hes1, Hes5* and *Hes7* as well as all *Hey* genes are induced by Notch activation. HES and HEY are helix-loop-helix transcription factors that function as transcriptional repressors and play an important role in development. *Hes1* knokout mice are not viable and display wide developmental defects (great overviews by Fischer and Gessler, 2007, Iso et al., 2003).
CD25 and the transcription factor GATA3 are direct Notch target genes activated in T-cell development. Two other Notch target genes *NRARP* and *Deltex1* are shown to be negative regulators of Notch signaling itself. Further Notch targets are *Myc*, *CyclinD1*, *p21*, *Bcl2*, *E2A, HoxA5, NFκB2* (broad review by Borggrefe and Oswald, 2009).

II. The Notch signaling in Cancer

A major challenge studying Notch is to understand how such a simple, direct pathway results in so varied outcomes. Given this broad range of processes that require normal Notch signaling, it is not surprising to find that a number of human diseases and cancers are caused by mutations in components of the Notch pathway and/or in the dysregulation of Notch signaling. Consequences of disruption of proper Notch signaling are very diverse. Here, two faces of Notch signaling in cancer will be discussed: the role as oncogene and tumor suppressor as well as the role of Notch in tumor related Epithelial-to-Mesenchymal Transition (for comprehensive review see Koch and Radtke, 2007).

Notch as an oncogene

The pure oncogenic role of Notch can be found in T-acute lymphoblastic leukemia (T-ALL) an aggressive neoplasm of immature T-cells. About 1% of the cases possesses a specific chromosomal translocation resulting in the fusion of the C-terminal region of Notch 1 to the enhancer sequences of the T cell antigen receptor β subunit (Ellisen et al., 1991). That results in constitutive expression of active *Notch* (NIC). More recently two other types of activated mutations within Notch1 were found to be much more common (56%) in T-ALL. The first occurs in the heterodimerisation region and results in ligand-independent proteolytic cleavage thereby activating Notch. The second is in the PEST domain and appears to increase NIC half-life. Interestingly, in all mentioned cases Notch1 activation still requires γ-secretase cleavage for activation. Since γ-secretase inhibitors are well described, their therapeutic use is considered. However, resistance to γ-secretase inhibitors is very common. The primary way in which abnormal Notch1 activity drives T-AL Leukemia is activation of *Myc* and *CyclinD* as well as inhibition of p53. All of them promote oncogenesis through increased proliferation, survival and genomic instability (T-ALL – Notch relationship is reviewed by Demarest et al., 2008). The study shows that Myc inhibitors interfere with pro-growth effects of activated Notch1 and that forced Myc expression rescues Notch1-dependent T-ALL cell lines from Notch withdrawal (Weng et al., 2006).

The second most compelling evidence for a Notch oncogenic function comes from studies of breast and cervical cancer as well as melanoma. The first indications of Notch playing a role in mammary gland tumorigenesis come from characterization of a mouse mammary tumor virus, which often integrates within the *Notch4* gene leading to its misexpression. Additional studies using *Notch4* overexpressing transgenic mice revealed importance of this pathway for mammary epithelium branching and differentiation. Moreover, mice are developing tumors within 7 months. Molecular analysis revealed that *Notch4* overexpresion activates TGFβ and HGF (hepatocyte growth factor) signaling and promotes tumor invasion. Although, involvement of Notch signaling in murine mammary tumorigenesis has been established, the information about similar mechanisms in human breast cancer is scares. Recent reports indicate Notch1 and Notch4 overexpression in the majority of breast ductal carcinoma *in situ* lesions (extensive review by Brennan, 2008).

A role for aberrantly active Notch signaling has been proposed in cervical cancer, largely due to observation of intensive Notch1 and Notch2 protein accumulation as well as consistent expression of Jagged1. It is speculated that two oncogenic effector mechanisms are triggered by Notch: activation of PI3K/AKT pathway and up-regulation of *Myc* (review by Maliekal et al., 2008).
Melanomas are highly aggressive tumors that originate from melanocytes, which are positioned at the epidermal-dermal junction and interspersed among the basal keratinocytes of the skin. The Notch signaling is commonly upregulated in primary human melanomas. However, models in which Notch is constitutively activated show that it is not sufficient for malignant transformation, although it promotes growth and metastasis. The pro-oncogenic functions of Notch in melanomas is linked with activation of Wnt signaling and promotion of N-cadherin expression. Additionally ablation of Notch in the melanocytes lineage leads to hair graying (Moriyama et al., 2006, Liu et al., 2006) in a dose-dependent manner (Schouwey et al., 2007).
Finally, overexpression of Notch pathway components has been observed in renal cell carcinoma, endometrical cancer, meduloblastoma and neuroblastoma however, details of the mechanisms and potential role of Notch is unclear (review by Koch and Radtke, 2007).

Notch as a tumor suppressor

Notch is often associated with maintaining immature progenitor cells and in order to induce differentiation Notch signaling has to be downregulated. In such cells Notch promotes cell growth, proliferation and survival and therefore, its aberrant activation is inevitably associated with oncogenesis. However, the Notch pathway can also induce cell fate decisions and differentiation in which it is associated with growth suspension and/or apoptosis. In this context the Notch signaling pathway has tumor suppressor proclivity (reviewed by Dotto, 2008).
The most emblematic example of Notch tumor suppressor function comes from studies on the skin. In primary mouse keratinocytes Notch induces cell cycle arrest and entry into differentiation. Conditional ablation of Notch1 in murine epidermis leads to epidermal hyperplasia and skin carcinoma over time (Nicolas, 2003 and Chapter 2). The tumor suppressive effect of Notch1 in the epidermis appears to be mediated by induction of p21, an important inhibitor of cell cycle progression (Rangarajan et al., 2001) and inhibition of β-catenin signaling (Nicolas et al., 2003). Similar results were reported in studies of inhibited Notch signaling *via* expression of a dominant-negative form of MAM in the epidermis (Proweller et al., 2006). As mentioned above this indicates that in the normal epithelium Notch1 suppresses Wnt/β-catenin signaling, which is associated with maintenance of keratinocytes in their stem cell compartment thus leading to terminal differentiation by withdrawal of proliferating cells from the cell cycle (more about Notch role in the skin tumor development see Chapter 3).

Notch and Epithelial-to-Mesenchymal Transition

Epithelial–mesenchymal transition (EMT) is a fundamental process that involves the switch from polarized epithelial cells to contractile and motile mesenchymal cells. EMT takes place at critical phases of embryonic development such as gastrulation, formation of the neural crest cells from the neural tube, formation

of the cardiac valve primordium during heart development etc. (reviewed by Thiery and Sleeman, 2006). Numerous observations support the idea that EMT is also involved in tumor metastasis during which primary tumor cells lose epithelial character and acquire mesenchymal features. This results in changed adhesive properties, and the activation of proteolysis and motility, which in turn allows tumor cells to metastasize and establish secondary tumors at distant sites. It is striking that the same signaling pathways that regulate developmental EMT are also activated during tumor progression, that includes activation of transforming growth factor-β (TGFβ), Wnt and Notch pathways (see also chapter 2). EMT involves repression of E-cadherin (that facilitates cell-cell adhesion) by Snail, Slug, Twist family of zinc-finger transcription factors, which can be induced by Notch in tissue specific context. For instance, in primary human breast cancer cells activation of Notch signaling upregulates the transcriptional repressor Slug and initiates EMT, which facilitates cancer cell metastasis (Leong et al., 2007). Notch signaling has also been suggested to be required in hypoxia-induced EMT, cell migration and invasion (Sahlgren et al., 2008, Chen et al., 2009). Moreover, Notch interacts with the TGFβ signaling pathway, which is a well-known inducer of EMT during embryonic development and in later stages of tumor progression. TGFβ can induce *Hey1* and *Jagged1* expression at the onset of EMT in epithelial cells and the subsequent activation of Notch signaling that in turn is necessary for the sustained induction of EMT (Zavadil et al., 2004, see also Chapter 2).

Notch and pancreatic cancer

The Notch signaling plays an important role in pancreatic development. In the adult pancreas, low expression of Notch receptors can be detected. Of note, increased expression levels of *Notch* pathway components during caerulein-induced acute pancreatitis will be analyzed in Chapter 4 (see also Gomez et al., 2004). Pancreatic-specific *Notch1* conditional knockout mice exhibit impaired regeneration after caerulein-induced pancreatitis. Epithelial differentiation, which is an early feature of pancreatic cancer, is also associated with Notch activity. Furthermore, cumulative observations now suggest re-activation of Notch signaling and robust activity of downstream target gene *Hes1* in the pre-neoplastic lesions as well as cancer and metastasis in both human and murine pancreatic malignancies (Miyamoto et al., 2003, Kimura et al., 2007, Hingorani et al., 2003). These results suggest that Notch activity is an early event leading to neoplasia. However, mouse models using a pancreas specific NIC overexpression approach fail to induce neoplasia, though combined with oncogenic Kras accelerate pre-neoplastic lesions formation (De La et al., 2008. Additionally, recent studies provide evidence that γ-secretase activity, probably by inducing Notch signaling, is required for the progression of pre-malignant to malignant pancreatic cells *in vivo* (Plentz et al., 2009). Additional description and author's findings considering the role of Notch receptors in development of pancreatic cancer are described in Chapter 2.

III. The pancreas

Many factors regulating pancreas development and regeneration are altered during pancreatic diseases including cancer and pancreatitis. Therefore, understanding the development of this organ and the pathways involved is crucial (see also chapter 5). This part briefly surveys the current knowledge about pancreas development.

Pancreas anatomy and physiology

The pancreas has two functionally different compartments: one exocrine, which is producing digestive enzymes, and one endocrine compartment that is responsible primarily for glucose homeostasis. The endocrine cells are clustered in groups called islets. The exocrine tissue (acinar) forms grape-lake structures connected with the ductal system of the pancreas through which the secreted digestive enzymes are transported into the duodenum (Fig. 1.4C). A robust vasculature provides functional support. However, the functionally divided pancreas forms a uniform organ localized against the posterior wall of the abdomen cavity (Fig. 1.4A and B), (Edlund, 2002).

Pancreas development

Pancreas organogenesis in the mouse starts at embryonic day 8.5 (E8.5) because of/through activation of PDX1 transcription factor expression in the posterior foregut. However, first morphological changes can be observed at day E9.5. Thickening of the dorsal and ventral surfaces of the gut endoderm forms pancreatic buds (Fig. 1.4D). Growing buds meet eventually at day E12-E13, coalescence leads to fusion of both parts. In the next 24 hours dramatic cellular and architectural changes occur. The embryonic pancreas starts branching, producing endocrine hormones and forming acinar cells. Over the next days (E14 to E18) endocrine cells are producing all secreted hormones and start aggregating but fully formed islet emerge after birth. The whole process of pancreas development is well orchestrated however, our knowledge of involved pathways (see Chapter 5) and molecular sequence remains unclear (excellent overview by Edlund, 2002).

Pancreatic stem cells, pancreatitis and pancreas regeneration

Narrow treatment modalities for pancreatic cancer, chronic pancreatitis and diabetes are urging for new cures. Pancreatic progenitor cells are providing most hope for regenerative therapies of diabetes. However the very existence of potential stem cells, their biology and function is elusive (review by Ku, 2008).
Do pancreatic stem cells exist? Yes, during embryogenesis, the pancreas progenitors cells are well defined i.e. co-express PDX1, PTF1, have active Notch signaling and share qualities of stem cells. However, those cells undergo differentiation resulting in a mature pancreas and those early progenitors seem to disappear. No spatial niche where adult stem cells would resign has been identified in the pancreas. The existence of 'resident' adult stem cells, which resign among normal tissue cells, is controversial as well. It must be considered however that the definition and proof of such cell existence in not

straightforward. A method known as BrdU retention indicates that slow-cycling, thus retaining BrdU cells are located around pancreatic islets, and express PDX1. Additionally, a method based on selecting cells expressing common stem cell markers like CD44, CD133, cMet suggests the existence of scattered progenitor cells in the pancreas. Finally, a number of studies suggest that centroacinar cells may have stem cell-like features. The centroacinar cell is located at the terminal end of the duct tube adjacent to acinus (Fig. 1.4C). The nature of these cells is elusive. They share some properties of duct cells but are in large part unique i.e. have active Notch signaling, express HES1 and PDX1. Given the absence of lineage tracing of centroacinar cells, formal prove of properties has yet to be obtained (see also Chapter 3).

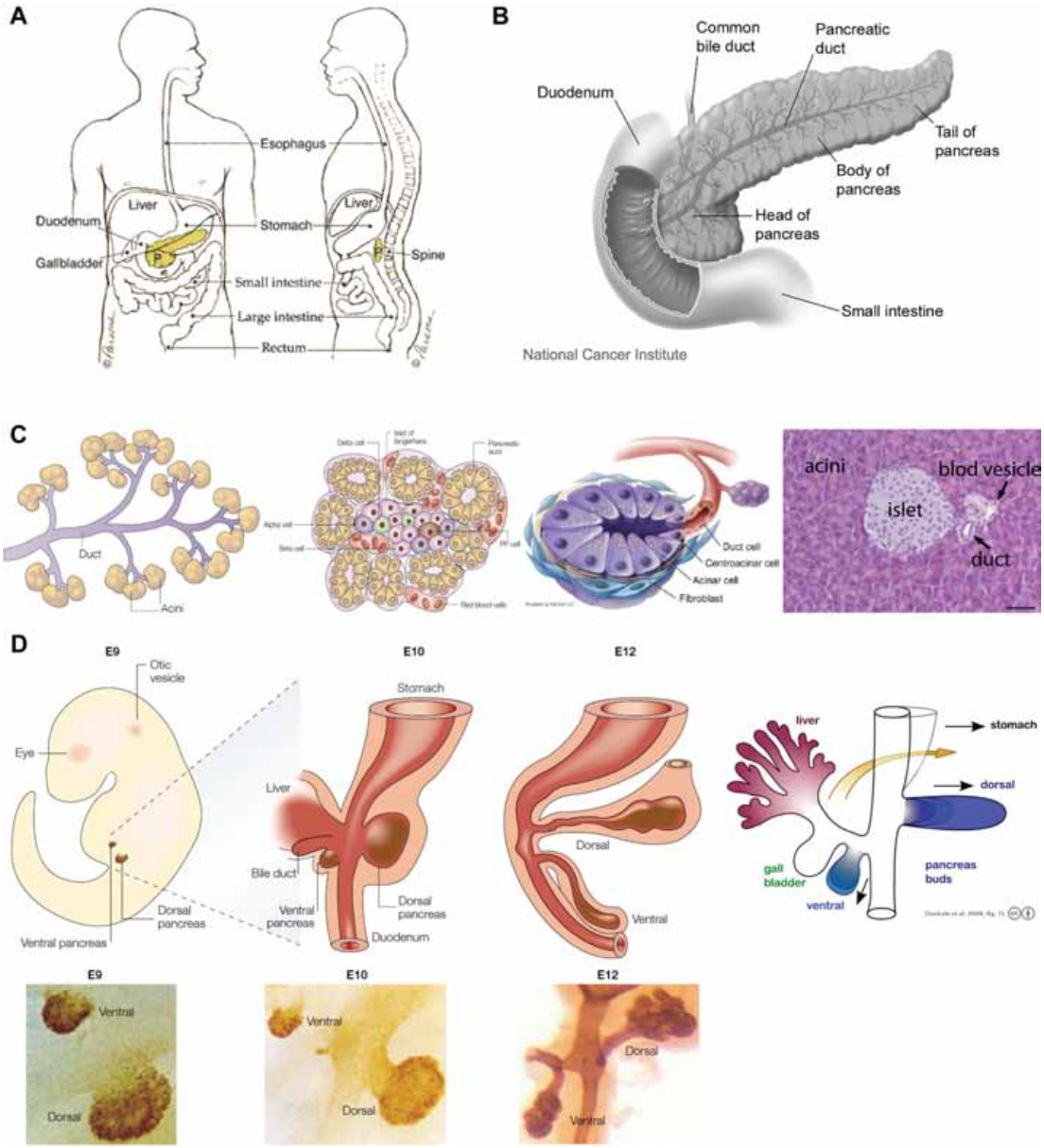

Figure 1.4. Pancreas anatomy and development.
(A) Localization of pancreas in the human body. (B) Gross anatomy of pancreas. (C) Morphology and structural elements of pancreas. (D) Schematic representation of the developing pancreas at embryonic day E9, E10 and E12 of a mouse embryo and photographs of the corresponding stages (Edlund, 2002).

IV. Pancreatic cancer

Pancreatic neoplasias can be classified based on their cellular lineage meaning which histologic type of the pancreas they recapitulate. Such a classification is an essential determinant of pathological and biological characteristics, which in turn is a key prognostic factor. Nearly all cell types of the pancreas have been associated with neoplasia. The most common and important entities of pancreas neoplasia will be presented.

Pancreatic ductal adenocarcinoma

Pancreatic Ductal Adenocarcinomas (PDACs) are recapitulating ductal lineage characteristics and represent the vast majority of pancreatic cancers. It is one of the deadliest of all cancers, with a 5-year survival below 5%, and it is the fourth leading cause of cancer deaths in the Western World (Jemal et al., 2008). It is estimated that PDAC is responsible for a substantial number of carcinomas of unknown primacy because it is often widely disseminated at the time of diagnosis when the origin of the primary tumor is hardly obvious. PDAC is difficult to diagnose because the tumor rarely forms lesions above 5 cm and is often metastatic at the stage of <2 cm in diameter. Differential diagnosis for PDAC is challenging and clinical pathologies are often missed. At the time of diagnosis only 20% of the cases are resectable and thus potentially curable.

One of the characteristic features of PDAC is its dense desmoplastic stroma (Fig. 1.5I) with ubiquitous fibrosis and inflammatory changes. Though PDAC presents often a well-differentiated glandular pattern that closely resembles duct-like structures (Fig. 1.5D), there are subtypes of these tumors representing more undifferentiated characteristics. Undifferentiated PDACs represent 2-5% of all PDACs but have an even more aggressive behavior and characteristic glandular PDAC duct-like structures are replaced by a more uniform cell mass. Undifferentiated PDACs include: sarcomatoid carcinoma with spindle-like cells (Fig. 1.5F, see also Chapter 2), anaplastic carcinoma (Fig. 1.5E) and carcinosarcoma. More about the molecular characteristics in part IX of the introduction and in Chapter 2.

Precursor lesions of pancreatic ductal adenocarcinoma

The prognosis of PDAC can be improved by early detection of precancerous lesions. Moreover, certain lesions are associated with specific molecular aberrations thus, diagnosing precursors is essential for treatment. The most common noninvasive precursor lesions are Pancreatic Intraepithelial Neoplasia (PanIN), Intraductal Papillary Mucinous Neoplasia (IMPN) and Mucinous Cystic Neoplasia (MCN). The cell of origin of these lesions is unknown however, it is believed that the lesions originate from epithelial cells of pancreatic ducts or trans-differentiated acinar cells (review by Schmid, 2008).

PanINs are most prevalent of all precursor lesions and are associated with high-risk PDACs. A classification system for PanINs based on morphologic structures has been developed and three grades have been defined: PanIN-1, PanIN-2 and PanIN-3. The degree of cell architecture abnormalities and nuclear atypia increases from grade 1 to 3. The PanIN-1 (subcategorized as 1A and 1B) is characterized as elongated duct cells with abundant mucin production and in

case of PanIN-1B with papillary instead of flat architecture. PanIN2 represents a consecutive step in the architectural disintegration and acquires moderate to severe nuclear aberrations. PanIN3 regarded as carcinoma in situ has cells budding into the lumen of duct (Fig. 1.5A) and is suggested to be the origin of PDAC, the so called PanIN-to-PDAC paradigm is widely accepted. Along with morphological changes molecular abnormalities and genetic mutations are observed (see part VIII).

IPMNs are defined as grossly visible cystic lesions with mucin producing, papillary epithelial cells filling the lumen (Fig. 1.5B). A classification of IPMNs has been developed distinguishing: gastric, intestinal, pancreatobiliary and oncocytic types based on morphology and characteristic mucin expression pattern. IPMNs have a broad histological spectrum from hyperplasia to adenoma and carcinoma. Though IPMN-to-PDAC progression remains unclear piling stack of evidence suggests such a possibility.

MCNs are lesions composed of multiocular cysts filled with mucin and lined with columnar epithelial cells (Fig. 1.5C). Characteristic of MCN is an ovarian-like stroma expressing progesterone and/or estrogene receptors. Moreover, MCNs usually occur in women only and are generally located in the splenic part of the pancreas. Progression of MCN-to-PDAC although reported remains controversial (see chapter 2).

Endocrine cancers

Most pancreatic tumors of endocrine lineage represent well differentiated Pancreatic Endocrine Neoplasms (PENs) formerly referred to as islet cell tumors. PENs are solid, circumscribed tumors recapitulating the morphology of the pancreatic islets. The cells of PENs are uniform, round with moderate amounts of cytoplasm and nuclei having a visible characteristic salt-and-pepper chromatin structure (Fig. 1.5H). Half of the PENs are functionally active thus, giving clinical symptoms of inappropriate production of endocrine hormones. These tumors are often named upon hormonal aberration represented e.g. insulinoma, glucagonoma, somatinostatinoma, gastrinoma etc. PENs tend to be non-aggressive (Hruban et al., 2006).

Acinar cancers

Neoplasms showing pure acinar phenotype are called Acinar Cell Carcinomas (ACCs) of the pancreas and account for less than 1% of all pancreatic cancers. The tumors are usually very cellular, homogenous with abundant cytoplasm and rarely showing desmoplastic reaction (Fig. 1.5G). Immunohistochemical stains reveal that ACCs are positive for pancreas-enzymes (trypsin, chymotrypsisn, lipase). Opposite to ductal carcinomas *Kras* gene mutations are usually absent (Hruban et al., 2006).

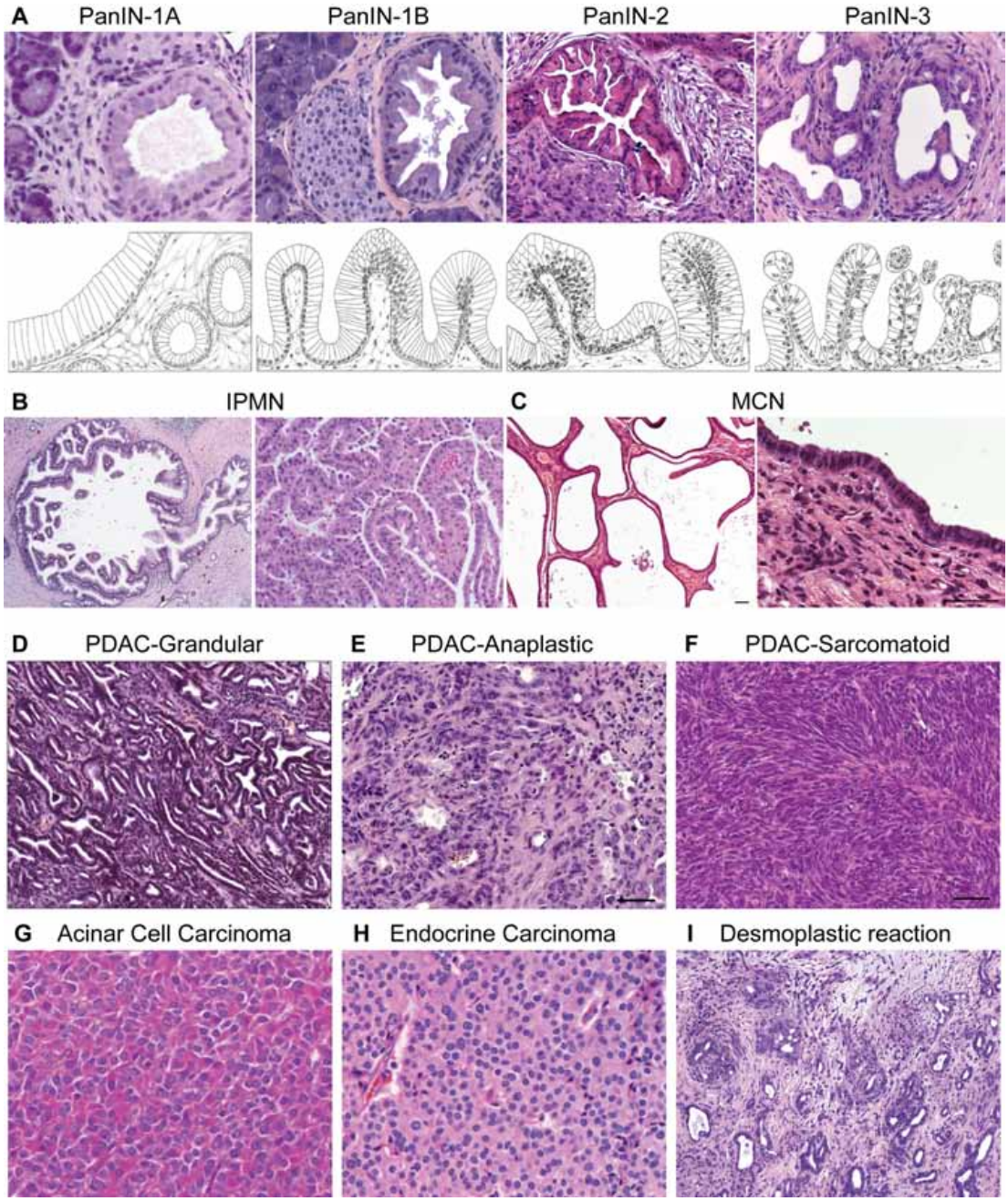

Figure 1.5. Pancreatic neoplasias.
(A-C) Precursor lesions of PDAC: PanIN, IPMN and MCN.
(D) Glandular PDAC shows prominent ductal differentiation.
(E) In anaplasitic PDAC undifferentiated features predominate.
(F) In sarcomatoid PDAC, note spindle cell morphology
(G) Characteristic acini formation in acinar cell carcinoma.
(H) Endocrine carcinoma
(I) Strong desmoplastic reaction is characteristic for PDAC

V. Models of pancreatic cancer

To unravel the molecular basis of pancreatic cancer a variety of model systems is used. Additionally, we rely on many of those models to help evaluating novel therapies for pancreatic cancer. A brief discussion of the models used to help us understand the pancreatic cancer is presented below (see also review by Ryan and Lowy, 2005, Melstrom and Grippo, 2008).

Pancreatic cancer cells in culture

As the study of molecular aberrations that lead to invasive pancreatic cancer was difficult to analyze on tissue level, investigating pancreatic cancer cell lines in culture offers an excellent alternative. Although isolation and culturing of pancreatic cancer cells proved to be very difficult, , there are now cell lines of various sources and aberrations that are stably growing *in vitro* (Table 1). Pancreatic cancer cells are used to assess the genetic background of the tumor but are also useful to evaluate the response to various therapies. This is particularly relevant to individualized medical treatment when patient tumor cells can be cultured and tested. However, a considerable limitation of studying pancreatic cancer *in vitro* is that procedures of isolation and maintenance of the cells change their interaction surroundings alternating the behavior and gene expression. This cell-culture effect renders it unlikely that cells *in vitro* recapitulate all *in situ* features of PDAC. Taking into consideration that isolated cells represent usually advanced stages of carcinogenesis it is difficult to study the role of molecular pathways, which might have contributed to tumorigenesis. High accumulation of genetic aberrations also makes it difficult to apply reverse genetic approaches to study pancreatic cancer. Partially, the above-mentioned limitations can be overcome by culturing normal duct cells *in vitro* or using xenografts (Melstrom and Grippo, 2008).

Table 1. Examples of pancreatic cancer cell lines and their genetic and histological background (Melstrom and Grippo, 2008)

Cell line	Source	Genetic mutations	Histology and grade
AsPC-1	Ascites	*Kras, p53, p16*	PDAC, G2/G3
BxPC-3	Primary tumor	*p53, p16, Smad4*	PDAC, G2/G3
CaPan-1	Liver metastasis	*Kras, p53, p16, Smad4*	PDAC, G1
CaPan-2	Primary tumor	*Kras, p16, Smad4*	PDAC, G1
MiaPaCa-2	Primary tumor	*Kras, p53, p16*	PDAC, G3
Panc-1	Primary tumor	*Kras, p53, p16*	PDAC, G3
Panc89	Lymph node met.	p53, p16	PDAC, G2
PancTu-I	Primary tumor	*Kras, p53, p16*	PDAC, G3
Pt45P1	Primary tumor	*Kras, p53, p16*	PDAC, G3

Subcutaneous and orthotopic xenografts

An approach to study pancreatic cancer cells *in vivo* employs xenografts transplantation into nude or Severe Combined Immunodeficient (SCID) mice. Nude or athymic mice have an aberrant thymus thus, lacking T-lymphocytes. SCID mice are defective in the immunoglobulin and T-cell receptor gene and therefore lack mature B- and T-lymphocytes. Both model types allow transplantation of cells in culture or pieces of resected tumor either

subcutaneously or orthotopically into the pancreas. That allows studying of pancreatic cancer cells in semi-natural conditions recapitulating some aspects (e.i. angiogenesis, invasion) and tissue context of tumor growth (for cross-examination of benefits and drawbacks see table 2).

Table 2. Subcutaneous vs. orthotopic xenografts (Melstrom and Grippo, 2008).

	Subcutaneous Xenografts	Orthotopic Xenografts
Disadvantages	-not suitable to study metastasis -do not show signs and symptoms that may arise as a consequence of pancreatic tumor growth -tumor-stroma interaction is lost -exchange of enzymes, cytokines is inhibited	-technically challenging -potential pancreas disruption or intra-peritoneal cancer cell spillage may result in hemorrhage or early artificial tumor spared and growth in abdomen -tumor establishment is anywhere between 50-100%
Advantages	-good model to assess tumor growth/volume in a temporal fasion -allow to obtain human pancreatic cancer tissue from cells -easy method to assess therapy response	-recapitulate primary tumor environment -give good correlation between the histology of the primary tumor and xenograft -allow imaging of disseminating cells

Mouse models of pancreatic cancer

Animal models recapitulating the course of disease including preneoplastic and microenvironment features are a major advance to study human malignancies. Genetically engineered mouse (GEM) models have the potential to mimic genotype-phenotype relationships found in cancer therefore advancing our understanding of the pathobiology of neoplasia (for review of wide number of mouse models see Van Dyke and Jacks, 2002). GEM have been successfully created using different transgenic and gene targeting strategies that mimic pancreatic cancer (Table 3). Moreover GEM have the potential to identify early markers of disease, recognize cooperating genetic alterations, and provide better preclinical models for therapy. A crucial consideration building a GEM model is how to target mutant alleles to the organ and in these projects to specific pancreatic cell lineages. First, models targeting mutations to elastase (EL) producing acinar cells were only partially successful regarding developing PDAC. Discoveries in the field of developmental biology of the pancreas allowed the generation of more refine GEM. Most remarkable was the use of *Pdx1* and *Ptf1a* transcription factors that are expressed predominantly in the developing pancreas (see, part III and Chapter 5) to drive expression of Cre recombinase. This allowed the usage of Cre/lox based mice for pancreas-specific gene modifications. The next milestone was the generation of a *Kras* mutant in the endogenous mouse allele. *Pdx1-Cre* or $Ptf1^{Cre}$ triggered $Kras^{G12D}$ expression results in PanIN formation and PanIN-to-PDAC tumor development faithfully recapitulating the human disease. Recent years brought further GEM that closely mirror many of the genetic and histologic characteristics of human PDAC including preneoplastic lesions. The most significant models include *El-TGFα;* $Ptf1^{Cre}$*;* $Kras^{G12D}$ mice that recapitulate IPMN-to-PDAC tumorigenesis and Ptf^{Cre}*(and Pdx1-Cre);* $Kras^{G12D}$*; Smad4* forming MCN-to-PDAC and IPMN-to-PDAC cancers. However, despite of these advances, controversy regarding the cell of origin of PDAC is still of ongoing debate.

Table 3. List of mouse models of the pancreatic cancer.

Genetic modification	Lesions	Cancer (age at onset in months, freq in %)	Metastasis (freq in %)
El-TAg (Ornitz et al., 1987)	Acinar dysplasia	ACC (2-3, 100%)	Rare (<2%)
El-Hras^{G12V} (Quaife et al., 1987)	Disrupted organogenesis	ACC (12, 100%)	None
El-myc (Sandgren et al., 1991)	Mixed acinar-ductal	ACC (2-4, 100%)	Liver (10%)
El-TGFα (Sandgren et al., 1990)	Acinar metaplasia, fibrosis	PDAC (12+, 20%)	None
El-TGFα; p53null (Wagner et al., 2001)	Tubular/cystic, acinar hyperplasia	ACC (12+, 30%)	None
MT-TGFα; p16/p19 / p53$^{-/-}$ (Bardeesy et al., 2002)	Tubular metaplasia	Serous cystic adenoma	None
El-Kras^{G12D} (Grippo et al., 2003)	Tubular metaplasia	None (>12)	None
CK19-Kras^{G12V} (Brembeck et al., 2003)	Ductal dysplasia, hyperplasia	None (>12)	None
Mist1-Kras^{G12D} (Tuveson et al., 2006)	Acinar-ductal metaplasia	ACC, PDAC (11, 100%)	None
Pdx1-Shh (Thayer et al., 2003)	Tubular complex	None (survival <1)	None
Pdx-1-Cre/Ptf-Cre; Kras$^{G12D/+}$ (Hingorani et al., 2003)	PanIN, desmoplasia	PDAC, glandular (16, 50%)	Liver (7%)
Pdx-1-Cre; Kras^{G12D};p16/p19$^{lox/lox}$ (Aguirre et al., 2003)	PanIN	PDAC, sarcomatoid (2-3, 100%)	Duod., Liver, diaphragm
Pdx-1-Cre; Kras^{G12D}; p53$^{R172H/+}$ (Hingorani et al., 2005)	PanIN	PDAC, glandular (5, 100%)	Yes
Pdx-1-Cre; Kras$^{G12D/+}$; p16$^{lox/lox}$ (Bardeesy et al., 2006a	PanIN	PDAC (<6)	Duodenum, Liver, bile d.
Pdx-1-Cre; Kras$^{G12D/+}$; p53$^{lox/lox}$ (Bardeesy et al., 2006a)	PanIN	PDAC, glandular (6, 100%)	None
Pdx-1-Cre;Kras$^{G12D/+}$; p16$^{-/-}$; p53$^{lox/lox}$ (Bardeesy et al., 2006a)	PanIN	PDAC, grandular, anaplastic (2, 100%)	Yes (20%)
Pdx-1-Cre; PTEN $^{lox/lox}$ / p53 $^{lox/+}$ (Stanger et al., 2005)	Ductal metaplasia, PanIN	PDAC (12, 10%)	Yes
MT-TGFα; El-myc (Liao et al., 2006)	Dysplastic duct, cystic neoplasia	PDAC & Mixed acinar-ductal carcinoma (2-7)	Liver (33%)
Ptf-Cre; Kras$^{G12D/+}$; TGFβIIR$^{lox/lox}$ (Ijichi et al., 2006)	PanIN	PDAC, glandular and sarcomatoid (2, 100%)	Yes
El-TGFα; Ptf-Cre; Kras$^{G12D/+}$ (Siveke et al., 2007)	IPMN	PDAC (12, 100%)	
Ptf-Cre; Kras$^{G12D/+}$; ca.Gli-2 (Pasca di Magliano et al., 2006)	PanIN, desmoplasia	PDAC, undifferentiated (1, 100%)	Yes
Ptf-Cre; Kras$^{G12D/+}$; Smad4 $^{lox/lox}$ (Kojima et al., 2007, Izeradjene et al., 2007, Bardeesy et al., 2006b)	MCN, IPMN	PDAC (9, 100%)	Yes
Ptf-Cre; Kras$^{G12D/+}$; ca.Akt (Elghazi et al., 2009)	Acinar-ductal metaplasia	PDAC (8, 100%)	
Ptf-Cre; Kras$^{G12D/+}$; Muc1 (Tinder et al., 2008)	PanIN	PDAC (6, 100%)	Yes
El-tTA/tetO-Cre; Kras$^{G12D/+}$ (Guerra et al., 2007)	PanIN	PDAC only with induced pancreatitis	

VI. Molecular signaling pathways in pancreatic cancer

The molecular pathogenesis of pancreatic ductal adenocarcinoma (PDAC) involves the stepwise accumulation of genetic alternations. Key mutations occurring during pancreas tumorigenesis involve genes encoding critical regulators of signal transduction networks that regulate cell cycle, differentiation and survival (Table 4). The signaling pathways involved in PDAC are now better understood. KRAS, p16, p53, TGFβ/Smad4 are among the most important and best studied. Recently, there has been given more attention to new pathways in particular to developmental signaling like Wnt, Notch and Hedgehog. These pathways are suggested to play a crucial role in directing local cellular behavior and oncogenic transformation (plenty excellent reviews covering the topic i.e. Bardeesy and DePinho, 2002, Hezel et al., 2006, Soto et al., 2006).

Table 4. Oncogenes and tumor suppressor genes alternated in human pancreatic cancer (Soto et al., 2006, Hruban et al., 2008)

Genetic mutation	Incidence of mutation
Kras	90-95%
p16	80-95%
p53	50-75%
Smad4	50%
p15	27-48%
Akt2	10-20%
Myb	10%
BRCA2	7%

Progression model of PDAC

Genetic studies strongly support the paradigm that multistep accumulation of genetic alternations is critical for the development of PDAC. The earliest pancreatic lesions confine constitutive activation of RAS signaling usually marked by *Kras* activating mutations, overexpression of EGF ligands (e.g. *TGFα*) leading to autocrine RAS activation or by amplification of EGF receptors (e.g. *HER2/Neu*). The aberrant RAS activation is though to be necessary and sufficient to initiate pancreatic cancer. At an early stage of tumor initiation Notch and Hedgehog signaling pathways are reactivated. Further advancements of pre-neoplastic lesions are usually associated with mutation or deletion of tumor suppressor genes e.g. *p16* or *p53*. Additional aberrations like centrosome abnormalities are observed in 85% of cases and chromosomal instability is a characteristic feature for the last act of PanIN-to-PDAC progression (reviewed by Schneider, 2005). The most important pathways implicated with pancreatic malignancies are described below (see also Fig. 1.6).

Kras pathway

Activating mutations of KRAS are the first genetic changes detected in yet normal appearing pancreatic cells that initiate tumorigenesis. Moreover, Kras mutations increase in frequency with disease progression and are found to be a predominant and necessary passage for PDAC. In fact the mouse models described in the previous section support the notion that oncogenic *Kras* is

sufficient to induce malignant transformation. Merely, one single point mutation can unleash the oncogenic potential of *Kras.* Activation occurs when codons 12 and 13, less frequently 59, 61 and 63 are mutated, commonly by conversion of glycine to aspartic acid, glutamic acid or valine. Intriguingly, sometimes Kras mutations emerge in normal pancreata over human lifespan not causing neoplastic transformation. The only caveat would revolve around the supposition that critical, yet to be characterized progenitor cells need to be targeted in order to drive malignant transformation. Oncogenic KRAS produces a remarkable array of cellular effects including induction of cell cycle, survival and invasion by activating downstream signaling (Fig. 1.6C). An overwhelming number of evidence supports the role of these downstream effectors in both the initiation and the maintenance of PDAC (reviewed in Hezel et al., 2006). However, the importance of each of the KRAS effectors is not fully understood yet is crucial for future therapeutic strategies.

Tumor suppressor genes and pathways: p16, p53, TGFβ-Smad4

P16*.* Germline mutations of *p16* (*Ink/Cdkn2a*) tumor suppressor gene confer a 13-fold increased risk of pancreatic cancer (Goldstein, 1995). Loss of p16 function brought by mutations, deletion, or promoter methylation, occurs in 80-95% of PDAC (Table 4). p16 (INK4) is often (ca. 40%) lost together with p19 (ARF) as they share physical juxtaposition in the genome, thereby disrupting two main tumor-suppressor pathways: RB (retinoblastoma) and p53. P16 inhibits CDK4 mediated phosphorylation/deactivation of RB cell cycle checkpoint thus, blocking entry to S phase of mitosis. P19 stabilizes p53 by inhibiting its MDM2-dependent ubiquitination followed by degradation (Fig. 1.6B). Normally *p16* expression is induced by environmental stress and inappropriate growth or DNA damage. Although loss of *p16* facilitates the oncogenic pressure of activated KRAS, as shown in mouse models (see part VIII of this Chapter 2), its occurrence late in the pancreatic tumorigenesis (Fig. 1.6A) indicates that both pathways synergy requires other events.

P53. Mutations in the tumor suppressor p53 are among the most common somatic alternations found consistently in most of human malignancies. In ca. 50% of all PDACs p53 is found mutated. p53 is a cell cycle gatekeeper sensitive for DNA damage, cytotoxic stress and hypoxia. Mutations in *p53* occur late in pancreas tumorigenesis and correlate with high levels of dysplasia and invasiveness. Loss of proper p53 function is associated with cell growth, increased survival and genetic instability. The latter is commonly found in the pancreatic cancer leading to chromosomal instability (CIN) and subsequent gene amplifications and/or deletions (Hingorani et al., 2005).

TGFβ-Smad4. TGFβ-mediated signaling results in Smad4 translocation, in complex with other proteins, to the nucleus (Fig. 1.6D). There Smad4 controls cell proliferation, differentiation, migration and apoptosis although the role of the TGFβ-Smad4 axis is biologically very complex and depends on the cell type and context. Overall, the current theory regarding the role of TGFβ signaling in PDAC claims that the mutation or loss of Smad4 renders an impossible execution of TGFβ-induced cell growth inhibition through stimulation of p21 (CIP1) and p15 (INK4B) expression and MYC repression as well as induction of apoptosis. On the other hand TGFβ promotes epithelial-to-mesenchymal transition (EMT),

thereby promoting invasiveness (Fig. 1.6E). A common manifestation of this fact is that tumors with an intact TGFβ-Smad4 pathway have a higher propensity to show poorly differentiated features (see Chapter 2). Therefore, TGFβ seems to have a bi-phasic effect inhibiting tumor initiation yet promoting later advancement (Fig. 1.6E), (further review in Truty and Urrutia, 2007).

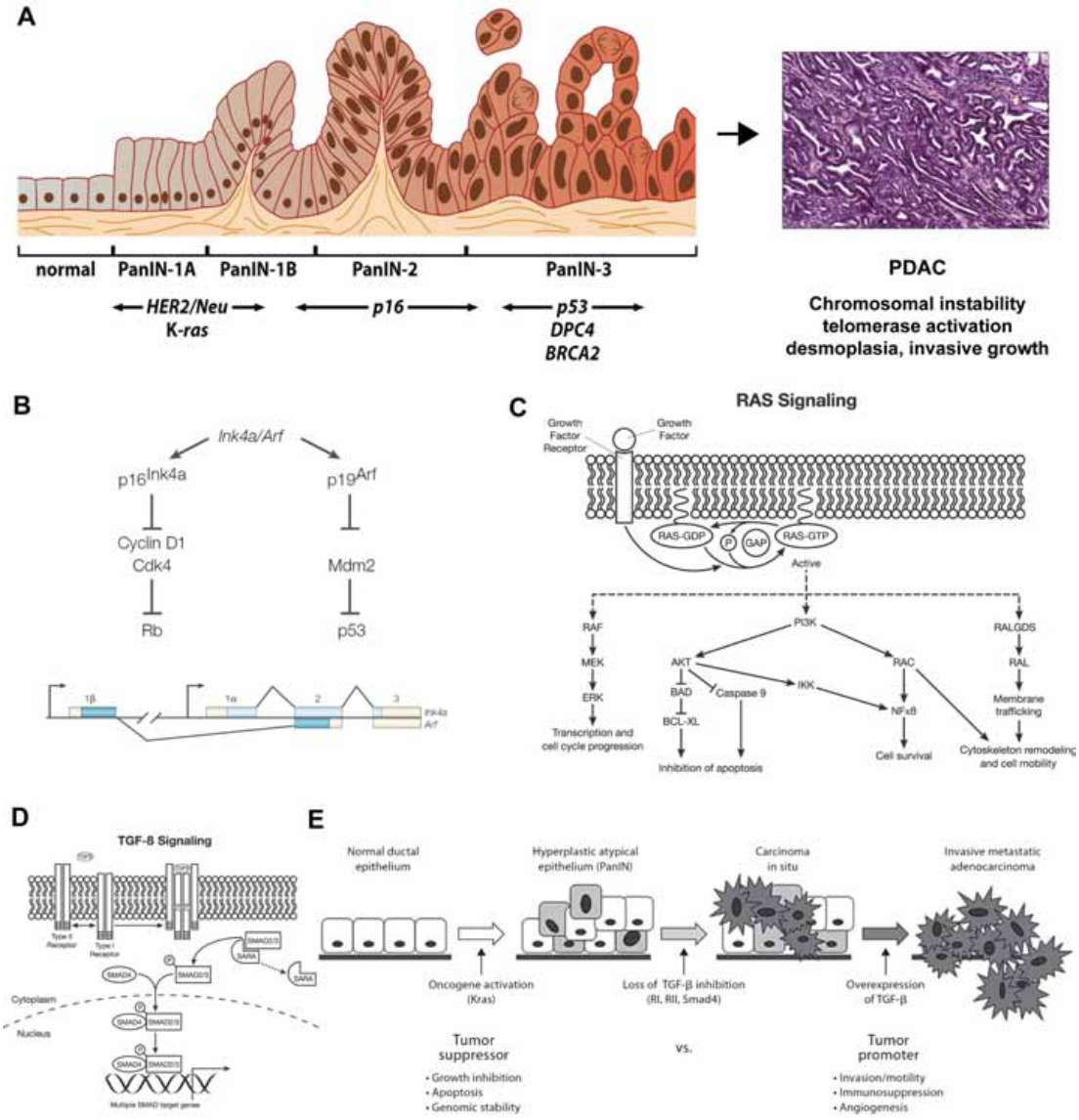

Figure 1.6. Model of PanIN precursor lesions progression and genetic events involved in PDAC development. (A) The PanIN grading scheme is shown, increasing grade (1–3) reflects increasing atypia, eventually leading to PDAC. The various genetic events are listed and divided into those that predominantly correlate with depicted stage of neoplasia (modified Weinberg, 2006). (B) p16/p19 share physical juxtaposition in the genome, however regulate distinct molecular pathways. (C) Ras signaling pathway. (D) TGFβ-Smad4 signaling pathway. (E) Bi-phasic effect of TGFβ regulation (Truty and Urrutia, 2007

VII. References

Aguirre, A. J., Bardeesy, N., Sinha, M., *et al.* (2003). Activated Kras and Ink4a/Arf deficiency cooperate to produce metastatic pancreatic ductal adenocarcinoma. Genes Dev *17*, 3112-3126.

Artavanis-Tsakonas, S., Rand, M. D., and Lake, R. J. (1999). Notch signaling: cell fate control and signal integration in development. Science *284*, 770-776.

Bardeesy, N., Aguirre, A. J., Chu, G. C., *et al.* (2006a). Both p16(Ink4a) and the p19(Arf)-p53 pathway constrain progression of pancreatic adenocarcinoma in the mouse. Proc Natl Acad Sci U S A *103*, 5947-5952.

Bardeesy, N., Cheng, K. H., Berger, J. H., *et al.* (2006b). Smad4 is dispensable for normal pancreas development yet critical in progression and tumor biology of pancreas cancer. Genes Dev *20*, 3130-3146.

Bardeesy, N., and DePinho, R. A. (2002). Pancreatic cancer biology and genetics. Nat Rev Cancer *2*, 897-909.

Bardeesy, N., Morgan, J., Sinha, M., *et al.* (2002). Obligate roles for p16(Ink4a) and p19(Arf)-p53 in the suppression of murine pancreatic neoplasia. Mol Cell Biol *22*, 635-643.

Bate, M., Rushton, E., and Frasch, M. (1993). A dual requirement for neurogenic genes in Drosophila myogenesis. Dev Suppl, 149-161.

Borggrefe, T., and Oswald, F. (2009). The Notch signaling pathway: transcriptional regulation at Notch target genes. Cell Mol Life Sci *66*, 1631-1646.

Bowerman, B., Eaton, B. A., and Priess, J. R. (1992). skn-1, a maternally expressed gene required to specify the fate of ventral blastomeres in the early C. elegans embryo. Cell *68*, 1061-1075.

Brembeck, F. H., Schreiber, F. S., Deramaudt, T. B., *et al.* (2003). The mutant K-ras oncogene causes pancreatic periductal lymphocytic infiltration and gastric mucous neck cell hyperplasia in transgenic mice. Cancer Res *63*, 2005-2009.

Chen, J., Imanaka, N., and Griffin, J. D. (2009). Hypoxia potentiates Notch signaling in breast cancer leading to decreased E-cadherin expression and increased cell migration and invasion. Br J Cancer.

Conlon, R. A., Reaume, A. G., and Rossant, J. (1995). Notch1 is required for the coordinate segmentation of somites. Development *121*, 1533-1545.

D'Souza, B., Miyamoto, A., and Weinmaster, G. (2008). The many facets of Notch ligands. Oncogene *27*, 5148-5167.

De La, O. J., Emerson, L. L., Goodman, J. L., *et al.* (2008). Notch and Kras reprogram pancreatic acinar cells to ductal intraepithelial neoplasia. Proc Natl Acad Sci U S A *105*, 18907-18912.

de la Pompa, J. L., Wakeham, A., Correia, K. M., *et al.* (1997). Conservation of the Notch signalling pathway in mammalian neurogenesis. Development *124*, 1139-1148.

Demarest, R. M., Ratti, F., and Capobianco, A. J. (2008). It's T-ALL about Notch. Oncogene *27*, 5082-5091.

Domenga, V., Fardoux, P., Lacombe, P., *et al.* (2004). Notch3 is required for arterial identity and maturation of vascular smooth muscle cells. Genes Dev *18*, 2730-2735.

Dotto, G. P. (2008). Notch tumor suppressor function. Oncogene *27*, 5115-5123.

Duarte, A., Hirashima, M., Benedito, R.*, et al.* (2004). Dosage-sensitive requirement for mouse Dll4 in artery development. Genes Dev *18*, 2474-2478.

Dunwoodie, S. L., Clements, M., Sparrow, D. B.*, et al.* (2002). Axial skeletal defects caused by mutation in the spondylocostal dysplasia/pudgy gene Dll3 are associated with disruption of the segmentation clock within the presomitic mesoderm. Development *129*, 1795-1806.

Edlund, H. (2002). Pancreatic organogenesis--developmental mechanisms and implications for therapy. Nat Rev Genet *3*, 524-532.

Elghazi, L., Weiss, A. J., Barker, D. J.*, et al.* (2009). Regulation of pancreas plasticity and malignant transformation by Akt signaling. Gastroenterology *136*, 1091-1103.

Ellisen, L. W., Bird, J., West, D. C.*, et al.* (1991). TAN-1, the human homolog of the Drosophila notch gene, is broken by chromosomal translocations in T lymphoblastic neoplasms. Cell *66*, 649-661.

Fischer, A., and Gessler, M. (2007). Delta-Notch--and then? Protein interactions and proposed modes of repression by Hes and Hey bHLH factors. Nucleic Acids Res *35*, 4583-4596.

Fitzgerald, K., Wilkinson, H. A., and Greenwald, I. (1993). glp-1 can substitute for lin-12 in specifying cell fate decisions in Caenorhabditis elegans. Development *119*, 1019-1027.

Fortini, M. E. (2002). Gamma-secretase-mediated proteolysis in cell-surface-receptor signalling. Nat Rev Mol Cell Biol *3*, 673-684.

Fre, S., Huyghe, M., Mourikis, P.*, et al.* (2005). Notch signals control the fate of immature progenitor cells in the intestine. Nature *435*, 964-968.

Gomez, G., Englander, E. W., Wang, G.*, et al.* (2004). Increased expression of hypoxia-inducible factor-1alpha, p48, and the Notch signaling cascade during acute pancreatitis in mice. Pancreas *28*, 58-64.

Gordon, W. R., Arnett, K. L., and Blacklow, S. C. (2008). The molecular logic of Notch signaling--a structural and biochemical perspective. J Cell Sci *121*, 3109-3119.

Greenwald, I. (1998). LIN-12/Notch signaling: lessons from worms and flies. Genes Dev *12*, 1751-1762.

Greenwald, I. S., Sternberg, P. W., and Horvitz, H. R. (1983). The lin-12 locus specifies cell fates in Caenorhabditis elegans. Cell *34*, 435-444.

Grippo, P. J., Nowlin, P. S., Demeure, M. J.*, et al.* (2003). Preinvasive pancreatic neoplasia of ductal phenotype induced by acinar cell targeting of mutant Kras in transgenic mice. Cancer Res *63*, 2016-2019.

Guerra, C., Schuhmacher, A. J., Canamero, M.*, et al.* (2007). Chronic pancreatitis is essential for induction of pancreatic ductal adenocarcinoma by K-Ras oncogenes in adult mice. Cancer Cell *11*, 291-302.

Haines, N., and Irvine, K. D. (2003). Glycosylation regulates Notch signalling. Nat Rev Mol Cell Biol *4*, 786-797.

Hamada, Y., Kadokawa, Y., Okabe, M.*, et al.* (1999). Mutation in ankyrin repeats of the mouse Notch2 gene induces early embryonic lethality. Development *126*, 3415-3424.

Hass, M. R., Sato, C., Kopan, R., *et al.* (2009). Presenilin: RIP and beyond. Semin Cell Dev Biol *20*, 201-210.

Heitzler, P., and Simpson, P. (1991). The choice of cell fate in the epidermis of Drosophila. Cell *64*, 1083-1092.

Hezel, A. F., Kimmelman, A. C., Stanger, B. Z., *et al.* (2006). Genetics and biology of pancreatic ductal adenocarcinoma. Genes Dev *20*, 1218-1249.

Hingorani, S. R., Petricoin, E. F., Maitra, A., *et al.* (2003). Preinvasive and invasive ductal pancreatic cancer and its early detection in the mouse. Cancer Cell *4*, 437-450.

Hingorani, S. R., Wang, L., Multani, A. S., *et al.* (2005). Trp53R172H and KrasG12D cooperate to promote chromosomal instability and widely metastatic pancreatic ductal adenocarcinoma in mice. Cancer Cell *7*, 469-483.

Hrabe de Angelis, M., McIntyre, J., 2nd, and Gossler, A. (1997). Maintenance of somite borders in mice requires the Delta homologue DII1. Nature *386*, 717-721.

Hruban, R. H., Maitra, A., Schulick, R., *et al.* (2008). Emerging molecular biology of pancreatic cancer. Gastrointest Cancer Res *2*, S10-15.

Hruban, R. H., Rustgi, A. K., Brentnall, T. A., *et al.* (2006). Pancreatic cancer in mice and man: the Penn Workshop 2004. Cancer Res *66*, 14-17.

Huppert, S. S., Le, A., Schroeter, E. H., *et al.* (2000). Embryonic lethality in mice homozygous for a processing-deficient allele of Notch1. Nature *405*, 966-970.

Hutter, H., and Schnabel, R. (1994). glp-1 and inductions establishing embryonic axes in C. elegans. Development *120*, 2051-2064.

Ijichi, H., Chytil, A., Gorska, A. E., *et al.* (2006). Aggressive pancreatic ductal adenocarcinoma in mice caused by pancreas-specific blockade of transforming growth factor-beta signaling in cooperation with active Kras expression. Genes Dev *20*, 3147-3160.

Iso, T., Kedes, L., and Hamamori, Y. (2003). HES and HERP families: multiple effectors of the Notch signaling pathway. J Cell Physiol *194*, 237-255.

Izeradjene, K., Combs, C., Best, M., *et al.* (2007). Kras(G12D) and Smad4/Dpc4 haploinsufficiency cooperate to induce mucinous cystic neoplasms and invasive adenocarcinoma of the pancreas. Cancer Cell *11*, 229-243.

Jiang, R., Lan, Y., Chapman, H. D., *et al.* (1998). Defects in limb, craniofacial, and thymic development in Jagged2 mutant mice. Genes Dev *12*, 1046-1057.

Kimble, J., and Simpson, P. (1997). The LIN-12/Notch signaling pathway and its regulation. Annu Rev Cell Dev Biol *13*, 333-361.

Kimura, K., Satoh, K., Kanno, A., *et al.* (2007). Activation of Notch signaling in tumorigenesis of experimental pancreatic cancer induced by dimethylbenzanthracene in mice. Cancer Sci *98*, 155-162.

Koch, U., and Radtke, F. (2007). Notch and cancer: a double-edged sword. Cell Mol Life Sci *64*, 2746-2762.

Kojima, K., Vickers, S. M., Adsay, N. V., *et al.* (2007). Inactivation of Smad4 accelerates Kras(G12D)-mediated pancreatic neoplasia. Cancer Res *67*, 8121-8130.

Kopan, R., and Ilagan, M. X. (2009). The canonical Notch signaling pathway: unfolding the activation mechanism. Cell *137*, 216-233.

Kopan, R., and Turner, D. L. (1996). The Notch pathway: democracy and aristocracy in the selection of cell fate. Curr Opin Neurobiol *6*, 594-601.

Krebs, L. T., Iwai, N., Nonaka, S.*, et al.* (2003). Notch signaling regulates left-right asymmetry determination by inducing Nodal expression. Genes Dev *17*, 1207-1212.

Krebs, L. T., Xue, Y., Norton, C. R.*, et al.* (2000). Notch signaling is essential for vascular morphogenesis in mice. Genes Dev *14*, 1343-1352.

Ku, H. T. (2008). Minireview: pancreatic progenitor cells--recent studies. Endocrinology *149*, 4312-4316.

Kurooka, H., Kuroda, K., and Honjo, T. (1998). Roles of the ankyrin repeats and C-terminal region of the mouse notch1 intracellular region. Nucleic Acids Res *26*, 5448-5455.

Lai, E. C. (2004). Notch signaling: control of cell communication and cell fate. Development *131*, 965-973.

Leong, K. G., Niessen, K., Kulic, I.*, et al.* (2007). Jagged1-mediated Notch activation induces epithelial-to-mesenchymal transition through Slug-induced repression of E-cadherin. J Exp Med *204*, 2935-2948.

Liao, D. J., Wang, Y., Wu, J.*, et al.* (2006). Characterization of pancreatic lesions from MT-tgf alpha, Ela-myc and MT-tgf alpha/Ela-myc single and double transgenic mice. J Carcinog *5*, 19.

Liu, Z. J., Xiao, M., Balint, K.*, et al.* (2006). Notch1 signaling promotes primary melanoma progression by activating mitogen-activated protein kinase/phosphatidylinositol 3-kinase-Akt pathways and up-regulating N-cadherin expression. Cancer Res *66*, 4182-4190.

Lubman, O. Y., Korolev, S. V., and Kopan, R. (2004). Anchoring notch genetics and biochemistry; structural analysis of the ankyrin domain sheds light on existing data. Mol Cell *13*, 619-626.

Maliekal, T. T., Bajaj, J., Giri, V.*, et al.* (2008). The role of Notch signaling in human cervical cancer: implications for solid tumors. Oncogene *27*, 5110-5114.

McCright, B., Gao, X., Shen, L.*, et al.* (2001). Defects in development of the kidney, heart and eye vasculature in mice homozygous for a hypomorphic Notch2 mutation. Development *128*, 491-502.

Melstrom, L. G., and Grippo, P. J. (2008). Models of Pancreatic Cancer: Understanding Disease Progression Springer).

Miyamoto, Y., Maitra, A., Ghosh, B.*, et al.* (2003). Notch mediates TGF alpha-induced changes in epithelial differentiation during pancreatic tumorigenesis. Cancer Cell *3*, 565-576.

Moriyama, M., Osawa, M., Mak, S. S.*, et al.* (2006). Notch signaling via Hes1 transcription factor maintains survival of melanoblasts and melanocyte stem cells. J Cell Biol *173*, 333-339.

Mumm, J. S., and Kopan, R. (2000). Notch signaling: from the outside in. Dev Biol *228*, 151-165.

Nicolas, M., Wolfer, A., Raj, K.*, et al.* (2003). Notch1 functions as a tumor suppressor in mouse skin. Nat Genet *33*, 416-421.

Nye, J. S., and Kopan, R. (1995). Developmental signaling. Vertebrate ligands for Notch. Curr Biol *5*, 966-969.

Ohlstein, B., and Spradling, A. (2006). The adult Drosophila posterior midgut is maintained by pluripotent stem cells. Nature *439*, 470-474.

Ornitz, D. M., Hammer, R. E., Messing, A.*, et al.* (1987). Pancreatic neoplasia induced by SV40 T-antigen expression in acinar cells of transgenic mice. Science *238*, 188-193.

Pasca di Magliano, M., Sekine, S., Ermilov, A.*, et al.* (2006). Hedgehog/Ras interactions regulate early stages of pancreatic cancer. Genes Dev *20*, 3161-3173.

Plentz, R., Park, J. S., Rhim, A. D.*, et al.* (2009). Inhibition of gamma-secretase activity inhibits tumor progression in a mouse model of pancreatic ductal adenocarcinoma. Gastroenterology *136*, 1741-1749 e1746.

Poulson, D. F. (1937). Chromosomal Deficiencies and the Embryonic Development of Drosophila Melanogaster. Proc Natl Acad Sci U S A *23*, 133-137.

Proweller, A., Tu, L., Lepore, J. J.*, et al.* (2006). Impaired notch signaling promotes de novo squamous cell carcinoma formation. Cancer Res *66*, 7438-7444.

Quaife, C. J., Pinkert, C. A., Ornitz, D. M.*, et al.* (1987). Pancreatic neoplasia induced by ras expression in acinar cells of transgenic mice. Cell *48*, 1023-1034.

Rand, M. D., Grimm, L. M., Artavanis-Tsakonas, S.*, et al.* (2000). Calcium depletion dissociates and activates heterodimeric notch receptors. Mol Cell Biol *20*, 1825-1835.

Rangarajan, A., Talora, C., Okuyama, R.*, et al.* (2001). Notch signaling is a direct determinant of keratinocyte growth arrest and entry into differentiation. EMBO J *20*, 3427-3436.

Ryan, T., and Lowy, A. M. (2005). Models for pancreatic cancer: Giant steps forward, miles to go Drug Discovery Today *2*, 27-33.

Sahlgren, C., Gustafsson, M. V., Jin, S.*, et al.* (2008). Notch signaling mediates hypoxia-induced tumor cell migration and invasion. Proc Natl Acad Sci U S A *105*, 6392-6397.

Sandgren, E. P., Luetteke, N. C., Palmiter, R. D.*, et al.* (1990). Overexpression of TGF alpha in transgenic mice: induction of epithelial hyperplasia, pancreatic metaplasia, and carcinoma of the breast. Cell *61*, 1121-1135.

Sandgren, E. P., Quaife, C. J., Paulovich, A. G.*, et al.* (1991). Pancreatic tumor pathogenesis reflects the causative genetic lesion. Proc Natl Acad Sci U S A *88*, 93-97.

Schmid, R. M. (2008). Precancerous lesions. In The Pancreas: An Integrated Textbook of Basic Science, Medicine, and Surgery, 2nd, H.-G. Beger, M. Buchler, R. Kozarek*, et al.*, eds. (Wiley-Blackwell), pp. 614-620.

Schouwey, K., Delmas, V., Larue, L.*, et al.* (2007). Notch1 and Notch2 receptors influence progressive hair graying in a dose-dependent manner. Dev Dyn *236*, 282-289.

Siveke, J. T., Einwachter, H., Sipos, B.*, et al.* (2007). Concomitant pancreatic activation of Kras(G12D) and Tgfa results in cystic papillary neoplasms reminiscent of human IPMN. Cancer Cell *12*, 266-279.

Soto, J. L., Barbera, V. M., Saceda, M.*, et al.* (2006). Molecular biology of exocrine pancreatic cancer. Clin Transl Oncol *8*, 306-312.

Stanger, B. Z., Stiles, B., Lauwers, G. Y.*, et al.* (2005). Pten constrains centroacinar cell expansion and malignant transformation in the pancreas. Cancer Cell *8*, 185-195.

Swiatek, P. J., Lindsell, C. E., del Amo, F. F., *et al.* (1994). Notch1 is essential for postimplantation development in mice. Genes Dev *8*, 707-719.

Tamura, K., Taniguchi, Y., Minoguchi, S., *et al.* (1995). Physical interaction between a novel domain of the receptor Notch and the transcription factor RBP-J kappa/Su(H). Curr Biol *5*, 1416-1423.

Thayer, S. P., di Magliano, M. P., Heiser, P. W., *et al.* (2003). Hedgehog is an early and late mediator of pancreatic cancer tumorigenesis. Nature *425*, 851-856.

Thiery, J. P., and Sleeman, J. P. (2006). Complex networks orchestrate epithelial-mesenchymal transitions. Nat Rev Mol Cell Biol *7*, 131-142.

Tinder, T. L., Subramani, D. B., Basu, G. D., *et al.* (2008). MUC1 enhances tumor progression and contributes toward immunosuppression in a mouse model of spontaneous pancreatic adenocarcinoma. J Immunol *181*, 3116-3125.

Truty, M. J., and Urrutia, R. (2007). Basics of TGF-beta and pancreatic cancer. Pancreatology *7*, 423-435.

Tuveson, D. A., Zhu, L., Gopinathan, A., *et al.* (2006). Mist1-KrasG12D knock-in mice develop mixed differentiation metastatic exocrine pancreatic carcinoma and hepatocellular carcinoma. Cancer Res *66*, 242-247.

Van Dyke, T., and Jacks, T. (2002). Cancer modeling in the modern era: progress and challenges. Cell *108*, 135-144.

van Es, J. H., van Gijn, M. E., Riccio, O., *et al.* (2005). Notch/gamma-secretase inhibition turns proliferative cells in intestinal crypts and adenomas into goblet cells. Nature *435*, 959-963.

Wagner, M., Greten, F. R., Weber, C. K., *et al.* (2001). A murine tumor progression model for pancreatic cancer recapitulating the genetic alterations of the human disease. Genes Dev *15*, 286-293.

Weng, A. P., Millholland, J. M., Yashiro-Ohtani, Y., *et al.* (2006). c-Myc is an important direct target of Notch1 in T-cell acute lymphoblastic leukemia/lymphoma. Genes Dev *20*, 2096-2109.

Wharton, K. A., Johansen, K. M., Xu, T., *et al.* (1985). Nucleotide sequence from the neurogenic locus notch implies a gene product that shares homology with proteins containing EGF-like repeats. Cell *43*, 567-581.

Wright, T. R. (1970). The genetics of embryogenesis in Drosophila. Adv Genet *15*, 261-395.

Xue, Y., Gao, X., Lindsell, C. E., *et al.* (1999). Embryonic lethality and vascular defects in mice lacking the Notch ligand Jagged1. Hum Mol Genet *8*, 723-730.

Yochem, J., Weston, K., and Greenwald, I. (1988). The Caenorhabditis elegans lin-12 gene encodes a transmembrane protein with overall similarity to Drosophila Notch. Nature *335*, 547-550.

Zavadil, J., Cermak, L., Soto-Nieves, N., *et al.* (2004). Integration of TGF-beta/Smad and Jagged1/Notch signalling in epithelial-to-mesenchymal transition. EMBO J *23*, 1155-1165.

Chapter 2: Notch2 is required for PanIN progression and development of pancreatic ductal adenocarcinoma

This chapter is based on the original work published in *Proc Natl Acad Sci U S A*, July 2010, vol. 107, issue 30. The essential background and most important results are presented in this chapter whereas the full-submitted manuscript is attached as Appendix 1. The paper is reproduced with the publisher's permission.

Abstract

Notch signaling has been implicated in tumor development including pancreatic cancer. Here, we demonstrate the effect of pancreas-specific Notch receptor ablation in oncogenic *Kras^{G12D}*-driven carcinogenesis. We show that inactivation of Notch2 but not Notch1 leads to an increased survival, a progression stop at the PanIN1 level, and increased development of mucinous cystic neoplasms (MCN). Malignant transformation occurred late with a shift in tumor cell differentiation towards anaplastic and sarcomatoid cancers with an increased rate of epithelial-mesenchymal transition. By expression profiling, we identified that Myc is regulated by Notch2 with Notch2 transcriptionally regulating Myc expression through binding to the Myc promoter. Ablation of Myc in *Kras^{G12D}*-induced pancreata recapitulated the phenotype of Notch2-deficient mice. Our data place Notch2 at a central position during PanIN progression and malignant transformation through modulation of Myc signaling and epithelial-mesenchymal transition.

Introduction

Pancreatic ductal adenocarcinoma (PDAC) remains one of the most lethal human malignancies. PDAC characteristics go along with a growing number of evidence supporting the cancer stem cell concept in pancreatic cancer (Li et al., 2007, Hermann et al., 2007). In addition to the identification of pancreatic cancer cells with putative stem cell abilities, activation of embryonically active pathways such as Hedgehog, Wnt and Notch signaling has been reported in preneoplastic lesions and PDAC (Pasca di Magliano et al., 2007, Siveke et al., 2007, Pasca di Magliano et al., 2006, Stanger et al., 2005, Miyamoto et al., 2003, Thayer et al., 2003). In the adult pancreas, Notch signaling is activated after acute pancreatitis (see Chapter 4) and in carcinogenesis. In three different murine models of pancreatic cancer, the *Ela-Tgfa;p53KO* model, the conditional *Kras^{G12D}*-based models and the conditional *PtenKO* model, expression of HES1 (Nocth-target) was increased pointing to an important role of Notch signaling activation early during tumor initiation (Miyamoto et al., 2003, Stanger et al., 2005, Hingorani et al., 2003). Recent work has shown that ectopic activation of Notch signaling *in vivo* promotes PanIN initiation and progression (De La et al., 2008), while chemical inhibition using γ-secretase inhibitor effectively block development of PDAC from PanIN lesions in a *Kras;p53$^{+/lox}$* mouse model (Plentz et al., 2009).

Here, we describe the effect of conditional Notch1 and Notch2 ablation in *Kras^{G12D}*-driven pancreatic carcinogenesis. This study takes advantage of the non-essential role of Notch1 and Notch2 during pancreatogenesis, see Chapter 5. We show that ablation of Notch1 has no critical effect on the development of preneoplastic lesions and invasive and metastatic PDAC. Ablation of Notch2 however, leads to an abrogation of PanIN progression, the development of MCNs and a late induction of undifferentiated and anaplastic tumors. Consequently, Notch2 knockout mice have a prolonged survival compared to Notch2 wildtype *Kras^{G12D}* mice. Molecular analysis revealed a regulatory role of Notch2 in Myc signaling with Myc-deficient mice showing a similar phenotype. These data point to a central role of Notch2-Myc regulation of preneoplastic PanIN progression and tumor differentiation.

Results

Notch1 and Notch2 are expressed in different compartments in adult pancreata; Notch2 is activated in Kras-induced tumorigenesis

Using quantitative RT-PCR we found that of all Notch receptors, Notch1 and Notch2 were predominantly expressed in the 9-week old pancreas. Moreover, the tumor inducing *Kras^{G12D}* mutation lead over time to an increased expression of *Notch2* and the Notch target gene *Hes1*, whereas *Notch1* transcript levels dropped (Fig. 2.1A, B), similarly to previous reports (Miyamoto et al., 2003). Using transgenic *Notch1-GFP* and *Notch2^{lacZ}* reporter mice (Lewis et al., 1998, Hamada et al., 1999) we analyzed the Notch1 and Notch2 expression pattern. In wildtype pancreata, we found X-Gal as a surrogate for Notch2 expression in ductal but not acinar or islet cells and in centroacinar cell position thought to be the progenitor cell compartment. In *Kras^{G12D}* mice, Notch2 expression was detectable in PanIN lesions and was found throughout the carcinogenic process and in the surrounding stroma (Fig. 2.1C). Notch1 expression, on the other hand, was found in normal acinar cells as previously described (Chapter 4), but was hardly ever detectable in PanIN lesions (Fig. 2.1C).

In summary, these expression data are consistent with Notch2 as the predominantly expressed Notch receptor in ductal and potentially centroacinar cells and in PanIN lesions as suggested previously (Miyamoto et al., 2003).

PanIN development and progression in Notch-ablated pancreata

To study the role of Notch in pancreatic carcinogenesis, we crossed conditional Notch1 and Notch2 knockout mice and Kras$^{+/LSL\text{-}G12D}$ (Radtke et al., 1999, Besseyrias et al., 2007, Hingorani et al., 2003) with Ptf1a$^{+/Cre(ex1)}$ mice (Nakhai et al., 2007) for generation of *Ptf1a$^{+/Cre(ex1)}$; Kras$^{+/LSL\text{-}G12D}$; Notch1$^{lox/lox}$* (*Kras;N1ko*) and *Ptf1a$^{+/Cre(ex1)}$; Kras$^{+/LSL\text{-}G12D}$; Notch2$^{lox/lox}$* (*Kras;N2ko*).

Kras and *Kras;N1ko* mice share a similar tumorigenesis process through the previously described pattern of PanIN lesions progression (Hingorani et al., 2003). *Kras;N2ko* mice however, developed almost no PanIN2 and -3 lesions but an increased amount of cystic lesions at 9 months of age (Fig. 2.1D, E), suggesting that Notch2 may be involved in PanIN progression.

Development of MCN-like lesions in Kras;N2ko mice

Kras;N2ko mice starting at about 9 months of age, often develop soft abdominal masses due to the development of moderate to very large multilocular cysts in

the splenic part of the pancreas (Fig. 2.2A). Histologically, most of these cysts showed a mucinous columnar epithelium, and low or no dysplasia (Fig. 2.2B). Seldom, goblet cells, high-grade dysplasia and invasion into the adjacent stroma were noted suggesting that these lesions may resemble mucinous cystic neoplasms (MCN). Further characterization revealed that these lesions express various markers found in human MCNs including ovarian-like type of stroma surrounding the cystic lesions with ER^+ and PR^+ nuclei (Fig. 2.2B).

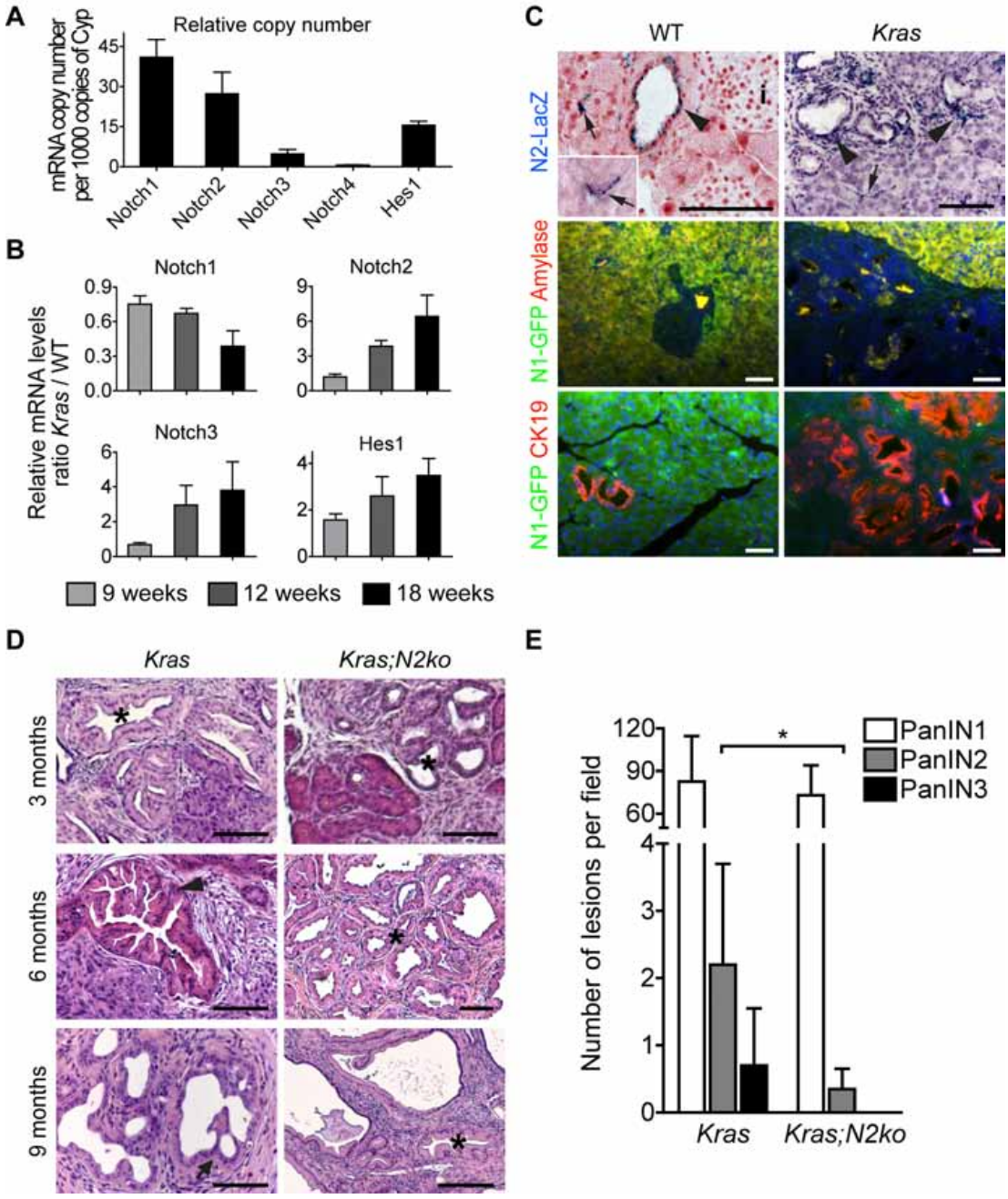

Figure 2.1. Expression analysis of Notch receptors in pancreata of wildtype vs. *Kras*^{G12D}-induced mice and PanIN lesion development in *Kras* vs. *Kras;N2ko* mice (detail description in text).

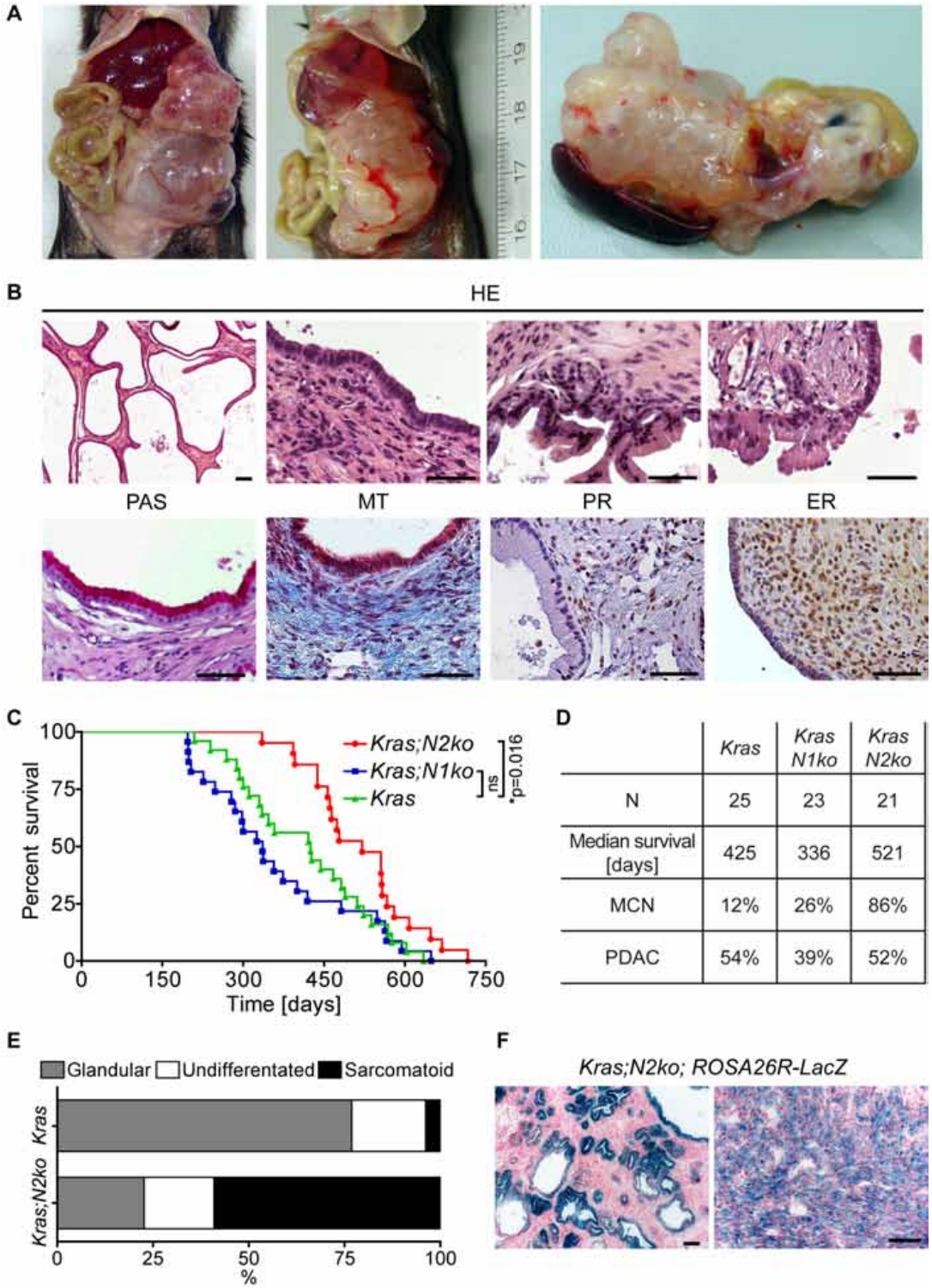

	Kras	Kras N1ko	Kras N2ko
N	25	23	21
Median survival [days]	425	336	521
MCN	12%	26%	86%
PDAC	54%	39%	52%

Figure 2.2. *Kras;N2ko* mice develop invasive and metastatic PDAC with a significant delay compared to *Kras* mice (detailed description in text).

Tumor development is different in Kras;N1ko and Kras;N2ko mice

For analysis of PDAC development and survival, a cohort of mice was followed until development of tumor-associated signs of disease or death. *Kras* and *Kras;N1ko* mice developed invasive PDAC with similar characteristics regarding age of tumor development, tumor differentiation, invasiveness and rate as well assites of metastasis (for details see the paper in Appendix 1).

However, *Kras;N2ko* mice had a largely altered carcinogenic process. These mice survived significantly longer than *Kras* and *Kras;N1ko* mice and only very rarely developed PDAC with ductal differentiation (Fig. 2.2C-E). Instead, *Kras;N2ko* mice either died without development of PDAC or developed highly aggressive anaplastic and sarcomatoid tumors at advanced age (Fig. 2.2D, E). Positive X-gal staining of these tumors proved their origin from a Notch2-ablated pancreatic precursor cell (Fig. 2.2F). *Kras;N2ko* PDAC often metastasize reconstituting undifferentiated cancer sometimes with MCN-like lesions (Appendix 1).

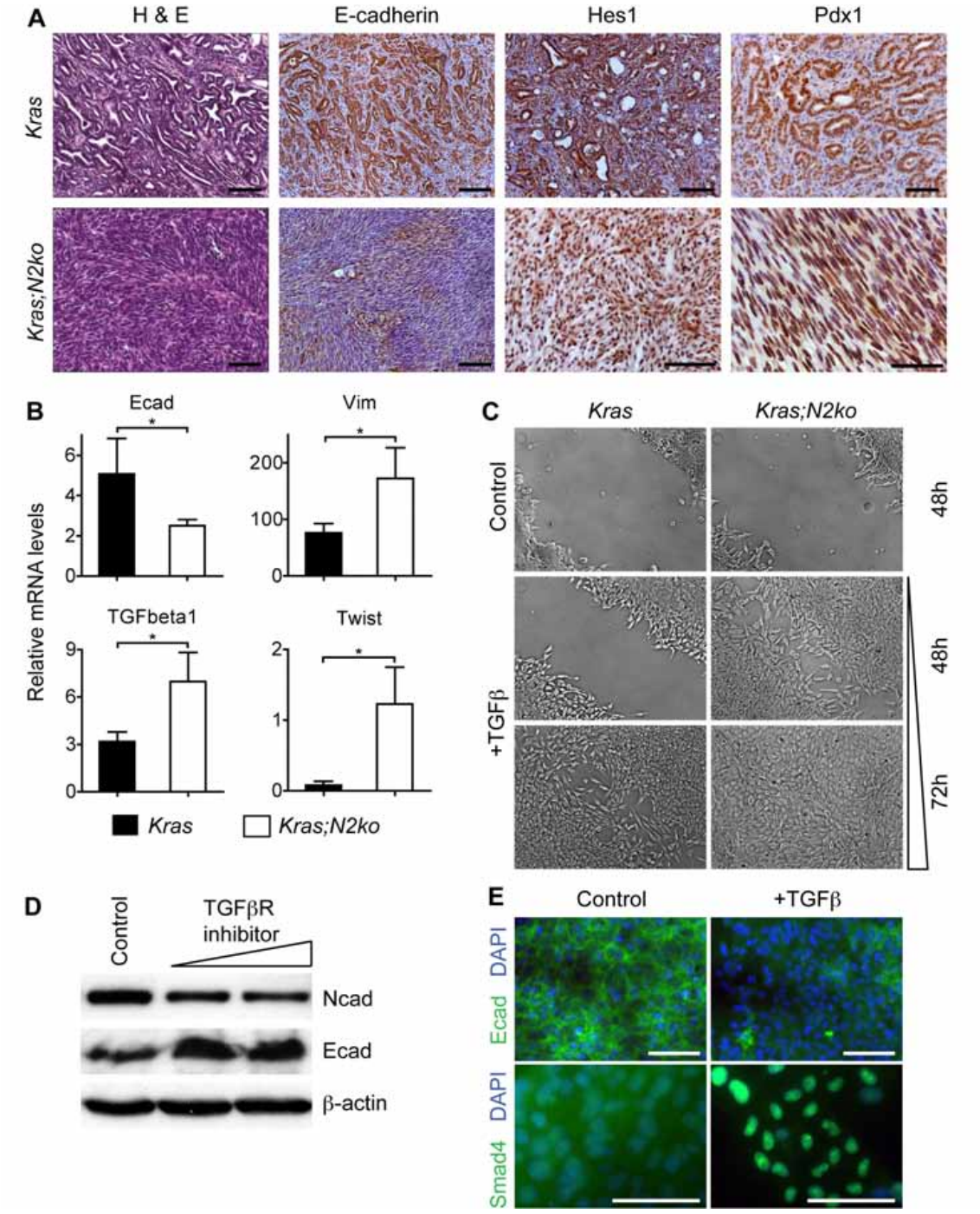

Figure 2.3. Epithelial-to-mesenchymal transition is a prominent feature in *Kras;N2ko* tumors and tumor-derived primary cell cultures (description in text).

Anaplastic/sarcomatoid Kras;N2ko PDAC have distinct molecular properties

Histologically *Kras;N2ko* tumors were very large, showing a sarcomatoid cell pattern with a high proliferative index (Fig. 2.3A). While we also observed areas within the tumors that displayed low differentiation, we practically never observed PDAC with high or moderate differentiation. All sarcomatoid tumors expressed PDX1 pointing to their pancreatic origin. Surprisingly, many cells expressed HES1, suggesting that its expression was not stopped by Notch2 ablation (Fig. 2.3A). To determine whether ablation of Notch2 led to upregulation of other Notch receptors, we tested isolated and cultivated cancer cells from *Kras* and *Kras;N2ko* PDAC and did not detect a consistent compensatory pattern.

Kras;N2ko cancers expressed low or no E-cadherin. Consistent with this, we found downregulation of E-cadherin and increased levels of Twist, Snail and Slug as well as Vimentin and TGFβ1 on protein and mRNA levels in isolated tumor cells (Fig. 2.3B). These data suggest that tumors developing in *Kras;N2ko* mice have a high rate of epithelial-to-mesenchymal transition (EMT) compared with ductal PDAC from *Kras* mice (Fig. 2.3A, B). Wound healing assay indicated that *Kras;N2ko* cancer cells have also an increased motility that is in consistence with elevation of EMT. Interestingly, we could reverse the EMT process with a TGFβR inhibitor (Fig. 2.3D, E) that suggests EMT is driven by a TFGβ ligand modulation rather than downstream regulation (e.g. Notch regulation of Snail).

Similarly to human PDAC, we noted a high incidence of p16Ink4a loss/mutation or promoter hypermethylation in all three genotypes. Somewhat surprisingly, we only rarely detected mutations in the p53 gene however, at the same time a significantly higher rate of chromosomal instability compared to *Kras* or *Kras;N1ko* cell lines was noted. Additionally, we found frequent loss of the wildtype *Kras* allele in *Kras;N2ko* mice, featured seldom in *Kras* and *Kras;N1ko* mice. Analyzing KRAS protein activation using a RAS activity immunoprecipitation showed a reduction in *Kras;N2ko* vs. *Kras* cells. However, analysis of phospho-EGFR and Ras-dependent pathways did not reveal significant differences between *Kras* and *Kras;N2ko* mice in cancer cell lines or at 7-day pancreata (for details see Appendix 1)

Deficiency of Notch2 leads to modulation of Myc signaling

Investigated molecular properties of the cell lines did not explain the observed oncogenic role of Notch2 during carcinogenesis, which we hypothesized to be a block in PanIN progression. For a screening approach we performed microarray-based Gene Set Enrichment Analysis (GSEA) on a set of 984 signatures derived from the GSEA signature library. We found a significant enrichment of various TGFβ signatures in *Kras;N2ko* cells, supporting our findings of alterated TGFβ signaling in *Kras;N2ko* PDAC. However, we also noted a highly significant enrichment of several MYC signatures in *Kras* cancer cells and in preneoplastic pancreatic tissue suggesting that Notch2 modulates MYC signaling (Fig. 2.4A-C and Appendix 1). Since deregulation of MYC signaling is known to occur in many tumor types we verify MYC relevance in our model. Indeed, we found an increased expression of MYC in PanIN lesions as well as increasing mRNA levels in $Kras^{G12D}$-induced precancerous pancreata (Fig. 2.4D, E). We next examined MYC protein and mRNA expression in isolated *Kras* and *Kras;N2ko* cancer cells and found reduced levels in *Kras;N2ko* cells (Fig. 2.4G). Additionally, strong MYC

staining was detected in ductal PDAC of *Kras* mice whereas sarcomatoid *Kras;N2ko*-derived cancers revealed a low expression (Fig. 2.4F), suggesting that *Myc* expression is downregulated in Notch2-ablated pancreatic tumors.

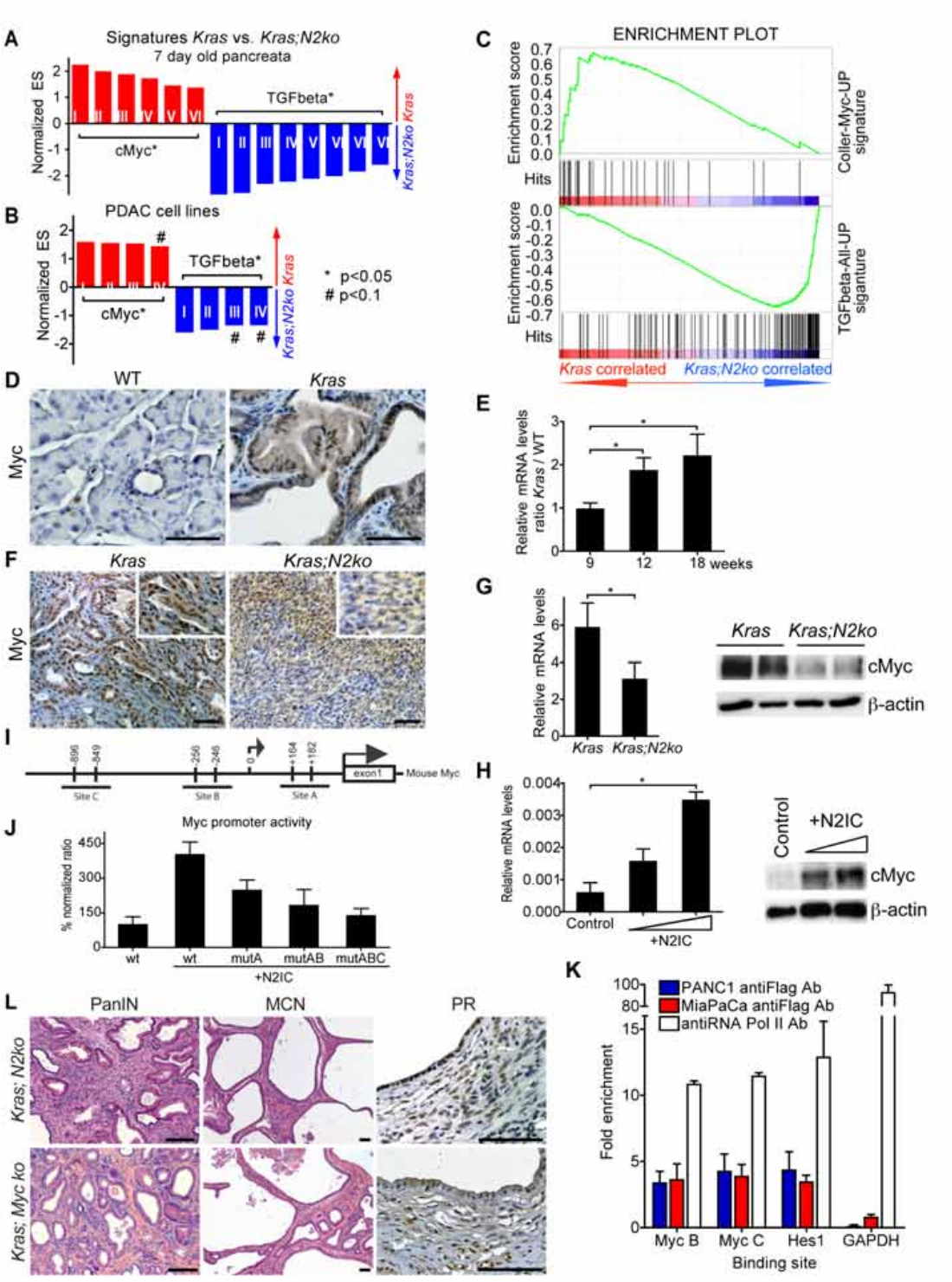

Figure 2.4. Myc is upregulated during pancreatic carcinogenesis and downregulated in *Kras;N2ko* mice. Myc is a downstream target of Notch and its ablation resembles features of the *Notch2*-deficient phenotype (detailed description in text).

To further analyze transcriptional regulation of *Myc*, we considered three Notch signaling binding sites in the *Myc* promoter (Fig. 2.4I). To test the relevance of each binding site, we transfected *Kras;N2ko* cancer cells with constitutively active Notch2 (N2IC) and luciferase reporter vectors with one, two or all three Notch sites mutated. As shown in Fig. 2.4K, all three regions seemed to be functional for transcriptional regulation. We next performed chromatin immunoprecipitation (ChIP) to further substantiate our finding. In the human pancreatic cancer cell lines MiaPaCa2 and Panc1, Notch2 binds to the *Myc* promoter. In fact, the three times increased *Myc* promoter occupation by Notch2 compared to non-specific IgG-binding was comparable to that of Notch2 binding to the *Hes1* promoter (Fig. 2.4J). Additionally, we observed an increase of Myc mRNA and protein expression in *Kras;N2ko* and Panc1 cells with forced expression of N2IC, which suggests transcriptional regulation of MYC by Notch2 (Fig. 2.4H)

To provide further evidence for a major role of MYC signaling in pancreatic carcinogenesis, we interbred previously described $Myc^{lox/lox}$ conditional knockout mice (Nakhai et al., 2008) with $Pdx1\text{-}Cre;Kras^{+/LSL\text{-}G12D}$ mice (*Kras;MycKO*). Intriguingly, preliminary analysis of two mice 11 and 12 months of age showed a similar phenotype as *Kras;N2ko* mice with development of MCN-like lesions with an ovarian-like stroma (Fig. 2.4L and data not shown). More importantly however, only PanIN1 but not higher grade lesions were observed strongly supporting our hypothesis of Myc signaling as an essential cornerstone of PanIN progression.

Discussion

In this study, we show that loss of Notch1 has no apparent effect on the course of PanIN progression, development of PDAC, tumor differentiation and survival. Ablation of Notch2 however, was found to inhibit PanIN progression and PDAC development and changed the differentiation of late-appearing pancreatic cancer to an undifferentiated and sarcomatoid phenotype.

Notch signaling activation in pancreatic carcinogenesis

The Notch signaling pathway plays a pivotal role in cell fate and differentiation decisions and its activation early in the carcinogenic process suggests a role in the cellular transformation under oncogenic stress. While the cell of origin issue in pancreatic cancer has not been decisively answered, activation of Notch signaling early during PanIN initiation probably presents a pivotal step for transformation. In a recent study using the $Kras^{G12D}$; $p53^{+/-}$ model, Notch signaling was found to be active in PDAC precursors and advanced tumors (Plentz et al., 2009). Notably, inhibition of Notch activation through use of a γ-secretase inhibitor (GSI) completely blocked tumor progression in vivo, supporting the central role of active Notch in tumor progression. Conversely, the synergistic PanIN-promoting effect of Notch activation in $Kras^{G12D}$-driven PanIN development has been recently reported (De La et al., 2008).

While observed inhibition of PanIN progression in Notch2-ablated pancreata goes along with the results of suppressed Notch signaling through GSI treatment (Plentz et al., 2009), some differences are notable. The authors found a relative high increase of *Notch3* mRNA in duct cells and PDAC. Although we also found an

increase in expression of *Notch3* in precancerous pancreas compared to wildtype pancreata, we only found very low copy numbers for *Notch3* compared to those of *Notch1* and *Notch2*. Reasons for these differences may include analysis of different tissue samples, whole pancreatic tissue in our study vs. isolated cells by Plentz and coworkers, and usage of different mouse models. In cancer cells isolated from PDAC of *Kras* mice however, we also found much lower mRNA and protein levels of Notch3 compared to Notch2. In fact, Notch2 was by far the most prominently expressed Notch receptor, a finding supported by earlier studies (Miyamoto et al., 2003). Importantly, we found that Notch2-loss has not led to any compensation by any other Notch receptor. Interestingly, we did not observe loss of HES1 expression in either Notch1- or Notch2-ablated pancreata suggesting that *Hes1* may still be activated by other Notch receptors or additional signaling pathways as previously suggested (Chapter 5).

Kras;N2ko mice develop MCN-like lesions and undifferentiated PDAC

The inability of Notch2-deficient $Kras^{G12D}$-mutated pancreatic cells to progress through the PanIN process and to form moderately and well differentiated PDAC goes along with a longer survival of these mice. Eventually, these mice develop large cysts resembling MCNs and succumb from either pancreatic insufficiency or from the development of undifferentiated and sarcomatoid pancreatic cancer. Since PanIN progression is blocked, development of MCN-like lesions may be a bypass route for pancreatic cells exposed to oncogenic stress. Interestingly, an association of sarcomatoid PDAC and MCN has been repeatedly described in patients (Hakamada et al., 2008, Pan and Wang, 2007, van den Berg et al., 2000, Wenig et al., 1997). Characterization of human MCN showed common overexpression of *Myc* and *Hes1*, which seems contradictory to our findings (Fukushima et al., 2004). In addition, we did not observe mutations or loss of the Smad4 gene, characteristic for PDAC arising from MCN (Izeradjene et al., 2007).
The very late occurrence and high incidence of LOH of the wildtype Kras allele in *Kras;N2ko* PDAC supports a model of deficient Notch2 and/or MYC signaling as an inhibitor of cancer progression. Further analysis will be required to understand the cellular and molecular cues in Notch2-deficient malignant transformation. Thus, whether the MCN-like lesions encountered in this specific setting truly relate to human MCN pathogenesis remains unclear.

TGFβ and MYC signaling in pancreatic cancer

Molecular characterization of the anaplastic and sarcomatoid PDAC in *Kras;N2ko* mice showed evidence for an EMT. Several reports have described an activating role of increased Notch signaling on the acquisition of an EMT phenotype by regulation of repressors such as Snail or interaction with TGFβ signaling (Wang et al., 2009, Sahlgren et al., 2008, Timmerman et al., 2004, Zavadil et al., 2004). TGFβ is known to play an ambivalent role in cancer biology (see Chapter 1). In the pancreas, conditional inactivation of *Tgfβr2* led to an accelerated development and progression of well-differentiated PDAC (Ijichi et al., 2006). Thus, the development of sarcomatoid PDAC is compatible with increased TGFβ signaling. The late appearance of tumors however argues against an oncogenic role of TGFβ in our model. In addition, the effect of TGFβR inhibition suggests an intact TGFβ signaling axis arguing for a non-essential role of Notch2 on TGFβ signaling and EMT regulation. Indirect regulation of TGFβ may be through

alternated MYC signaling, which is known to suppress the activation of TGFβ - induced genes e.g. p21CIP1 (Wu et al., 2003). Interestingly, p21CIP1 has recently been described as regulator of RAS- and MYC-dependent EMT in breast cancer that also interact with Notch in various organs (Liu et al., 2009, Rangarajan et al., 2001). However, we could not detect consistent differences in *p21* expression or signatures between *Kras* and *Kras;N2ko* tumors.

Decreased MYC signaling in Notch2-ablated pancreatic cancer supports the hypothesis of MYC as a key regulator of the carcinogenic process in the pancreas. Deregulation of MYC in PDAC has been described and amplification with gains of chromosome 8q occurs in about 30% of PDAC (Schleger et al., 2000, Schleger et al., 2002, Schreiner et al., 2003, Bardeesy et al., 2006). Interestingly, amplification is a typical event detectable already in precursor lesions suggesting that MYC has an important role in the preneoplastic carcinogenic process (Schleger et al., 2002). In a recent quantitative proteomic screen of peneoplastic PanIN lesions, MYC expression was identified in PanIN3 lesions (Pan et al., 2009). Notably, network analysis predicted MYC as the most important regulatory protein in this screen.

We and others have previously characterized the important role of MYC in progenitor and acinar cell proliferation during pancreas development and homeostasis (Bonal et al., 2009, Nakhai et al., 2008, Strom et al., 2007). Consistently, we found an increased MYC expression throughout the development of PanIN lesions in *Kras* mice, suggesting that MYC-dependent gene regulation plays a role during preneoplastic progression. It is tempting to speculate that MYC and RAS signaling cooperatively promote tumor progression in a setting of active Notch. Notch signaling has been reported to cooperate with RAS (Weijzen et al., 2002) and several studies have reported direct transcriptional regulation of *Myc* by Notch1 (Klinakis et al., 2006, Palomero et al., 2006, Sharma et al., 2006, Weng et al., 2006, Satoh et al., 2004). Our finding that active Notch2 induces *Myc* expression in pancreatic cancer cells supports these reports, placing Notch as an important regulator of Myc signaling during carcinogenesis in pancreatic cancer. While still preliminary, the phenotypic similarities of Notch2 and Myc-ablated $Kras^{G12D}$-induced pancreata with development of cystic lesions and a PanIN progression blockage strongly support this hypothesis.

Previously reported success of using Notch inhibitors to prevent tumor formation (Plentz et al., 2009) is now supported by our results. Of note, the same group has reported *Myc* amplification in $Kras^{G12D}$-driven PDAC mouse models adding evidence for an important role of this signaling pathway during the carcinogenic process. It will be of high interest to study the integration of the transcriptional programs regulated by Myc and Notch signaling respectively in further detail, which may eventually help explain the permissive signals regulating pancreatic plasticity and malignant transformation.

Experimental procedures

Detailed description of experimental procedures in Appendix 1.

Mouse strains

Kras$^{+/LSL\text{-}G12D}$, *Notch1*$^{lox/lox}$, *Notch2* $^{lox/lox}$, *Myc* $^{lox/lox}$, *Ptf1a*$^{+/Cre}$, *Pdx1-Cre* and Rosa26$^{+/LSL\text{-}lacZ}$ mice have been described before (Hingorani et al., 2003, Radtke et al., 1999, Besseyrias et al., 2007, Nakhai et al., 2008, Nakhai et al., 2007, Gu et al., 2003, Soriano, 1999). Animals had mixed C57BL/6;129SV background.

Affymetrix gene chip analysis and GSEA

For Microarray analysis 7-day old pancreata of two to four mice and six PDAC low-passage cultured cell lines from *Kras* and *Kras;N2ko* PDAC were used. Mouse expression gene chip arrays (Affymetrix Mouse Genome 430A 2.0 Array) were used according to Affymetrix protocols. Gene chips were scanned and analyzed using Affymetrix Microarray Suite 5.0 software (MAS 5.0). GSEA software was provided by the Broad Institute of MIT and Harvard (http://www.broad.mit.edu/gsea/), (Subramanian et al., 2005). For analysis we used the default parameters (number of permutations =1000).

Disclosure

Pawel K. Mazur participation in the publication included: designing and performing the experiments, analysis of data, writing the manuscript.

References

Bardeesy, N., Aguirre, A. J., Chu, G. C.*, et al.* (2006). Both p16(Ink4a) and the p19(Arf)-p53 pathway constrain progression of pancreatic adenocarcinoma in the mouse. Proc Natl Acad Sci U S A *103*, 5947-5952.

Besseyrias, V., Fiorini, E., Strobl, L. J.*, et al.* (2007). Hierarchy of Notch-Delta interactions promoting T cell lineage commitment and maturation. J Exp Med *204*, 331-343.

Bonal, C., Thorel, F., Ait-Lounis, A.*, et al.* (2009). Pancreatic inactivation of c-Myc decreases acinar mass and transdifferentiates acinar cells into adipocytes in mice. Gastroenterology *136*, 309-319 e309.

De La, O. J., Emerson, L. L., Goodman, J. L.*, et al.* (2008). Notch and Kras reprogram pancreatic acinar cells to ductal intraepithelial neoplasia. Proc Natl Acad Sci U S A *105*, 18907-18912.

Fukushima, N., Sato, N., Prasad, N.*, et al.* (2004). Characterization of gene expression in mucinous cystic neoplasms of the pancreas using oligonucleotide microarrays. Oncogene *23*, 9042-9051.

Gu, G., Brown, J. R., and Melton, D. A. (2003). Direct lineage tracing reveals the ontogeny of pancreatic cell fates during mouse embryogenesis. Mech Dev *120*, 35-43.

Hakamada, K., Miura, T., Kimura, A.*, et al.* (2008). Anaplastic carcinoma associated with a mucinous cystic neoplasm of the pancreas during pregnancy: report of a case and a review of the literature. World J Gastroenterol *14*, 132-135.

Hamada, Y., Kadokawa, Y., Okabe, M.*, et al.* (1999). Mutation in ankyrin repeats of the mouse Notch2 gene induces early embryonic lethality. Development *126*, 3415-3424.

Hermann, P. C., Huber, S. L., Herrler, T., *et al.* (2007). Distinct populations of cancer stem cells determine tumor growth and metastatic activity in human pancreatic cancer. Cell Stem Cell *1*, 313-323.

Hingorani, S. R., Petricoin, E. F., Maitra, A., *et al.* (2003). Preinvasive and invasive ductal pancreatic cancer and its early detection in the mouse. Cancer Cell *4*, 437-450.

Ijichi, H., Chytil, A., Gorska, A. E., *et al.* (2006). Aggressive pancreatic ductal adenocarcinoma in mice caused by pancreas-specific blockade of transforming growth factor-beta signaling in cooperation with active Kras expression. Genes Dev *20*, 3147-3160.

Izeradjene, K., Combs, C., Best, M., *et al.* (2007). Kras(G12D) and Smad4/Dpc4 haploinsufficiency cooperate to induce mucinous cystic neoplasms and invasive adenocarcinoma of the pancreas. Cancer Cell *11*, 229-243.

Klinakis, A., Szabolcs, M., Politi, K., *et al.* (2006). Myc is a Notch1 transcriptional target and a requisite for Notch1-induced mammary tumorigenesis in mice. Proc Natl Acad Sci U S A *103*, 9262-9267.

Lewis, A. K., Frantz, G. D., Carpenter, D. A., *et al.* (1998). Distinct expression patterns of notch family receptors and ligands during development of the mammalian inner ear. Mech Dev *78*, 159-163.

Li, C., Heidt, D. G., Dalerba, P., *et al.* (2007). Identification of pancreatic cancer stem cells. Cancer Res *67*, 1030-1037.

Liu, M., Casimiro, M. C., Wang, C., *et al.* (2009). p21CIP1 attenuates Ras- and c-Myc-dependent breast tumor epithelial mesenchymal transition and cancer stem cell-like gene expression in vivo. Proc Natl Acad Sci U S A *106*, 19035-19039.

Miyamoto, Y., Maitra, A., Ghosh, B., *et al.* (2003). Notch mediates TGF alpha-induced changes in epithelial differentiation during pancreatic tumorigenesis. Cancer Cell *3*, 565-576.

Nakhai, H., Sel, S., Favor, J., *et al.* (2007). Ptf1a is essential for the differentiation of GABAergic and glycinergic amacrine cells and horizontal cells in the mouse retina. Development *134*, 1151-1160.

Nakhai, H., Siveke, J. T., Mendoza-Torres, L., *et al.* (2008). Conditional inactivation of Myc impairs development of the exocrine pancreas. Development *135*, 3191-3196.

Palomero, T., Lim, W. K., Odom, D. T., *et al.* (2006). NOTCH1 directly regulates c-MYC and activates a feed-forward-loop transcriptional network promoting leukemic cell growth. Proc Natl Acad Sci U S A *103*, 18261-18266.

Pan, S., Chen, R., Reimel, B. A., *et al.* (2009). Quantitative proteomics investigation of pancreatic intraepithelial neoplasia. Electrophoresis *30*, 1132-1144.

Pan, Z. G., and Wang, B. (2007). Anaplastic carcinoma of the pancreas associated with a mucinous cystic adenocarcinoma. A case report and review of the literature. JOP *8*, 775-782.

Pasca di Magliano, M., Biankin, A. V., Heiser, P. W., *et al.* (2007). Common activation of canonical Wnt signaling in pancreatic adenocarcinoma. PLoS One *2*, e1155.

Pasca di Magliano, M., Sekine, S., Ermilov, A., *et al.* (2006). Hedgehog/Ras interactions regulate early stages of pancreatic cancer. Genes Dev *20*, 3161-3173.

Plentz, R., Park, J. S., Rhim, A. D., *et al.* (2009). Inhibition of gamma-secretase activity inhibits tumor progression in a mouse model of pancreatic ductal adenocarcinoma. Gastroenterology *136*, 1741-1749 e1746.

Radtke, F., Wilson, A., Stark, G., *et al.* (1999). Deficient T cell fate specification in mice with an induced inactivation of Notch1. Immunity *10*, 547-558.

Rangarajan, A., Talora, C., Okuyama, R., *et al.* (2001). Notch signaling is a direct determinant of keratinocyte growth arrest and entry into differentiation. EMBO J *20*, 3427-3436.

Sahlgren, C., Gustafsson, M. V., Jin, S., *et al.* (2008). Notch signaling mediates hypoxia-induced tumor cell migration and invasion. Proc Natl Acad Sci U S A *105*, 6392-6397.

Satoh, Y., Matsumura, I., Tanaka, H., *et al.* (2004). Roles for c-Myc in self-renewal of hematopoietic stem cells. J Biol Chem *279*, 24986-24993.

Schleger, C., Arens, N., Zentgraf, H., *et al.* (2000). Identification of frequent chromosomal aberrations in ductal adenocarcinoma of the pancreas by comparative genomic hybridization (CGH). J Pathol *191*, 27-32.

Schleger, C., Verbeke, C., Hildenbrand, R., *et al.* (2002). c-MYC activation in primary and metastatic ductal adenocarcinoma of the pancreas: incidence, mechanisms, and clinical significance. Mod Pathol *15*, 462-469.

Schreiner, B., Greten, F. R., Baur, D. M., *et al.* (2003). Murine pancreatic tumor cell line TD2 bears the characteristic pattern of genetic changes with two independently amplified gene loci. Oncogene *22*, 6802-6809.

Sharma, V. M., Calvo, J. A., Draheim, K. M., *et al.* (2006). Notch1 contributes to mouse T-cell leukemia by directly inducing the expression of c-myc. Mol Cell Biol *26*, 8022-8031.

Siveke, J. T., Einwachter, H., Sipos, B., *et al.* (2007). Concomitant pancreatic activation of Kras(G12D) and Tgfa results in cystic papillary neoplasms reminiscent of human IPMN. Cancer Cell *12*, 266-279.

Soriano, P. (1999). Generalized lacZ expression with the ROSA26 Cre reporter strain. Nat Genet *21*, 70-71.

Stanger, B. Z., Stiles, B., Lauwers, G. Y., *et al.* (2005). Pten constrains centroacinar cell expansion and malignant transformation in the pancreas. Cancer Cell *8*, 185-195.

Strom, A., Bonal, C., Ashery-Padan, R., *et al.* (2007). Unique mechanisms of growth regulation and tumor suppression upon Apc inactivation in the pancreas. Development *134*, 2719-2725.

Subramanian, A., Tamayo, P., Mootha, V. K., *et al.* (2005). Gene set enrichment analysis: a knowledge-based approach for interpreting genome-wide expression profiles. Proc Natl Acad Sci U S A *102*, 15545-15550.

Thayer, S. P., di Magliano, M. P., Heiser, P. W., *et al.* (2003). Hedgehog is an early and late mediator of pancreatic cancer tumorigenesis. Nature *425*, 851-856.

Timmerman, L. A., Grego-Bessa, J., Raya, A., *et al.* (2004). Notch promotes epithelial-mesenchymal transition during cardiac development and oncogenic transformation. Genes Dev *18*, 99-115.

van den Berg, W., Tascilar, M., Offerhaus, G. J., *et al.* (2000). Pancreatic mucinous cystic neoplasms with sarcomatous stroma: molecular evidence for monoclonal origin with subsequent divergence of the epithelial and sarcomatous components. Mod Pathol *13*, 86-91.

Wang, Z., Li, Y., Kong, D., *et al.* (2009). Acquisition of epithelial-mesenchymal transition phenotype of gemcitabine-resistant pancreatic cancer cells is linked with activation of the notch signaling pathway. Cancer Res *69*, 2400-2407.

Weijzen, S., Rizzo, P., Braid, M., *et al.* (2002). Activation of Notch-1 signaling maintains the neoplastic phenotype in human Ras-transformed cells. Nat Med *8*, 979-986.

Weng, A. P., Millholland, J. M., Yashiro-Ohtani, Y., *et al.* (2006). c-Myc is an important direct target of Notch1 in T-cell acute lymphoblastic leukemia/lymphoma. Genes Dev *20*, 2096-2109.

Wenig, B. M., Albores-Saavedra, J., Buetow, P. C., *et al.* (1997). Pancreatic mucinous cystic neoplasm with sarcomatous stroma: a report of three cases. Am J Surg Pathol *21*, 70-80.

Wu, S., Cetinkaya, C., Munoz-Alonso, M. J., *et al.* (2003). Myc represses differentiation-induced p21CIP1 expression via Miz-1-dependent interaction with the p21 core promoter. Oncogene *22*, 351-360.

Zavadil, J., Cermak, L., Soto-Nieves, N., *et al.* (2004). Integration of TGF-beta/Smad and Jagged1/Notch signalling in epithelial-to-mesenchymal transition. EMBO J *23*, 1155-1165.

Chapter 3: Pdx1 expression in the skin discloses different roles of Notch1 and Notch2 in murine KrasG12D-induced skin carcinogenesis in vivo

This chapter is based on the original work published in *PloS One*, October 2010, vol. 5, issue 10. The critical background and essential results are presented in this chapter whereas the full-published paper is attached as Appendix 2. The paper is reproduced with the publisher's permission.

Abstract

The Ras and Notch signaling pathways are frequently activated during development to control many diverse cellular processes and are often dysregulated during tumorigenesis. To study the role of Notch and oncogenic Kras signaling in a progenitor cell population, *Pdx1-Cre* mice were utilized to generate conditional oncogenic $Kras^{G12D}$ mice with ablation of *Notch1* and/or *Notch2*. Surprisingly, mice with activated $Kras^{G12D}$ and *Notch1* but not *Notch2* ablation developed skin papillomas progressing to squamous cell carcinoma providing evidence for *Pdx1* expression in the skin. Immunostaining and lineage tracing experiments indicate that PDX1 is present predominantly in the suprabasal layers of the epidermis and rarely in the basal layer. Further analysis of keratinocytes *in vitro* revealed differentiation-dependent expression of PDX1 in terminally differentiated keratinocytes. Our study revealed that loss of Notch1 but not Notch2 is critical for skin tumor development. Reasons for this include distinct Notch expression with Notch1 in all layers and Notch2 in the suprabasal layer as well as distinctive p21 and β-catenin signaling inhibition capabilities.

Introduction

Conditional tissue-specific modulation of genes using Cre/loxP recombination in genetically engineered mice provides an enormous leap forward to study gene function in detail yet requires detailed knowledge of gene regulation and expression patterns. For pancreatic targeting of genes, *Pdx1-Cre* mice are commonly used (Gannon et al., 2000; Gu et al., 2002; Hingorani et al., 2003), in which Cre-recombinase is expressed under a 4.5 to 5.5kb fragment of the *Pdx1* promoter. The transcription factor *Pdx1* (pancreas and duodenum homeobox gene 1) directs pancreatic cell formation, maintenance and function. *Pdx1* is expressed in the region of the endoderm that ultimately gives rise to stomach, pancreas and duodenum and its function is critical for posterior foregut development (Gannon et al., 2001). Postnatally, Pdx1 is mainly expressed in insulin-producing endocrine cells of the pancreas. Ablation of *Pdx1* results in defects of different cell types including malformations of the pylorus and duodenum, absence of Brunner's glands and reduced numbers of specific enteroendocrine cell types in the stomach and intestine. Loss of *Pdx1* function results in pancreatic agenesis, while heterozygous expression leads to defects in glucose homeostasis. *Pdx1*-deficient mice survive up to 6.5 days after birth, are severely dehydrated, have no fur and a delicate, cracking skin (Brissova et al., 2002; Jonsson et al., 1994; Larsson et al., 1996; Offield et al., 1996). Here, we

report epidermal PDX1 expression observed due to an unexpected skin tumor formation in *Pdx1-Cre* mice with activation of oncogenic *Kras^{G12D}* and loss of *Notch1* but not *Notch2.*

Notch receptors are expressed in the skin, although their precise functions remain uncertain (reviewed in Dotto, 2008; Lefort and Dotto, 2004). Gain- and loss-of-function studies have suggested various functions for Notch including proliferation control, differentiation switch of developing epidermis and formation of hair follicles (Demehri et al., 2009; Lin et al., 2000; Nicolas et al., 2003; Pan et al., 2004; Uyttendaele et al., 2004; Vauclair et al., 2005). Mice with epidermal loss of Notch1 as well as *Presenilin*-deficient mice develop epidermal hyperplasia and skin cancers (Nicolas et al., 2003; Xia et al., 2001). Of note, most studies have focused on Notch1 and downstream signaling members such as Rbpj or Hes1 (Blanpain et al., 2006; Moriyama et al., 2008). Very little is known about the function of Notch2 and other receptors in skin physiology and carcinogenesis. Here, we investigate the role of Notch1 and Notch2 using two different *Cre* expression systems. Our results provide evidence for different roles of Notch1 and Notch2 in skin development and carcinogenesis.

Results

Notch1 but not *Notch2* deletion increases susceptibility to *Kras^{G12D}* induced carcinogenesis in *Pdx1-Cre* mice

To analyze the effect of *Notch1* and *Notch2* deficiency during pancreas carcinogenesis, we crossed previously described *Pdx1-Cre* (Gu et al., 2002), *Notch1$^{fl/fl}$* (Radtke et al., 1999), *Notch2$^{fl/fl}$* (Besseyrias et al., 2007) and *Kras$^{+/LSL-G12D}$* (Hingorani et al., 2003) mice for generation of *Pdx1-Cre;Kras$^{+/LSL-G12D}$*, *Pdx1-Cre;Kras$^{+/LSL-G12D}$;Notch1$^{fl/fl}$* and *Pdx1-Cre*;*Kras$^{+/LSL-G12D}$*;*Notch2$^{fl/fl}$* mice (referred to as *Pdx1-Cre;Kras*, *Pdx1-Cre;Kras;N1ko* and *Pdx1-Cre;Kras;N2ko,* respectively). These mice were born at the expected Mendelian ratio and successful recombination of the floxed loci in the pancreas was confirmed by PCR (Fig. 3.1C). Surprisingly, *Pdx1-Cre;Kras;N1ko* mice developed focal skin hyperplasia at 10-15 days of age and as early as 4 weeks of age developed massive skin papillomas (Fig. 3.1D). These lesions and tumors showed recombination of the floxed loci (Fig. 3.1C) pointing to epidermal *Cre* expression, which was further corroborated using *Pdx1-Cre;Kras;N1ko;ROSA26R-LacZ* reporter mice (Fig. 3.1F), (Soriano, 1999). The penetrance of the skin papilloma development was 78%. In contrast, *Pdx1-Cre;Kras;N2ko* mice rarely developed any skin phenotype. However, double *Notch1* and *Notch2* knockout mice (*Pdx1-Cre;Kras;N1ko;N2ko)* featured an accelerated skin tumor formation (Fig. 3.1A and B) suggesting an essential role of Notch1 ablation in epidermal lesion development and a promoting role of Notch2 deletion. *Pdx1-Cre;Kras* mice manifested a skin phenotype with low penetrance, which has been observed previously (Hingorani et al., 2003; Hingorani et al., 2005). Most tumors encountered in *Pdx1-Cre;Kras;N1ko* mice were benign papillomas but often grew large and ulcerating, requiring euthanasia of animals for ethical reasons. Hence, the intended pancreatic carcinogenesis study was inconclusive (data not shown).

Pdx1-Cre;Kras;N1ko mice developed the following skin pathologies: squamous papillomas involving the ear, neck, lips, anal and vulvo-vaginal skin, epidermal cysts, and sebaceous gland hyperplasia and cutaneous horns to lesser extend

(Fig. 1D and E). Moreover, 32% of the animals developed squamous cell carcinomas (SCC), (Fig. 3.1E), supporting the previous observations that papillomas progressing to SCC are a common manifestation of activated Ras signaling (Greenhalgh et al., 1993; Tuveson et al., 2004; Vitale-Cross et al., 2004). Mice without oncogenic *Kras^{G12D}* but ablation of *Notch1* and *Notch2* (*Pdx1-Cre;N1ko*, *Pdx1-Cre;N2ko)* only very rarely developed skin abnormalities (not shown).

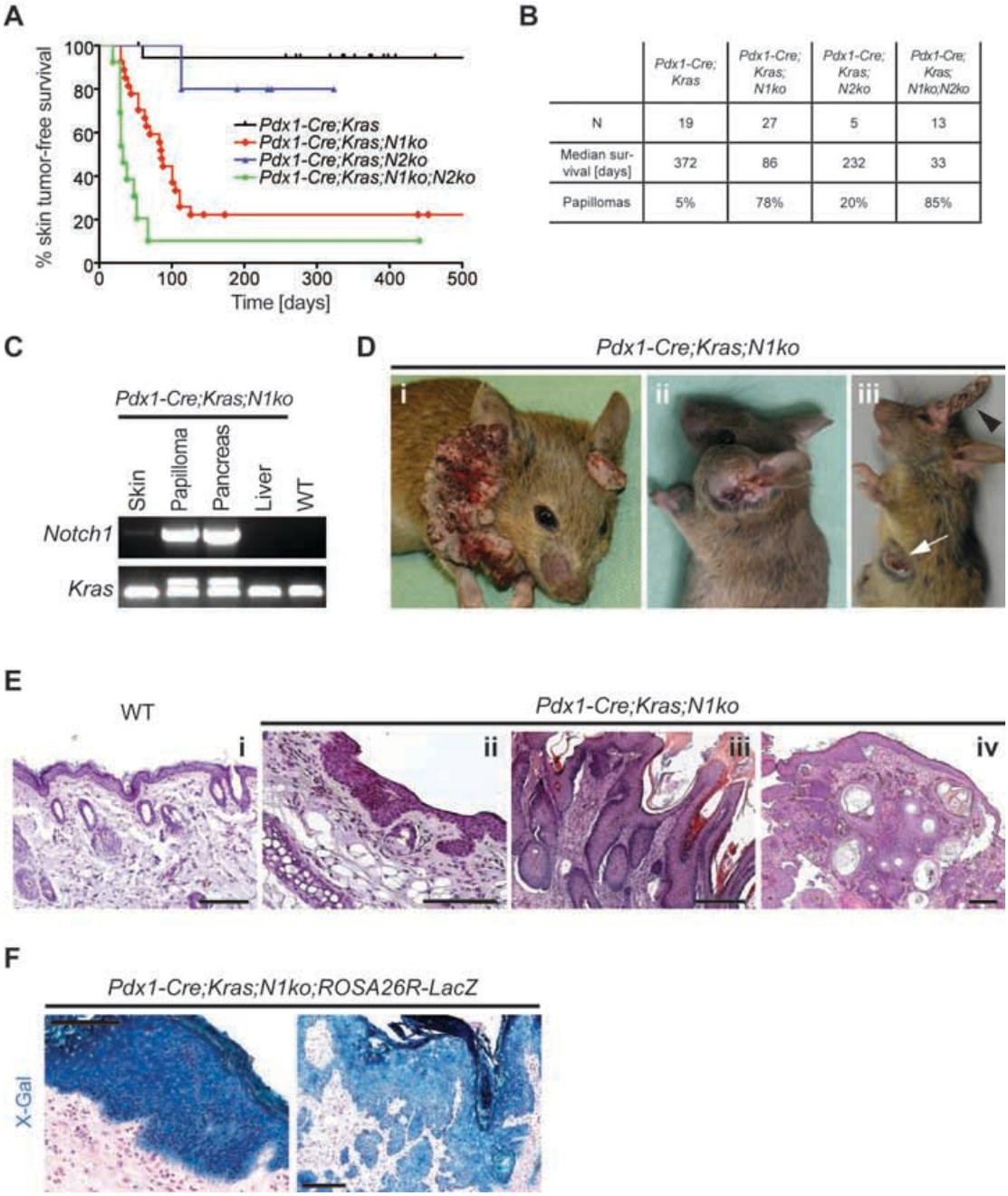

Figure 3.1. *PDX1-Cre;Kras^{G12D};N1ko* mice develop skin tumors (description in text).

Evidence of Pdx1 expression in vivo and in vitro

The observation that *Pdx1-Cre;Kras;N1ko* mice develop skin neoplastic lesions with high penetrance and undergo Cre-mediated recombination are evidence of *Cre* expression in the epidermis possibly due to *Pdx1-Cre* transgene misexpression or physiological PDX1 expression in the skin. To test both hypotheses, immunohistochemical expression analysis was performed in the skin of wildtype and *Pdx1-Cre* mice, which showed a small subset of PDX1$^+$ cells (Fig. 3.2A). Thus, the observed phenotype is due to physiological PDX1 expression in the skin rather than transgenic misexpression of Cre recombinase.

Immunofluorescent staining of PDX1 shows that the intensity of staining was comparable to that in the duodenum and much lower than in pancreatic islet cells (Fig. 3.2Bi and ii). Double immunofluorescent staining revealed that PDX1 co-localizes with Keratin10 (K10) in the spinous layer of the epidermis (Fig. 2Biii; arrowheads). Noteworthy, a very small fraction of PDX1$^+$ cells was located in the basal layer of the epidermis suggesting that PDX1 expression may be initiated also in this layer (Fig. 3.2Bi and iii; arrows).

Above-mentioned experiments demonstrate that PDX1 is predominantly present in differentiated keratinocytes of the skin. To test whether PDX1 expression is regulated during keratinocyte differentiation we induced terminal differentiation in cultured wildtype keratinocytes by calcium as described (Hennings et al., 1980). As early as 12 hours after calcium addition growth arrest and a switch in keratin expression occurred. As expected, treated keratinocytes showed a three-fold induction of the differentiation markers *Keratin10* and *Loricrin* and a five fold reduction of *p63* associated with amplifying keratinocytes in the basal layer of the epidermis. In addition, we found a robust 10-fold induction of *Pdx1* transcript expression in treated keratinocytes (Appendix 2). These findings strongly support the hypothesis that *Pdx1* is predominantly expressed in suprabasal layers of the epidermis (Appendix 2).

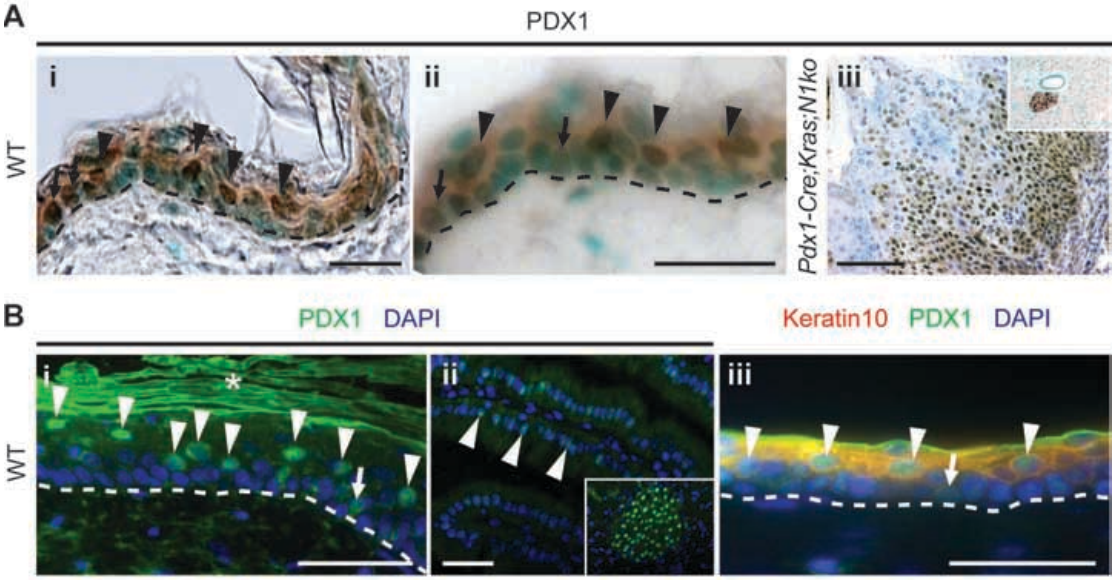

Figure 3.2. Pdx1 is expressed in the skin

Mosaic epidermal Cre expression in Pdx1-Cre mice

Physiological PDX1 expression in the epidermis does not explain the stochastic character of papilloma formation in the *Pdx1-Cre;Kras,N1ko* mice. Hence, we

speculated that *Cre* expression has a mosaic character or alternatively may be induced by mechanical skin irritation. To address the first hypothesis we examined X-Gal expression in *Pdx1-Cre;ROSA26R-LacZ* reporter mice (Soriano, 1999). Consistent with previous studies, we found that *Pdx1-Cre* mice showed a mosaic recombination pattern in the pancreas (Gannon et al., 2000), (Fig. 3.3Ai). Interestingly, similar mosaic staining was observed in the skin (Fig. 3.3Aii). Microscopic evaluation of X-Gal positive areas indicated that suprabasal keratinocytes underwent recombination (Fig. 3Aiii; arrowheads), supporting the hypothesis that PDX1 is mainly expressed in differentiated keratinocytes. However, we found sporadically X-Gal$^+$ keratinocytes residing in the basal layer (Fig. 3.3Aiii; arrow). All examined skin hyperplasia had X-Gal$^+$ basal layer cells suggesting that neoplastic structures originate from the basal keratinocytes of the skin (Fig. 3.3Aiv; arrow).

To further asses the scale of recombination in the basal layer (K14$^+$) and the spinous layer (K10$^+$) of the epidermis we tested freshly isolated keratinocytes from *Pdx1-Cre;N1ko* mice. Cells were fractioned for K14 and K10 expression respectively using fluorescent activated cell sorting (FACS). Cre-mediated recombination was measured using quantitative PCR amplifying the recombined allele of floxed *Notch1* that was normalized to input and then compared to fully recombined DNA. We found that only 5% of DNA isolated from total keratinocytes underwent recombination in *Pdx-Cre;N1ko* mice and most of them were found in the suprabasal layer. We sporadically (below 0.5%) found K14$^+$ cells with recombined Notch1 loci hypothesizing that these cells could be the cell-of-origin for papilloma development (Fig. 3.3B).

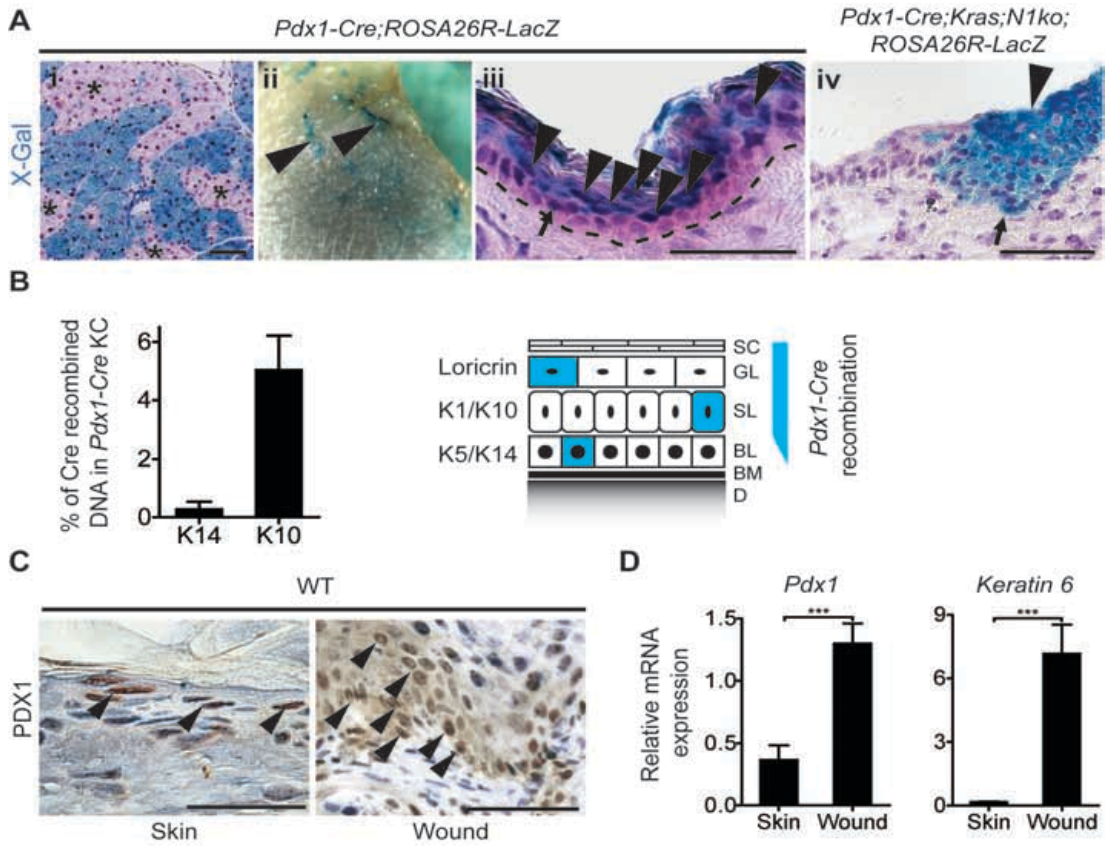

Figure 3.3. Mosaic epidermal Cre expression in *Pdx1-Cre* mice

As papilloma development in *Pdx1-Cre* mice usually occurred in regions susceptible to grooming, scratching and wounding, we speculated that PDX1 expression may be induced in wounded skin triggering Cre-mediated $Kras^{G12D}$ activation and *Notch1* ablation. To test this hypothesis, wounds were induced on the back skin of wild type mice. Six days after wound formation mice were sacrificed and sections of scared skin were dissected and analyzed. Increased PDX1 expression was found in the scar tissue and in the transition zone between normal and wounded epidermis (Fig. 3.3C). PDX1 staining pattern was nuclear and partially cytoplasmic as previously described (Buettner et al., 2004; Kawamori et al., 2003; Macfarlane et al., 1999; Wescott et al., 2009). Quantitative RT-PCR indicated a three-fold induction of *Pdx1* and highly increased *Keratin6* transcript levels in wounded compared to normal epidermis (Fig. 3.3D) supporting PDX1 expression in wounded skin. In summary these results denote (i) physiological *Pdx1* expression in the skin, (ii) restricted to differentiated keratinocytes but sporadically present in $K14^+$ basal cells, (iii) mosaic *Pdx1-Cre* epidermal expression, and (iv) *Pdx1* induction in wounded skin.

Notch1 but not Notch2 is a tumor suppressor in the skin

Although the role of Notch receptors in the skin has already been intensively studied (Demehri et al., 2009; Lin et al., 2000; Nicolas et al., 2003; Pan et al., 2004; Uyttendaele et al., 2004; Vauclair et al., 2005), we aimed to characterize epidermal *Notch1* and *Notch2* deficiency in our model. To do so, $Notch1^{fl/fl}$ (Radtke et al., 1999) and $Notch2^{fl/fl}$ (Besseyrias et al., 2007) mice were crossed with basal keratinocyte-specific *Keratin5-Cre* mice (Tarutani et al., 1997), (named *K5;N1ko* and *K5;N2ko* respectively). These mice were born at the expected Mendelian ratio and successful recombination of the floxed loci was confirmed in isolated primary keratinocytes by immunoblot (Fig. 3.5A).

Consistent with previous studies, *K5;N1ko* mice did not develop proper hair follicles showing a 'naked' phenotype. Additionally, the epidermis was thinner, easily cracking and prone to injury (Fig. 3.4B, D and E). Such a phenotype has been attributed to a role of Notch1 in the stimulation of keratinocyte differentiation (Blanpain et al., 2006; Lowell et al., 2000; Rangarajan et al., 2001). Before the age of 9 months, *K5;N1ko* mice developed extensive hyperplasia and keratinization of the corneal epithelium, which resulted in opaque plague formation and blindness (Fig. 3.4B and C), (Nicolas et al., 2003). All analyzed mice (n=4) developed skin neoplasia at 9 to 12 months of age and additionally BCC, SCC and papillomas were noticed (Fig. 3.4B and C). By contrast, *K5;N2ko* mice featured a non-pathological skin and hair follicle formation (Fig. 3.4B and D) with normal growth cycles. However, impairment of hair growth direction that manifested in more upwards-ruffle appearance of fur was observed (Fig. 3.4B). Mice followed up to 12 months of age (n=4) did not show any sign of tumorigenesis. Taken together, our findings confer that Notch1, but not Notch2 is a tumor suppressor and plays a crucial role in proper skin development and differentiation.

Since expression in different compartments may explain distinct Notch1 and Notch2 functions, we analyzed the expression pattern of these receptors using immunohistochemical staining as well as transgenic *Notch1-GFP (*Lewis et al., 1998) and $Notch2^{lacZ}$ knockin (Hamada et al., 1999) reporter mice. We found Notch2 and X-Gal as a surrogate for Notch2 expression in spinous and granular

layers of the epidermis (Fig. 3.4A). Notch1 and GFP expression in *Notch1-GFP* mice was found throughout the epidermal layers as previously described (Rangarajan et al., 2001), including the basal layer of keratinocytes formed by stem cells and highly proliferative transit amplifying cells (Fig. 3.4A).

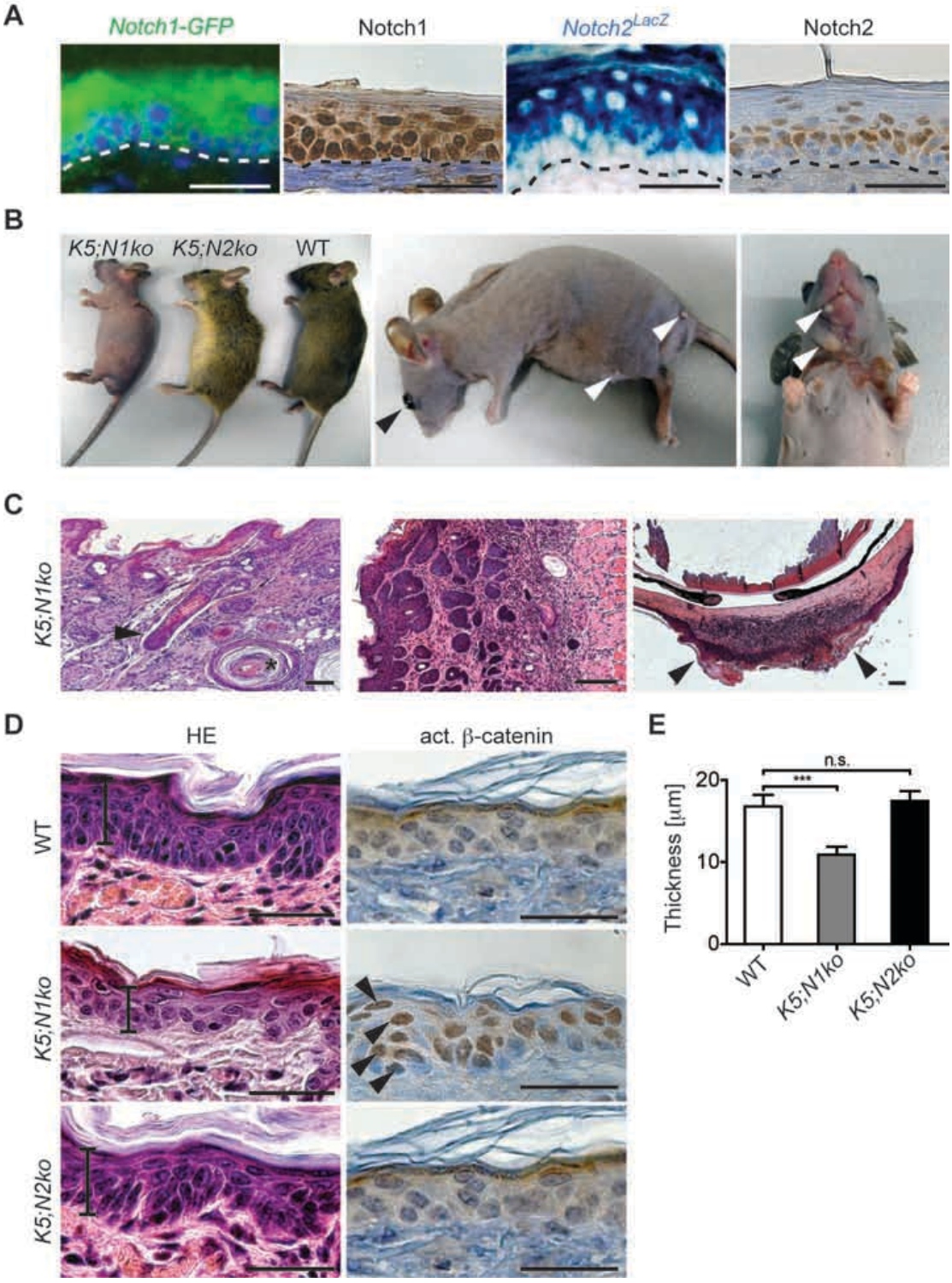

Figure 3.4. Phenotype and biochemical analysis of *K5;N1ko* and *K5;N2ko* mice.

Notch1 but not Notch2 is a suppressor of β-catenin in the skin

As an increased level of active β-catenin is commonly associated with skin malignancies (Chan et al., 1999; Reya and Clevers, 2005; Xia et al., 2001), we investigated the regulation of this pathway in *Notch1* and *Notch2* ablated epidermis. Immunohistochemical analysis revealed increased levels of nuclear localized β-catenin (active β-catenin) in *K5;N1ko* mice in agreement with previous studies Nicolas et al., 2003. Remarkably, neither wildtype nor *K5;N2ko* mice showed strong epidermal active β-catenin staining (Fig. 3.4D). Furthermore, immunoblot analysis of primary keratinocytes isolated from *K5;N1ko and K5;N2ko* mice exhibited a similar pattern (Fig. 3.5A).

Differences in expression of Notch1 and Notch2 in the epidermal layers as well as receptor-specific regulatory mechanisms may contribute to distinct and potentially tumorigenic alterations of β-catenin activity. Therefore, we examined the capabilities of active Notch1 (N1IC) and Notch2 (N2IC) to inhibit β-catenin signaling activity in primary keratinocytes using a luciferase reporter assay. Both Notch receptors were able to inhibit β-catenin activity but N1IC was a significantly stronger inhibitor. Forced expression of N1IC represses β-catenin signaling by over 90% whereas N2IC overexpression leads only to a modest reduction of 30% (Fig. 3.5B). At the same time both Notch receptors showed a similar induction of *Hes1* promoter activity, serving as a read-out for similar activation of canonical Notch signaling (Fig. 3.5 B).

Taken together, these results support a context- and cell-specific function in addition to a distinct expression pattern of Notch and Notch2 in keratinocytes.

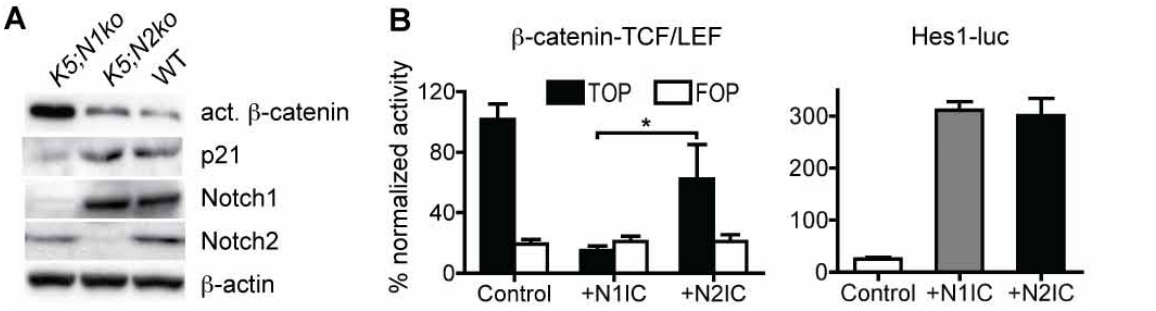

Figure 3.5. Notch1 but not Notch2 is a suppressor of β-catenin in the skin.

Discussion

Neoplasms originating from cutaneous epithelial cells are the most common cancer-type in the United States with an annual incidence of over 1 million cases (Bagheri and Safai, 2001). Developmental signaling pathways play a key role in the induction and progression of cancer. Our study reports a previously unrecognized epidermal expression of PDX1 and adds further evidence for a pivotal role of Notch1 but not Notch2 as a tumor suppressor in the skin, which may be particularly interesting in the light of new therapeutic approaches targeting single Notch receptors (Moellering et al., 2009; Wu et al., 2010).

Epidermal PDX1 expression

As PDX1 is mainly expressed in the pancreas and duodenum, the *Pdx1* promoter is commonly utilized for pancreas-specific transgenic mouse lines. Surprisingly, we found conditional gene deletion in the skin using a *Pdx1-Cre* strain (Gu et al., 2002). Further research provided strong evidence that PDX1 is physiologically expressed in the suprabasal layers of the skin (Fig. 3.2A and B; arrowheads) and rarely in basal keratinocytes (Fig. 3.2A and B; arrows). A similar pattern of *Pdx1* expression was observed in differentiation induced cultured keratinocytes (Fig. 3.2C). This hypothesis is supported by reports indicating a skin phenotype of *Pdx1* knockout mice, which survive 6.5 days postpartum and have, among other characteristic features, thin and cracking skin with little or no fur (Offield et al., 1996). While these skin abnormalities may be due to indirect effects, they suggest a role of PDX1 during skin development, which should be addressed in further studies, e.g. by analyzing keratinocyte-specific *Pdx1* knockout mice, which however is beyond the scope of this report.

In contrast to the ubiquitous expression of Pdx1 in the suprabasal layers of the skin, *Pdx1-Cre;Kras,N1ko* mice developed skin papillomas and other cutaneous lesions only in preferred sites suggesting that Cre-mediated recombination may be mosaic and/or occurs in the cells resistant to neoplastic transformation. Notably, *Cre* expression in *Pdx1-Cre* mice is mosaic such that Cre-mediated recombination occurs far less frequently as would be suggested by the observed PDX1 expression. In addition, papillomas and most other skin tumors typically originate from the basal layer; in fact development from the suprabasal layer is a rather unlikely scenario. Although PDX1 is mainly expressed in the suprabasal keratinocytes, we occasionally found PDX1 expression and Cre-mediated recombination in $K14^+$ cells (Fig. 3.3A, B). These observations may be the reason for the relatively few tumors developing per animal. Interestingly, tumors of *Pdx1-Cre;Kras,N1ko* mice usually develop around exposed areas of the skin (Fig. 1D), possibly due to *Pdx1* activation in wound and scar associated basal layer keratinocytes (Fig. 3.3C). We speculate that cutaneous aggravation or micro-wounds due to grooming and scratching may trigger an inflammatory reaction and wound healing processes with upregulated Pdx1 and Notch expression (Chigurupati et al., 2007), thus forming a tumor-prone environment in *Pdx1-Cre;Kras;N1ko* mice.

Intriguingly, other studies have reported skin phenotypes using *Pdx1-Cre* mice despite the fact that different transgenic strains were utilized (Hingorani et al., 2003; Hingorani et al., 2005). These reports support our finding that *Pdx1* is expressed in the skin. However, only defined genetic alterations lead to a cutaneous phenotype. In the most often analyzed *Pdx1-Cre;Kras* mouse model, skin lesions were only rarely observed (below 5%, Fig.1B and (Hingorani et al., 2003; Hingorani et al., 2005). In our study, *Pdx1-Cre;Kras;N1ko* but not *Pdx1-Cre;Kras;N2ko* or *Pdx1-Cre;Kras* developed skin lesions (Fig. 3.1A and B) which points to the importance of Notch1 but not Notch2 for skin tumor development.

Notch1 and Notch2 play different roles in skin tumorigenesis

Different Notch receptors have often distinct expression patterns, ligand preferences and discrete downstream signaling. Although different Notch receptors can compensate each other e.g. in pancreas development (Nakhai et al., 2008), individual Notch receptors commonly have distinct functions in

development (Geisler et al., 2008), tumorigenesis (Fan et al., 2004; Kopan and Ilagan, 2009; Mazur et al., 2010; Wu et al., 2010) or tissue regeneration (Siveke et al., 2008). The result of this study points to differences in expression pattern and distinctive cellular effectors as main cause of the diverse Notch1 and Notch2 knockout phenotypes. First, we found that Notch1 and Notch2 are present only in partially overlapping layers of the epidermis. Consistent with previous studies, Notch1 is present throughout all skin layers including the tumor-prone basal layer of the skin, whereas Notch2 is expressed exclusively in suprabasal keratinocytes (Rangarajan et al., 2001). These findings were confirmed using immunohistochemical staining as well as *Notch1-GFP* and *Notch2*^{LacZ} reporter mice (Fig. 5A). This divergent expression pattern is very likely at least partially responsible for the downregulation of p21 in *Notch1*- but not *Notch2*-deficient keratinocytes and in line with previous studies (Mammucari et al., 2005; Rangarajan et al., 2001). The second notable difference between Notch1 and Notch2 was their ability to inhibit β-catenin-mediated signaling. β-catenin is responsible for hair-follicle morphogenesis and epidermal stem cell maintenance Huelsken et al., 2001, whereas the disruption of the β-catenin signaling has been associated with several malignancies of the skin (Chan et al., 1999; Reya and Clevers, 2005; Xia et al., 2001). *Notch1* deficiency leading to accumulation of β-catenin in the nucleus has been associated with tumorigenesis (Nicolas et al., 2003). Surprisingly, we did not observe a similar effect when the *Notch2* receptor was abrogated (Fig. 3.4D and 6A). Additionally, we provide *in vitro* evidence of different inhibition capacities between both receptors (Fig. 3.5C) further supporting the postulate of distinct molecular functions of Notch1 and Notch2.

In line with the non-redundant roles of Notch1 and Notch2 in keratinocytes is the accelerated papilloma formation in double *Notch1/2*-deficient mice (Fig. 3.1A and B), suggesting that Notch2 cannot fully compensate for Notch1 loss. Besides different roles in regulation of p21 and β-catenin, Notch expression dosage may play a role as was recently shown (Demehri et al., 2009). In this study *Notch1* loss promoted skin tumorigenesis in a non-cell autonomous manner by impairing skin-barrier integrity and creating a wound-like microenvironment in the epidermis. Of note, *Notch2* ablation alone had no such capabilities unless combined with a *Notch3* knockout, suggesting that a certain threshold of Notch signaling is essential for skin homeostasis.

In conclusion, our results provide strong evidence for epidermal expression of *Pdx1* as of yet not identified function as well as distinctive roles of Notch1 and Notch2 in skin tumorigenesis potentially *via* different p21 and β-catenin pathway modulation.

Experimental Procedures

For detailed description of experimental procedures see Appendix 2.

Disclosure

Pawel K. Mazur contribution to the publication included: designing and performing the experiments, analysis of data, writing the manuscript.

References

Bagheri, M. M., and Safai, B. (2001). Cutaneous malignancies of keratinocytic origin. Clin Dermatol *19*, 244-252.

Besseyrias, V., Fiorini, E., Strobl, L. J.*, et al.* (2007). Hierarchy of Notch-Delta interactions promoting T cell lineage commitment and maturation. J Exp Med *204*, 331-343.

Blanpain, C., Lowry, W. E., Pasolli, H. A.*, et al.* (2006). Canonical notch signaling functions as a commitment switch in the epidermal lineage. Genes Dev *20*, 3022-3035.

Brissova, M., Shiota, M., Nicholson, W. E.*, et al.* (2002). Reduction in pancreatic transcription factor PDX-1 impairs glucose-stimulated insulin secretion. J Biol Chem *277*, 11225-11232.

Buettner, M., Dimmler, A., Magener, A.*, et al.* (2004). Gastric PDX-1 expression in pancreatic metaplasia and endocrine cell hyperplasia in atrophic corpus gastritis. Mod Pathol *17*, 56-61.

Chan, E. F., Gat, U., McNiff, J. M.*, et al.* (1999). A common human skin tumour is caused by activating mutations in beta-catenin. Nat Genet *21*, 410-413.

Chigurupati, S., Arumugam, T. V., Son, T. G.*, et al.* (2007). Involvement of notch signaling in wound healing. PLoS One *2*, e1167.

Demehri, S., Turkoz, A., and Kopan, R. (2009). Epidermal Notch1 loss promotes skin tumorigenesis by impacting the stromal microenvironment. Cancer Cell *16*, 55-66.

Dotto, G. P. (2008). Notch tumor suppressor function. Oncogene *27*, 5115-5123.

Gannon, M., Gamer, L. W., and Wright, C. V. (2001). Regulatory regions driving developmental and tissue-specific expression of the essential pancreatic gene pdx1. Dev Biol *238*, 185-201.

Gannon, M., Herrera, P. L., and Wright, C. V. (2000). Mosaic Cre-mediated recombination in pancreas using the pdx-1 enhancer/promoter. Genesis *26*, 143-144.

Geisler, F., Nagl, F., Mazur, P. K.*, et al.* (2008). Liver-specific inactivation of Notch2, but not Notch1, compromises intrahepatic bile duct development in mice. Hepatology *48*, 607-616.

Greenhalgh, D. A., Rothnagel, J. A., Quintanilla, M. I.*, et al.* (1993). Induction of epidermal hyperplasia, hyperkeratosis, and papillomas in transgenic mice by a targeted v-Ha-ras oncogene. Mol Carcinog *7*, 99-110.

Gu, G., Dubauskaite, J., and Melton, D. A. (2002). Direct evidence for the pancreatic lineage: NGN3+ cells are islet progenitors and are distinct from duct progenitors. Development *129*, 2447-2457.

Hamada, Y., Kadokawa, Y., Okabe, M.*, et al.* (1999). Mutation in ankyrin repeats of the mouse Notch2 gene induces early embryonic lethality. Development *126*, 3415-3424.

Hennings, H., Michael, D., Cheng, C.*, et al.* (1980). Calcium regulation of growth and differentiation of mouse epidermal cells in culture. Cell *19*, 245-254.

Hingorani, S. R., Petricoin, E. F., Maitra, A.*, et al.* (2003). Preinvasive and invasive ductal pancreatic cancer and its early detection in the mouse. Cancer Cell *4*, 437-450.

Hingorani, S. R., Wang, L., Multani, A. S.*, et al.* (2005). Trp53R172H and KrasG12D cooperate to promote chromosomal instability and widely metastatic pancreatic ductal adenocarcinoma in mice. Cancer Cell *7*, 469-483.

Huelsken, J., Vogel, R., Erdmann, B., *et al.* (2001). beta-Catenin controls hair follicle morphogenesis and stem cell differentiation in the skin. Cell *105*, 533-545.

Jonsson, J., Carlsson, L., Edlund, T., *et al.* (1994). Insulin-promoter-factor 1 is required for pancreas development in mice. Nature *371*, 606-609.

Kawamori, D., Kajimoto, Y., Kaneto, H., *et al.* (2003). Oxidative stress induces nucleo-cytoplasmic translocation of pancreatic transcription factor PDX-1 through activation of c-Jun NH(2)-terminal kinase. Diabetes *52*, 2896-2904.

Kopan, R., and Ilagan, M. X. (2009). The canonical Notch signaling pathway: unfolding the activation mechanism. Cell *137*, 216-233.

Larsson, L. I., Madsen, O. D., Serup, P., *et al.* (1996). Pancreatic-duodenal homeobox 1 - role in gastric endocrine patterning. Mech Dev *60*, 175-184.

Lefort, K., and Dotto, G. P. (2004). Notch signaling in the integrated control of keratinocyte growth/differentiation and tumor suppression. Semin Cancer Biol *14*, 374-386.

Lewis, A. K., Frantz, G. D., Carpenter, D. A., *et al.* (1998). Distinct expression patterns of notch family receptors and ligands during development of the mammalian inner ear. Mech Dev *78*, 159-163.

Lin, M. H., Leimeister, C., Gessler, M., *et al.* (2000). Activation of the Notch pathway in the hair cortex leads to aberrant differentiation of the adjacent hair-shaft layers. Development *127*, 2421-2432.

Lowell, S., Jones, P., Le Roux, I., *et al.* (2000). Stimulation of human epidermal differentiation by delta-notch signalling at the boundaries of stem-cell clusters. Curr Biol *10*, 491-500.

Macfarlane, W. M., McKinnon, C. M., Felton-Edkins, Z. A., *et al.* (1999). Glucose stimulates translocation of the homeodomain transcription factor PDX1 from the cytoplasm to the nucleus in pancreatic beta-cells. J Biol Chem *274*, 1011-1016.

Mammucari, C., Tommasi di Vignano, A., Sharov, A. A., *et al.* (2005). Integration of Notch 1 and calcineurin/NFAT signaling pathways in keratinocyte growth and differentiation control. Dev Cell *8*, 665-676.

Mazur, P. K., Einwächter, H., Lee, M., *et al.* (2010). Notch2 is required for PanIN progression and development of pancreatic ductal adenocarcinoma. Proc Natl Acad Sci U S A *in press*.

Moellering, R. E., Cornejo, M., Davis, T. N., *et al.* (2009). Direct inhibition of the NOTCH transcription factor complex. Nature *462*, 182-188.

Moriyama, M., Durham, A. D., Moriyama, H., *et al.* (2008). Multiple roles of Notch signaling in the regulation of epidermal development. Dev Cell *14*, 594-604.

Nakhai, H., Siveke, J. T., Klein, B., *et al.* (2008). Conditional ablation of Notch signaling in pancreatic development. Development *135*, 2757-2765.

Nicolas, M., Wolfer, A., Raj, K., *et al.* (2003). Notch1 functions as a tumor suppressor in mouse skin. Nat Genet *33*, 416-421.

Novak, A., Guo, C., Yang, W., *et al.* (2000). Z/EG, a double reporter mouse line that expresses enhanced green fluorescent protein upon Cre-mediated excision. Genesis *28*, 147-155.

Offield, M. F., Jetton, T. L., Labosky, P. A., *et al.* (1996). PDX-1 is required for pancreatic outgrowth and differentiation of the rostral duodenum. Development *122*, 983-995.

Pan, Y., Lin, M. H., Tian, X., *et al.* (2004). gamma-secretase functions through Notch signaling to maintain skin appendages but is not required for their patterning or initial morphogenesis. Dev Cell *7*, 731-743.

Radtke, F., Wilson, A., Stark, G., *et al.* (1999). Deficient T cell fate specification in mice with an induced inactivation of Notch1. Immunity *10*, 547-558.

Rangarajan, A., Talora, C., Okuyama, R., *et al.* (2001). Notch signaling is a direct determinant of keratinocyte growth arrest and entry into differentiation. EMBO J *20*, 3427-3436.

Reya, T., and Clevers, H. (2005). Wnt signalling in stem cells and cancer. Nature *434*, 843-850.

Sakai, T., Johnson, K. J., Murozono, M., *et al.* (2001). Plasma fibronectin supports neuronal survival and reduces brain injury following transient focal cerebral ischemia but is not essential for skin-wound healing and hemostasis. Nat Med *7*, 324-330.

Siveke, J. T., Einwachter, H., Sipos, B., *et al.* (2007). Concomitant pancreatic activation of Kras(G12D) and Tgfa results in cystic papillary neoplasms reminiscent of human IPMN. Cancer Cell *12*, 266-279.

Siveke, J. T., Lubeseder-Martellato, C., Lee, M., *et al.* (2008). Notch signaling is required for exocrine regeneration after acute pancreatitis. Gastroenterology *134*, 544-555.

Soriano, P. (1999). Generalized lacZ expression with the ROSA26 Cre reporter strain. Nat Genet *21*, 70-71.

Tarutani, M., Itami, S., Okabe, M., *et al.* (1997). Tissue-specific knockout of the mouse Pig-a gene reveals important roles for GPI-anchored proteins in skin development. Proc Natl Acad Sci U S A *94*, 7400-7405.

Tuveson, D. A., Shaw, A. T., Willis, N. A., *et al.* (2004). Endogenous oncogenic K-ras(G12D) stimulates proliferation and widespread neoplastic and developmental defects. Cancer Cell *5*, 375-387.

Uyttendaele, H., Panteleyev, A. A., de Berker, D., *et al.* (2004). Activation of Notch1 in the hair follicle leads to cell-fate switch and Mohawk alopecia. Differentiation *72*, 396-409.

Vauclair, S., Nicolas, M., Barrandon, Y., *et al.* (2005). Notch1 is essential for postnatal hair follicle development and homeostasis. Dev Biol *284*, 184-193.

Vitale-Cross, L., Amornphimoltham, P., Fisher, G., *et al.* (2004). Conditional expression of K-ras in an epithelial compartment that includes the stem cells is sufficient to promote squamous cell carcinogenesis. Cancer Res *64*, 8804-8807.

Wescott, M. P., Rovira, M., Reichert, M., *et al.* (2009). Pancreatic ductal morphogenesis and the Pdx1 homeodomain transcription factor. Mol Biol Cell *20*, 4838-4844.

Wu, Y., Cain-Hom, C., Choy, L., *et al.* (2010). Therapeutic antibody targeting of individual Notch receptors. Nature *464*, 1052-1057.

Xia, X., Qian, S., Soriano, S., *et al.* (2001). Loss of presenilin 1 is associated with enhanced beta-catenin signaling and skin tumorigenesis. Proc Natl Acad Sci U S A *98*, 10863-10868.

Chapter 4: Notch signaling is required for exocrine regeneration after acute pancreatitis

This chapter is based on the original work published in *Gastroenterology*, February 2008, vol. 134, issue 2. The required background and the most essential results are presented in this chapter whereas the full-published paper is attached as Appendix 3. The paper is reproduced with the publisher's permission.

Abstract

The mechanisms for tissue regeneration and renewal after acute pancreatitis are not well understood but may involve activation of Notch signaling. To study the role of Notch signaling in a murine model of acute pancreatitis, we used: the γ-secretase inhibitor dibenzazepine (DBZ) to ablate Notch activation or conditional Notch1 knockout mice. Acute pancreatitis was induced by cerulein treatment. Loss of Notch signaling results in impaired regeneration after acute pancreatitis with fewer mature acinar cells in DBZ-treated and Notch1-deficient mice. β-catenin expression was increased and prolonged during exocrine regeneration. We found that the RAM domain of active Notch inhibits β-catenin-mediated transcriptional activity. Our results suggest an interaction of Notch and Wnt signaling in pancreatic acinar cells, providing evidence for a role of these pathways in the regulation of the maturation process of acinar cells.

Introduction

Regenerative processes after organ injury are essential for tissue homeostasis and include the activation and proliferation of progenitor cells. Recently, acinar cell proliferation along with a dedifferentiation and re-differentiation process was described after cellular damage in a model of cerulein-induced acute pancreatitis. This process involved activation of embryonic pathways including Notch signaling (Jensen et al., 2005), Gomez et al., 2004) for which an important role in organ regeneration and self-renewal is known (Wilson and Radtke, 2006). In murine adult pancreata, *Notch1* (mRNA) is strongly upregulated in the acute and regenerative phase of acute pancreatitis (Jensen et al., 2005), Gomez et al., 2004).

In this study, we have investigated the effect of Notch inhibition in the adult pancreas and during cerulein-induced pancreatitis by either blocking Notch cleavage using the γ-secretase inhibitor DBZ or by generating conditional pancreas-specific Notch1 knockout mice. We show that Notch1 is an important regulator of pancreatic regeneration after acute pancreatitis and provide evidence for a close interaction of the Notch and β-catenin signaling pathways as a possible underlying cause.

Results

DBZ treatment in adult pancreas and cerulein-induced acute pancreatitis

To investigate the effect of Notch pathway inactivation in the adult pancreas, the γ-secretase inhibitor DBZ was utilized. While most of the exocrine pancreas consisted of normal-looking acinar tissue, we also noted decreased intercellular adhesion of acinar cells in some lobules. Western blot analysis showed decreased amylase and enhanced β-catenin expression in the pancreata of DBZ-treated mice (Fig. 4A). Interestingly, we found cytoplasmic staining of β-catenin and E-cadherin in some acinar cells of DBZ treated mice but not in vehicle-treated cells. Immunohistochemical staining for clusterin, a marker of immature acinar cells, showed increased expression in DBZ-treated pancreata (for details see the paper in Appendix 4). These results indicate that administration of DBZ induces moderate histologic alterations in the exocrine pancreas *in vivo* correlating with the molecular changes in genes defining exocrine differentiation.

Impaired regeneration after cerulein-induced pancreatitis in DBZ-treated mice

To test if Notch signaling affects pancreatic regeneration after cellular insult, we used the model of cerulein-induced acute pancreatitis (Jensen et al., 2005). We found upregulation of Notch1 expression on day 3 (d3) after induction of pancreatitis, confirming previous results using transgenic *Notch1-GFP* mice (Shou et al., 2001). Unstimulated and injured pancreata however, showed no or only a very low expression. Evaluation of chemical ablated Notch signaling (DBZ) during acute pancreatitis revealed substantial differences in exocrine tissue regeneration at d3 (Fig. 4B). Histomorphologically, control mice revealed a mixed cellular picture with large areas of almost complete exocrine regeneration and only minor post-inflammatory residues left. DBZ-treated mice showed a marked reduction of differentiated acinar cells. Quantification of acinar regeneration confirmed the morphologic findings, showing significantly less differentiated acini in DBZ-treated animals (Fig. 4C). Additionally, we found an increased expression of Clusterin, E-cadherin and β-catenin (Fig. 4B), which is indicative for dedifferentiated acinar cells, reflecting a transient progenitor status (Jensen et al., 2005).

Pancreas-specific inactivation of Notch1 impair regeneration after cerulein-mediated pancreatitis

Due to possible Notch-independent effects of γ-secretase inhibition, we next generated pancreas-specific *Ptf1a$^{+/Cre(ex1)}$; Notch1* knockout mice (*N1KO*), (Fig. 4E) as previously described (Nakhai et al., 2007, Radtke et al., 1999). *N1KO* mice developed normally, showing no signs of disease up to an observation period of 18 months (data not shown).

Similarly to the chemical inhibition of Notch approach we have seen an elevated β-catenin expression (Fig. 4D), then we examined the *N1KO* response to pancreatitis. Likewise impaired regeneration of exocrine tissue in *N1KO* mice, comparing to WT, was observable at d3 after induced pancreatitis. (Fig. 4F). Acini regenerated significantly slower. Analysis of acinar regeneration showed significantly less acini in *N1KO* mice at d3 (Fig. 4G). Analogously, with the DBZ-treatment experiment we found elevated E-cadherin, Clusterin and β-catenin

(Fig. 4F). These data suggest that Notch1 has a direct or indirect influence on the β-catenin pathway during regeneration of the exocrine pancreas.

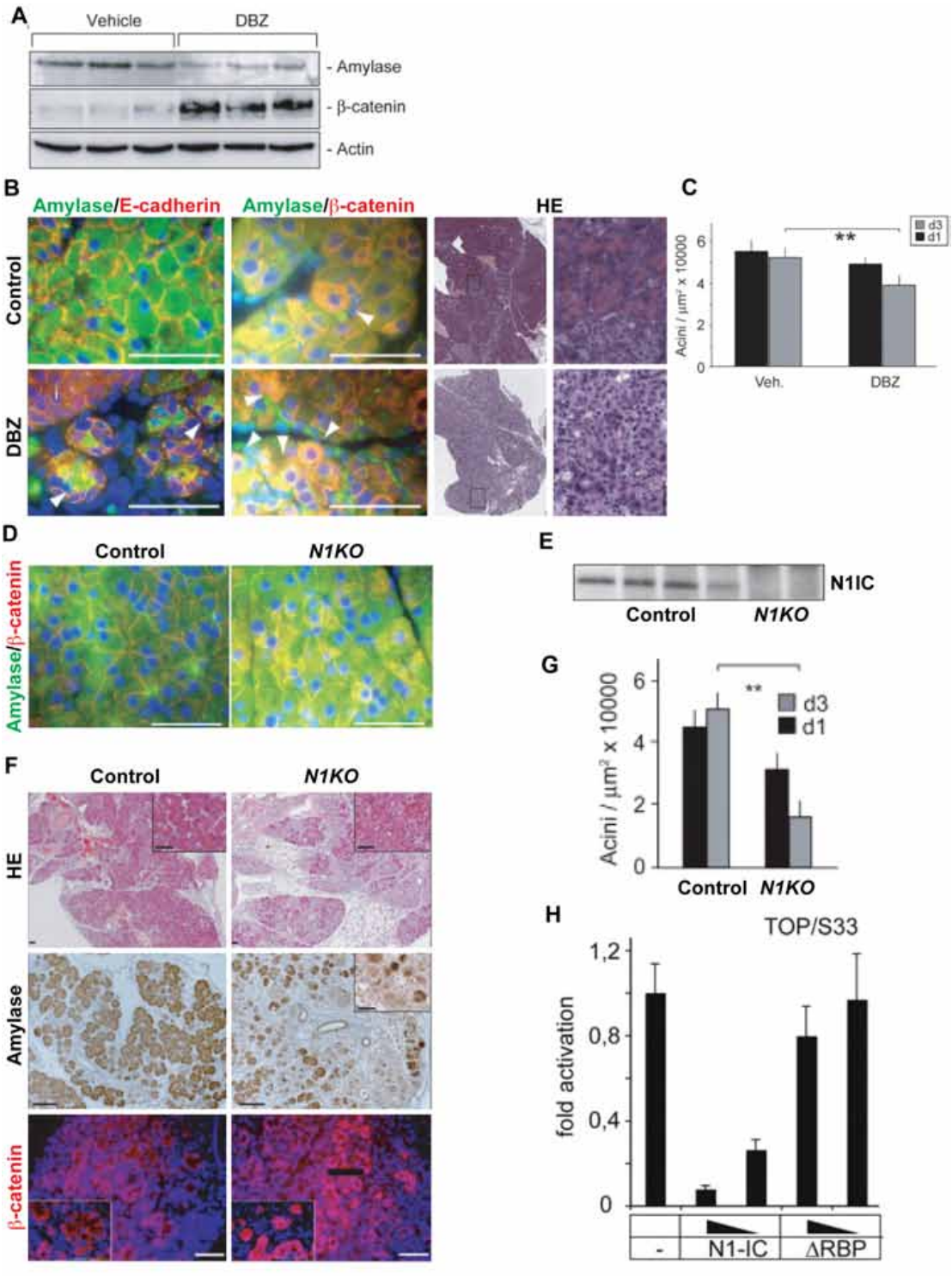

Figure 4. Notch signaling is required for exocrine regeneration after acute pancreatitis (detailed description in text).

Notch1 inhibits β-Catenin/Tcf activity in the acinar tumor cell line 266-6

To analyze a possible interaction between β-catenin and Notch signaling in acinar cells, we sought to establish a cell culture system using the murine acinar cell tumor cell line 266-6 (Ornitz et al., 1985). Due to the low intrinsic transcriptional activity of β-catenin in 266-6 cells measured by using the β-catenin–responsive TCF reporter construct (TOP) and mutant control (FOP), cells were stimulated with Wnt1 or constitutively active S33/β-catenin. To test if increased Notch signaling alters β-catenin activity, we co-transfected 266-6 cells with either S33/β-catenin or Wnt1 together with different Notch1 constructs. We found that Notch1-IC (N1-IC, constructively active Notch1) but not Notch1-ICΔRBP (Notch lacking a functional RAM domain) were able to inhibit both Wnt1 and S33/β-catenin–induced TOP activity (Fig. 4H). These data suggest an inhibitory role of Notch1 on the Wnt signaling pathway dependent on Notch1 signaling *via* RBPJκ.

Discussion

In this study, we investigated the role of the Notch pathway during acute pancreatitis using a chemical and genetic approach for ablation of Notch signaling. Impaired recovery after acute pancreatitis in Notch inhibited pancreata may be due to different mechanisms. Notch signaling inhibition in the pancreatic mesenchyme, such as in fibroblasts or blood vessels, would be a potential mechanism in DBZ-treated mice, yet these compartments are not targeted in *N1KO* mice and can thus not sufficiently explain the very similar phenotype of chemically and genetically Notch-ablated mice. Another mechanism may be that inhibition of Notch signaling could increase the susceptibility of pancreatic cells to cerulein-induced damage. However, cerulein effects peak at 1d, in time of which there were no observable differences between Notch ablated and WT pancreata. Additionally, low expression of Notch1 in normal acini and elevated expression at d3 suggest that Notch is not sensitizing acini to injury, rather plays a role in the regeneration phase (Jensen et al., 2005). Another possibility would be exhaustion of the adult progenitor cell compartment by defective Notch signaling before or during injury. Recent evidence suggests that exocrine regeneration occurs primarily from preexisting acinar cells (Jensen et al., 2005, Desai et al., 2007). From our experiments and in the absence of cell lineage tracing experiments, we cannot conclude which cells are responsible for regeneration in our model. However, our results of impaired regeneration of the exocrine compartment support a model of Notch-regulated acinar cell regeneration. Because we do not find evidence for an essential role of Notch signaling in acinar proliferation (details see Appendix 4), the role of Notch may be regulating the differentiation status of acinar cells versus regulation of an adult progenitor compartment during acute pancreatitis, and both hypotheses should be addressed by lineage tracing experiments in future studies.

A potential mechanism for Notch1 regulating acinar differentiation is by interacting with β-catenin. Recent studies have found evidence for an interaction of both pathways in various organs, including skin and the hematopoietic system (Hayward et al., 2005, Nicolas et al., 2003, Reya et al., 2003). In the pancreas, β-catenin is essential for acinar specification during organogenesis, pointing to a

central role of this pathway in acinar differentiation (Murtaugh et al., 2005, Dessimoz et al., 2005, Heiser et al., 2006). The finding of increased acinar β-catenin mRNA expression early in acute pancreatitis and its decline later during regeneration (Jensen et al., 2005) suggests that β-catenin may also be required during acinar maturation processes. Our results of a prolonged and increased expression of β-catenin in Notch-ablated acini during acute pancreatitis suggest its modulatory function. We find strong indications that Notch and β-catenin are involved in acinar differentiation and it is consistent with the role of β-catenin in embryonic exocrine development (Murtaugh et al., 2005).
In conclusion, we have identified Notch signaling to be important for regeneration of the adult murine pancreas during acute pancreatitis. We show that Notch1 is required for the exocrine regeneration of the pancreas *in vivo*. Molecular studies using a cell culture–based system provide evidence for an interaction of Notch1 with β-catenin. However, further characterization of affected cellular compartment and mechanism of the Notch and β-catenin signaling interaction is required.

Experimental procedures

For detailed description of experimental procedures see Appendix 3.

Mouse Strains

For generation of *Notch1*-deficient mice, *Notch1*$^{lox/lox}$ mice (Radtke et al., 1999) were bred with *Ptf1a*$^{+/Cre(ex1)}$ knockin mice (Nakhai et al., 2007). Mice were of mixed 129SV/C57BL/6 genetic background. For Notch1 expression studies, Notch1-GFP mice were used (Shou et al., 2001).

DBZ and Cerulein Treatment

For DBZ experiments, C57BL/6 mice 8–12 weeks of age were used. DBZ (<99.9% purity) was custom synthesized by Syncom (Groningen, The Netherlands) and suspended in 0.5% hydroxypropyl methylcellulose (Methocel E4, Dow Chemical Co, Midland, MI), 1% ethanol, and 0.1% Tween 80 (Sigma-Aldrich, Steinheim, Germany) in water and injected intraperitoneally (10 umol/kg, 0.2 mL/mouse) for indicated periods. Pancreatitis was induced by administration of 8 hourly intraperitoneal injections of cerulein (10 ug/mL, 0.2 mL/mouse) over 2 consecutive days. At indicated time points, mice were killed and pancreata removed. All experiments were performed according to the guidelines of the local animal use and care committees.

Disclosure

Pawel K. Mazur contribution to the publication included: acquisition of data.

References

Desai, B. M., Oliver-Krasinski, J., De Leon, D. D., *et al.* (2007). Preexisting pancreatic acinar cells contribute to acinar cell, but not islet beta cell, regeneration. J Clin Invest *117*, 971-977.

Dessimoz, J., Bonnard, C., Huelsken, J., *et al.* (2005). Pancreas-specific deletion of beta-catenin reveals Wnt-dependent and Wnt-independent functions during development. Curr Biol *15*, 1677-1683.

Gomez, G., Englander, E. W., Wang, G., *et al.* (2004). Increased expression of hypoxia-inducible factor-1alpha, p48, and the Notch signaling cascade during acute pancreatitis in mice. Pancreas *28*, 58-64.

Hayward, P., Brennan, K., Sanders, P., *et al.* (2005). Notch modulates Wnt signalling by associating with Armadillo/beta-catenin and regulating its transcriptional activity. Development *132*, 1819-1830.

Heiser, P. W., Lau, J., Taketo, M. M., *et al.* (2006). Stabilization of beta-catenin impacts pancreas growth. Development *133*, 2023-2032.

Jensen, J. N., Cameron, E., Garay, M. V., *et al.* (2005). Recapitulation of elements of embryonic development in adult mouse pancreatic regeneration. Gastroenterology *128*, 728-741.

Murtaugh, L. C., Law, A. C., Dor, Y., *et al.* (2005). Beta-catenin is essential for pancreatic acinar but not islet development. Development *132*, 4663-4674.

Nakhai, H., Sel, S., Favor, J., *et al.* (2007). Ptf1a is essential for the differentiation of GABAergic and glycinergic amacrine cells and horizontal cells in the mouse retina. Development *134*, 1151-1160.

Nicolas, M., Wolfer, A., Raj, K., *et al.* (2003). Notch1 functions as a tumor suppressor in mouse skin. Nat Genet *33*, 416-421.

Ornitz, D. M., Palmiter, R. D., Messing, A., *et al.* (1985). Elastase I promoter directs expression of human growth hormone and SV40 T antigen genes to pancreatic acinar cells in transgenic mice. Cold Spring Harb Symp Quant Biol *50*, 399-409.

Radtke, F., Wilson, A., Stark, G., *et al.* (1999). Deficient T cell fate specification in mice with an induced inactivation of Notch1. Immunity *10*, 547-558.

Reya, T., Duncan, A. W., Ailles, L., *et al.* (2003). A role for Wnt signalling in self-renewal of haematopoietic stem cells. Nature *423*, 409-414.

Shou, J., Ross, S., Koeppen, H., *et al.* (2001). Dynamics of notch expression during murine prostate development and tumorigenesis. Cancer Res *61*, 7291-7297.

Wilson, A., and Radtke, F. (2006). Multiple functions of Notch signaling in self-renewing organs and cancer. FEBS Lett *580*, 2860-2868.

Chapter 5: Conditional ablation of Notch signaling in pancreatic development.

This chapter is based on the original work published in *Development*, August 2008, vol. 135, issue 16. The essential background and results are presented in this chapter whereas the full-published paper is attached as Appendix 4. The paper is reproduced with the publisher's permission.

Abstract

The role of Notch signaling and *Rbpj* in exocrine pancreatic development is not well defined. We therefore analyzed conditional pancreas-specific *Rbpj* and combined *Notch1/Notch2* knockout mice. Animals were invastigated at different embryonic stages for pancreatic exocrine and endocrine development. The absence of *Rbpj* in pancreatic progenitor cells impaired exocrine pancreas development up to embryonic day 18.5 and led to premature differentiation of pancreatic progenitors into endocrine cells. In *Rbpj*-deficient pancreata, amylase expressing acini and islets formed during late embryonic and postnatal development, suggesting an essential role of *Rbpj* in early but not late development. Contrary to this severe phenotype, the concomitant inactivation of *Notch1* and *Notch2* only moderately disturbed the proliferation of pancreatic epithelial cells during early embryonic development, and did not inhibit pancreatic development. Our results show that, in contrast to *Rbpj*, *Notch1* and *Notch2* are not essential for pancreatogenesis. These data favor a Notch-independent role of *Rbpj* in the development of the exocrine pancreas. Furthermore, our findings suggest that in late stages of pancreatic development exocrine cell differentiation and maintenance are independent of *Rbpj*.

Introduction

Loss-of-function studies have proposed that Notch signaling regulates self-renewal leading to depletion of pancreatic progenitor cells and accelerated differentiation of endocrine cells (Apelqvist et al., 1999, Fujikura et al., 2006, Fujikura et al., 2007, Jensen et al., 2000). While these studies have provided evidence for an important role of Notch signaling in endocrine development, the dependence of the exocrine compartment on specific Notch signaling members is not well understood. Recently, RBPJκ, the transcriptional mediator of Notch signaling, was found to be a binding partner of PTF1A in the PTF1 complex (details of pancreas development in Chapter 1), suggesting a Notch-independent function during pancreatic development (Beres et al., 2006, Masui et al., 2007). During pancreatic organogenesis, Notch1 and Notch2 expression has been described in the pancreatic epithelium, whereas Notch3 and Notch4 are expressed in mesenchymal and endothelial cells (Lammert et al., 2000). In order to clarify the role of the Notch1 and Notch2 receptors versus the abrogation of RBPJκ signaling, we analyzed conditional *Notch1/Notch2* double-knockout and *Rbpj* knockout mice by using *Ptf1a*$^{+/Cre(ex1)}$ mice for targeting pancreatic progenitor and exocrine cells.

Results

Generation of pancreas-specific Rbpj and Notch1/Notch2 knockout mice

To abrogate Notch signaling in the pancreas, an approach generating conditional *Rbpj* (see Experimental Procedures) or previously described *Notch1* plus *Notch2* knockout mice (Radtke et al., 1999, Besseyrias et al., 2007) were crossed with pancreas specific *Ptf1a*$^{+/Cre(ex1)}$ mice (Nakhai et al., 2007). *Ptf1a*$^{+/Cre(ex1)}$*; Rbpj*$^{lox/lox}$ mice will be termed *RbpjKO* whereas, *Ptf1a*$^{+/Cre(ex1)}$*; Notch1*$^{lox/lox}$*; Notch2*$^{lox/lox}$ will be referred to as *N1N2KO.* Using *Rosa26R-lacZ* reporter mice (*R26R*) as a surrogate for Cre-recombinase induced deletion of *Rbpj* or *Notch1/2,* we observed a positive X-gal stain in all exocrine cells in adult pancreata (Fig. 5.1-3). Homozygous *Notch1KO*, *Notch2KO* and *N1N2KO* mice showed no gross abnormalities and developed normally. *RbpjKO* mice survived only until 4-5 days postpartum. The premature death was caused by insufficient postnatal growth with impaired milk digestion (Fig. 5.4). Examination of the *RbpjKO;R26R* mice at day 1 postpartum (dpp) revealed a small and severely altered pancreas (Fig. 5.3, 2.7). In the duodenal part of the mutant pancreas, weakly branched ducts were observable (Fig. 5.3, arrowhead), whereas the splenic part of the pancreas showed no branching (Fig. 5.3, arrows). Histological examination demonstrated a lack of acinar tissue with large duct-like structures being present in the splenic and duodenal portion of the pancreas (Fig. 5.7, blue). Interestingly, *N1N2KO* mice did not reveal striking abnormalities in pancreatic tissue organization or cell lineage distribution, except being slightly smaller, suggesting a non-essential role for Notch1 and Notch2 during pancreatic development (Fig. 5.1-2).

Early development of RbpjKO and N1N2KO pancreata

The pancreatic buds of E13.5 *N1N2KO* appeared smaller and less branched than in control littermates (Fig. 5.8-9, 2.11). By contrast, *RbpjKO* embryos revealed a significantly reduced epithelial mass with weakly branched structures in both buds (Fig. 5.10-11), suggesting that *Rbpj* is essential for their development. The reduced branching and epithelial mass in the *N1N2KO* and *RbpjKO* embryos was accompanied by a decreasing number of the proliferating cells in pancreatic epithelium, as detected by phospho-histone H3 (PHH3), (Fig. 5.15-18).

As the premature differentiation of pancreatic progenitor to endocrine cells has been suggested previously as a possible cause for the reduction of pancreatic epithelium in *Rbpj* deficient buds (Fujikura et al., 2006), pancreatic sections at E11.5 were stained for X-gal and glucagon expression. Similar to control mice (Fig. 5.12), *N1N2KO* mice showed no increased number of glucagon-positive cells (Fig. 5.13). By contrast, we observed an increased number of glucagon-positive cells in *RbpjKO;R26R* embryos at this time point, consistent with the premature differentiation of pancreatic progenitors to endocrine cells. These cells were found within and peripheral from the ventral and dorsal buds (Fig. 5.14).

In summary, *RbpjKO* embryos show severe defects in the pancreas development whereas, *N1N2KO* have only a minor loss of pancreatic mass, without defects in the development of the exocrine and endocrine compartments.

Acinar cells development in *Rbpj*-deficient pancreas

In contrast to control and *N1N2KO*, *RbpjKO* embryos showed no amylase expression at E14.5 (Fig. 5.19-21). At E18.5, the exocrine pancreas of Notch1 and 2-deficent mice was morphologically normal (Fig. 5.22-23) however, *RbpjKO*

littermates have a few amylase positive (+) acini in the duodenal part and amylase+ duct-like structures in the splenic portion of the rudimentary pancreas (Fig. 5.24).

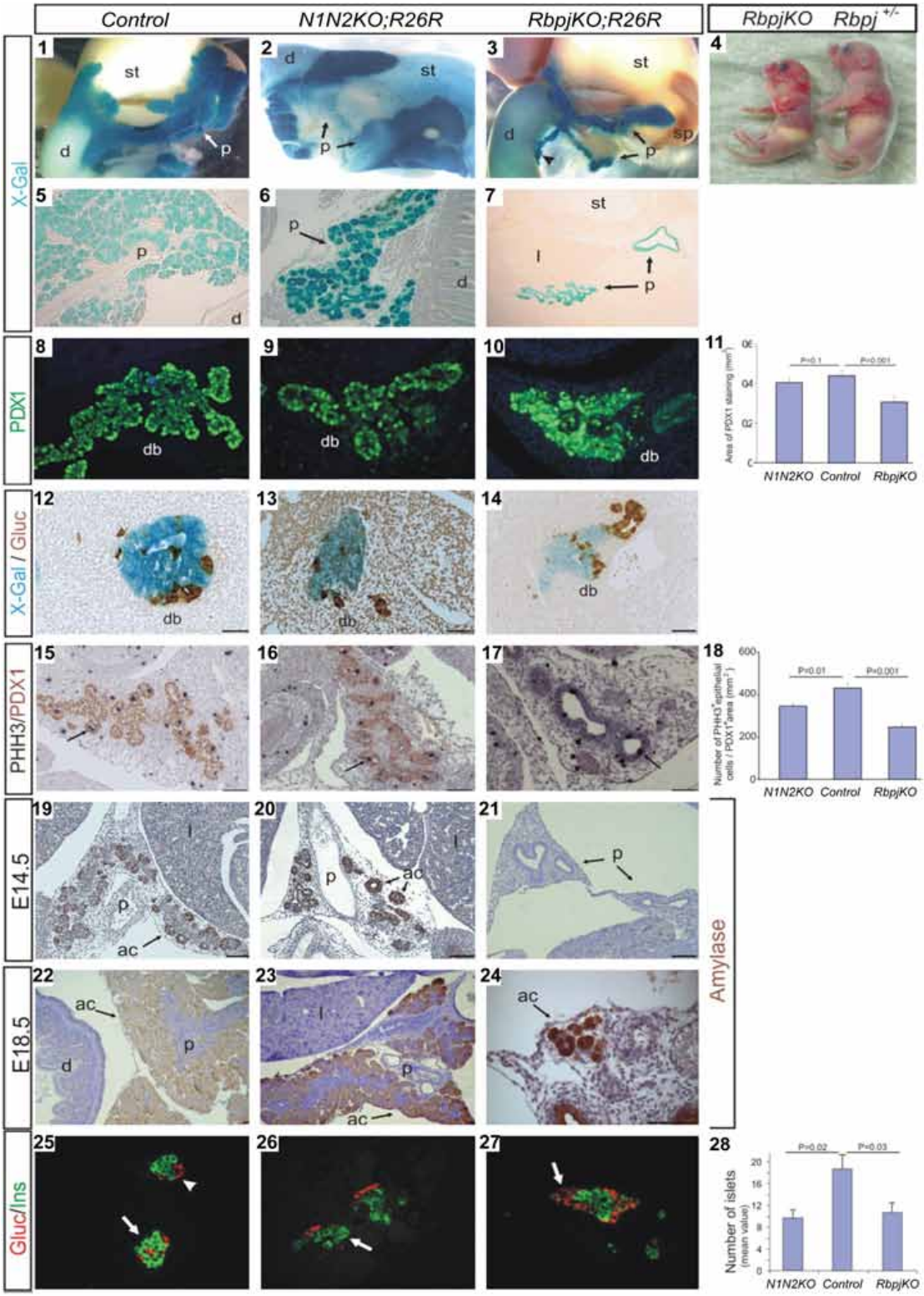

Figure 5. Conditional ablation of Notch signaling in pancreatic development (detailed description in text).

In *RbpjKO* pups, the duct-like structures showed positive staining with CK19, a marker of differentiated ductal cells. These cells were also positive for X-gal staining, suggesting that all of them derived from *Rbpj*-deficient cells. In *RbpjKO* mice at E18.5, the majorities of amylase+ cells were also PDX1+ (PDX is active in developing pancreas – Chapter 1) and were mitotically active, as determined by BrdU labeling. We also found PTF1A+ cells outside the main duct and in the duodenal part of the rudimentary pancreas. The PTF1 complex is required for the expression of acinar genes, such as amylase (Appendix 1).

Endocrine cell development in RbpjKO and N1N2KO pancreas

Most mature endocrine cells appeared after E14 in both *N1N2KO* and *RbpjKO* embryos, similar to littermate controls. At E18.5, we could detect all endocrine cell lines. In *RbpjKO* mice, these cells were detectable in the rudimentary pancreas within the tubular duct wall and in the protruding formations of the pancreatic tubule. The endocrine epithelium in *N1N2KO* embryos, and more prominently in *RbpjKO* embryos, had a disturbed appearance and formed less islets than control embryos (Fig. 5.28). In most of the endocrine cell clusters, α cells were not organized around β cells, and the morphology of these islet-like structures appeared to be long rather than circular like in the control mice (Fig. 5.25-27). In adult pancreata of *N1N2KO* mice, however, the islets appeared normal and were indistinguishable from wild-type controls (data not shown).

Discussion

The regulation of organogenesis and proper cell fate determination in the pancreas has been found to involve the activation of the Notch pathway. The canonical Notch signaling activates target genes through the transcription factor RBPJκ. During early pancreatic development, *RbpjKO* mice revealed an essential role for *Rbpj* with premature glucagon+ cell development and a severe decrease in acinar cell differentiation. In our model, *RbpjKO* mice do not survive more than 4-5 days after birth, most probably as a result of the clinically apparent pancreatic insufficiency with impaired weight gain, a high content of milk in the stomach of animals and no apparent neurological phenotype. We favor a pancreas related cause of death over, for example, extra-pancreatic causes, as we could not detect any defects in other PTF1A-expressing organs, such as the retina or the CNS (data not shown). The reason why *RbpjKO* mice do not develop a normal adult exocrine compartment is not clear, but may possibly be explained by a more rigorous deletion of early progenitors in our mice. Nevertheless, the late appearance of acinar cells during organogenesis in our and other *Rbpj*-deficient pancreata (Fujikura et al., 2006, Fujikura et al., 2007) is surprising, and may occur through *Rbpj*-independent mechanisms involving a recently identified regulator of acinar cell development, the *Rbpj* homolog *Rbpjl* (Beres et al., 2006). These authors showed that the initiation of the acinar differentiation program by the PTF1 complex involves RBPJκ binding to PTF1A to form the PTF1-J complex. This complex then activates RBPJL, which itself binds to PTF1A to form the PTF1-L complex. PTF1-L has been shown to be the more active complex, activating acinar genes such as amylase and elastase (Beres et al., 2006). The finding of delayed expression of acinar genes at E18.5 in *RbpjKO* mice may be explained by two mechanisms. First, Cre activation may not be complete in a few proacinar cells, which will eventually form the exocrine pancreas. However, our

results showing Cre-induced recombination (Fujikura et al., 2007) do not support this hypothesis. Secondly, spontaneous activation of *Rbpjl* in precursor cells expressing PTF1A may lead to the formation of PTF1-L and, thus, to a positive-feedback loop activating the *Rbpjl* promoter. The delayed appearance and the small initial population of acinar cells would be consistent with a stochastic activation of *Rbpjl*, a hypothesis as yet unproven however.
The defective ductal branching observed in our, as well as in other models of ablated Notch signaling, may be due to an early reduction of the epithelial progenitor pool (suggested previously by Fujikura et al., 2006, Fujikura et al., 2007). Interestingly, the ductal cells in *RbpjKO* and *N1N2KO* mice expressed CK19, suggesting that the differentiation of progenitor cells into ductal cells is not inhibited by inactivated *Rbpj*-dependent Notch signaling. Future studies may help to determine the factors regulating ductal differentiation.
Studies with ectopic overexpression of Notch1 show inhibition of exocrine and endocrine differentiation of pancreatic progenitor cells, leaving them in an undifferentiated state (Esni et al., 2004, Hald et al., 2003, Murtaugh et al., 2003). Despite technical issues, such as the potentially non-physiological Notch1 levels, these results, as well as our studies, point to a role for Notch in the regulation of pancreatic progenitor cells, with one of the main conclusions being a premature endocrine differentiation caused by insufficient Notch signaling. Interestingly however, we found such an effect in *RbpjKO* but not in *N1N2KO* mice, possibly indicating the requirement of *Rbpj* but not of *Notch1* or *Notch2* for endocrine differentiation. However, we cannot rule out an inefficient early Cre-induced inactivation of *Notch1* and *Notch2*. The modest phenotype of *N1N2KO* mice was unexpected and is in contrast to the skin, where genetic inactivation of *Rbpj* and *Notch1*/*Notch2* leads to similar phenotypes (Schouwey et al., 2007).
The different impact of pancreatic *Notch1/2* and *Rbpj* inactivation in our study strongly suggests a Notch-independent role of *Rbpj* in pancreatic organogenesis. The almost complete absence of acinar cells until late gestation suggests that RBPJκ is required for the formation of the acinar lineage. Our results are in line with a Notch-independent role of RBPJκ as an obligate partner of PTF1A to form a functional PTF1 complex, a pivotal event during early pancreatic development. Thus, RBPJκ in *N1N2KO* mice might still function as a PTF1A-binding partner independently of its transducer role in the Notch siganling pathway.
In conclusion, we demonstrate an essential role of *Rbpj*, but not of *Notch1* and *Notch2*, in pancreatic organogenesis. This finding strongly suggests that these receptors, but not *Rbpj*, are dispensable for exocrine and endocrine development. Thus, at least in the pancreas, a Notch-independent role of *Rbpj* during development seems to be a likely mechanism.

Experimental procedures

Detailed description in the paper (Appendix 4)

Generation of *Rbpj*$^{lox/lox}$ mice

In order to generate conditional gene *Rbpj*-knockout mice, *loxP* sites were inserted flanking exons 6 and 7. Cre-recombination leads to deletion of an *Rbpj* gene fragment encoding the DNA-binding domain (details in Appendix 1).

Disclosure

Pawel K. Mazur contribution to the publication included: acquisition of data and reagents contribution.

References

Apelqvist, A., Li, H., Sommer, L.*, et al.* (1999). Notch signalling controls pancreatic cell differentiation. Nature *400*, 877-881.

Beres, T. M., Masui, T., Swift, G. H.*, et al.* (2006). PTF1 is an organ-specific and Notch-independent basic helix-loop-helix complex containing the mammalian Suppressor of Hairless (RBP-J) or its paralogue, RBP-L. Mol Cell Biol *26*, 117-130.

Besseyrias, V., Fiorini, E., Strobl, L. J.*, et al.* (2007). Hierarchy of Notch-Delta interactions promoting T cell lineage commitment and maturation. J Exp Med *204*, 331-343.

Esni, F., Ghosh, B., Biankin, A. V.*, et al.* (2004). Notch inhibits Ptf1 function and acinar cell differentiation in developing mouse and zebrafish pancreas. Development *131*, 4213-4224.

Fujikura, J., Hosoda, K., Iwakura, H.*, et al.* (2006). Notch/Rbp-j signaling prevents premature endocrine and ductal cell differentiation in the pancreas. Cell Metab *3*, 59-65.

Fujikura, J., Hosoda, K., Kawaguchi, Y.*, et al.* (2007). Rbp-j regulates expansion of pancreatic epithelial cells and their differentiation into exocrine cells during mouse development. Dev Dyn *236*, 2779-2791.

Hald, J., Hjorth, J. P., German, M. S.*, et al.* (2003). Activated Notch1 prevents differentiation of pancreatic acinar cells and attenuate endocrine development. Dev Biol *260*, 426-437.

Jensen, J., Pedersen, E. E., Galante, P.*, et al.* (2000). Control of endodermal endocrine development by Hes-1. Nat Genet *24*, 36-44.

Lammert, E., Brown, J., and Melton, D. A. (2000). Notch gene expression during pancreatic organogenesis. Mech Dev *94*, 199-203.

Masui, T., Long, Q., Beres, T. M.*, et al.* (2007). Early pancreatic development requires the vertebrate Suppressor of Hairless (RBPJ) in the PTF1 bHLH complex. Genes Dev *21*, 2629-2643.

Murtaugh, L. C., Stanger, B. Z., Kwan, K. M.*, et al.* (2003). Notch signaling controls multiple steps of pancreatic differentiation. Proc Natl Acad Sci U S A *100*, 14920-14925.

Nakhai, H., Sel, S., Favor, J.*, et al.* (2007). Ptf1a is essential for the differentiation of GABAergic and glycinergic amacrine cells and horizontal cells in the mouse retina. Development *134*, 1151-1160.

Radtke, F., Wilson, A., Stark, G.*, et al.* (1999). Deficient T cell fate specification in mice with an induced inactivation of Notch1. Immunity *10*, 547-558.

Schouwey, K., Delmas, V., Larue, L.*, et al.* (2007). Notch1 and Notch2 receptors influence progressive hair graying in a dose-dependent manner. Dev Dyn *236*, 282-289.

Chapter 6: Liver-specific inactivation of Notch2, but not Notch1, compromises intrahepatic bile duct development in mice.

This chapter is based on the original work published in *Hepatology*, August 2008, vol. 48, issue 2. The essential background and the most important findings are presented in this chapter whereas the full-published paper is attached as Appendix 5. The paper is reproduced with the publisher's permission.

Abstract

In humans, mutations in the Notch receptor ligand *Jagged1* gene result in defective intrahepatic bile duct (IHBD) development and subsequently in the Alagille Syndrome (AGS). In mice, heterozygous mutations in *Jagged1* and *Notch2* lead to IHBD defects suggesting their interaction is crucial for IHBD. Here, we investigated the effect of combined or single targeted disruption of *Notch1* and *Notch2* specifically in hepatoblasts and hepatoblast-derived lineage cells on liver development using *Alb-Cre* transgenic mice. Hepatocyte differentiation and homeostasis were not impaired in mice after combined deletion of *Notch1* and *Notch2*. However, we detected irregular ductal plate structures in mutated newborns. Moreover, postnatal development of IHBD was severely impaired resulting in disorganized primitive biliary structures accompanied by portal inflammation fibrosis, and foci of hepatocyte feathery degeneration in adulthood. Further characterization of mutant mice showed that *Notch2* but not *Notch1*, is crucial for normal perinatal and postnatal IHBD development.

Introduction

In humans and rodents intrahepatic bile duct (IHBD) development begins with the condensation of hepatoblasts forming a single continuous cell layer around the larger portal veins called the ductal plate. Later, parts of the ductal plate reduplicate and dilate to form tubular structures eventually forming biliary tree (Crawford, 2002, Lazaridis et al., 2004, Shiojiri, 1997). In humans, abnormalities of this process lead to diseases such as Congenital Hepatic Fibrosis, Caroli's syndrome, Alagille syndrome (AGS). The latter is caused by mutations in the Notch ligand *Jagged1* (Li et al., 1997 Oda et al., 1997). Mice with a heterozygous mutation of *Jagged1* and a hypomorphic *Notch2* allele showed features of human AGS (McCright et al., 2002). Conditional hepatoblast-specific inactivation of *Jagged1* using *Alfp-Cre* mice with a concomitant hypomorphic mutation of the *Notch2* allele leads to bile duct abnormalities in 50% of mice (Loomes et al., 2007). All studies indicate that *Jagged1* is important for bile duct development; it may primarily not act cell-autonomously in hepatoblasts but in adjacent cells to activate Notch signaling in hepatic progenitor cells and/or other cell compartments that are crucial for proper IHBD development. On the other hand, the Notch2 site of action is unclear and a possible contribution of other Notch receptors in tissue-specific knockout models has not been investigated.

Here, we investigated the effects of combined or single conditional ablation of *Notch1* and *Notch2* in hepatobiliary development and homeostasis using *Alb-Cre* mice. We proof that *Notch2* but not *Notch1*, is essential for normal IHBD development and morphogenesis in mice.

Results

Targeted liver-specific disruption of Notch1 and Notch2

To study the function of Notch-signaling in perinatal and postnatal liver we generated conditional knockout mice in which both *Notch1* and *Notch2* are inactivated specifically in the liver (*Alb-Cre;N1N2KO*), (Fig. 6.13). The embryonic liver albumin expression occurs in hepatoblasts as early as 13.5 days of gestation before intrahepatic bile ducts start to differentiate from periportal hepatoblasts at E15 (Shiojiri, 1997). Consistently, when crossing *Alb-Cre* mice with a *Rosa26-LacZ* reporter mouse (Soriano, 1999), liver parenchymal cells and the vast majority of bile ducts but not hematopoietic cells or portal vein mesenchyme were X-gal positive (see the paper in Appendix 5).

Because IHBD development in the mouse continues beyond the first weeks after birth we first analyzed the histological organization of the liver architecture after postnatal bile duct development in 4-week old *Alb-Cre;N1N2KO* mice. Livers of 4-week old *Alb-Cre;N1N2KO* mice were not distinguishable from controls on gross examination. However, histological analysis revealed that combined deletion of *Notch1* and *Notch2* resulted in a very disorganized biliary system. In all mice investigated (n=12), portal and periportal areas and interlobular septs displayed multiple arborizing pan-CK positive ductular structures that extended far into the hepatic lobe (Fig. 6-1-6). Besides these irregular ductular structures which were abundant in all *Alb-Cre;N1N2KO* mice, portal areas with proliferation and distortion of mature bile ducts accompanied by mild portal inflammation was observed in 9/12 animals with mild deposits of collagen (see Appendix 5). These morphological changes were most pronounced in the periphery of the hepatic lobes and are suggestive of local cholestasis. In this context, small foci of hepatocyte feathery degeneration were also observed in 5/12 animals.

Early postnatal IHBD development is impaired in Alb-Cre;N1N2KO mice

Typical ductal plate remodeling at postnatal day 1 (P1) was apparent by the detection of pan-CK-positive epithelial cells forming tubular and non-tubular structures around the larger portal veins (Fig. 6.7-8). At day P10 (Fig. 6.9-10) and P20 (Fig. 6.11-12) the tubular structures further progressed into mature differentiated bile ducts and well integrated into the portal mesenchyme. However, ductal plate cells were also detected in *Alb-Cre;N1N2KO* animals at P1, cells were mostly arranged irregularly around the portal veins and did not form typical tubular structures (Fig. 6.8). At P10 (Fig. 6.10), the vast majority of portal tracts did not contain differentiated bile ducts. Instead, ductal plate remnants and abnormal CK-positive epithelial cells were abundant in the periportal area.

At P20 (Fig. 6.12) the number of these cells further increased now forming tubular structures disorganized and mostly not integrated into the portal mesenchyme.

In summary, cell-specific combined disruption of *Notch1* and *Notch2* leads to a disorganized irregular bile duct system most likely due to impaired morphogenesis and branching of the biliary tree.

Notch2, but not Notch1, is indispensable for normal IHBD development

To elucidate whether both *Notch1* and *Notch2* are required for normal bile duct development and morphogenesis, we analyzed a single Notch mutant at 4-week

of age. The phenotype observed in *Alb-Cre;N1N2KO* animals was completely rescued in mice carrying only one or two WT *Notch2* alleles, indicating that disruption of *Notch1* alone does not alter liver development. When analyzing *Alb-Cre;Notch2* knockout mice (*Alb-Cre;N2KO*) we found the same morphological phenotype as in double mutant *Alb-Cre;N1N2KO* (Fig. 6.15, 5.4). That suggests that Notch1 and Notch2 have non-redundant functions in IHBD development. We used transgenic *Notch1-GFP* (Lewis et al., 1998) and *Notch2*$^{+/lacZ}$ reporter mice (Hamada et al., 1999) to analyze the Notch expression pattern during IHBD development.

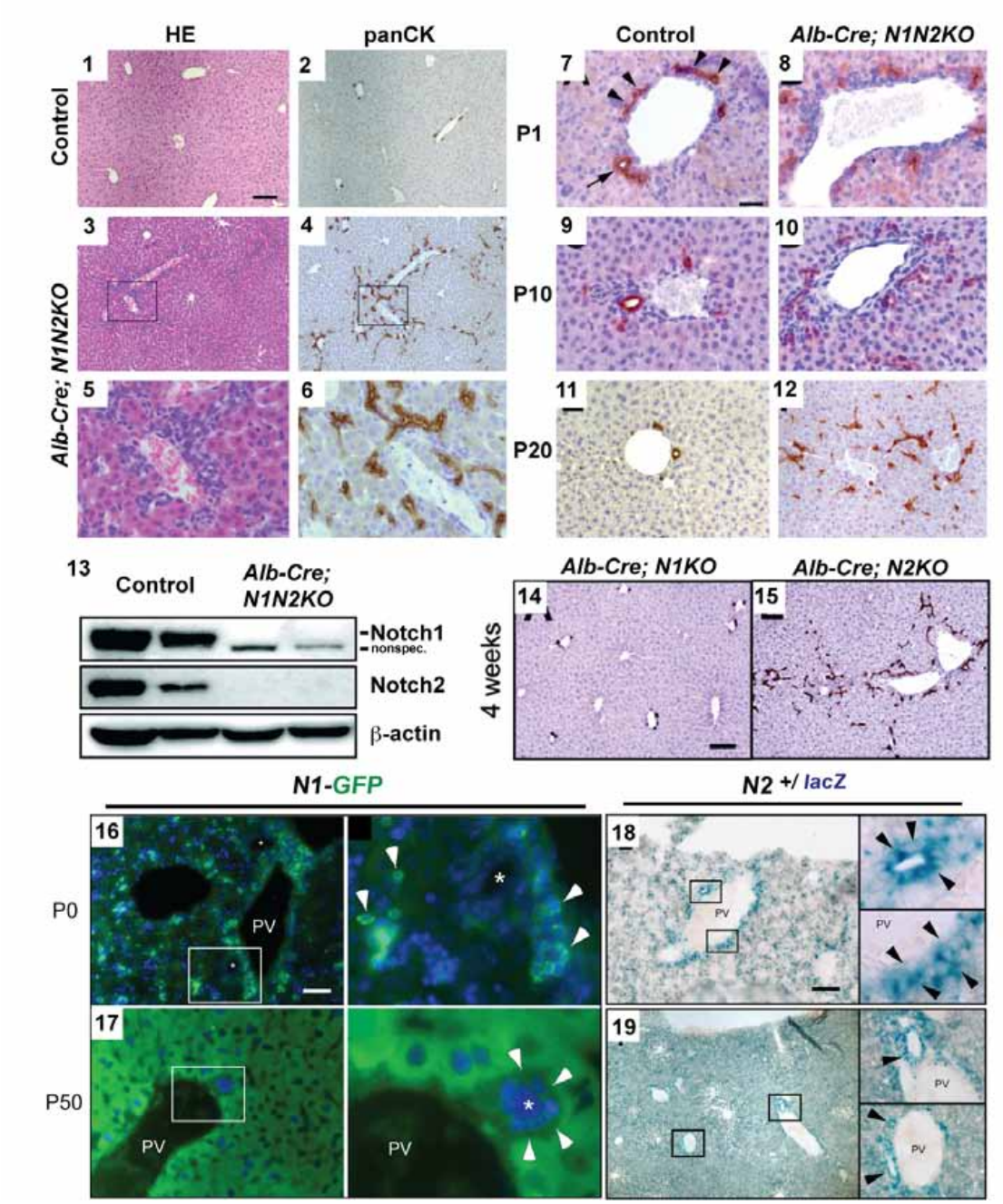

Figure 6. Liver-specific inactivation of Notch2, but not Notch1, compromises intrahepatic bile duct development in mice (detailed description in text).

Notch1 was absent in bile ducts but could be detected in hepatocytes and in a number of cells with small cytoplasm distributed throughout the liver at P1, most likely cells of the hematopoetic system (Fig. 6.16-17). In contrast, X-Gal staining of *Notch2*$^{+/lacZ}$-liver revealed strong staining in developing and mature bile ducts (Fig. 6-18-19) whereas only a weak stain marked hepatocytes and other liver cells. This expression profile further supports our conclusions deduced from morphological findings in single mutant mice that Notch2, but Notch1, plays a decisive role in IHBD development.

Discussion

In this study, we analyzed the role of liver-specific Notch1 and Notch2 ablation to hepatobiliary development and homeostasis. Mice lacking liver Notch2 have strongly disorganized ductal cells along with impaired early postnatal remodeling of ductal plate structures. Additionally, we found local cholestasis, feathery necrosis, portal inflammation, and enlarged portal tract expansion with collagen deposits. Since non of these abnormalities were found analyzing *Alb-Cre;N1KO* we conclude that impaired Notch2 but not Notch1 signaling, is responsible for the observed liver pathology.

In all *Notch2* deficient animals we have investigated, the structural IHBD abnormalities were most pronounced in the periphery of the liver lobes whereas in the central regions most portal tracts contained mature, albeit frequently distorted bile ducts next to primitive pan-CK-positive ductular structures. Similar spatial disparities of IHBD morphology have been described for human AGS supporting the concept that Notch signaling is crucial for normal postnatal branching and elongation of IHBD (Libbrecht et al., 2005). However, it must be considered that in *Alb-Cre* animals Cre-mediated deletion of *floxed* alleles occurs progressively with age (Postic and Magnuson, 2000) and bile duct development and morphogenesis around larger central portal veins starts at around E15 before development of the biliary tree branches. Thus, it may be the case that embryonic Notch2 levels still allow largely regular development and morphogenesis of functional IHBD in the central parts of the liver thus preventing mice from severe generalized cholestasis and liver damage. Progressive and cumulative *Alb-Cre* recombination my partially explain the phenotype. Since Notch2 ablation below level capable to drive proper bile duct branches development occurs late, only the peripheral branches are predominantly handicapped.

How does impaired Notch2 signaling in biliary precursor cells lead to impaired IHBD development? Two sequential steps are necessary for IHBD formation: lineage commitment of hepatoblasts to differentiate into biliary epithelial cells and further morphogenesis and maturation to form the intrahepatic biliary tree. The detection of ductal plate cells and biliary epithelial structures in *Alb-Cre;N2KO* mice suggests that Notch2 is not decisive for initial lineage commitment, although we cannot rule out that trace amounts of Notch2 might suffice for this process during embryogenesis. Nevertheless, Notch2 signaling seems to be especially important for normal ductal plate remodeling and further maturation of primitive biliary structures to mature bile ducts. We speculate that Jagged1 signals from adjacent portal vein and hepatic artery endothelial cells (Kodama et al., 2004, McCright et al., 2002) are necessary to properly guide bile

duct development along portal veins thus leading to disorganized biliary structures once Notch2 signaling is impaired in biliary epithelial cells.
In conclusion, we provide evidence, that single targeted disruption of *Notch2*, but not *Notch1*, leads to impaired IHBD development supporting a central role of Notch2 in biliary cell maturation and morphogenesis. Additional genetic and *in vitro* studies are required to further unravel the molecular mechanisms to define the role of Notch1 and Notch2 in hepatobiliary development and disease.

Experimental procedures

For detailed description of experimental procedures see Appendix 5.

Mice
Mice carrying conditional knockout alleles for *Notch1* (Radtke et al., 1999) and *Notch2* (Besseyrias et al., 2007) were crossed with transgenic mice carrying a Cre gene under control of the albumin enhancer promoter (Postic et al., 1999).

Disclosure

Pawel K. Mazur participation in the publication included: acquisition of data and reagents contribution.

References

Besseyrias, V., Fiorini, E., Strobl, L. J.*, et al.* (2007). Hierarchy of Notch-Delta interactions promoting T cell lineage commitment and maturation. J Exp Med *204*, 331-343.

Crawford, J. M. (2002). Development of the intrahepatic biliary tree. Semin Liver Dis *22*, 213-226.

Hamada, Y., Kadokawa, Y., Okabe, M.*, et al.* (1999). Mutation in ankyrin repeats of the mouse Notch2 gene induces early embryonic lethality. Development *126*, 3415-3424.

Kodama, Y., Hijikata, M., Kageyama, R.*, et al.* (2004). The role of notch signaling in the development of intrahepatic bile ducts. Gastroenterology *127*, 1775-1786.

Lazaridis, K. N., Strazzabosco, M., and Larusso, N. F. (2004). The cholangiopathies: disorders of biliary epithelia. Gastroenterology *127*, 1565-1577.

Lewis, A. K., Frantz, G. D., Carpenter, D. A.*, et al.* (1998). Distinct expression patterns of notch family receptors and ligands during development of the mammalian inner ear. Mech Dev *78*, 159-163.

Li, L., Krantz, I. D., Deng, Y.*, et al.* (1997). Alagille syndrome is caused by mutations in human Jagged1, which encodes a ligand for Notch1. Nat Genet *16*, 243-251.

Libbrecht, L., Spinner, N. B., Moore, E. C.*, et al.* (2005). Peripheral bile duct paucity and cholestasis in the liver of a patient with Alagille syndrome: further evidence supporting a lack of postnatal bile duct branching and elongation. Am J Surg Pathol *29*, 820-826.

Loomes, K. M., Russo, P., Ryan, M.*, et al.* (2007). Bile duct proliferation in liver-specific Jag1 conditional knockout mice: effects of gene dosage. Hepatology *45*, 323-330.

McCright, B., Lozier, J., and Gridley, T. (2002). A mouse model of Alagille syndrome: Notch2 as a genetic modifier of Jag1 haploinsufficiency. Development *129*, 1075-1082.

Oda, T., Elkahloun, A. G., Pike, B. L.*, et al.* (1997). Mutations in the human Jagged1 gene are responsible for Alagille syndrome. Nat Genet *16*, 235-242.

Postic, C., and Magnuson, M. A. (2000). DNA excision in liver by an albumin-Cre transgene occurs progressively with age. Genesis *26*, 149-150.

Postic, C., Shiota, M., Niswender, K. D.*, et al.* (1999). Dual roles for glucokinase in glucose homeostasis as determined by liver and pancreatic beta cell-specific gene knock-outs using Cre recombinase. J Biol Chem *274*, 305-315.

Radtke, F., Wilson, A., Stark, G.*, et al.* (1999). Deficient T cell fate specification in mice with an induced inactivation of Notch1. Immunity *10*, 547-558.

Shiojiri, N. (1997). Development and differentiation of bile ducts in the mammalian liver. Microsc Res Tech *39*, 328-335.

Soriano, P. (1999). Generalized lacZ expression with the ROSA26 Cre reporter strain. Nat Genet *21*, 70-71.

Chapter 7: Overview and Conclusions

Conclusions

The topic of this thesis poses a great challenge. The Notch signaling pathways is of high complexity despite the rather basic-appearing downstream signaling, affects nearly every tissue lineage of every higher animal and is involved in many diseases. Although we know about Notch mutations causing defects in *Drosophila* development for almost 100 years now, the field of Notch research has only recently taking momentum as a result of a few milestone papers including Notch gene cloning form *Drosophila* in 1983 (Artavanis-Tsakonas et al., 1983) and the accurate model of Notch activation and signal transduction in mid 1990's (Struhl et al., 1993, Jarriault et al., 1995). Thus, we observe an utter explosion of Notch-related studies in the past decade with over for 300 original articles published only in 2008 alone and several thousands of publications so far.

This thesis contributes to the Notch field with following conclusions that have been achieved:

1. *Rbpj* but not *Notch1* or *Notch2* is essential for exocrine pancreas development and proper endocrine cell differentiation.

2. *Notch2* but not *Notch1* is crucial for normal perinatal and postnatal intrahepatic bile duct development.

3. Notch signaling is required for exocrine regeneration after acute pancreatitis *via* modulation of β-catenin signaling.

4. Notch1 and Notch2 receptors are expressed in different compartments in adult pancreata.

5. Notch2 but not Notch1 is activated in $Kras^{G12D}$-induced tumorigenesis.

6. Notch2 acts as a pro-oncogene and is crucial for PanIN lesion development and progression.

7. *Notch2* ablation in $Kras^{G12D}$-induced tumorigenesis leads to MCN-like lesions and late appearing undifferentiated cancers development.

8. In pancreatic cancer Notch2 acts through modulation of MYC signaling

9. Notch1 but not Notch2 is a tumor suppressor in the skin, having different influences on β-catenin signaling

10. PDX1 is expressed in the skin.

Perspectives

Frontiers of pancreatic cancer research

The conquest of pancreatic cancer continuous to pose a great challenge to biomedical science. To date the so-called Whipple Operation, pancreatico-duodenectomy in medical terms, is the only effective treatment of PDAC. However, it involves the removal of the gallbladder, common bile duct, duodenum, pancreas with tumor, requires extensive experience by the surgeons performing the operation and imposes often a dramatically reduced comfort of living for the patient. Moreover, such curative operations are possible in less than 20 percent of patients. On the other hand, the results of standard chemotherapy in the management of patients with unresectable pancreatic cancer have been very disappointing, although occasional patients benefit significantly from the use of gemcitabine or 5-flourouracil. Because of the inadequacy of present methods of treatment, pancreatic cancer represents an ideal setting in which to explore the efficacy of many of the newly developed forms of biological anti-tumor treatment.

New less toxic agents for cancer treatment include antibodies, enzymes inhibitors and target-specific molecules that block mutated protein functions. These therapies are often referred to as "targeted" because although they are still a type of chemotherapy they interact only with a specific, mutated protein. Therapy success is additionally limited to tumors reflecting a particular molecular aberration, whereas the current classification of cancers is mainly based on morphology than DNA and RNA analysis.

Oncogene addiction vs. moving target

Why there is so much excitement about new target cancer therapy? One reason is based on a somehow surprising consequence of oncogene suppression i.e. tremendous reduction of cancer cell number due to cell death. The hypothesis that a cancer cell is dependent on a particular oncogene for viability and not just growth is known as oncogene addiction. This concept foster efforts to identify new therapeutics against mutated oncogenes. The flip side of oncogene addiction is addiction to lack of a tumor suppressor. It is the most evident in the case of p53. This tumor suppressor pathway is mutated in the majority of human cancers and p53 restoration leads to tumor retraction.

Second, the hypothesis of cancer emergence proposes that stochastic accumulation of tumor suppressor inactivation and oncogene activation mutations progressively drives the evolution of cancer from benign expansion of cells to an invasive malignancy. This concept perceives cancer as a "moving target" that is very difficult to destroy because it is constantly changing (review by Sharma and Settleman, 2007).

Pancreatic cancer is believed to occur through sequential acquisition of mutations, which would favor the 'moving target ' hypothesis, although 95% of cancers are associated with mutations of *Kras* leaving this oncogene a hallmark for PDAC. Targeting the oncogenic RAS has been a goal in cancer research for over 20 years, but success has been elusive. Approaches include inhibition of posttranslational farnesylation, using rybozymes and RNAi technology. Blocking the posttranslational processing by farnesyltransferase inhibitors has a weakness. It blocks modification of other cellular proteins and what is more

important KRAS among other RAS proteins is the only one resistant to farnesyltransferase inhibition. The only one feasible and precise tool is RNA interference using shRNA to target the transcript degradation. Successfully applied by Zhu et al., 2006, it could be proven that reduction of the *Kras* transcript by shRNA and thus reduced protein production completely inhibited growth of human cancer cells *in vitro* and in xenograft mice. These results suggest dependence of pancreatic cancer cells on the KRAS oncogene. However, reliable therapeutic agents are currently lacking and the RNAi approach remains an experimental tool so far.

Tumor environment

Understanding tumor environment is providing new opportunities to develop new therapies. The best known is the anti-angiogenic strategy for 'starving the tumor' by restricting blood supply. Successful use of antibodies against VEGF (that stimulates endothelial cell proliferation) has been reported, although pancreatic cancer is largely resistant to this therapy (Saif, 2006). There are, however grounds for optimism about other approaches to address tumor's milieu by interfering with growth-promoting signals from non-cancerous 'stromal cells' particularly active in the pancreatic cancer, inhibiting specific proteases (matrix metalloproteases, MMP) that promote tumor metastasis (Coussens et al., 2002) and by promoting an immune response by inactivating factors like T-cell surface protein CTLA-4 (overview by Egen et al., 2002). However, none of these approaches have yet led to clinical therapeutic advancements.

Notch as a target for therapy

Only a few malignancies such as leukemia (T-ALL) are directly caused by Notch mutations leading to constitutive activation. However, Notch receptors are overexpressed in a broad spectrum of tumors that includes activation of Notch2 in pancreatic cancer (Chapter 2). Most of the studies indicate that such a hyperactivation can be oncogenic. In fact, enforced expression of Notch in mouse models leads or promotes the development of various tumors e.g. T-cell lymphoma, T-ALL, mammary gland carcinoma, pancreatic cancer (De La et al., 2008, Gallahan and Callahan, 1997, Bellavia et al., 2000). Moreover, certain cancers exploit Notch downstream signaling in order to maintain the transformed phenotype. In the best-known case of Epstein-Barr virus-driven B-cell lymphoma viral protein Nuclear Antigen-2 binds to RBPJκ and mimics Notch activation (Zimber-Strobl and Strobl, 2001). Additionally, it is believed that Notch being implicated in self-renewal and stem cell maintenance is contributing to neoplasia through for instance cell death inhibition or sustaining the undifferentiated state of the cell.

All above provides rationale for Notch inhibition in cancer. This can be achieved in many ways: blocking ligand binding, preventing ligand trafficking, inhibiting intramembranous proteolysis or interfering with already activated Notch. First, the ligand binding blocking can be reached by competitive inhibition using recombinant protein binding to EGF-repeats Garces et al., 1997 or monoclonal antibodies.

Notch proteolysis can be inhibited by inactivation of ADAM metalloproteases or γ-secretase in the presenilin complex. Only the latter is feasible since ADAM

proteases have a broad range of cellular targets, whereas γ-secretase is implicated mainly with APP processing. In fact, the pharmaceutical industry has directed an immense interest in γ-secretase inhibitors (GSI), because of its ability to cleave APP, producing amyloid peptides, which are believed to play an important role in the pathogenesis of Alzheimer's disease. However, the lack of specificity prevents it from providing a treatment for Alzheimer's disease. The side effects of GSI include altered lymphopoiesis and intestinal cell differentiation (Wong et al., 2004), which correlates well with the effect of blocking Notch in these systems (Chapter 4). However, despite the adverse effects, there is a chance that a periodic treatment with GSI may produce an acceptable level of toxicity and at the same time is tumor-suppressive in Notch dependent neoplasias. The successful use of GSI as a chemo-preventive therapy has been recently reported in a mouse model of pancreatic cancer (Plentz et al., 2009)

The last but most promising way of inhibiting Notch is direct interference with the transcription complex Notch-RBPJκ-MAM that activates downstream target genes. Recently, the group of Dr. Bradner used a synthetic, cell-permeable 'stapled peptide' that targets the Notch transactivation domain with a high-affinity thus preventing assembly of the active transcription complex. The method was proved working in a mouse model of T-ALL, where it induced a Notch-specific anti-proliferative effect (Moellering et al., 2009).

Less explored areas of using Notch as a target for therapy involved its activation. Theoretically, neoplasias where Notch was proven to act as a tumor suppressor (e.g. skin, see Chapter 3) are good targets for Notch activation, however taking into consideration the consequences of an increased Notch activity in other tissues such a therapy is possible difficult and dangerous.

Nevertheless, the Notch activation might be potentially important for stem cell maintenance, tissue engineering and regenerative medicine. Notch activation can be achieved by addition of soluble ligands, inhibition of processing and degradation or activation of direct target genes. All of which require a unique condition possible so far in cell cultures. However, successful immortalization of hematopoietic stem cells by constitutive activation of Notch reported by Varnum-Finney et al., 2000 proofs enormous potential.

References

Artavanis-Tsakonas, S., Muskavitch, M. A., and Yedvobnick, B. (1983). Molecular cloning of Notch, a locus affecting neurogenesis in Drosophila melanogaster. Proc Natl Acad Sci U S A *80*, 1977-1981.

Bellavia, D., Campese, A. F., Alesse, E.*, et al.* (2000). Constitutive activation of NF-kappaB and T-cell leukemia/lymphoma in Notch3 transgenic mice. EMBO J *19*, 3337-3348.

Coussens, L. M., Fingleton, B., and Matrisian, L. M. (2002). Matrix metalloproteinase inhibitors and cancer: trials and tribulations. Science *295*, 2387-2392.

De La, O. J., Emerson, L. L., Goodman, J. L.*, et al.* (2008). Notch and Kras reprogram pancreatic acinar cells to ductal intraepithelial neoplasia. Proc Natl Acad Sci U S A *105*, 18907-18912.

Egen, J. G., Kuhns, M. S., and Allison, J. P. (2002). CTLA-4: new insights into its biological function and use in tumor immunotherapy. Nat Immunol *3*, 611-618.

Gallahan, D., and Callahan, R. (1997). The mouse mammary tumor associated gene INT3 is a unique member of the NOTCH gene family (NOTCH4). Oncogene *14*, 1883-1890.

Garces, C., Ruiz-Hidalgo, M. J., Font de Mora, J.*, et al.* (1997). Notch-1 controls the expression of fatty acid-activated transcription factors and is required for adipogenesis. J Biol Chem *272*, 29729-29734.

Jarriault, S., Brou, C., Logeat, F.*, et al.* (1995). Signalling downstream of activated mammalian Notch. Nature *377*, 355-358.

Moellering, R. E., Cornejo, M., Davis, T. N.*, et al.* (2009). Direct inhibition of the NOTCH transcription factor complex. Nature *462*, 182-188.

Plentz, R., Park, J. S., Rhim, A. D.*, et al.* (2009). Inhibition of gamma-secretase activity inhibits tumor progression in a mouse model of pancreatic ductal adenocarcinoma. Gastroenterology *136*, 1741-1749 e1746.

Saif, M. W. (2006). Anti-angiogenesis therapy in pancreatic carcinoma. JOP *7*, 163-173.

Sharma, S. V., and Settleman, J. (2007). Oncogene addiction: setting the stage for molecularly targeted cancer therapy. Genes Dev *21*, 3214-3231.

Struhl, G., Fitzgerald, K., and Greenwald, I. (1993). Intrinsic activity of the Lin-12 and Notch intracellular domains in vivo. Cell *74*, 331-345.

Varnum-Finney, B., Xu, L., Brashem-Stein, C.*, et al.* (2000). Pluripotent, cytokine-dependent, hematopoietic stem cells are immortalized by constitutive Notch1 signaling. Nat Med *6*, 1278-1281.

Wong, G. T., Manfra, D., Poulet, F. M.*, et al.* (2004). Chronic treatment with the gamma-secretase inhibitor LY-411,575 inhibits beta-amyloid peptide production and alters lymphopoiesis and intestinal cell differentiation. J Biol Chem *279*, 12876-12882.

Zhu, H., Liang, Z. Y., Ren, X. Y.*, et al.* (2006). Small interfering RNAs targeting mutant K-ras inhibit human pancreatic carcinoma cells growth in vitro and in vivo. Cancer Biol Ther *5*, 1693-1698.

Zimber-Strobl, U., and Strobl, L. J. (2001). EBNA2 and Notch signalling in Epstein-Barr virus mediated immortalization of B lymphocytes. Semin Cancer Biol *11*, 423-434.

Biographical note

Name:	Pawel Karol MAZUR,
Date of birth:	August 7, 1981
Place of birth:	Kolbuszowa, Poland

Education

9/2005-11/2010	PhD, *Summa cum laude,* Technical University of Munich – International Max Planck Research School,
10/2003-9/2005	MSc, *Summa cum laude*, Molecular biology, Warsaw University
10/2000-9/2003	BSc, *Summa cum laude*; Biology, Warsaw University
9/1996-6/2000	Matura (A-levels) *Summa cum laude,* Janek Bytnar High School
9/1991-6-1998	Graduated with distinction*,* State Music School, piano, voice class
9/1988-6/1996	Graduated with distinction, Henryk Sienkiewicz Elementary School

Research Experience

1/2006-present	International Max Planck Research School, Fellowship of University Hospital Technical University of Munich
9-12/2005	International Max Planck Research School, Fellowship of Max Planck Institute orientation, coursework and laboratory rotations
6-9/2004	Summer Undergraduate Research Program, Cold Spring Harbor Laboratory, New York, USA; Advisor Prof. M. Timmermans, miRNA166 in development
9/2003-7/2005	Laboratory of Plant Molecular Biology, Warsaw University; Advisor: Prof. A. Jerzmanowski; BSc and MSc thesis: Retinoblastoma protein in development
6-9/2002	Research Internship in Institute of Biochemistry and Biophysics, Polish Academy of Science, Mentor Prof. Zagorski-Ostoja, GM plants generation
4/2000	Research Internship in Faculty of Chemistry; Warsaw University, Mentor: Dr. D.Pawlak, Sponsored by Polish Children's Found
3/2000	Research Internship in Medical Research Center, Polish Academy of Science, Mentor: Prof. P. Grieb, Sponsored by Polish Children's Found;
1-2/1999	Research Internship in Institute of Organic Chemistry, Polish Academy of Science, Mentor Prof. M. Makosza, Sponsored by Polish Children's Found;
6/1998	40th Summer Research School of Physics; Jagiellonian University in Krakow
3/1998	Research Internship in The Nencki Institute of Experimental Biology; Mentor: Prof. E. Wyroba, Sponsored by Polish Children's Found;

Honors and Awards

7/2009	American Association of Cancer Research Scholarship for Course in Pathobiology of Cancer-The Edward A. Smuckler Memorial
6/2009	Conference Scholarship awarded by Keystone Symposia
	EMBO Scholarship for Course in Mouse Anatomy and Embryology

9/2006	Conference Stipend awarded by Symposia 'Horizons of molecular biology'
10/2001-7/2005	Ministry of Education Scholarship, granted for highly talented students
12/2002	Mayor of Warsaw Prize for the Best Student of All-Warsaw Universities
5/2002	Global Leader Award-The Goldman Sachs Foundation and Institute of International Education, London, UK
4/2002	Student Representative in Warsaw University Senate
6/2000	First Prize on European Essay Contest
6/2000	Representative to Polish Youth Parliament-VI term of office
4/2000	Laureate of National Biology Olympiad for high school students the top 25
5/1999	Second Prize on United Nations Literary Competition for Essay "Seniors-towards generation solidarity"
11/1998	President of Poland Scholarship for Extraordinary Academic Achievements
9/1998-6/1999	Prime Minister Scholarship for the Best High School Student
5/1998; 5/1999	Honorable Mention in Category Research Papers in 6th and 7th International Competition First step to Nobel Prize in Physics
9/1997-9/2000	Polish Children's Fund Scholarship granted for three consecutive years; only ca. 15 scholarships per year are awarded
1997,1998,1999	Honorable Mentions on the 6th, 7th, 8th All-Poland Research Paper Competition

Publications

1/2010	Identification of Pdx1 expression in the skin discloses different roles of Notch1 and Notch2 in *Kras^{G12D}*-induced skin carcinogenesis, *PlosONE*
1/2010	Notch2-induced regulation of Myc signaling is crucial in pancreatic carcinogenesis, *PNAS*
9/2008	Conditional ablation of Notch signaling in pancreatic development, *Development*; Co-author
9/2008	Liver-specific inactivation of Notch2, but not Notch1, compromises intrahepatic bile duct development in mice, *Hepatology*; Co-author
1/2008	Notch signaling is required for exocrine regeneration after acute pancreatitis, *Gastroenterology*; Co-author
1/2003	Arabidopsis mutants education set, *Polish Journal of Natural Sciences*; Co-author

Other Publications and Presentations

8/2009	Talk on FEBS/EACR Course Molecular Mechanisms of Signal Transduction and Cancer, Spates, Greece
6/2009	Poster on Keystone Symposium Deregulation of Transcription in Cancer, Kerry, Ireland
2/2008	Poster on International Congress for Integrative Cancer Genomics Munich
9/2007	Poster on Gordon Conference: Mechanism of Cell Signaling, Oxford, UK
9/2006	Poster on International PhD Student Symposium, Gottingen, Germany
1/2006	Article: Evolution of Eukaryota, *Biology* [polish]
6/2005	Invited lecture for Academic Science Television (ATVN): Genes which makes a male: http://www.atvn.pl/archiwum/ram_new2.php?ID=2005-06-23/1

3/2005	Article: Plasmids, *Biology* [polish]
1/2005	Article: Storm of Hormones, *Science and life* [polish]
9/2003	Poster on Conference of the Polish Society for Plant Experimental Biology
7/2000	Talk on London International Youth Science Forum, London, UK

Professional Development

8/2009	FEBS and EACR Course in Molecular Mechanisms of Signal Transduction and Cancer, Spates, Greece
7/2009	AACR Course in Pathobiology of Cancer, The Edward A. Smuckler Memorial Workshop, Snowmass Village Resort - Aspen, Colorado, USA
9/2008	EMBO Course in Mouse Anatomy and Embryology, Zagreb, Croatia
6/2007-3/2009	Max Planck Institute Advanced Courses in: Statistics for Biologists, Fluorescence Activated Cell Sorting, Light Microscopy for Biologists, Histological and Immunohisto-chemical Techniques, Access to genes and genomes with Ensembl
9/2005-12/2009	Soft skills workshops: Effective Scientific Writing, Project Management, Presentation Skills, Designing and presenting a poster, Self and Time Management, Speed reading and memory enhancement, Intercultural Communication, Negotiation Skills, Presentation with Confidence, The Art of Small Talk, Application Skills, Self-management for Junior Scientists, Getting Funded
10/2003	20th European Evolutionary Biology Workshops, Warsaw
9/2003 – 6/2005	School of Science-Lecturer and instructor, Warsaw, Poland
5/2002	Global Leaders Program Meeting, London, UK
7/2000	London International Youth Science Forum, Sponsored by British Council
6/1999	European Youth Congress in the Netherlands, Sponsored by European Union

Affiliations/Memberships

9/2009-present	Member of American Association of Cancer Research (AACR)
8/2009-present	Member of European Association of Cancer Research (EACR)
9/2003-present	Founder, Chairman and Honorary Member of Warsaw University Students Scientific Society of Genetics and Epigenetics
6/2002-present	Alumnus of Goldman Sachs Foundation Global Leaders Program
1/2003-present	Polish Biochemical Society / Federation of European Biochemical Societies
10/2000-present	Alumnus Association of Polish Children Found

Interests

- Stand-up comedy: Best Stand-up Comedy performance at the 1st, 2nd, 3rd Youth Art Creation Festival "Feta" (1998-2000), Kolbuszowa, Poland
- Theater/acting: Theatre workshops-Siemaszkowa's Theatre (9/1998-6/1999), Rzeszow, Poland
- Music/piano: Member of chorus "Acordare" (9/1995-6/2000) in 1999 Best Acappella performance, Finished Music School (piano)
- Cybernetics, politics, economy (Laissez-faire, Austrian School)
- Sports: gym/workout, running, swimming

Lebenslauf

Name:	Pawel Karol MAZUR
Geburtsdatum:	7 August, 1981
Geburtsort:	Kolbuszowa, Polen

Ausbildung

9/2005-11-2010	Dr. rer. nat. (*summa cum laude*) Technische Universität München International Max Planck Research School,
10/2003-9/2005	Master of Science in Molekularbiologie (*summa cum laude*), Universität Warschau
10/2000-9/2003	Bachelor of Science in Biologie (*summa cum laude*), Universität Warschau
9/1996-6/2000	Matura/entspricht Abitur (*summa cum laude*), Janek Bytnar Gymnasium
9/1991-6-1998	Abschluss an der staatlichen Musikschule (Klavier-und Gesangsunterricht) mit Auszeichnung
9/1988-6/1996	Abschluss an der Henryk Sienkiewicz Grundschule, mit Auszeichnung

Forschung

Seit 1/2006	International Max Planck Research School und Klinikum rechts der Isar, Universitätsklinikum der Technischen Universität München
9-12/2005	Stipendiat des Max-Planck-Instituts, International Max Planck Research School-Lehrveranstaltungen und rotierende Laborkurse
6-9/2004	Forschungs-Programm für Studenten vor dem ersten akademischen Grad Cold Spring Harbor Labor, New York, USA; Betreuerin Prof. M. Timmermans. Thema: miRNA166 in development
9/2003-7/2005	Labor für Molekularbiologie der Pflanze, Universität Warschau, Betreuer Prof. A.Jerzmanowski; Bachelor- und Masterarbeit: Retinoblastoma protein
6-9/2002	Forschungspraktikum am Institut für Biochemie und Biophysik, Polnische Akademie der Wissenschaften, Betreuer Prof. Zagorski-Ostoja, Thema: Genmodifizierte Pflanzen

Auszeichnungen und Preise

7/2009	American Association of Cancer Research Stipendium für die Fortbildung: Pathobiology of Cancer – Edward A. Smuckler Memorial
6/2009	Stipendium für einen Konferenzbesuch verliehen durch das Keystone Symposia
9/2008	EMBO Stipendium für den Kurs Mouse Anatomy and Embryology
9/2006	Stipendium für einen Konferenzbesuch verliehen durch das Doktorandensymposium „Horizons of molecular biology“
10/2001-7/2005	Stipendium des Bundesministeriums für Bildung, vergeben an hochtalentierte Studenten

12/2002	Preis für den besten Studenten aller Warschauer Universitäten, verliehen durch den Bürgermeister Warschaus
5/2002	Global Leader Preis-The Goldman Sachs Foundation and Institute of International Education
4/2002	Studentischer Vertreter im Senat der Universität Warschau
6/2000	Erster Platz beim Europäischen Wettbewerb im Aufsatzschreiben
6/2000	Vertreter des Polnischen Jugendparlaments – 6 Amtszeiten
5/2000	Preisträger der National Biology Olympiad für Gymnasiasten (unter den 25 Besten)
5/1999	Zweiter Platz beim literarischen Aufsatzwettbewerb der Vereinigten Nationen
11/1998	Präsident des Polnischen Stipendiums für außergewöhnliche akademische Leistungen
9/1998-6/1999	Stipendium für den besten Gymnasiasten, verliehen durch den Ministerpräsidenten
5/1998; 5/1999	Lobende Anerkennung in der Kategorie Forschungsarbeiten im sechsten und siebten internationalen Wettbewerb: First step to Nobel Prize in Physics
9/1997-9/2000	Polish Children`s Fund Stipendium, gewährt für drei hintereinander folgende Jahre; nur etwa 15 Stipendien werden pro Jahr vergeben
1997,1998,1999	Lobende Anerkennungen im sechsten, siebten und achten Wettbewerb über Forschungsarbeiten in ganz Polen

Veröffentlichungen

1/2010	Notch2-induced regulation of Myc signaling is crucial in pancreatic carcinogenesis, *Manuskript*; Erstautor
1/2010	Identification of Pdx1 expression in the skin discloses different roles of Notch1 and Notch2 in $Kras^{G12D}$-induced skin carcinogenesis, *Manuskript*; Erstautor
9/2008	Conditional ablation of Notch signaling in pancreatic development, *Development*; Co-author
9/2008	Liver-specific inactivation of Notch2, but not Notch1, compromises intrahepatic bile duct development in mice, *Hepatology*; Co-author
1/2008	Notch signaling is required for exocrine regeneration after acute pancreatitis, *Gastroenterology*; Co-author
1/2003	Arabidopsis mutants education set, *Polish Journal of Natural Sciences*; Co-author

Andere Veröffentlichungen und Präsentationen

8/2009	Vortrag auf dem FEBS/EACR Lehrgang: Molecular Mechanisms of Signal Transduction and Cancer, Spetses, Griechenland
6/2009	Posterpräsentation auf dem Keystone Symposium: Deregulation of Transcription in Cancer, Kerry, Irland
2/2008	Posterpräsentation auf dem Internationalen Kongress: Integrative Cancer Genomics, München, Deutschland
9/2007	Posterpräsentation auf der Gordon Konferenz: Mechanism of Cell Signalling, Oxford, GB
9/2006	Posterpräsentation auf dem Internationalen Symposium in Göttingen, Deutschland
1/2006	Artikel: Evolution der Eukaryonten, Biologie [auf Polnisch]

6/2005	Gastredner im Akademischen Wissenschaftsfernsehen (ATVN): *Gene, die einen Mann ausmachen* [auf Polnisch]: http://www.atvn.pl/archiwum/ram_new2.Php?ID=2005-06-23/1; http://www.atvn.pl/archiwum/ram_new2.php?ID=2005-06-24/1
3/2005	Artikel: Plasmide, Biologie [auf Polnisch]
1/2005	Artikel: Sturm der Hormone, Wissenschaft und Leben [auf Polnisch]
9/2003	Posterpräsentation auf der Konferenz: Polish Society for Plant Experimental Biology
7/2000	Vortrag auf dem London International Youth Science Forum, London, GB

Beruflicher Werdegang

8/2009	FEBS/EACR Lehrgang: Molecular Mechanism of Signal Transduction and Cancer, Spetses, Griechenland
7/2009	AACR Lehrgang in Pathobiology of Cancer, Edward A. Smuckler Memorial Workshop, Snowmass Village Resort – Aspen, Colorado, USA
9/2008	EMBO Lehrgang in Mausanatomie und –embryologie, Zagreb, Kroatien
6/2007-3/2009	Fortgeschrittenenkurs in Statistik für Biologen, Durchflusszytometrie (FACS), Lichtmikroskopie für Biologen, Histologische und Immunohistochemische Techniken, Max-Planck Institut für Biochemie, Martinsried, Deutschland
9/2005-12/2009	Workshops der Soft Skills Serie, International Max-Planck Research School
5/2002	Treffen des Global Leaders Programms in London, GB
7/2000	London International Youth Science Forum, gefördert durch die British Council (Großbritanniens internationale Organisation für Bildung und Kultur)
6/1999	European Youth Congress in den Niederlanden, gefördert durch die Europäische Union

Mitgliedschaften

Seit - 9/2009	Mitglied der American Association of Cancer Research (AACR)
Seit - 8/2009	Mitglied der European Association of Cancer Research (EACR)
Seit - 9/2003	Gründer, Vorsitzender und Ehrenmitglied der wissenschaftlichen Gesellschaft Genetik und Epigenetik Warschauer Studenten
Seit - 6/2002	Alumnus des Global Leader Programms der Goldman Sachs Foundation
Seit - 1/2003	Mitglied der FEBS/Polnischen Gesellschaft für Biochemie
Seit - 10/2000	Alumnus des Polish Children Fund

Interessen

- Stand-up Comedy im Juni 1998, 1999, 2000 Bester Stand-up Comedian beim ersten, zweiten und dritten Jugendfestival für Kunst und Gestaltung „Feta“, Kolbuszowa, Polen
- Theater/Schauspiel, September 1998 bis Juni 1999 Theaterworkshops – Siemaszkowa Theater, Rzeszow, Polen
- Musik, Klavier, September 1995 bis Juni 2000 Mitglied des Chors „Acordare“, Abschluss an der Musikschule
- Kybernetik, Politik, Wirtschaftswissenschaft (Österreichischen Schule der Ökonomie)
- Sport: Fitnessstudio, Joggen, Schwimmen

Acknowledgments

I would especially like to thank the following people:

My supervisor prof. **Roland M. Schmid,** for taking me on as a PhD student in the beginning. You opened up the door to science for me, made me curious, and inspired me. I am grateful for your wisdom, patience and for your never exceeding encouragement.

My co-supervisor and my main scientific advisor Dr. **Jens T. Siveke**, for your immense knowledge of the scientific field, your generosity, positive attitude towards me and all the projects, and for letting me be a part of your team. I have particularly cherished your caring and joyful ways of work, making it strictly impossible to be in a bad mood around you.

My co-supervisor prof. Michael Schemann for your vast enthusiasm on science, support and practical guidance in the early time of my study.

International Max Planck Research school in particular prof. **Ulrich Hartl**, Dr. **Hans Joerg Schaeffer** and the coordination office for taking chances on me and for continuous support and great opportunities you gave me over the year.

Hassan Nakhai for your can-do spirit. I am utterly grateful that we could collaborate in the Notch field. I really miss our talks and your wise sayings.

Fabian Geisler for pleasure of working with you. Your strong and positive attitude really speeded things up, and made life in the lab more exciting.

Whole Siveke's lab: Barbara, Clara, Irina, Marcel, Roxanne, Silke and Mathilde, all of you for your sunny spirit and for never exhausting will to help out. Thanks for all good times!

I would like to express gratitude to my **Thesis Advisory Committee:** Prof. Dr. Roland M. Schmid, Prof. Dr. Hermann Wagner, Prof. Dr. Reinhard Faessler, Prof. Dr. Michael Schemann, PD Dr. med. Jens Siveke, PD Dr. med. Rudolf Rupec and Dr. Elke Burgermeister for great scientific input over the years

In particular I would like to express my gratitude to prof. **Reinhard Faessler** and his lab, for sharing their extensive knowledge and know-how.

Simone for being part of my life. Your support the last few months has been invaluable. Also, thank you for revising and proofreading my thesis.

Krzysztof, my brother and best friend, you give me strength and motivation. Thank you for always believing in me!

Mom and Dad, my two favorite persons in the whole world. I am truly grateful for your immense support and never-ending love.

Appendix 1

Pawel K. Mazur, Henrik Einwächter, Bence Sipos, Marcel Lee, Hassan Nakhai, Horst Hameister, Roland Rad, Nathalie Conte, Allan Bradley, Ursula Zimber-Strobl, Lothar J. Strobl, Freddy Radtke, Günter Klöppel, Roland M. Schmid, and Jens T. Siveke.

Notch2 is required for PanIN progression and development of pancreatic ductal adenocarcinoma

Proc Natl Acad Sci USA. 2010 Jul 27;107(30):13438-43.

Notch2 is required for progression of pancreatic intraepithelial neoplasia and development of pancreatic ductal adenocarcinoma

Pawel K. Mazur[a], Henrik Einwächter[a], Marcel Lee[a], Bence Sipos[b], Hassan Nakhai[c], Roland Rad[d], Ursula Zimber-Strobl[e], Lothar J. Strobl[e], Freddy Radtke[f], Günter Klöppel[g], Roland M. Schmid[a], and Jens T. Siveke[a,1]

[a]Second Department of Internal Medicine and [g]Institute of Pathology, Technical University of Munich, 81675 Munich, Germany; [b]Department of Pathology, University Hospital Tübingen, 72076 Tubingen, Germany; [c]Department of Biological Sciences, University of Warwick, Coventry CV4 7AL, United Kingdom; [d]The Wellcome Trust Sanger Institute, Cambridge CB10 1SA, United Kingdom; [e]Department of Gene Vectors, Helmholtz Center, 81377 Munich, Germany; and [f]Ecole Polytechnique Fédérale de Lausanne (EPFL SV ISREC), SV/Swiss Institute for Experimental Cancer Research, 1015 Lausanne, Switzerland

Edited by Elliott Kieff, Harvard Medical School and Brigham and Women's Hospital, Boston, MA, and approved June 8, 2010 (received for review February 26, 2010)

Pancreatic cancer is one of the most fatal malignancies lacking effective therapies. Notch signaling is a key regulator of cell fate specification and pancreatic cancer development; however, the role of individual Notch receptors and downstream signaling is largely unknown. Here, we show that Notch2 is predominantly expressed in ductal cells and pancreatic intraepithelial neoplasia (PanIN) lesions. Using genetically engineered mice, we demonstrate the effect of conditional Notch receptor ablation in *Kras^{G12D}*-driven pancreatic carcinogenesis. Deficiency of *Notch2* but not *Notch1* stops PanIN progression, prolongs survival, and leads to a phenotypical switch toward anaplastic pancreatic cancer with epithelial–mesenchymal transition. By expression profiling, we identified increased Myc signaling regulated by Notch2 during tumor development, placing Notch2 as a central regulator of PanIN progression and malignant transformation. Our study supports the concept of distinctive roles of individual Notch receptors in cancer development.

genetically engineered mice | K-Ras | Myc | Notch | pancreatic cancer

Pancreatic ductal adenocarcinoma (PDAC) remains a devastating disease despite tremendous therapeutical efforts. PDAC derives from several preneoplastic lesions, including pancreatic intraepithelial neoplasia (PanIN), intraductal papillary mucinous neoplasm, and mucinous cystic neoplasm (MCN), of which PanINs are the most common precursors (1). PanINs typically progress through defined histological and molecular stages, with the most advanced PanIN3 lesion being defined as carcinoma in situ (2). Because of early metastatic spread, PanIN3 represents the latest curable precursor lesion. Thus, defining the regulators of PanIN initiation and progression is of utmost importance.

Recapitulation of human pancreatic carcinogenesis was greatly advanced by generating mice with pancreas-specific activation of endogenous oncogenic *Kras^{G12D}* (3). The ongoing characterization of relevant signaling pathways in pancreatic carcinogenesis using genetically engineered mouse models has helped to depict the enormous plasticity in precursors to PDAC. Despite activation of cell fate regulating signaling pathways such as Hedgehog, Wnt, and Notch signaling (3–9), the precise role of these pathways remains largely unclear.

The Notch signaling pathway plays a pivotal role in cell fate and differentiation decisions, and its activation early in the carcinogenic process suggests a role in initiation of transformation. Although the cell of origin in PDAC has not been decisively identified, activation of Notch signaling during PanIN initiation probably presents a pivotal step for transformation. In several murine models of PDAC, expression of the Notch target gene *Hes1* was increased in PanIN lesions (3, 5, 8, 9). In a recent study, chemical inhibition of Notch activation completely blocked tumor progression in vivo (10). Conversely, Murtaugh and co-workers (11) described a PanIN-promoting effect of Notch activation in *Kras^{G12D}*-driven PanIN development. However, the specific role of individual Notch receptors and the downstream events have so far not been determined.

Here, we describe the effect of pancreas-specific ablation of *Notch1* and *Notch2* in *Kras^{G12D}*-driven pancreatic carcinogenesis, taking advantage of the nonessential role of Notch1 and Notch2 during pancreatogenesis (12). We show that Notch1 and Notch2 are expressed in pancreatic acinar and ductal cells, respectively. Conditional ablation of *Notch2* but not *Notch1* leads to an abrogation of PanIN progression, development of MCN-like lesions, and increased survival. Identification of Notch2-regulated Myc signaling during carcinogenesis points to a central role of Notch2 in controlling PanIN progression and tumor differentiation.

Results

Notch1 and Notch2 Are Expressed in Different Compartments in Adult Pancreata and Are Activated in *Kras* Mice During PanIN Development. To determine the expression of members of the Notch signaling family during pancreatic carcinogenesis, *Kras$^{+/LSL\text{-}G12D}$* mice were crossed to *Ptf1a$^{+/Cre(ex1)}$* mice (referred to as *Kras*; Fig. S1*C*), as previously described (9). Notch1 and Notch2 were predominantly expressed in whole-tissue mRNA from WT and *Kras^{G12D}*-induced pancreata compared with low expression of Notch3 and Notch4 (Fig. 1*A*). In *Kras* pancreata at 9 wk of age, when only a few PanIN1 lesions are notable, increased expression of Notch2 and the Notch target gene Hes1 but not Notch1 was observed, similar to previous reports (5). During progression, we noted a significant increase in Notch2 and Hes1 expression, whereas Notch1 was further reduced. Notch3 was also increased, albeit at lower total expression levels (Fig. 1*B*). This expression pattern correlated well with an increase in CK19 and a decrease in amylase expression, suggesting that Notch2 is expressed in CK19$^+$ PanINs, whereas Notch1 may be predominantly expressed in acinar cells. To test this hypothesis, we used transgenic *Notch1-GFP* and *Notch2^{lacZ}* knockin reporter mice (13, 14) to localize Notch1 and Notch2 expression in WT and *Kras* mice. In WT pancreata, we found X-Gal as a surrogate for Notch2 expression in ductal but not acinar or islet cells (Fig. 1*C*). Moreover, X-Gal$^+$ cells were notable in the typical centroacinar position thought to be a presumed progenitor cell compartment (15) (Fig. 1*C*). In

Author contributions: R.M.S. and J.T.S. designed research; P.K.M., H.E., M.L., B.S., H.N., R.R., and J.T.S. performed research; U.Z.-S., L.J.S., and F.R. contributed new reagents/analytic tools; P.K.M., H.E., M.L., B.S., H.N., R.R., G.K., and J.T.S. analyzed data; and P.K.M. and J.T.S. wrote the paper.

The authors declare no conflict of interest.

This article is a PNAS Direct Submission.

[1]To whom correspondence should be addressed. E-mail: jens.siveke@web.de.

This article contains supporting information online at www.pnas.org/lookup/suppl/doi:10.1073/pnas.1002423107/-/DCSupplemental.

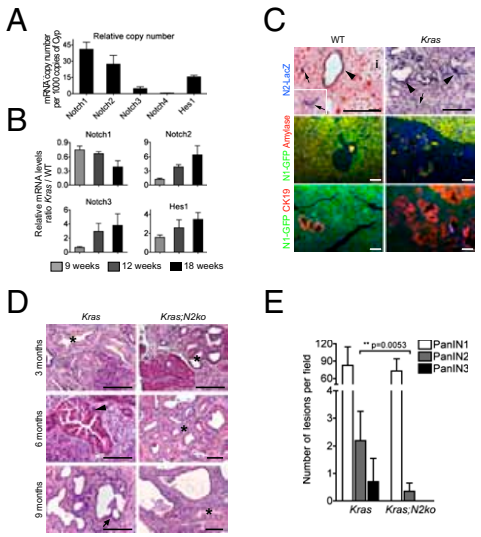

Fig. 1. Expression analysis of Notch receptors in WT and *Kras*^{G12D}-induced pancreata. (*A*) Transcript levels of Notch receptors and Hes1 in relation to cyclophilin gene expression in WT pancreata (n = 3). (*B*) Quantification of Notch receptor and Hes1 gene expression at indicated time points in *Kras* pancreatic tissue. Values represent WT-to-*Kras* tissue ratios of relative expression levels (n = 4). (*C*) Expression of Notch1 and Notch2 in distinct compartments of 18-wk-old WT and *Kras* pancreas using Notch1 and Notch2 reporter mice. Arrows indicate centroacinar cells, and arrowheads point to X-Gal$^+$ ducts and PanINs. i, islets. (*D*) H&E staining of 3-, 6-, and 9-mo-old *Kras* and *Kras;N2ko* pancreata. Asterisks indicate PanIN1, arrowhead points to PanIN2, and arrow indicates PanIN3 lesions. Note the absence of PanIN2/3 in *Kras;N2ko* mice. (Scale bars: 50 μm.) (*E*) Quantification of PanINs in 9-mo-old *Kras* (n = 4) and *Kras;N2ko* (n = 5) mice shows a significant reduction in PanIN2 and absence of PanIN3 lesions in *Kras;N2ko* mice.

Kras:Notch2^{lacZ} mice, X-Gal expression was detectable in PanIN lesions and the surrounding stroma (Fig. 1*C*). GFP expression as a surrogate for Notch1 was found in normal acinar cells, as previously described (16), but was hardly ever detectable in PanIN lesions (Fig. 1*C*). In summary, these expression data are consistent with Notch2 as the predominant Notch receptor in ductal, centroacinar, and PanIN cells as suggested previously (5).

PanIN Development and Progression in *Notch*-Ablated Pancreata. To analyze the effect of *Notch1* and *Notch2* deficiency in pancreatic carcinogenesis, we crossed previously described floxed *Notch1*$^{fl/fl}$ and *Notch2*$^{fl/fl}$ mice (17) with *Ptf1a*$^{+/Cre(ex1)}$ mice (18) for generation of *Ptf1a*$^{+/Cre(ex1)}$;*Notch1*$^{fl/fl}$ and *Ptf1a*$^{+/Cre(ex1)}$;*Notch2*$^{fl/fl}$ mice, respectively (called *N1ko* and *N2ko* mice hereafter). These mice were born at the expected Mendelian ratio, and successful recombination of the floxed loci was confirmed by PCR (Fig. S1 *A* and *B*). *N1ko* mice have been previously described to show no major pancreatic abnormalities (16). Similarly, *N2ko* adult pancreata displayed no obvious morphological or functional abnormalities (Fig. S2). However, in mice older than 12 mo of age, we often noted a slight to moderate degree of focal exocrine atrophy with adipose tissue accumulation.

To study the role of Notch1 and Notch2 during pancreatic carcinogenesis, we crossed *N1ko* and *N2ko* mice with *Kras* mice for generation of *Kras;N1ko* and *Kras;N2ko* mice, respectively. Notably, *Kras;N2ko* mice showed no PanIN progression over time, whereas *Kras* and *Kras;N1ko* mice developed higher grade PanIN lesions, suggesting that Notch2 is involved in PanIN progression (Fig. 1 *D* and *E*). PanIN lesions from all genotypes expressed typical markers such as CK19 and MUC5AC and, somewhat surprisingly, HES1 (Tables S1–S3).

Development of MCN-Like Lesions in *Kras;N2ko* Mice. Frequently, albeit not in all mice, *Kras;N2ko* mice developed moderate to very large multilocular cysts. These cysts most often developed in the splenic part of the pancreas and showed a mucinous columnar epithelium resembling human MCN (Fig. S3 *A* and *B*). Rarely, goblet cells, high-grade dysplasia, and invasion into the adjacent stroma were noted. To characterize these lesions further, various markers, including those found in human MCNs, were analyzed. The cystic epithelial cells expressed PDX1, MUC5AC, and HES1, thus showing similar characteristics as PanIN lesions (Table S3). Consistent with the observation of an MCN-like preneoplastic lesion, we found an ovarian-like stroma surrounding the cystic lesions with estrogen receptor (ER)-positive and progesterone receptor-positive nuclei characteristic for human MCNs (19) (Fig. S3*B* and Table S7). To see whether the MCN-like lesions were derived from *Notch2*-deficient cells, cell lineage analysis was performed by crossing the *Rosa26R*$^{+/LSL\text{-}lacZ}$ reporter strain to *Kras;N2ko* mice. Indeed, we found all PanIN and MCN lesions to be X-Gal$^+$ (Fig. 2*C*).

Distinct Roles for Notch1 and Notch2 During Tumor Development. For analysis of PDAC development, a cohort of mice was followed for signs of disease progression or death. *Kras* and *Kras;N1ko* mice developed PDAC with similar characteristics regarding age of tumor development, tumor differentiation, rate, and sites of metastasis (Tables S4–S6). *Kras;N1ko* mice showed a slight, albeit not significant, reduction in median survival compared with *Kras* mice, supporting a nononcogenic role of Notch1 in *Kras*^{G12D}-driven pancreatic carcinogenesis (Fig. 2*A*). However, in *Kras;N2ko* mice, a largely altered carcinogenic process was notable. These mice survived significantly longer than *Kras* and *Kras;N1ko* mice and only very rarely developed PDAC with ductal differentiation. Instead, *Kras;N2ko* mice either died without development

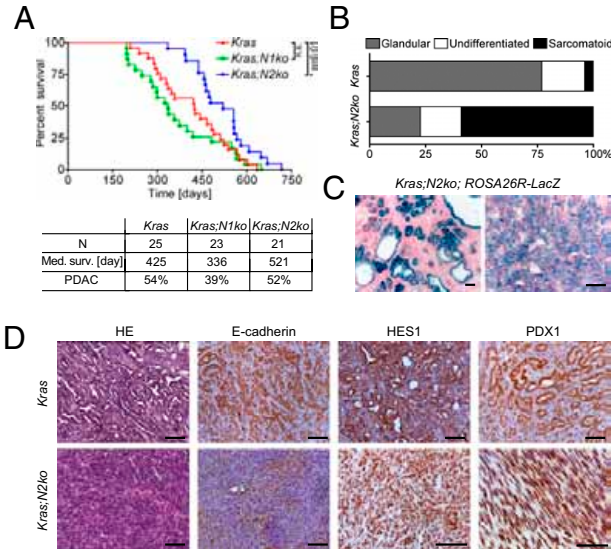

	Kras	Kras;N1ko	Kras;N2ko
N	25	23	21
Med. surv. [day]	425	336	521
PDAC	54%	39%	52%

Fig. 2. Deficiency of *Notch2* prolongs survival and delays development of anaplastic PDAC. (*A*) Kaplan–Meier survival data and PDAC development of *Kras*, *Kras;N1ko*, and *Kras;N2ko* mice. *Kras;N2ko* mice have significantly prolonged survival compared with *Kras* and *Kras;N1ko* mice ($P < 0.02$). n.s., not significant. (*B*) Tumor differentiation analysis reveals more anaplastic PDAC in *Kras;N2ko* mice compared with *Kras* mice. (*C*) Positive X-Gal staining shows Cre-induced recombination in cells of MCN-like cysts and anaplastic PDAC in *Kras;N2ko;Rosa26R*$^{+/LSL\text{-}lacZ}$ mice. (*D*) Histological and immunohistochemical analysis of *Kras* and *Kras;N2ko* tumors. Expression of E-cadherin in *Kras* PDAC and low to absent expression in *Kras;N2ko* tumors. The Notch targets HES1 and PDX1 are expressed in tumors derived from both genotypes. (Scale bars: 50 μm.)

of PDAC or developed highly aggressive anaplastic PDAC at a very advanced age (Fig. 2 *A* and *B* and Tables S4–S6). Histologically, most of these tumors were very large, showing a sarcomatoid cell pattern with a high proliferative index. Although we observed tumor areas that displayed features of poorly differentiated PDAC, we practically never observed G1/2 grades. Anaplastic PDAC showed an absence or low expression of E-cadherin and expressed PDX1, indicating its pancreatic origin (Fig. 2*D*). Lineage tracing showed PanIN and anaplastic PDAC development from *Notch2*-ablated pancreatic cells (Fig. 2*C*). Surprisingly, as was seen in MCN-like lesions, many cells expressed HES1, suggesting Notch2-independent regulation (Fig. 2*D*). *Kras;N1ko* and *Kras;N2ko* PDAC showed an absence of the respective Notch receptor, whereas expression was notable in *Kras* cancer cells (Figs. S1*D* and S4). To determine whether deficiency of *Notch2* led to up-regulation of other Notch receptors, we tested *Kras* and *Kras;N2ko* PDAC cells for expression of Notch1–4. Here, we did not detect a consistent compensatory expression pattern of other Notch receptors in *Kras;N2ko* mice (Fig. S4).

Molecular Analysis of Key Signaling Pathways in *Notch2*-Deficient PDAC. Analysis of genetic alterations typically found in PDAC showed no differences in *p16Ink4a*, *p19Arf*, *p53*, and *Smad4* status between low-passage cancer cells isolated from *Kras* and *Kras;N2ko* PDAC (Tables S8 and S9). Consistent with low E-cadherin expression, we found increased levels of Twist, Snail, Slug, vimentin, and TGF-β1 in *Kras;N2ko* cancer cells, suggesting a high rate of epithelial-to-mesenchymal transition (EMT) (Fig. 3*A*). Because EMT has been associated with TGF-β signaling, we next tested integration of the pathway. Using a wound-healing assay, we found significantly increased cell migration of *Notch2*-deficient cancer cells (Fig. 3*B*). Gene set enrichment analysis (GSEA) was performed using pancreatic tissue at 7 d of age and cancer cells isolated from *Kras* and *Kras;N2ko* PDAC, as previously described (9), and revealed significant enrichment of several TGF-β signatures in *Kras;N2ko* preneoplastic tissue and cancer cells (Fig. 3*C* and Tables S10 and S11). Next, expression of E- and N-cadherin was studied in the presence of a TGF-β receptor inhibitor. Here, we found a reversed EMT process with increased expression of E-cadherin and down-regulation of N-cadherin (Fig. 3*E*), whereas addition of TGF-β led to down-regulation of E-cadherin and translocation of SMAD4 to the nucleus (Fig. 3*D*). These results suggest that TGF-β signaling is increased in *Kras;N2ko* PDAC yet responsive to either inhibition or activation in the absence of Notch2.

Deficiency of *Notch2* Modulates Myc Signaling. To elucidate the oncogenic role of Notch2 further, we screened *Kras* and *Kras;N2ko* preneoplastic pancreatic tissue and cancer cells using GSEA. Here, we noted highly significant enrichment of several Myc signatures, suggesting that Notch2 modulates Myc signaling (Fig. 4*A* and Tables S12 and S13). Compatible with deregulation of Myc signaling during early carcinogenesis, we found increased Myc expression in PanIN lesions as well as increasing mRNA levels in $Kras^{G12D}$-induced pancreatic tissue during preneoplastic progression (Fig. 4 *B* and *C* and Tables S1–S3). We next examined *Kras* and *Kras;N2ko* cancer cells and found reduced mRNA and, most importantly, reduced protein levels in *Kras;N2ko* cells (Fig. 4*D*). Immunohistochemistry of Myc in PDAC of *Kras* mice and anaplastic PDAC of *Kras;N2ko* mice revealed a heterogeneous yet decreased expression pattern in *Kras;N2ko* mice (Fig. 4*E* and Tables S1–S3), suggesting that Myc protein expression is indeed down-regulated in *Notch2*-ablated preneoplastic and malignant pancreatic cells.

Recently, several Notch/Rbpj binding sites in the murine *Myc* promoter have been described (20). To analyze transcriptional regulation of *Myc* further, we considered three Notch/Rbpj signaling binding sites of interest in the *Myc* promoter (Fig. 5*A*). To test the relevance of each binding site, we transfected *Kras;N2ko* cancer cells with activated Notch2 (N2IC) and luciferase reporter vectors with one, two, or all three Notch/Rbpj sites mutated. As shown in Fig. 5*B*, all three sites seemed to be functional for transcriptional regulation. Intriguingly, we found *Myc* promoter induction through Notch2 in every cell line tested. We next performed ChIP to substantiate the reporter assay results in *Kras* cancer cells. ChIP demonstrated Notch2 and RbpJ binding to the *Myc* promoter. In fact, the increased *Myc* promoter occupation by Notch2 and RbpJ was comparable to that of Notch2 binding to the *Hes1* promoter (Fig. 5*C*). Intriguingly, a similar result was obtained in the human PDAC cell lines MiaPaCa2 and Panc1, in which two Notch/Rbpj binding sites are conserved between humans and mice (Fig. S5). We next tested whether N2IC would increase Myc expression in *Kras;N2ko* and Panc1 cells. As shown in Fig. 5*D*, Myc mRNA and protein expression was increased in N2IC-transfected cells, suggesting transcriptional regulation.

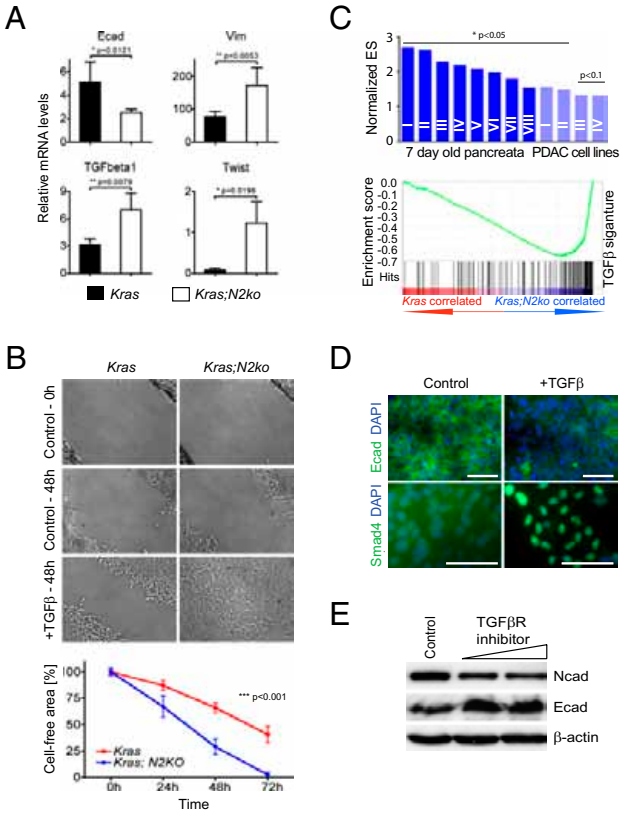

Fig. 3. EMT is a prominent feature in *Kras;N2ko* PDAC. (*A*) Quantitative RT-PCR analysis of EMT-associated genes expressed by cancer cells from *Kras* and *Kras;N2ko* PDAC (n = 4 for each genotype). (*B*) Assessment of cell migration in wound closure assays performed in *Kras* and *Kras;N2ko* cells treated with TGF-β. Wound closure is delayed in *Kras* cells compared with *Kras;N2ko* cells. Quantification of wound closure is plotted as the percentage of the cell-free area over time. (*C*) Comparison of TGF-β gene sets by GSEA reveals significantly up-regulated TGF-β signatures in *Kras;N2ko* pancreata isolated from 7-d-old mice (dark blue, n = 2 and 4) and cancer cells (light blue, n = 6 each). A positive normalized enrichment score indicates elevated TFG-β–associated gene expression. Roman numbers refer to the detailed analysis in Tables S10 and S11. (*D*) *Kras;N2ko* cells reveal morphological and molecular responses characteristic of EMT in response to TGF-β, including loss of E-cadherin expression and nuclear translocation of SMAD4. (Scale bars: 50 μm.) (*E*) Treatment with the TGF-β receptor inhibitor SB431542 is sufficient to reverse the EMT-associated cadherin switch, suggesting that EMT in *Kras;N2ko* cells is dependent on a TGF-β autocrine loop.

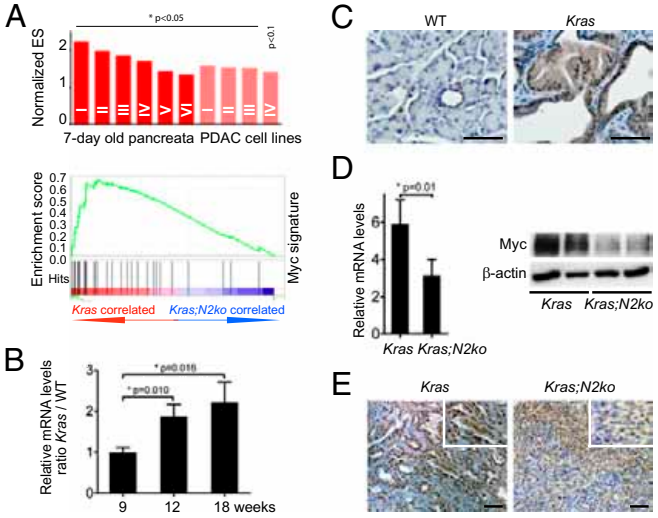

Fig. 4. Myc is up-regulated during pancreatic carcinogenesis and down-regulated in *Kras;N2ko* mice. (*A*) GSEA shows significantly enriched Myc signatures in *Kras* vs. *Kras;N2ko* pancreata isolated from 7-d-old mice (dark red, $n = 2$ and 4) and primary cancer cells (light red, $n = 6$ each). Roman numbers refer to detailed analysis in Tables S12 and S13. (*B*) Myc transcript levels increase during carcinogenesis in *Kras* pancreata at indicated time points. Values represent WT-to-*Kras* ratio of relative expression levels ($n = 3$ for each time point). (*C*) Expression of Myc is low in the normal pancreas and increases in PanIN lesions of *Kras* mice. (*D*) *Kras;N2ko* cancer cells ($n = 4$) show decreased Myc mRNA and protein expression compared with *Kras* cells ($n = 5$). (*E*) Immunohistochemical staining in *Kras;N2ko*-derived anaplastic PDAC shows lower expression of Myc compared with *Kras* PDAC. (Scale bar: 50 μm.)

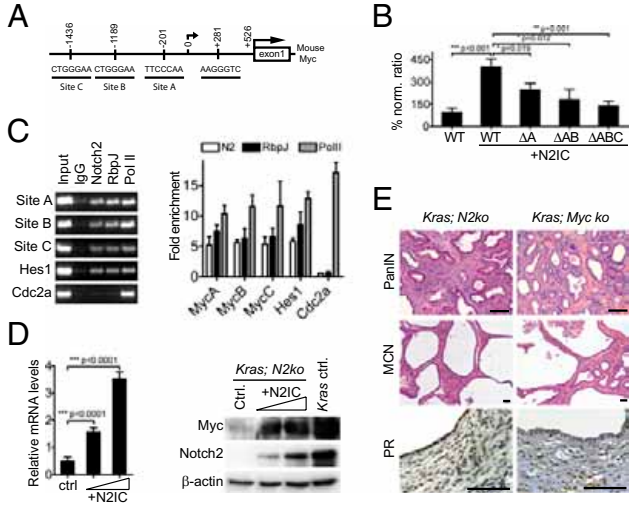

Fig. 5. Myc is a downstream target of Notch, and its ablation resembles features of the *Notch2*-deficient phenotype. (*A*) Analysis of Notch/Rbpj binding sites in the mouse *Myc* promoter using the consensus RTGGGAA motif reveals three sites: A, B, and C. (*B*) Activity of a *Myc* promoter fragment containing binding regions A, B, and C was analyzed using luciferase reporter assays. *Kras;N2ko* cells were cotransfected with *Myc* luciferase plasmids and N2IC. Mutations in the respective binding sites decrease activation of Myc. Activities were corrected for transfection efficiency by normalizing with Renilla luciferase activity and are expressed as a percentage of induction. (*C*) ChIP analyses using the indicated antibodies were analyzed by PCR for sites of interests. Products of the exponential phase of PCR are shown. *Hes1* promoter primer served as positive control, and *Cdc2a* promoter primers as negative control. Quantitative PCR indicates that Notch2 binds to regions A, B, and C of the *Myc* promoter comparable to a binding site in the *Hes1* promoter. (*D*) Transfection of N2IC stimulates Myc expression in *Kras;N2ko* cells in a dose-dependent manner. Notch2 and Myc expression levels of *Kras* control are shown for comparison. (*E*) *Myc* and *Notch2* ablation in *Kras* mice results in similar phenotypes. *Kras;N2ko* and *Kras;Myc-ko* mice develop PanIN1 but not advanced PanIN2/3 lesions and MCN-like lesions with progesterone receptor-positive (PR^+) surrounding stroma. Brightness and contrast levels were adjusted across the whole image for each panel. (Scale bar: 50 μm.)

To analyze Myc signaling in pancreatic carcinogenesis in vivo, we interbred previously described $Myc^{fl/fl}$ mice (21) with *Pdx1-Cre;* $Kras^{+/LSL\text{-}G12D}$ mice to obtain *Myc*-ablated *Kras* mice. Although breeding was hindered by exocrine atrophy occurring in most animals, we could analyze two mice 11 and 12 mo of age that showed a phenotype of only PanIN1 but not higher grade lesions, strongly supporting our hypothesis of Myc signaling being essential for PanIN progression. Additionally, we observed the development of MCN-like lesions with ovarian-like stroma, similar to *Kras;N2ko* mice (Fig. 5*E*).

Discussion

Notch Signaling Activation in Pancreatic Carcinogenesis. In this study, we have evaluated the role of the Notch receptors 1 and 2 in pancreatic carcinogenesis in vivo using the well-established conditional $Kras^{G12D}$ model generated by Tuveson and co-workers (3). Although inhibition of PanIN progression in *Kras;N2ko* mice goes along with the results of inhibition of Notch signaling through γ-secretase inhibitor treatment (10), some differences between the models are notable. Plentz et al. (10) found a high relative increase of Notch3 mRNA in duct cells derived from PanIN-bearing pancreata and cells isolated from PDAC. Although we also found an increase in expression of Notch3 in PanIN-bearing compared with WT pancreata, expression was low compared with Notch1 and Notch2 levels. Reasons may include use of different mouse models as well as analysis of different tissue samples. In cancer cells isolated from PDAC of *Kras* mice, however, we also found much lower mRNA and protein levels of Notch3 compared with Notch2. In fact, Notch2 was by far the most prominently expressed Notch receptor during PanIN development and in PDAC, a finding supported by earlier studies (5). Importantly, we found no consistent up-regulation of any other Notch receptor in *Notch2*-deficient PDAC cells, suggesting that these cells could not easily reconstitute loss of Notch2 by any other Notch receptor. Interestingly, we did not observe loss of HES1 expression in either *Notch1*- or *Notch2*-ablated pancreata, suggesting that Hes1 may be regulated by other signaling pathways, as suggested previously (12, 16).

Although the downstream signaling of different Notch receptors and ligand specificity are complex, the differential pancreatic expression of Notch1 and Notch2 is noteworthy. The predominant expression of Notch1 in acinar cells goes along with our previous result of impaired regeneration in conditional *Notch1*-deficient mice during acute pancreatitis (16). Interestingly, Murtaugh and co-workers (11) found Notch1-activated mature acinar cells to be susceptible to PanIN initiation and progression. The hypothesis of acinar cells as potential cells of origin for PDAC has recently gained much interest because of the plasticity of this cell type, its potential for initiation of preneoplastic lesions (22–25), and the involvement of Notch signaling (5, 11). Although Notch1 is expressed in the acinar compartment, expression was absent in PanIN lesions when analyzed using transgenic *Notch1-GFP* reporter mice. Along this line, we did not observe fewer PanINs when Notch1 was ablated in our model. Instead survival and tumor incidence was reduced, although this finding was not significant. Of note, Notch1 ablation in $Pdx1\text{-}Cre;Kras^{G12D}$ mice was recently shown to result in increased PanIN progression, supporting the concept that Notch1 has no oncogenic role in pancreatic carcinogenesis (26).

Expression of Notch2 in ductal cells has been described previously and increases in metaplastic ductal cells (27, 28). Recently, centroacinar cells were described to show features of progenitor cells, including respective marker expression, sphere formation ability, and differentiation into different pancreatic lineages (15).

These and our results suggest that a potential progenitor compartment in small ducts such as centroacinar cells expresses Notch2, a hypothesis supported by our expression studies using *Notch2*$^{+/lacZ}$ reporter mice. Because we observed PanIN1 initiation but no higher grade PanINs in *Kras;N2ko* mice, activation of Notch2 may be required for progression of PanIN lesions. However, other explanations remain possible. Because PanIN1 lesions are often encountered in pancreata of elderly people, it is possible that PanIN1 lesions may not actually precede PanIN2 and PanIN3 lesions but are mainly default lesions that may form from different pancreatic cells, including the acinar compartment. Consistent with this hypothesis is the induction of PanIN lesions but usually no development of invasive PDAC from acinar cells in *Ela-Cre-ER*;*Kras*^{G12D} mice. Although our study did not directly address this intriguing question, it remains possible that PanIN1 lesions may originate from acinar cells, whereas initiation or progression of PanIN2/3 lesions may require a Notch-regulated potential progenitor compartment or an additional stimulus such as ongoing inflammation (25, 29).

Development of MCN-Like Lesions and Anaplastic PDAC in *Kras;N2ko* Mice. The blockade of PanIN progression and PDAC development in *Notch2*-deficient *Kras*^{G12D} mice goes along with the longer survival of these mice. Eventually, these mice develop large cysts resembling MCNs and succumb from either pancreatic insufficiency or from the development of anaplastic PDAC. Development of MCN-like lesions may thus be a bypass route for pancreatic cells undergoing oncogenic stress. However, two scenarios are possible with either (*i*) a common cell of origin for PanIN and MCN development, in which the route to higher grade PanINs is blocked by Notch2 deficiency, or (*ii*) different cells of origin for each lesion type that respond differentially to *Kras*^{G12D} in the presence or absence of Notch2.

Interestingly, an association of anaplastic PDAC and MCN has been repeatedly described in patients (30). However, we do not have enough evidence to conclude that MCNs are the direct precursors for PDAC in *Kras;N2ko* mice. Further analysis is required to understand the cellular and molecular cues in *Notch2*-deficient malignant transformation. However, the clinical and experimental observations of the combined occurrence of MCN and anaplastic PDAC highlight the potential predictive capability of genotype-phenotype correlations in complex cancer mouse models.

TGF-β Signaling and EMT in *Notch2*-Deficient PDAC. Molecular characterization of the anaplastic PDAC in *Kras;N2ko* mice showed evidence of EMT. Several reports have described an activating role of increased Notch signaling in EMT by regulation of E-cadherin repressors such as Snail or interaction with TGF-β signaling (31–34). TGF-β is known to play an ambivalent role in cancer biology. In the pancreas, conditional inactivation of TGF-β receptor 2 led to accelerated development and progression of well-differentiated PDAC (35). The development of late-occurring anaplastic PDAC with increased EMT is compatible with the dual role of TGF-β signaling in epithelial tumorigenesis. The effect of TGF-β receptor inhibition on E- and N-cadherin expression and exogenous TGF-β–induced nuclear translocation of SMAD4 suggest an intact TGF-β signaling axis. Indirect regulation of TGF-β may occur through deregulated Myc signaling, which is known to suppress the activation of TGF-β–induced genes such as p21CIP1, which has been shown to interact with Notch in various organs (36, 37). However, we could not detect consistent differences in p21CIP1 expression or related signatures between *Kras* and *Kras;N2ko* tumors.

Myc Signaling Is Regulated by Notch2 in PDAC. Decreased Myc signaling in *Kras;N2ko* mice supports the hypothesis of Notch2-dependent Myc signaling as a key regulator of the carcinogenic process in the pancreas. Deregulation of Myc in PDAC has been described in many studies, and amplification occurs in about 30% of human PDAC as well as in murine PDAC (38–40). In recent studies, Myc signaling has been identified to play a key role in cell cycle regulation of PDAC cells (41, 42). Although these studies demonstrate the importance of deregulated Myc signaling in PDAC, our results suggest an early role during PanIN progression supported by early Myc amplification in precursor lesions (38). In a recent quantitative proteomic screen of preneoplastic PanIN lesions, Myc expression was identified in PanIN3 lesions (43).

We and others have previously characterized the important role of Myc in progenitor and acinar cell proliferation during development and adult homeostasis (21, 44, 45). Consistently, we found increased Myc expression throughout PanIN development in *Kras* mice. It is tempting to speculate that Myc and Ras signaling cooperatively promote tumor progression in a setting of active Notch. Notch signaling has been reported to cooperate with Ras, and several studies have reported direct transcriptional regulation of Myc by Notch1 (20, 46–48). Our finding that active Notch2 induces Myc expression in PDAC cells supports these reports. Although preliminary, the phenotypical similarities of *Notch2* and *Myc*-ablated *Kras*^{G12D}-induced pancreata with development of cystic lesions and a PanIN progression stop strongly support this hypothesis. Of consideration is the use of different Cre mice, *Ptf1a*$^{+/Cre(ex1)}$ and *Pdx1-Cre* mice, in *Kras;N2ko* and *Kras;Myc-ko* mice, respectively, because of extensive exocrine hypoplasia and early postnatal death of *Ptf1a*$^{+/Cre(ex1)}$;*Myc*$^{fl/fl}$ mice (21). Although we cannot rule out different target compartments in both Cre lines, this seems unlikely, given the similar phenotype in *Kras*^{G12D}-activated mice (3).

The results from luciferase reporter and ChIP assays suggest that all three reported Notch/Rbpj binding sites in the *Myc* promoter are relevant for transcriptional regulation of Myc. On the basis of our findings, we report that Myc is regulated by Notch2. Why *Notch1* ablation did not lead to similar alterations in early tumor progression in our model is not clear. A possible explanation would be a context- and cell-specific role of Myc and its regulation through Notch. A possible scenario may thus be that a progenitor cell (e.g., within the centroacinar compartment) is the target cell for cooperative Myc-Ras–induced tumor development propagated by Notch2 activation. The success of Notch inhibition as a chemopreventive approach to inhibit PanIN progression has been shown (10). This outcome is supported by our results. Of note, the same group has reported *Myc* amplification in *Kras*^{G12D}-driven PDAC mouse models, adding evidence for a key role of this signaling pathway during the carcinogenic process (40). It will be of great interest to study the integration of the transcriptional programs regulated by Myc and Notch signaling in further detail, which may eventually help to explain the permissive signals regulating pancreatic plasticity and malignant transformation.

In summary, our results provide evidence for an essential role of Notch2 and Myc in the initiation of a neoplastic transformation program in pancreatic cells, whereas Notch1 has no oncogenic role, supporting the concept of distinctive roles of individual Notch receptors in cancer development. In addition, the data demonstrate the integrative interaction of regulators of cell fate and cell cycle signaling, thereby enhancing our biological understanding for unique approaches in this still untreatable disease.

Materials and Methods

Mouse Strains. *Kras*$^{+/LSL-G12D}$, *Notch1*$^{fl/fl}$, *Notch2*$^{fl/fl}$, *Myc*$^{fl/fl}$, *Ptf1a*$^{+/Cre(ex1)}$, *Pdx1-Cre*, and Rosa26$^{+/LSL-lacZ}$ mice have been described before (3, 9, 17, 21). All experiments were performed according to the guidelines of the local animal use and care committees.

Detailed descriptions of additional procedures, including protein and mRNA analysis, immunohistochemistry, microarray/GSEA, luciferase-based reporter assays, and ChIP, are provided in *SI Text*.

ACKNOWLEDGMENTS. We thank W. Gao (Genentech, Inc., CA), Y. Hamada (National Institute for Basic Biology, Okazaki, Japan), and C. A. Klug (University of Alabama, Birmingham, AB) for the generous gift of Notch reporter mice

and A. Klinakis (Biochemical Research Foundation, Athens, Greece) for Myc plasmids. We are grateful to T. Sudo (Toray Industries Inc., Kamakura, Japan) for HES1 and to C. V. Wright (Vanderbilt University Medical Center, Nashville, TN) for PDX1 antibodies. We thank M. Neuhofer, S. Ruberg, and C. Köhler for excellent technical assistance. This work was supported by grants from the German Cancer Aid (Grant 107195), German Federal Ministry of Education and Research (Grant 01GS08115), Lustgarten Foundation (RFP05-14 and 06-12), and German Research Foundation (Grant SI 1549/1-1).

1. Hezel AF, Kimmelman AC, Stanger BZ, Bardeesy N, Depinho RA (2006) Genetics and biology of pancreatic ductal adenocarcinoma. *Genes Dev* 20:1218–1249.
2. Hruban RH, Iacobuzio-Donahue C, Wilentz RE, Goggins M, Kern SE (2001) Molecular pathology of pancreatic cancer. *Cancer J* 7:251–258.
3. Hingorani SR, et al. (2003) Preinvasive and invasive ductal pancreatic cancer and its early detection in the mouse. *Cancer Cell* 4:437–450.
4. Pasca di Magliano M, et al. (2006) Hedgehog/Ras interactions regulate early stages of pancreatic cancer. *Genes Dev* 20:3161–3173.
5. Miyamoto Y, et al. (2003) Notch mediates TGF alpha-induced changes in epithelial differentiation during pancreatic tumorigenesis. *Cancer Cell* 3:565–576.
6. Pasca di Magliano M, et al. (2007) Common activation of canonical Wnt signaling in pancreatic adenocarcinoma. *PLoS ONE* 2:e1155.
7. Thayer SP, et al. (2003) Hedgehog is an early and late mediator of pancreatic cancer tumorigenesis. *Nature* 425:851–856.
8. Stanger BZ, et al. (2005) Pten constrains centroacinar cell expansion and malignant transformation in the pancreas. *Cancer Cell* 8:185–195.
9. Siveke JT, et al. (2007) Concomitant pancreatic activation of Kras(G12D) and Tgfa results in cystic papillary neoplasms reminiscent of human IPMN. *Cancer Cell* 12: 266–279.
10. Plentz R, et al. (2009) Inhibition of gamma-secretase activity inhibits tumor progression in a mouse model of pancreatic ductal adenocarcinoma. *Gastroenterology* 136:1741–1749.e6.
11. De La O JP, et al. (2008) Notch and Kras reprogram pancreatic acinar cells to ductal intraepithelial neoplasia. *Proc Natl Acad Sci USA* 105:18907–18912.
12. Nakhai H, et al. (2008) Conditional ablation of Notch signaling in pancreatic development. *Development* 135:2757–2765.
13. Lewis AK, Frantz GD, Carpenter DA, de Sauvage FJ, Gao WQ (1998) Distinct expression patterns of notch family receptors and ligands during development of the mammalian inner ear. *Mech Dev* 78:159–163.
14. Hamada Y, et al. (1999) Mutation in ankyrin repeats of the mouse Notch2 gene induces early embryonic lethality. *Development* 126:3415–3424.
15. Rovira M, et al. (2010) Isolation and characterization of centroacinar/terminal ductal progenitor cells in adult mouse pancreas. *Proc Natl Acad Sci USA* 107:75–80.
16. Siveke JT, et al. (2008) Notch signaling is required for exocrine regeneration after acute pancreatitis. *Gastroenterology* 134:544–555.
17. Besseyrias V, et al. (2007) Hierarchy of Notch-Delta interactions promoting T cell lineage commitment and maturation. *J Exp Med* 204:331–343.
18. Nakhai H, et al. (2007) Ptf1a is essential for the differentiation of GABAergic and glycinergic amacrine cells and horizontal cells in the mouse retina. *Development* 134: 1151–1160.
19. Zamboni G, et al. (1999) Mucinous cystic tumors of the pancreas: clinicopathological features, prognosis, and relationship to other mucinous cystic tumors. *Am J Surg Pathol* 23:410–422.
20. Klinakis A, et al. (2006) Myc is a Notch1 transcriptional target and a requisite for Notch1-induced mammary tumorigenesis in mice. *Proc Natl Acad Sci USA* 103: 9262–9267.
21. Nakhai H, Siveke JT, Mendoza-Torres L, Schmid RM (2008) Conditional inactivation of Myc impairs development of the exocrine pancreas. *Development* 135:3191–3196.
22. Habbe N, et al. (2008) Spontaneous induction of murine pancreatic intraepithelial neoplasia (mPanIN) by acinar cell targeting of oncogenic Kras in adult mice. *Proc Natl Acad Sci USA* 105:18913–18918.
23. Ji B, et al. (2009) Ras activity levels control the development of pancreatic diseases. *Gastroenterology*, 137:1072–1082 1082.e1–6..
24. Zhu L, Shi G, Schmidt CM, Hruban RH, Konieczny SF (2007) Acinar cells contribute to the molecular heterogeneity of pancreatic intraepithelial neoplasia. *Am J Pathol* 171: 263–273.
25. Guerra C, et al. (2007) Chronic pancreatitis is essential for induction of pancreatic ductal adenocarcinoma by K-Ras oncogenes in adult mice. *Cancer Cell* 11:291–302.
26. Hanlon L, et al. (2010) Notch1 functions as a tumor suppressor in a model of K-ras-induced pancreatic ductal adenocarcinoma. *Cancer Res* 70:4280–4286.
27. Rooman I, et al. (2006) Expression of the Notch signaling pathway and effect on exocrine cell proliferation in adult rat pancreas. *Am J Pathol* 169:1206–1214.
28. Lee KM, Yasuda H, Hollingsworth MA, Ouellette MM (2005) Notch 2-positive progenitors with the intrinsic ability to give rise to pancreatic ductal cells. *Lab Invest* 85:1003–1012.
29. Morris JP, IV, Cano DA, Sekine S, Wang SC, Hebrok M (2010) Beta-catenin blocks Kras-dependent reprogramming of acini into pancreatic cancer precursor lesions in mice. *J Clin Invest* 120:508–520.
30. Pan ZG, Wang B (2007) Anaplastic carcinoma of the pancreas associated with a mucinous cystic adenocarcinoma. A case report and review of the literature. *JOP* 8: 775–782.
31. Sahlgren C, Gustafsson MV, Jin S, Poellinger L, Lendahl U (2008) Notch signaling mediates hypoxia-induced tumor cell migration and invasion. *Proc Natl Acad Sci USA* 105:6392–6397.
32. Wang Z, et al. (2009) Acquisition of epithelial-mesenchymal transition phenotype of gemcitabine-resistant pancreatic cancer cells is linked with activation of the notch signaling pathway. *Cancer Res* 69:2400–2407.
33. Timmerman LA, et al. (2004) Notch promotes epithelial-mesenchymal transition during cardiac development and oncogenic transformation. *Genes Dev* 18:99–115.
34. Zavadil J, Cermak L, Soto-Nieves N, Böttinger EP (2004) Integration of TGF-beta/Smad and Jagged1/Notch signalling in epithelial-to-mesenchymal transition. *EMBO J* 23: 1155–1165.
35. Ijichi H, et al. (2006) Aggressive pancreatic ductal adenocarcinoma in mice caused by pancreas-specific blockade of transforming growth factor-beta signaling in cooperation with active Kras expression. *Genes Dev* 20:3147–3160.
36. Liu M, et al. (2009) p21CIP1 attenuates Ras- and c-Myc-dependent breast tumor epithelial mesenchymal transition and cancer stem cell-like gene expression in vivo. *Proc Natl Acad Sci USA* 106:19035–19039.
37. Rangarajan A, et al. (2001) Notch signaling is a direct determinant of keratinocyte growth arrest and entry into differentiation. *EMBO J* 20:3427–3436.
38. Schleger C, Verbeke C, Hildenbrand R, Zentgraf H, Bleyl U (2002) c-MYC activation in primary and metastatic ductal adenocarcinoma of the pancreas: Incidence, mechanisms, and clinical significance. *Mod Pathol* 15:462–469.
39. Schreiner B, et al. (2003) Murine pancreatic tumor cell line TD2 bears the characteristic pattern of genetic changes with two independently amplified gene loci. *Oncogene* 22:6802–6809.
40. Bardeesy N, et al. (2006) Both p16(Ink4a) and the p19(Arf)-p53 pathway constrain progression of pancreatic adenocarcinoma in the mouse. *Proc Natl Acad Sci USA* 103: 5947–5952.
41. Konig A, et al. (2010) NFAT-induced histone acetylation relay switch promotes c-myc-dependent growth in pancreatic cancer cells. *Gastroenterology* 138:1189–1199.e1-2.
42. Schild C, et al. (2009) PI3K signaling maintains c-myc expression to regulate transcription of E2F1 in pancreatic cancer cells. *Mol Carcinog* 48:1149–1158.
43. Pan S, et al. (2009) Quantitative proteomics investigation of pancreatic intraepithelial neoplasia. *Electrophoresis* 30:1132–1144.
44. Bonal C, et al. (2009) Pancreatic inactivation of c-Myc decreases acinar mass and transdifferentiates acinar cells into adipocytes in mice. *Gastroenterology* 136: 309–319.e9.
45. Strom A, et al. (2007) Unique mechanisms of growth regulation and tumor suppression upon Apc inactivation in the pancreas. *Development* 134:2719–2725.
46. Palomero T, et al. (2006) NOTCH1 directly regulates c-MYC and activates a feed-forward-loop transcriptional network promoting leukemic cell growth. *Proc Natl Acad Sci USA* 103:18261–18266.
47. Sharma VM, et al. (2006) Notch1 contributes to mouse T-cell leukemia by directly inducing the expression of c-myc. *Mol Cell Biol* 26:8022–8031.
48. Weng AP, et al. (2006) c-Myc is an important direct target of Notch1 in T-cell acute lymphoblastic leukemia/lymphoma. *Genes Dev* 20:2096–2109.

Supporting Information

Mazur et al. 10.1073/pnas.1002423107

SI Materials and Methods

Histology and Immunohistology. Specimens were fixed in 4% neutral buffered formaldehyde and embedded in paraffin. Pancreata were sectioned at 3 μm and stained with H&E or used for immunohistochemical studies with antibodies against amylase, insulin (Sigma), CK19 (DSHB), ER, glucagon (Dako), E-cadherin (R&D Systems), PDX1 (gift of C. V. Wright, Vanderbilt University Medical Center, Nashville, TN), HES1 (gift of T. Sudo, Toray Industries Inc., Kamakura, Japan), Myc (Santa Cruz Biotechnology), progesterone receptor (NeoMarkers), and p53 (Novocastra). Staining for mucin content was carried out using a periodic acid–Schiff reaction. X-Gal staining of cryosections (10 μm) was carried out according to standard protocols, and cryosections were counterstained with nuclear fast red. Double-immunofluorescence was performed using Alexa 488 and Alexa 555 (1:1,000; Invitrogen). Nuclei were stained with DAPI. Pictures were taken using an Axiovert 200M fluorescence inverse microscope (Zeiss) equipped with Axiovision software (Zeiss).

Histopathological Evaluation. H&E-stained sections were evaluated by pathologists with expertise in human and mouse PDAC pathology (B.S. and G.K.).

Western Blot Analysis. Protein extracts from tissues or cells were obtained using radioimmunoprecipitation assay buffer, separated on standard SDS/PAGE electrophoresis, transferred to nitrocellulose filters, and incubated with antibodies: β-actin (Sigma), Myc, Notch1 (BD Pharmingen), Notch2 (DSHB), Notch3, Notch4, Delta, Jagged (Santa Cruz Biotechnology), and p53 (Novocastra). Antibody binding was visualized using HRP-labeled secondary antibodies and ECL reagent (Amersham).

Primary Cell Culture and Cell Assays. Cells were maintained in DMEM medium with 10% (vol/vol) FCS, 1% nonessential amino acids, and 1% penicillin/streptomycin. For TGF-β receptor inhibition experiments, the SB431542 inhibitor (Sigma) was used for 48 h at final concentrations of 5 and 10 μM. For migration assays (wound healing), confluent cells were starved with minimal medium (0.5% FCS), scratched with a 20-μL pipette tip to form wounds, and incubated with human recombinant TGF-β1 (R&D Systems) at a final concentration of 5 ng/mL for 48 h. Representative photographs were taken from several high-power fields. Quantification of the wound closure area was performed using Axiovision 4.8 software (Zeiss). Six representative photographs for each time point were analyzed, and the percentage of cell-free area was plotted. For all assays, analysis was performed on low passage number cell lines (fewer than eight passages).

ChIP. Experiments were performed using the EZ-ChIP Kit (Upstate). The following antibodies were used: Notch2 (DSHB), RBP-Jκ (Institute of Immunology Co.), Pol II (Upstate) as a positive control, and IgG as background control. Quantitative PCR was performed on a Lightcycler (Roche) using the primers listed in Table S11. Calculation of average cycle threshold (Ct) and SD for triplicate reactions was performed, and each DNA fraction was normalized to the input to account for chromatin sample preparation differences: $\Delta Ct_{\text{normalized ChIP}} = Ct_{\text{ChIP}} - Ct_{\text{input}} - \text{Log}_2(\text{dilution})$, where "dilution" is input dilution factor = 100. Normalized background was then subtracted using the following equation: $\Delta\Delta Ct = \Delta Ct_{\text{normalized ChIP}} - \Delta Ct_{\text{normalized IgG}}$. The SD was calculated using propagation of error: $SD_{\Delta\Delta Ct} = \sqrt{SD_{ChIP}^2 + SD_{input}^2 + SD_{IgG}^2}$.

Calculation of the relative quantity of amplified sequence (fold enrichment) was carried out according to the following equation: $Q = 2^{-\Delta\Delta Ct}$. Calculation of error for relative quantity was carried out according to the following equation: $Q_{error\pm} = Q \pm 2^{-(\Delta\Delta Ct \pm SD\Delta\Delta Ct)}$.

RT-PCR Assay. RNA was isolated using the Qiagen RNeasy Isolation Kit, followed by cDNA synthesis (SuperScript II; Invitrogen). Real-time PCR was performed with 800-nM primers diluted in a final volume of 20 μL in SYBR Green Reaction Mix (Applied Biosystems). RT-PCR assays were performed as follows: 95 °C for 10 min, followed by 35 cycles of 95 °C for 15 s and 60 °C for 1 min using a LightCycler (Roche). All samples were analyzed in triplicate. Cyclophilin and hypoxanthine guanine phosphoribosyl transferase expression was used for normalization. Primers used are shown in Table S14.

Mutation Analysis of *p53*, *p16/Ink4a*, and *Smad4*. RNA isolated from PDAC cell lines (RNeasy Isolation Kit) was used to generate cDNA (Superscript II) for further analysis essentially as described previously (32[1]). Briefly, amplified (with PfuUltra polymerase; Stratagene) *p53* and *Smad4* gene sequences were cloned into the pCR3.1-TOPO (Invitrogen) plasmid, and *p16/Ink4a*, *p19/Arf* was cloned into pBluescript (Stratagene; restriction sites BamHI and HindIII) and sequenced bidirectionally. Three to eight independent clones were sequenced for each cell line.

Bisulfite Modification and Methylation-Specific PCR Assay. DNA isolated from primary cancer cells was modified by bisulfite treatment (Invitrogen) and PCR-amplified using primers specific for methylated and unmethylated regions of the 5′ UTR of the *p16/Ink4a* locus. Primers used are listed in Table S11.

Luciferase Reporter Assay. A luciferase reporter assay was performed with the following luciferase reporter constructs: Myc-luc, containing three WT *Rbpj* binding sites; Myc-mutA-luc, containing mutated binding site A; Myc-mutAB-luc, including mutated binding sites A and B; and Myc-mutABC-luc, with mutated binding sites A, B, and C. Primary *Kras;N2ko* cancer cells were cultured in a six-well plate and transiently transfected in triplicate with luciferase reporter plasmids, N2IC expression plasmids and pRL-TK (internal control reporter; Promega) using Fugene 6 following the manufacturer's instructions (Roche). Luciferase activity was measured with the dual-luciferase reporter assay system (Promega) 48 h after transfection, with the Renilla luciferase activity serving as an internal control. Results are expressed as a percentage of induction over control (100%).

Gene Chip Analysis and GSEA. Pancreata of two to four mice per genotype were dissected 7 d postnatally. For analysis of PDAC, six different low-passage (fewer than eight passages) cultured cell lines from *Kras* and *Kras;N2ko* PDAC were used. Total RNA was prepared as described above. A total of 1–5 μg of labeled RNA was hybridized to mouse expression gene chip arrays (Mouse Genome 430A 2.0 Array; Affymetrix) according to the manufacturer's protocols. Gene chips were scanned and analyzed using Affymetrix Microarray Suite 5.0 software (MAS 5.0), as described previously (10[2]).

GSEA software was provided by the Broad Institute of the Massachusetts Institute of Technology and Harvard University (http://www.broad.mit.edu/gsea/). We acknowledge the use of the GSEA and GSEA software (60). For both gene sets, we used

the default parameters of the GSEA software package, except for the number of permutations (n = 1,000).

Statistical Analyses. Kaplan–Meier curves were calculated using the survival time for each mouse from all littermate groups (*wt*, *Kras, Kras;N1ko*, and *Kras;N2ko*). The log-rank test was used to test for significant differences between the four groups. For gene expression analysis, the unpaired two-tailed Student's t test was used. $P < 0.05$ was considered significant.

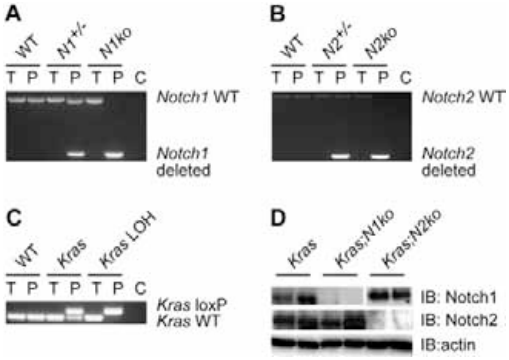

Fig. S1. Targeting endogenous *Kras*^{G12D} expression and *Notch1* and *Notch2* deletion in the pancreas. (*A*) Specific PCR analysis of genomic DNA from pancreata (P) but not tails (T) of *N1ko* mice reveals the expected *Notch1* deletion (C = negative control). (*B*) Specific PCR analysis of genomic DNA from pancreata but not tails of *N2ko* mice reveals the expected *Notch2* deletion. (*C*) Specific PCR analysis of genomic DNA from pancreata but not tails of *Kras* mice reveals the expected stop cassette removal and *Kras*^{G12D} activation. Some pancreata show loss of heterozygosity of the remaining WT *Kras* allele. (*D*) Western blot analysis confirms *Notch1* and *Notch2* ablation in the pancreas. IB, immunoblot.

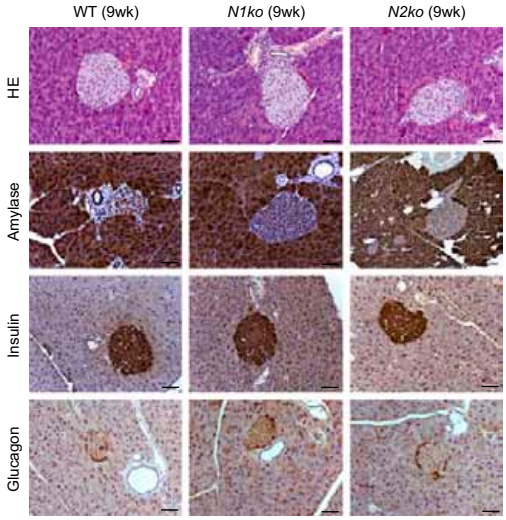

Fig. S2. Architectural and functional integrity of the pancreas in 9-wk-old WT, *N1ko*, and *N2ko* animals and in 12-mo-old *N2ko* animals. Immunohistological detection of amylase, insulin, and glucagon reveals no differences between genotypes.

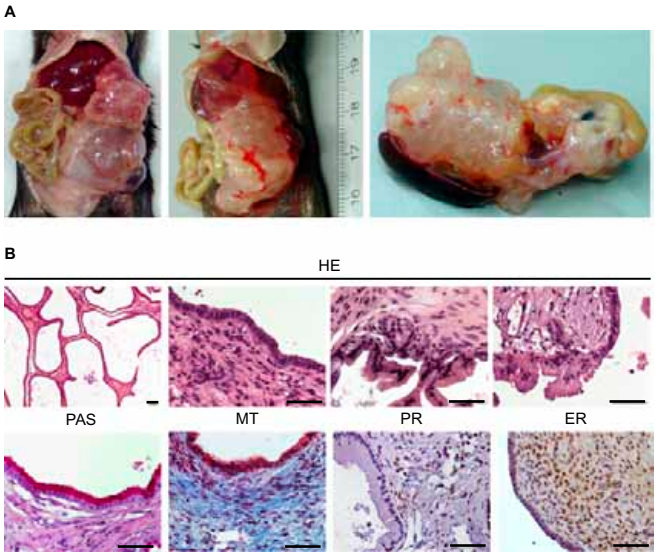

Fig. S3. *Kras;N2ko* mice develop cystic lesions resembling human MCN. (*A*) Typical multilocular cysts develop in the splenic part of the pancreas in aged *Kras;N2ko* mice. (*B*) Cystic lesions are lined by mucinous columnar epithelium positive by PAS staining, focally demonstrating low to moderate levels of dysplasia (*Top Right*). The surrounding highly cellular stromal compartment has abundant collagen deposits, as indicated by Masson–Trichrome staining (MT) and prominent nuclear expression of progesterone receptor (PR) and/or ER. (Scale bar: 50 μm.)

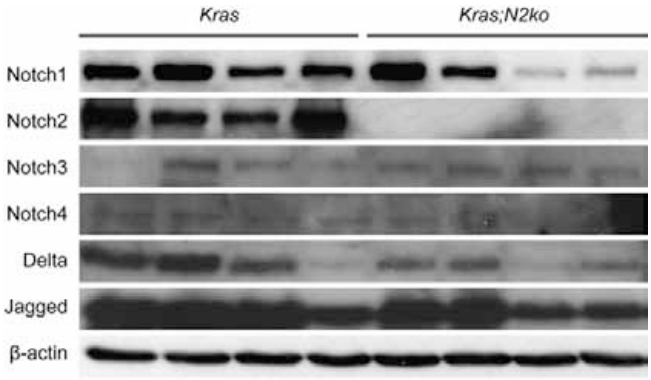

Fig. S4. Notch receptor and ligand protein expression in *Kras* and *Kras;N2ko* primary tumor cells.

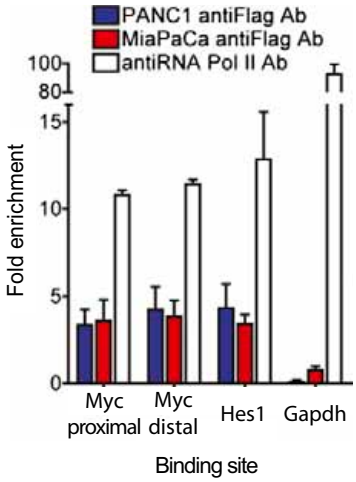

Fig. S5. ChIP was performed in human pancreatic cancer cell lines Panc1 and MiaPaCa2. Cells were transiently transfected with pCMV-Notch2-IC-Flag construct, and anti-Flag antibody was used to analyze whether Myc is a direct transcriptional target of Notch2. Quantitative PCR indicates that Notch2 binds to regions proximal and distal in the human *Myc* promoter (corresponding to Myc site A and B + C in the murine promoter, respectively), comparable to a binding site of the *Hes1* promoter. A nonbinding *Gapdh* promoter region and RNA Polymerase III binding serve as controls.

Table S1. Immunohistochemical analyses of PanINs, MCN, invasive PDA, and metastases in *Kras* mice

	PanIN				MCN				Tumor				Metastases			
Marker	N	F	P	I	N	F	P	I	N	F	P	I	N	F	P	I
TP53	5/9	+++	++	++	2/3	++	++	+	4/9	++	++	+	1/3	+++	+++	++
PDX1	9/9	++	++	+	3/3	+++	+++	++	9/9	++	++	+	2/3	+++	+++	+++
CK19	9/9	+++	+++	++	3/3	+++	+++	+++	9/9	+++	+++	++	3/3	+++	+++	+++
E-CAD	9/9	+++	+++	++	3/3	+++	+++	+++	9/9	+++	+++	++	3/3	+++	+++	+++
HES1	9/9	+++	+++	+	3/3	+++	+++	+	9/9	+++	++	+	3/3	+++	++	+
MYC	8/8	+++	+++	+++	2/2	++	++	+	8/8	+++	+++	+++	3/3	+++	+++	+++

F, frequency of lesions (or discrete regions of tumor) that scored positive per tissue sample (+, <10%; ++, 10–50%; +++, >50%); I, intensity of expression per positive cell (+, weak; ++, moderate; +++, strong); N; number of tissue samples with positive lesions over total evaluated; P, percentage of cells within a specified lesion that were positive (+ <10%; ++, 10–50%; +++, >50%).

Table S2. Immunohistochemical analyses of PanINs, MCN, invasive PDA, and metastases in *Kras;N1ko* mice

	PanIN				MCN				Tumor				Metastases			
Marker	N	F	P	I	N	F	P	I	N	F	P	I	N	F	P	I
TP53	6/9	++	+	+	2/4	++	+	+	0/7	n/a	n/a	n/a	n/d			
PDX1	5/8	++	++	+	4/4	++	++	+	2/8	++	++	+	n/d			
CK19	6/6	+++	+++	++	3/3	+++	+++	+++	6/6	+++	+++	++	n/d			
E-CAD	6/6	+++	+++	++	3/3	+++	+++	+++	6/6	+++	+++	++	n/d			
HES1	9/9	+++	+++	+	4/4	+++	+++	+	9/9	++	++	+	n/d			
MYC	3/3	+++	+++	+++	n/d				3/3	+++	+++	+++	n/d			

F, frequency of lesions (or discrete regions of tumor) that scored positive per tissue sample (+, <10%; ++, 10–50%; +++, >50%); I, intensity of expression per positive cell (+, weak; ++, moderate; +++, strong); N; number of tissue samples with positive lesions over total evaluated; n/a, not applicable; n/d, not determined; P, percentage of cells within a specified lesion that were positive (+ <10%; ++, 10–50%; +++, >50%).

Table S3. Immunohistochemical analyses of PanINs, MCN, invasive PDA, and metastases in *Kras;N2ko* mice

	PanIN				MCN				Tumor				Metastases			
Marker	N	F	P	I	N	F	P	I	N	F	P	I	N	F	P	I
TP53	8/10	++	+	+	5/7	++	++	+	6/10	+	+	+	0/3	n/a	n/a	n/a
PDX1	10/10	+++	+++	+++	7/7	+++	+++	+++	10/10	+++	+++	++	3/3	+++	+++	++
CK19	10/10	+++	+++	+++	7/7	+++	+++	+++	5/10	++	+	+	1/3	Z	++	+
E-CAD	10/10	+++	+++	+++	7/7	+++	+++	+++	5/10	++	+	+	1/3	Z	++	+
HES1	10/10	+++	+	+	7/7	++	+	+	10/10	+++	++	+	3/3	+++	++	+
MYC	8/8	++	++	+	5/5	++	++	+	8/8	++	++	+	2/2	++	+	+

F, frequency of lesions (or discrete regions of tumor) that scored positive per tissue sample (+, <10%; ++, 10–50%; +++, >50%); I, intensity of expression per positive cell (+, weak; ++, moderate; +++, strong); N; number of tissue samples with positive lesions over total evaluated; n/a, not applicable; P, percentage of cells within a specified lesion that were positive (+ <10%; ++, 10–50%; +++, >50%); Z, presence of stochastic heterogeneity.

Table S4. Clinical spectrum of disease in *Kras* mice

				Histology						
Identification no.	Age, d	MCN	PDAC	>50%	<50%	Liver	Lung	Ascites	Cachexia	Other
2190	467	N	Y	G	U, S	Y^{M}	Y^{M}	Y	Y	
4874	358	N	N			N	N	N	N	Postmortem
5630	538	N	N			N	N	N	N	FAP
9801	300	N	Y	G		Y^{M}	Y^{M}	Y^{B}	Y	LN^{M}
9425	209	N	N			N	N	N	N	F
9907	444	N	Y	G		Y^{M}	N	N	N	
10265	603	N	Y	G		Y^{M}	Y^{M}	N	N	F
10266	425	N	Y	G		Y^{M}				SM
10259	269	N	N							
10526	523	Y	Y	U		Y^{M}	N	N	N	
11752	347	N	N			N	N	N	Y	
14128	482	Y	Y	G		Y^{M}	N	Y^{B}	N	AD, LN^{M}, A^{m}, SM
17027	239	N	Y	G		Y^{M}	Y^{M}	N	N	
17165	576	N	N					Y		D^{inv}
17395	512	N	N							F
17654	335	N	N			N	N	N	N	
19476	630	N	N			N	N	N	N	F, FAP
20283	489	N	Y	G	U	N	N			Steatosis of liver
50709	635	Y	Y	G	U					F
52231	427	N	N			N	N	N	N	F
54474	311	N	N							
510042	569	N	Y	G		Y^{M}	Y^{M}	Y^{B}		SM
510046	330	N	N			N	N	Y^{B}	N	Hemorrhage, Panc necrosis
510242	421	N	Y	G		N	N	N	N	
510256	293	N	Y	U	G	N	N	N	N	LN^{M}, SM
610020	288	N	Y	G		Y^{M}	Y^{M}	N	N	F
Total		3/26	14/26			10/26	6/26	5/26	3/26	
%		12%	54%			38%	23%	19%	12%	

A, adrenal gland; AD, abdominal distention; ^{B}, bloody ascites; D^{inv}, duodenum invasion; F, fibrosis; FAP, fat atrophy of the pancreas; G, glandular; LN, lymph node; ^{M}, macrometastasis; ^{m}, micrometastasis; N, no; Panc, pancreas; S, sarcomatoid; SM, splenomegaly (spleen >20 mm); U, undifferentiated; Y, yes.

Table S5. Clinical spectrum of disease in *Kras;N1ko* mice

				Histology						
Identification no.	Age, d	MCN	PDAC	>50%	<50%	Liver	Lung	Ascites	Cachexia	Other
818	594	N	N			N	N	N	Y	SM, lymphoma
1015	198	N	Y	S		N	N	N	Y	A^{M}, D^{inv}, liver necrosis
1016	226	N	N			N	N	N	N	FAP
4894	337	Y	N			N	N	Y^{B}	Y	Panc necrosis
5051	278	N	N			N	N	N	Y	Respiration insufficiency
5306	357	N	Y	G		N	N	N	Y	FAP, spleen necrosis
6340	563	N	N			N	N	N	N	FAP
6344	325	N	Y	G	U, S	Y^{M}	Y^{M}	Y	Y	LN^{M}
6364	300	N	Y	U	S	Y^{M}	Y^{M}	N	N	
6361	549	Y	Y	S	G	N	N	N	N	LN^{M}, FAP
6367	248	N	Y	G		Y	N	N	Y	SM, bronchitis
7289	336	N	N			N	N	N	Y	Icterus, liver necrosis, lung thromboembolism
9372	482	N	N			N	N	N	Y	Panc granulomatous inflammation, hepatitis
9382	566	Y	Y	G	S	N	N	N	N	IPMN, FAP
9854	197	N	N			N	N	N	N	FAP
9857	659	N	N			N	N	N	N	FAP
11741	298	N	N			N	N	N	Y	
15625	203	Y	Y	G	S	N	N	N	N	AD, SM
17906	374	N	N			N	N	N	N	FAP
17908	285	N	N			N	N	N	N	
50825	199	Y	Y			N	N	Y^{B}	N	Liver necrosis, bronchitis
52138	400	N	N			N	N	N	N	
54665	419	N	N			N	N	N	N	Hemorrhage
Total		6/23	9/23			3/23	2/23	2/24	9/23	
%		26%	39%			13%	9%	9%	39%	

A, adrenal gland; AD, abdominal distention; D^{inv}, duodenum invasion; FAP, fat atrophy of the pancreas; G, glandular; IPMN, intraductal papillary mucinous neoplasm; LN, lymph node; ^{M}, macrometastasis; N, no; Panc, pancreas; S, sarcomatoid; SM, splenomegaly (spleen >20 mm); U, undifferentiated; Y, yes.

Table S6. Clinical spectrum of disease in *Kras;N2ko* mice

				Histology						
Identification no.	Age, d	MCN	PDAC	>50%	<50%	Liver	Lung	Ascites	Cachexia	Other
998	438	Y	N			N	N	N	N	AD
999	438	Y	N			N	N	N	N	AD
1002	478	Y	N			N	N	N	Y	
1003	474	Y	N			N	N	N	Y	AD, D^{inv}
1006	464	Y	Y	S		Y^{M}	N	Y	Y	AD, LN^{m}
1009	669	Y	Y	S	U^{G3}	Y^{M}	Y^{M}	N	N	LN^{m}, D^{inv}
1013	580	Y	Y	S		Y^{M}	Y^{m}	N	N	AD
1014	457	Y	N			N	N	N	Y	
3113	567	Y	Y	S	U^{G3}	Y^{M}	Y^{m}	N	N	AD
5111	648	Y	N			N	N	N	N	E, pneumonia
5112	558	Y	Y	S		Y^{M}	N	Y^{B}	N	D^{inv}, LN^{M}
5114	717	Y	N			N	N	N	N	Blind
10894	608	N	Y	S		Y^{M}	N	N	N	AD, D^{inv}
14054	557	Y	N			N	N	N	N	D^{inv}
17656	335	N	Y	G	U^{G3}	Y^{M}	Y^{M}	N	N	LN^{m}, A^{M}
17693	461	Y	Y	S	G	Y^{M}	N	N	N	Sudden death
17915	556	Y	N			N	N	N	N	Panc insufficiency
17916	556	Y	N	*	*	*	*	N	Y	AD, post mortem
50753	521	Y	Y	G		N	N	N	Y	
54658	393	Y	Y	G	U^{G3}	Y^{M}	N	N	N	Panc necosis
55079	396	N	Y	S		Y^{M}	Y^{m}	Y^{B}	N	D^{inv}
Total		18/21	11/21			10/20	5/20	3/21	6/21	
%		86%	52%			50%	25%	14%	29%	

A, adrenal gland; AD, abdominal distention; D^{inv}, duodenum invasion; E, edema; G, glandular; LN, lymph node; ^{M}, macrometastasis; ^{m}, micrometastasis; N, no; Panc, pancreas; S, sarcomatoid; U, undifferentiated; Y, yes.
*Not evaluable.

Table S7. Characteristics of the stromal compartments of *Kras, Kras;N1ko, and Kras;N2ko* mice

	Kras			*Kras;N1ko*			*Kras;N2ko*			*Myc ko*		
Marker	N	P	I	N	P	I	N	P	I	N	P	I
PR	8/15	+	+	4/11	+	+	17/18	++	++	2/2	++	++
ER	0/15	–	–	1/11	+	+	9/18	+	+	2/2	+	+

I, intensity of expression per positive cell (+, weak; ++, moderate); N, number of tissue samples with positive stroma over total evaluated; P, percentage of cells within a stroma that were positive (+, <10%; ++, 10–50%; +++, >50%); PR, progesterone receptor.

Table S8. Molecular profiles of *Kras* primary pancreatic cancer cell lines

	p16				p19			p53			Smad4	
Identification no.	DNA	mRNA	Protein	Promoter	DNA	Protein	Promoter	DNA	mRNA	Protein	mRNA	Protein
2190	del	–	–	n/a	del	–	n/a	mut	+	+	+	+
9801	del	–	–	n/a	del	–	n/a	wt	+	–	+	+
17027	mut	+	–	n/a	n/d	–	n/d	wt	+	–	+	+
10265	n/a	n/a	–	M	n/a	–	M	n/a	–	–	+	+
13092	n/a	n/a	–	M	n/a	–	M	mut	+	–	+	+

del, deletion; M, methylated; mut, mutation; n/a, not applicable; n/d, not determined; wt, wild type.

Table S9. Molecular profiles of *Kras;N2ko* primary pancreatic cancer cell lines

	p16				p19			p53			Smad4	
ID	DNA	mRNA	Protein	Promoter	DNA	Protein	Promoter	DNA	mRNA	Protein	mRNA	Protein
1006	del	–	–	n/a	del	–	n/a	wt	+	–	+	+
1009	mut	+	–	U	mut	–	n/a	wt	+	–	+	+
1013	wt	+	–	M	n/a	–	M	wt	+	–	+	+
3113	del	–	–	n/a	del	–	n/a	wt	+	–	+	+
5112	n/a	n/a	–	M	n/a	–	M	wt	+	–	+	+

del, deletion; M, methylated; mut, mutation; n/a, not applicable; U, unmethylated; wt, wild type.

Table S10. Top 20 and selected TGF-β GSEA signature analysis of *Kras;N2ko vs. Kras* in 7-d-old pancreata

TGF-β signature	No.	Name	Size	ES	NES	NOM *P* value	FDR Q value	FWER *P* value	Rank at maximum
	1	VEGF_MMMEC_6HRS_UP	63	−0.73973954	−2.7084892	0	0	0	2449
I	2	TGFBETA_ALL_UP	122	−0.6643366	−2.6893036	0	0	0	3697
II	3	TGFBETA_EARLY_UP	67	−0.7087745	−2.6222773	0	0	0	2828
	4	HTERT_DN	88	−0.67262614	−2.61393	0	0	0	2203
	5	CROONQUIST_RAS_STROMA_DN	35	−0.7753971	−2.526193	0	0	0	1506
	6	CROONQUIST_IL6_STROMA_UP	62	−0.6876837	−2.5074594	0	0	0	2646
	7	VEGF_MMMEC_12HRS_UP	40	−0.7396944	−2.4997904	0	0	0	2703
	8	CMV_ALL_DN	165	−0.5892903	−2.4887757	0	0	0	3137
	9	CMV_24HRS_DN	115	−0.60143775	−2.4474874	0	0	0	3137
	10	ADIP_VS_PREADIP_DN	61	−0.6479043	−2.3746915	0	0	0	2203
	11	SANA_TNFA_ENDOTHELIAL_DN	129	−0.5758857	−2.3746207	0	0	0	3153
	12	CORDERO_KRAS_KD_VS_CONTROL_UP	124	−0.5773957	−2.358846	0	0	0	3808
	13	VEGF_MMMEC_ALL_UP	134	−0.5670125	−2.3364904	0	0	0	3170
	14	JNK_DN	53	−0.6561161	−2.336097	0	0	0	1504
	15	EMT_UP	89	−0.595401	−2.3324068	0	0	0	1812
	16	ADIP_VS_FIBRO_DN	45	−0.6774173	−2.3317726	0	0	0	1704
	17	PASSERINI_EM	52	−0.65962523	−2.3163188	0	0	0	1188
	18	NI2_MOUSE_UP	68	−0.62407684	−2.3120317	0	0	0	2273
	19	CMV_HCMV_6HRS_DN	86	−0.5928433	−2.2827766	0	0	0	2639
III	20	TGFBETA_LATE_UP	55	−0.6278115	−2.2798045	0	0	0	3697
IV	27	TGFBETA_C1_UP	26	−0.71738595	−2.1937995	0	0	0	3125
V	50	TGFBETA_C2_UP	21	−0.7205094	−2.0788	0	1.08E-04	0.004	2481
VI	59	TGFBETA_C3_UP	20	−0.71528685	−1.978819	0	8.68E-04	0.038	2828
VII	103	TGF_BETA_SIGNALING_PATHWAY	73	−0.47657073	−1.8012985	0	0.005866292	0.356	3045
VIII	210	TGFBETA_C5_UP	28	−0.50880885	−1.5387949	0.03522505	0.04333228	1	3507

NOM, nominal; FDR, false discovery rate; FWER, familywise-error rate.

Table S11. Top 20 and selected TGF-β GSEA-signature analysis of *Kras;N2ko vs. Kras* in primary cancer cells

TGF-β signature	No.	Name	Size	ES	NES	NOM *P* value	FDR *Q* value	FWER *P* value	Rank at maximum
	1	BRCA1_SW480_DN	25	0.57281667	1.6047903	0.016260162	1	0.941	4867
	2	STANELLE_E2F1_UP	37	0.5446293	1.5969661	0.029411765	1	0.959	4800
	3	ROSS_MLL_FUSION	92	0.51262605	1.5786657	0.013779528	1	0.976	3624
	4	DFOSB_BRAIN_2WKS_UP	70	0.4554071	1.5774709	0.02258727	1	0.977	3462
	5	BECKER_ESTROGEN_RESPONSIVE_SUBSET_2	16	0.7206843	1.5664608	0.062248997	1	0.981	3974
	6	PITUITARY_FETAL_UP	20	0.5904766	1.5654356	0.020661157	1	0.981	2282
I	7	TGFBETA_C3_UP	22	0.7693509	1.557574	0.012048192	1	0.983	4837
	8	PASSERINI_EM	52	0.5384598	1.5406632	0.041420117	1	0.991	4491
	9	HIPPOCAMPUS_DEVELOPMENT_POSTNATAL	93	0.40995428	1.5284934	0.056092843	1	0.992	4648
	10	MATRIX_METALLOPROTEINASES	40	0.60774666	1.5278989	0.025590552	1	0.992	5098
	11	BCNU_GLIOMA_MGMT_48HRS_DN	236	0.38457447	1.5273094	0	1	0.992	3432
	12	CREB_BRAIN_2WKS_UP	50	0.5023513	1.5242647	0.02892562	1	0.992	5003
	13	BCNU_GLIOMA_NOMGMT_48HRS_DN	39	0.53599626	1.5200945	0.0480167	1	0.993	5916
	14	CMV_24HRS_DN	120	0.5040459	1.5176041	0.021568628	1	0.994	5554
	15	P21_ANY_UP	21	0.54496384	1.5051401	0.038934425	1	1	1451
	16	BRENTANI_CYTOSKELETON	36	0.49675605	1.494601	0.04733728	1	1	3546
	17	TSA_HEPATOMA_CANCER_UP	63	0.5483822	1.4906943	0.014141414	1	1	5229
	18	HOGERKORP_ANTI_CD44_DN	17	0.619508	1.4869046	0.02739726	1	1	3159
II	19	TGFBETA_C2_UP	23	0.6331687	1.4660585	0.058091287	1	1	3449
	20	AGED_MOUSE_CEREBELLUM_UP	87	0.40096402	1.4480395	0.019417476	1	1	3658
III	49	TGFBETA_C5_UP	29	0.5311824	1.3228422	0.13373253	1	1	2431
IV	60	TGFBETA_ALL_UP	131	0.44838282	1.3071258	0.13582677	1	1	3449
V	63	TGFBETA_EARLY_UP	74	0.46519884	1.3036715	0.14741036	1	1	3449
VI	99	TGFBETA_LATE_UP	57	0.4385211	1.2246829	0.19379845	0.9441126	1	2431
VII	300	TGF_BETA_SIGNALING_PATHWAY	77	0.27689424	0.90238446	0.6062992	0.95473385	1	5197

Table S12. Top 20 and selected Myc GSEA-signature analysis of *Kras vs. Kras;N2ko* in 7-day pancreata

Myc signature	No.	Name	Size	ES	NES	NOM *P* value	FDR *Q* value	FWER *P* value	Rank at maximum
	1	ELECTRON_TRANSPORT_CHAIN	158	0.5342571	2.300599	0	0	0	4326
	2	TRNA_SYNTHETASES	27	0.7419937	2.2859864	0	0	0	4208
I	3	COLLER_MYC_UP	32	0.6781227	2.216999	0	3.84E-04	0.002	2778
	4	IDX_TSA_UP_CLUSTER5	145	0.50770676	2.158931	0	8.76E-04	0.006	4059
	5	LEE_E2F1_DN	78	0.53141326	2.0727038	0	0.001649699	0.014	3441
	6	LEE_DENA_DN	91	0.5156025	2.0725226	0	0.001374749	0.014	1955
	7	IDX_TSA_UP_CLUSTER6	257	0.4502082	2.0651782	0	0.001441618	0.017	4497
	8	WELCSH_BRCA_DN	23	0.67598593	2.0217664	0.001945525	0.002307167	0.03	2810
	9	CANTHARIDIN_DN	78	0.5077346	1.9852358	0	0.003184209	0.047	5920
II	10	SCHUMACHER_MYC_UP	87	0.48875225	1.9593258	0	0.004319648	0.07	3945
III	11	ZELLER_MYC_UP	43	0.5399944	1.8503262	0	0.015880471	0.262	2889
	12	CAMPTOTHECIN_PROBCELL_UP	34	0.56002825	1.8316183	0	0.0168502	0.294	520
	13	WELCH_GATA1	31	0.5687488	1.8138825	0.004149378	0.018689869	0.337	3743
	14	LIZUKA_G2_GR_G3	49	0.4995041	1.8052945	0.004115226	0.019245178	0.368	2443
	15	FETAL_LIVER_VS_ADULT_LIVER_GNF2	82	0.46067837	1.7911378	0	0.021657487	0.422	3410
	16	HSC_INTERMEDIATEPROGENITORS_FETAL	193	0.39740488	1.7571981	0	0.029404327	0.542	4533
	17	TGZ_ADIP_UP	31	0.5390484	1.7285321	0	0.0372291	0.66	3874
	18	CHAUVIN_ANDROGEN_REGULATED_GENES	53	0.47623584	1.7251784	0	0.036329415	0.672	3578
	19	TARTE_PC	121	0.41285878	1.722183	0	0.035080407	0.68	2706
	20	FATTY_ACID_METABOLISM	86	0.43455413	1.7186521	0.00212766	0.03449751	0.695	3522
IV	23	LEE_MYC_E2F1_DN	70	0.4449714	1.6893218	0	0.040535	0.797	1955
V	46	LEE_MYC_TGFA_UP	86	0.38082185	1.4974045	0.01594533	0.10934354	1	1104
VI	50	LEE_MYC_TGFA_DN	74	0.38602623	1.4770054	0.027777778	0.11692726	1	3386
VII	55	LEE_MYC_DN	70	0.3735229	1.4269519	0.017699115	0.15354133	1	2455
VIII	69	MYC_TARGETS	71	0.34512275	1.335033	0.042600896	0.2337143	1	2254
IX	137	MENSSEN_MYC_UP	56	0.29244816	1.0630429	0.3197556	0.5902829	1	2950

Table S13. Top 20 and selected Myc GSEA-signature analysis of *Kras vs. Kras;N2ko* in primary cancer cells

Myc signature	No.	Name	Size	ES	NES	NOM *P* value	FDR *Q* value	FWER *P* value	Rank at maximum
	1	RADIATION_SENSITIVITY	41	−0.5413243	−1.7699555	0	0.6791079	0.406	345
	2	LIZUKA_L0_GR_L1	20	−0.63693947	−1.6705452	0.01996008	1	0.81	2738
	3	HIPPOCAMPUS_DEVELOPMENT_PRENATAL	58	−0.52234524	−1.6371815	0.013461539	1	0.9	1985
	4	FERRANDO_LYL1_NEIGHBORS	23	−0.5858673	−1.6352273	0.033264033	1	0.904	68
	5	SMITH_HTERT_UP	155	−0.45070013	−1.6220243	0.00591716	0.95484215	0.919	4327
	6	BYSTRYKH_HSC_BRAIN_CIS_GLOCUS	130	−0.45005926	−1.6199737	0.003752345	0.817574	0.919	4532
	7	CMV_HCMV_TIMECOURSE_18HRS_UP	101	−0.47429216	−1.6039898	0	0.81278753	0.951	5032
	8	YAMA_RECURRENT_HCC_UP	26	−0.6083519	−1.5693748	0.024	1	0.972	68
I	9	COLLER_MYC_UP	33	−0.64743054	−1.5649265	0.030425964	0.93578124	0.974	4101
	10	DAC_FIBRO_UP	32	−0.6267182	−1.5453129	0.02892562	1	0.98	434
II	11	ZELLER_MYC_UP	46	−0.54964083	−1.5182744	0.046511628	1	0.989	1941
	12	BYSTRYKH_HSC_CIS_GLOCUS	229	−0.36202464	−1.5155611	0	1	0.989	4357
III	13	MYC_TARGETS	74	−0.50701964	−1.508564	0.07170542	1	0.991	4478
	14	UVC_HIGH_D2_DN	57	−0.45448267	−1.4786458	0.041501977	1	0.998	3948
	15	STEMCELL_COMMON_UP	315	−0.4237171	−1.4669318	0.05511811	1	0.998	6368
	16	HDACI_COLON_SUL24HRS_UP	105	−0.43819037	−1.4586589	0.050403226	1	0.998	5993
	17	HDACI_COLON_CLUSTER10	50	−0.41208372	−1.4579145	0.017307693	1	0.998	4566
	18	HDACI_COLON_CLUSTER5	37	−0.44846	−1.4569557	0.028985508	1	0.998	3738
	19	VENTRICLES_UP	307	−0.3362042	−1.4472296	0.044624746	1	0.998	4557
	20	UVB_NHEK2_DN	160	−0.32544827	−1.4116431	0.020449897	1	1	5077
IV	25	SCHUMACHER_MYC_UP	92	−0.43308792	−1.3953692	0.12645914	1	1	3422
V	127	LEE_MYC_UP	95	−0.28379893	−1.1302445	0.29492188	0.9526402	1	3889
VI	321	LEE_MYC_TGFA_UP	88	−0.24205469	−0.7627981	0.7643312	1	1	4431
VII	342	FERNANDEZ_MYC_TARGETS	280	−0.17656198	−0.727881	0.91581106	1	1	4997
VIII	361	MENSSEN_MYC_UP	57	−0.23652063	−0.6912166	0.8199234	1	1	7119

Table S14. PCR primers (5′–3′) used

Name	Forward	Reverse
qRT-PCR-Notch1	TGTGCTTTCACACTGGCACAG	CCACTTAGAAGGAATTCCACC
qRT-PCR-Notch2	CCCAGAACCAATCAGGTTAGC	GCCGAGACTCTAGCAATCACAA
qRT-PCR-Notch3	TGGCTCTACTGCACTGATCCTG	CAAGCTCATCCACTGCATTGAC
qRT-PCR-Notch4	GGACTACACCTTTGATGCTGGC	TTCCCCTTTTATCCCTGGCTC
qRT-PCR-Hes1	CGGTGTTAACGCCCTCACA	CGGCTTCAGCGAGTGCAT
qRT-PCR-Ecad	CGTCCTGCCAATCCTGATGAA	ACCACTGCCCTCGTAATCGAA
qRT-PCR-Vim	CATCTCTGGTCTCACCGTCTT	GCCTCTGCCAACCTTTTCTT
qRT-PCR-TGFb1	GTACAGCAAGGTCCTTGCCCT	TAGTAGACGATGGGCAGTGGC
qRT-PCR-Twist	CGGGTCATGGCTAACGTG	CAGCTTGCCATCTTGGAGTC
qRT-PCR-Myc	AAGCTGGTCTCGGAGAA	GGTTTGCCTCTTCTCCAC
qRT-PCR-Cyp	ATGGTCAACCCCACCGTGT	TTCTGCTGTCTTTGGAACTTTGTC
ChIP-Myc SiteA	AAGAGAAAATGGTCGGGCGCGCAGTT	GCGGGGATTAGCCAGAGAATCTCTCT
ChIP-Myc SiteB	AACGTTACTTTGATCTGATCAGGGCC	AAGGCGCTAGACGCGAGAATATGCC
ChIP-Myc SiteC	AACGGAAGCATACACACACAATTCG	CGTTTTCTGAGTACAAAGACCAACCA
ChIP-Hes1	AGACCTTGTGCCTAGCGGCCAATG	AGGGCTACTTAGTGATCGGTAGCAC
ChIP-Cdc2a	GCATTTGAATTGTGTTAGTCTTGGAGGG	TCCGCCAATCCGATTGCACGTAGAC
ChIP-hMyc-proximal	CCCGAGACTGTTGCAAACC	ACTGAGTCCCCCAATTTGCT
ChIP-hMyc-distal	AGAGGGAGCAAAAGAAAATGG	AGAGGGAGCAAAAGAAAATGG
ChIP-hHes1	CCAAATCCAAACGAGGAATTT	GGACGGGTGTAAGAATGTGAG
ChIP-hGAPDH	TACTAGCGGTTTTACGGGCG	TCGAACAGGAGGAGCAGAGAGCGA
p16-methylated	CGATTGGGCGGGTATTGAATTTTCGC	CACGTCATACACACGACCCTAAACCG
p16-unmethylated	GTGATTGGGTGGGTATTGAATTTTTGTG	CACACATCATACACACAACCCTAAACCA
p19-methylated	AATCGAAAATAAATAACGTTTTCGC	TTTAAACCCTTAACGATACGTACG
p19-unmethylated	AAATTGAAAATAAATAATGTTTTTGG	TTAAACCCTTAACAATACACTACAT

Appendix 2

Pawel K. Mazur, Hassan Nakhei, Bence Sipos, Ursula Zimber-Strobl, Lothar Strobl, Freddy Radtke, Roland M. Schmid, Jens T. Siveke.

Identification of Pdx1 expression in the skin discloses different roles of Notch1 and Notch2 in Kras^{G12D}-induced skin carcinogenesis.

PLoS One. 2010 Oct 22;5(10):e13578.

OPEN ACCESS Freely available online

PLoS one

Identification of Epidermal Pdx1 Expression Discloses Different Roles of Notch1 and Notch2 in Murine *Kras^{G12D}*-Induced Skin Carcinogenesis *In Vivo*

Pawel K. Mazur[1], Barbara M. Grüner[1], Hassan Nakhai[2], Bence Sipos[3], Ursula Zimber-Strobl[4], Lothar J. Strobl[4], Freddy Radtke[5], Roland M. Schmid[1], Jens T. Siveke[1]*

1 2nd Department of Internal Medicine, Klinikum Rechts der Isar University Hospital, Technical University of Munich, Munich, Germany, **2** Department of Biological Sciences, University of Warwick, Coventry, United Kingdom, **3** Institute of Pathology, University Hospital, University of Tübingen, Tübingen, Germany, **4** Department of Gene Vectors, Helmholtz Zentrum, German Research Center for Environmental Health, Munich, Germany, **5** ISREC, Ecole Polytechnique Fédérale de Lausanne (EPFL SV ISREC), Lausanne, Switzerland

Abstract

Background: The Ras and Notch signaling pathways are frequently activated during development to control many diverse cellular processes and are often dysregulated during tumorigenesis. To study the role of Notch and oncogenic Kras signaling in a progenitor cell population, *Pdx1-Cre* mice were utilized to generate conditional oncogenic *Kras^{G12D}* mice with ablation of *Notch1* and/or *Notch2*.

Methodology/Principal Findings: Surprisingly, mice with activated *Kras^{G12D}* and *Notch1* but not *Notch2* ablation developed skin papillomas progressing to squamous cell carcinoma providing evidence for *Pdx1* expression in the skin. Immunostaining and lineage tracing experiments indicate that PDX1 is present predominantly in the suprabasal layers of the epidermis and rarely in the basal layer. Further analysis of keratinocytes *in vitro* revealed differentiation-dependent expression of PDX1 in terminally differentiated keratinocytes. PDX1 expression was also increased during wound healing. Further analysis revealed that loss of Notch1 but not Notch2 is critical for skin tumor development. Reasons for this include distinct Notch expression with Notch1 in all layers and Notch2 in the suprabasal layer as well as distinctive p21 and β-catenin signaling inhibition capabilities.

Conclusions/Significance: Our results provide strong evidence for epidermal expression of Pdx1 as of yet not identified function. In addition, this finding may be relevant for research using *Pdx1-Cre* transgenic strains. Additionally, our study confirms distinctive expression and functions of Notch1 and Notch2 in the skin supporting the importance of careful dissection of the contribution of individual Notch receptors.

Citation: Mazur PK, Grüner BM, Nakhai H, Sipos B, Zimber-Strobl U, et al. (2010) Identification of Epidermal Pdx1 Expression Discloses Different Roles of Notch1 and Notch2 in Murine *Kras^{G12D}*-Induced Skin Carcinogenesis In Vivo. *PLoS ONE* 5(10): e13578. doi:10.1371/journal.pone.0013578

Editor: Joseph Alan Bauer, Bauer Research Foundation, United States of America

Received February 6, 2010; **Accepted** September 22, 2010; **Published** October 22, 2010

Funding: This work was supported by grants from the German Cancer Aid (#107195), The Lustgarten Foundation (RFP05-14 and 06-12) and the German Research Foundation (SI 1549/1-1; all to J.T.S.). The funders had no role in study design, data collection and analysis, decision to publish, or preparation of the manuscript.

Competing Interests: The authors have declared that no competing interests exist.

* E-mail: jens.siveke@lrz.tum.de

Introduction

Conditional tissue-specific modulation of genes using Cre/loxP recombination in genetically engineered mice provides an enormous leap forward to study gene function in detail yet requires detailed knowledge of gene regulation and expression patterns. For pancreatic targeting of genes, *Pdx1-Cre* mice are commonly used [1–3], in which Cre-recombinase is expressed under a 4.5 to 5.5 kb fragment of the *Pdx1* promoter. The transcription factor *Pdx1* (pancreas and duodenum homeobox gene 1) directs pancreatic cell formation, maintenance and function. *Pdx1* is expressed in the region of the endoderm that ultimately gives rise to stomach, pancreas and duodenum and its function is critical for posterior foregut development [4]. Postnatally, Pdx1 is mainly expressed in insulin-producing endocrine cells of the pancreas. Ablation of *Pdx1* results in defects of different cell types including malformations of the pylorus and duodenum, absence of Brunner's glands and reduced numbers of specific enteroendocrine cell types in the stomach and intestine. Loss of *Pdx1* function results in pancreatic agenesis, while heterozygous expression leads to defects in glucose homeostasis. *Pdx1*-deficient mice survive up to 6.5 days after birth, are severely dehydrated, have no fur and a delicate, cracking skin. [5–8]. Here, we report epidermal PDX1 expression observed due to an unexpected skin tumor formation in *Pdx1-Cre* mice with activation of oncogenic *Kras^{G12D}* and loss of *Notch1* but not *Notch2*.

Notch proteins are evolutionarily conserved large transmembrane receptors, which upon ligand binding undergo proteolytic cleavage mediated by the γ-secretase-presenilin complex releasing the intracellular fragment (NIC). NIC is translocated to the nucleus where it binds and activates the mammalian repressor RBP-Jκ thereby regulating fetal and postnatal cell fate decisions

and differentiation processes [9]. Notch receptors are expressed in the skin, although their precise functions remain uncertain (reviewed in [10,11]). Gain- and loss-of-function studies have suggested various functions for Notch including proliferation control, differentiation switch of developing epidermis and formation of hair follicles [12–17]. Mice with epidermal loss of Notch1 as well as *Presenilin*-deficient mice develop epidermal hyperplasia and skin cancers [14,18]. Of note, most studies have focused on Notch1 and downstream signaling members such as Rbpj or Hes1 [19,20]. Very little is known about the function of Notch2 and other receptors in skin physiology and carcinogenesis. Here, we investigate the role of Notch1 and Notch2 using two different *Cre* expression systems. Our results provide evidence for different roles of Notch1 and Notch2 in skin development and carcinogenesis.

Results

Notch1 but not *Notch2* deletion increases susceptibility to $Kras^{G12D}$ induced skin carcinogenesis in *Pdx1-Cre* mice

To analyze the effect of *Notch1* and *Notch2* deficiency during pancreas carcinogenesis, we crossed previously described *Pdx1-Cre* [2], $Notch1^{fl/fl}$ [21], $Notch2^{fl/fl}$ [22] and $Kras^{+/LSL\text{-}G12D}$ [3] mice for generation of $Pdx1\text{-}Cre;Kras^{+/LSL\text{-}G12D}$, $Pdx1\text{-}Cre;Kras^{+/LSL\text{-}G12D};Notch1^{fl/fl}$ and $Pdx1\text{-}Cre;Kras^{+/LSL\text{-}G12D};Notch2^{fl/fl}$ mice (referred to as *Pdx1-Cre;Kras*, *Pdx1-Cre;Kras;N1ko* and *Pdx1-Cre;Kras;N2ko*, respectively). These mice were born at the expected Mendelian ratio and successful recombination of the floxed loci in the pancreas was confirmed by PCR (Fig. 1C). Surprisingly, *Pdx1-Cre;Kras;N1ko* mice developed focal skin hyperplasia at 10–15 days of age and as early as 4 weeks of age developed massive skin papillomas (Fig. 1D). These lesions and tumors showed recombination of the floxed loci (Fig. 1C) pointing to epidermal *Cre* expression, which was further corroborated using *Pdx1-Cre;Kras;N1-ko;ROSA26R-LacZ* reporter mice (Fig. 1F) [23]. The penetrance of the skin papilloma development was 78%. In contrast, *Pdx1-Cre;Kras;N2ko* mice rarely developed any skin phenotype. However, double *Notch1* and *Notch2* knockout mice (*Pdx1-Cre;Kras;N1ko;N2ko*) featured an accelerated skin tumor formation (Fig. 1A and B) suggesting an essential role of Notch1 ablation in epidermal lesion development and a promoting role of Notch2 deletion. *Pdx1-Cre;Kras* mice manifested a skin phenotype with low penetrance, which has been observed previously [3,24]. Most tumors encountered in *Pdx1-Cre;Kras;N1ko* mice were benign papillomas but often grew large and ulcerating, requiring euthanasia of animals for ethical reasons. Hence, the intended pancreatic carcinogenesis study was inconclusive (data not shown).

Pdx1-Cre;Kras;N1ko mice developed the following skin pathologies: squamous papillomas involving the ear, neck, lips, anal and vulvo-vaginal skin, epidermal cysts, and sebaceous gland hyperplasia and cutaneous horns to lesser extend (Fig. 1D and E). Moreover, 32% of the animals developed squamous cell carcinomas (SCC), (Fig. 1E), supporting the previous observations that papillomas progressing to SCC are a common manifestation of activated Ras signaling [25–27]. Mice without oncogenic $Kras^{G12D}$ but ablation of *Notch1* and *Notch2* (*Pdx1-Cre;N1ko*, *Pdx1-Cre;N2ko*) only very rarely developed skin abnormalities (not shown).

Evidence of *Pdx1* expression *in vivo* and *in vitro*

The observation that *Pdx1-Cre;Kras;N1ko* mice develop skin neoplastic lesions with high penetrance and undergo Cre-mediated recombination are evidence of *Cre* expression in the epidermis possibly due to *Pdx1-Cre* transgene misexpression or physiological PDX1 expression in the skin. To test both hypotheses, immunohistochemical expression analysis was performed in the skin of wildtype and *Pdx1-Cre* mice, which showed a small subset of $PDX1^+$ cells (Fig. 2A). Thus, the observed phenotype is due to physiological PDX1 expression in the skin rather than transgenic misexpression of Cre recombinase.

Immunofluorescent staining of PDX1 shows that the intensity of staining was comparable to that in the duodenum and much lower than in pancreatic islet cells (Fig. 2Bi and ii). Double immunofluorescent staining revealed that PDX1 co-localizes with Keratin10 (K10) in the spinous layer of the epidermis (Fig. 2Biii; arrowheads). Noteworthy, a very small fraction of $PDX1^+$ cells was located in the basal layer of the epidermis suggesting that PDX1 expression may be initiated also in this layer (Fig. 2Bi and iii; arrows).

Above-mentioned experiments demonstrate that PDX1 is predominantly present in differentiated keratinocytes of the skin. To test whether PDX1 expression is regulated during keratinocyte differentiation we induced terminal differentiation in cultured wildtype keratinocytes by calcium as described [28]. As early as 12 hours after calcium addition growth arrest and a switch in keratin expression occurred. As expected, treated keratinocytes showed a three-fold induction of the differentiation markers *Keratin10* and *Loricrin* and a five fold reduction of *p63* associated with amplifying keratinocytes in the basal layer of the epidermis. In addition, we found a robust 10-fold induction of *Pdx1* transcript expression in treated keratinocytes (Fig. 2C). These findings strongly support the hypothesis that *Pdx1* is predominantly expressed in suprabasal layers of the epidermis (Fig. 2D).

Mosaic epidermal *Cre* expression in *Pdx1-Cre* mice

Physiological PDX1 expression in the epidermis does not explain the stochastic character of papilloma formation in the *Pdx1-Cre;Kras,N1ko* mice. Hence, we speculated that *Cre* expression has a mosaic character or alternatively may be induced by mechanical skin irritation. To address the first hypothesis we examined X-Gal expression in *Pdx1-Cre;ROSA26R-LacZ* reporter mice [23]. Consistent with previous studies, we found that *Pdx1-Cre* mice showed a mosaic recombination pattern in the pancreas [1] (Fig. 3Ai). Interestingly, similar mosaic staining was observed in the skin (Fig. 3Aii). Microscopic evaluation of X-Gal positive areas indicated that suprabasal keratinocytes underwent recombination (Fig. 3Aiii; arrowheads), supporting the hypothesis that PDX1 is mainly expressed in differentiated keratinocytes. However, we found sporadically $X\text{-}Gal^+$ keratinocytes residing in the basal layer (Fig. 3Aiii; arrow). All examined skin hyperplasia had $X\text{-}Gal^+$ basal layer cells suggesting that neoplastic structures originate from the basal keratinocytes of the skin (Fig. 3Aiv; arrow).

To further asses the scale of recombination in the basal layer ($K14^+$) and the spinous layer ($K10^+$) of the epidermis we tested freshly isolated keratinocytes from *Pdx1-Cre;N1ko* mice. Cells were fractioned for K14 and K10 expression respectively using fluorescent activated cell sorting (FACS). Cre-mediated recombination was measured using quantitative PCR amplifying the recombined allele of floxed *Notch1* that was normalized to input and then compared to fully recombined DNA. We found that only 5% of DNA isolated from total keratinocytes underwent recombination in *Pdx-Cre;N1ko* mice and most of them were found in the suprabasal layer. We sporadically (below 0.5%) found $K14^+$ cells with recombined Notch1 loci hypothesizing that these cells could be the cell-of-origin for papilloma development (Fig. 3B).

As papilloma development in *Pdx1-Cre* mice usually occurred in regions susceptible to grooming, scratching and wounding, we speculated that PDX1 expression may be induced in wounded skin triggering Cre-mediated $Kras^{G12D}$ activation and *Notch1* ablation.

A

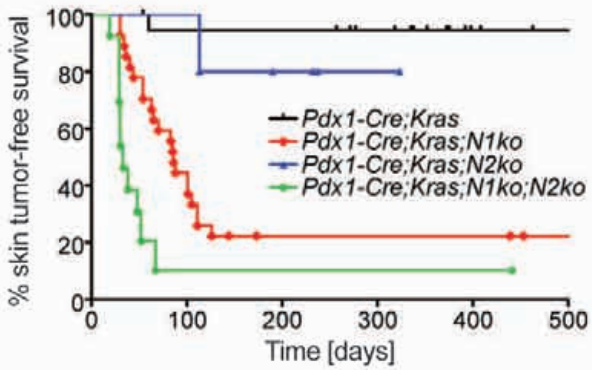

B

	Pdx1-Cre; Kras	*Pdx1-Cre; Kras; N1ko*	*Pdx1-Cre; Kras; N2ko*	*Pdx1-Cre; Kras; N1ko;N2ko*
N	19	27	5	13
Median survival [days]	372	86	232	33
Papillomas	5%	78%	20%	85%

C

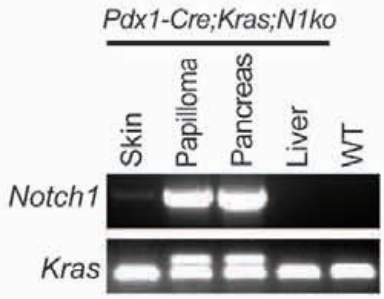

D

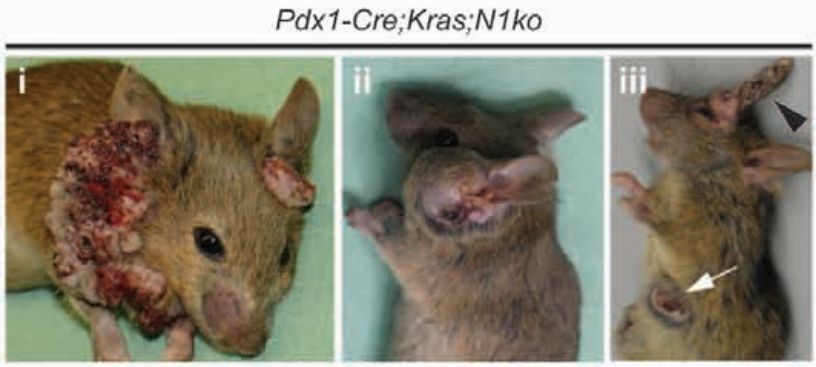

E

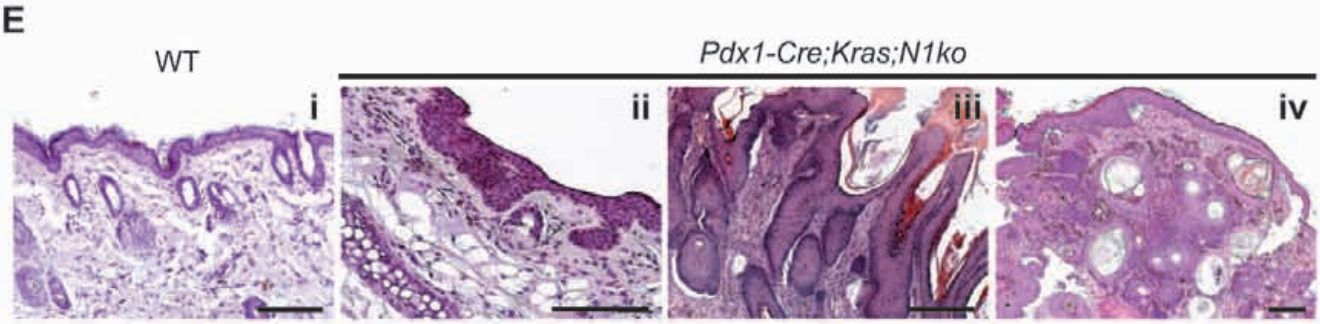

F

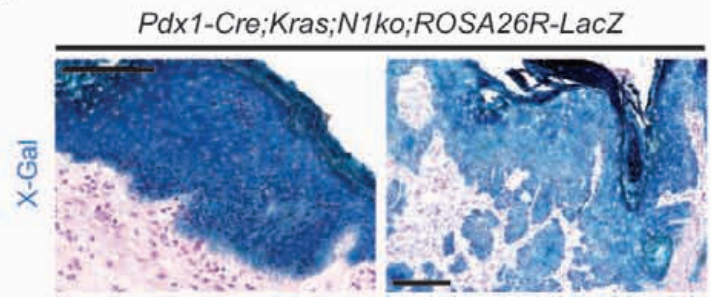

Figure 1. ***Pdx1-Cre;Kras;N1ko*** **mice develop skin tumors. A:** Kaplan-Meier tumor-free survival analysis of *Pdx1-Cre* mice. **B:** Table summarizing survival and skin tumor incidence observed in *Pdx1-Cre* mice. **C:** PCR results confirm *Notch1* deletion and $Kras^{G12D}$ activation in pancreas and skin papilloma while non-recombined status in unaffected skin, liver and in WT control DNA. **D:** Examples of skin neoplasia observed: papillomas of neck-head and ear (i), sebaceous gland tumor (ii), cutaneous horns (iii, black arrowhead) and SCC (iii, white arrow). **E:** Hematoxilin and eosin staining (HE) of WT skin (i) and characteristic cutaneous histopathologies found in *Pdx1-Cre;Kras;N1ko mice*: hyperplasia (ii), skin papilloma (iii) and SCC (iv). **F:** X-Gal staining indicates Cre-mediated recombination in skin hyperplasia (left) and papillomas (right) of *Pdx1-Cre;Kras;N1ko;ROSA26R-LacZ* reporter mice. The scale bars represent 50 μm.
doi:10.1371/journal.pone.0013578.g001

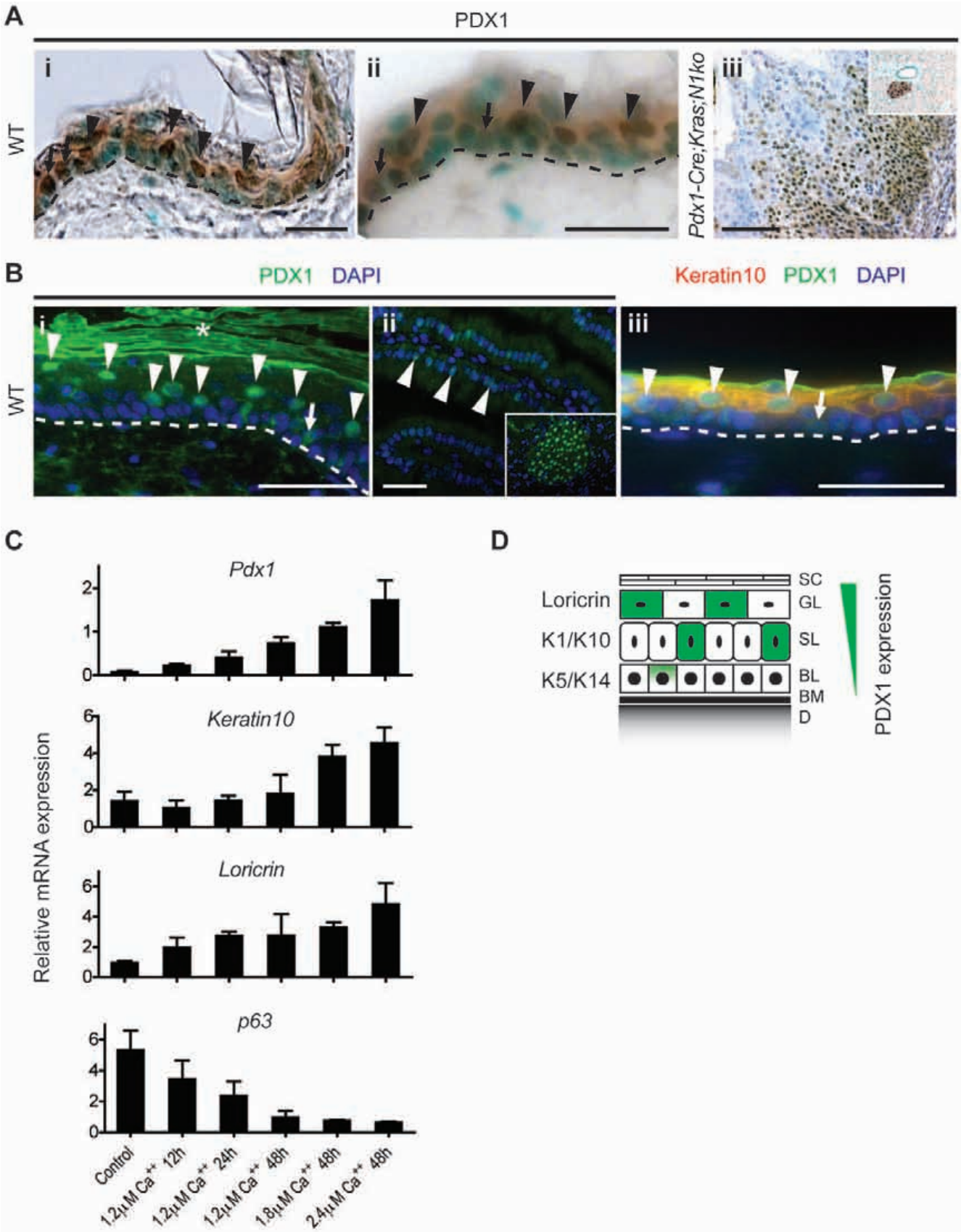
A
PDX1
WT
i
ii
iii
Pdx1-Cre;Kras;N1ko
B
PDX1 DAPI
Keratin10 PDX1 DAPI
WT
i
ii
iii
C
Pdx1
Keratin10
Loricrin
p63
Relative mRNA expression
Control
1.2μM Ca++ 12h
1.2μM Ca++ 24h
1.2μM Ca++ 48h
1.8μM Ca++ 48h
2.4μM Ca++ 48h
D
Loricrin
K1/K10
K5/K14
SC
GL
SL
BL
BM
D
PDX1 expression

Figure 2. Pdx1 is physiologically expressed in the adult mouse epidermis. A: Immunohistochemical PDX1 staining of normal wildtype epidermis (i, ii) reveals that PDX1 is expressed in suprabasal keratinocytes (black arrowheads) and only rarely in basal cells (black arrows). *Pdx1-Cre;Kras;N1ko* papilloma (iii) is strongly positive for PDX1. Inclusion (iii) shows positive staining of pancreatic islet cells. Nuclei were contrastained with methyl green (i, ii) or hematoxilin (iii). **B:** Immunofluorescent PDX1 staining (i) indicates positive keratinocytes in the suprabasal (white arrowheads) and the basal (arrow) layer of the skin. Signal strength is comparable to that in duodenum cells (ii, arrowheads) and weaker than in pancreatic islet cells (ii, inclusion). Double immunofluorescence (iii) demonstrates that the majority of $PDX1^+$ cells co-localize with a suprabasal marker Keratin10 (arrowheads) however, a small subset of $PDX1^+$ cells can be found in the basal layer of the epidermis (arrow). Asterisks indicate unspecific staining of stratum corneum. **C:** Pdx1 expression in cultured keratinocytes is increased during Ca^{++}-induced differentiation. Quantitative RT-PCR of *Pdx1*, *Keratin10*, *Loricrin* and *p63* transcripts in induced primary keratinocytes *in vitro*. **D:** Schematic representation of PDX1 expression in the epidermal layers: (SC) Stratum Corneum, (GL) Granular Layer, (SL) Spinous Layer, (BL) Basal Layer, (BM) Basement Membrane, (D) Dermis and their markers: Loricrin, K1/10, K5/14. The scale bars represent 50 μm.
doi:10.1371/journal.pone.0013578.g002

To test this hypothesis, wounds were induced on the back skin of wild type mice. Six days after wound formation mice were sacrificed and sections of scared skin were dissected and analyzed. Increased PDX1 expression was found in the scar tissue and in the transition zone between normal and wounded epidermis (Fig. 3C). PDX1 staining pattern was nuclear and partially cytoplasmic as previously described [29–32]. Quantitative RT-PCR indicated a three-fold induction of *Pdx1* and highly increased *Keratin6* transcript levels in wounded compared to normal epidermis (Fig. 3D) supporting PDX1 expression in wounded skin. In summary these results denote (i) physiological *Pdx1* expression in the skin, (ii) restricted to differentiated keratinocytes but sporadically present in $K14^+$ basal cells, (iii) mosaic *Pdx1-Cre* epidermal expression, and (iv) *Pdx1* induction in wounded skin.

Histopathology of skin tumors developing in *Pdx1-Cre;Kras;N1ko* mice

Histological investigations revealed that the papillomas and hyperplastic epithelium cover thin expansions of a fibroblastic stroma often with mild chronic inflammatory infiltrates. Local hyperplasia and squamous papillomas were well differentiated, rarely demonstrating focal dysplasia (Fig. 1E). Sections of typical papillomas were analyzed by immunofluorescence for differentiation markers including Keratin 14, 10 and Loricrin. In the papillomas all three keratins were expressed in a manner similar to normal skin, except that there was a delay in the onset of K10 expression consistent with an expansion of the proliferative compartment expressing K14 and CyclinD1 (Fig. 4). In line with the hyperplastic character was the expression of K6, a keratin usually expressed in hair follicles or in pathological conditions resulting in hyperplasia (Fig. 4). The observed keratin expression pattern is characteristic of well-differentiated squamous papillomas. Older mice developed hyperproliferative lesions that exhibited cellular atypia, increased mitosis and an invasive growth pattern with characteristic keratin 'pearls' formation and a high degree of keratinization that are diagnostic of well-differentiated SCC. Of note, no basal cell carcinomas (BCC) were observed in *Pdx1-Cre;Kras;N1ko* mice and no signs of a metastatic disease were observed.

Immunohistochemical characterization of papillomas revealed strong activation of Ras-dependent phospho-ERK consistent with previous studies [33] as well as robust MYC expression associated with skin neoplastic transformation [34]. Interestingly, robust p63 expression throughout the papilloma tissue was noted. Normally, the presence of p63 is restricted to the thin layer of basal keratinocytes due to inhibition by Notch1. Expression of p63 is characteristic for progenitor and multiplying cells of the epidermis. Expanded and strong CyclinD1 staining supports this conclusion (Fig. 4). This expression pattern is common and characteristic for cutaneous neoplasia.

Notch1 but not Notch2 is a tumor suppressor in the skin

Although the role of Notch receptors in the skin has already been intensively studied [12–17], we aimed to characterize epidermal *Notch1* and *Notch2* deficiency in our model. To do so, $Notch1^{fl/fl}$ [21] and $Notch2^{fl/fl}$ [22] mice were crossed with basal keratinocyte-specific *Keratin5-Cre* mice [35] (named *K5;N1ko* and *K5;N2ko* respectively). These mice were born at the expected Mendelian ratio (Fig. 5B) and successful recombination of the floxed loci was confirmed in isolated primary keratinocytes by immunoblot (Fig. 6A).

Consistent with previous studies, *K5;N1ko* mice did not develop proper hair follicles showing a 'naked' phenotype. Additionally, the epidermis was thinner, easily cracking and prone to injury (Fig. 5B, D and E). Such a phenotype has been attributed to a role of Notch1 in the stimulation of keratinocyte differentiation [19,36,37]. Before the age of 9 months, *K5;N1ko* mice developed extensive hyperplasia and keratinization of the corneal epithelium, which resulted in opaque plague formation and blindness (Fig. 5B and C) [14]. All analyzed mice (n = 4) developed skin neoplasia at 9 to 12 months of age and additionally BCC, SCC and papillomas were noticed (Fig. 5B and C). By contrast, *K5;N2ko* mice featured a non-pathological skin and hair follicle formation (Fig. 5B and D) with normal growth cycles. However, impairment of hair growth direction that manifested in more upwards-ruffle appearance of fur was observed (Fig. 5B). Mice followed up to 12 months of age (n = 4) did not show any sign of tumorigenesis. Taken together, our findings confer that Notch1, but not Notch2 is a tumor suppressor and plays a crucial role in proper skin development and differentiation.

Since expression in different compartments may explain distinct Notch1 and Notch2 functions, we analyzed the expression pattern of these receptors using immunohistochemical staining as well as transgenic *Notch1-GFP* [38] and $Notch2^{lacZ}$ knockin [39] reporter mice. We found Notch2 and X-Gal as a surrogate for Notch2 expression in spinous and granular layers of the epidermis (Fig. 5A). Notch1 and GFP expression in *Notch1-GFP* mice was found throughout the epidermal layers as previously described [37], including the basal layer of keratinocytes formed by stem cells and highly proliferative transit amplifying cells (Fig. 5A). Besides these differences in expression, different and context-specific functions of Notch1 and Notch2 have been described. We thus isolated and cultured primary keratinocytes from *K5;N1ko* and *K5;N2ko* mice, which showed no protein expression of the respective Notch receptor (Fig. 6A) and significantly downregulated levels of *Hes1* transcripts (Fig. 6B)

Notch1 signaling is essential for proper skin differentiation through induction of p21 (WAF1/Cip1) [37,40]. We speculated that Notch2 signaling might not be required for this process since it is expressed mainly by differentiated keratinocytes. p21 is a cyclin-dependent kinase inhibitor that induces cell cycle arrest [41], predictably its loss is commonly associated with skin malignancies, particularly in an active Ras context [34]. We found that p21 expression was highly reduced in Notch1 ablated cells whereas no significant differences were noted in *Notch2* deficient keratinocytes both on mRNA and protein level (Fig. 6A,

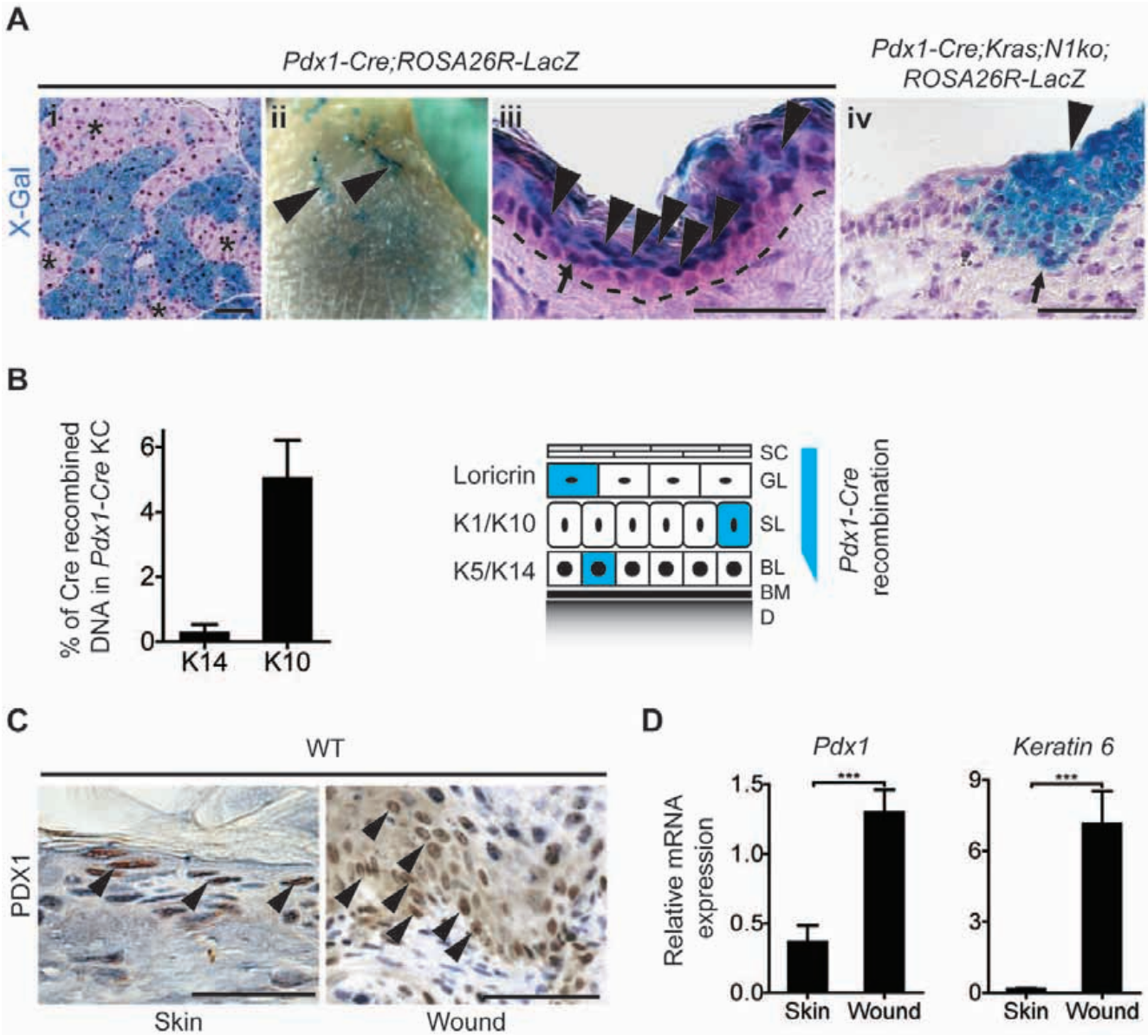

Figure 3. Mosaic Cre-mediated recombination in *Pdx1-Cre* mice. A: *Pdx1-Cre;ROSA26R-LacZ* reporter mice reveal patchy X-Gal staining as surrogate for the Pdx1 cell lineage in the pancreas (i) and in whole mount skin (ii). Analysis of X-Gal$^+$ areas of the epidermis indicates that recombined keratinocytes are localized primarily in suprabasal layers of the skin (iii). Early cutaneous hyperplasia sections demonstrate that X-Gal$^+$ cells are also located in the basal layer of the epidermis (iv). Asterisks indicate non-recombined areas of pancreatic tissue; arrowheads point to recombined X-Gal$^+$ cells and regions; arrows show positive basal layer keratinocytes. **B:** Cre-mediated recombination of the *Notch1* locus occurs predominantly in suprabasal keratinocytes (K10$^+$) with a small fraction of recombined basal cells (K14$^+$). Schematic depiction of areas of possible *Pdx1-Cre* driven recombination in the epidermis (right): (SC) Stratum Corneum, (GL) Granular Layer, (SL) Spinous Layer, (BL) Basal Layer, (BM) Basement Membrane, (D) Dermis, (KC) Keratinocytes. **C:** Immunohistochemical staining of healing wound epidermis indicates increased expression of PDX1 in keratinocytes comparing to normal skin. **D:** Expression of *Pdx1* along with *Keratin6* is induced in wounded skin as revealed by qRT-PCR. The scale bars represent 50 μm.
doi:10.1371/journal.pone.0013578.g003

B). These results support the hypothesis that p21 is mainly regulated by Notch1 but not by Notch2 potentially due to cell- and context-specific differences.

Notch1 but not Notch2 is a suppressor of β-catenin in the skin

As an increased level of active β-catenin is commonly associated with skin malignancies [18,42,43], we investigated the regulation of this pathway in *Notch1* and *Notch2* ablated epidermis. Immunohistochemical analysis revealed increased levels of nuclear localized β-catenin (active β-catenin) in *K5;N1ko* mice in agreement with previous studies [14]. Remarkably, neither wildtype nor *K5;N2ko* mice showed strong epidermal active β-catenin staining (Fig. 5D). Furthermore, immunoblot analysis of primary keratinocytes isolated from *K5;N1ko and K5;N2ko* mice exhibited a similar pattern (Fig. 6A).

Differences in expression of Notch1 and Notch2 in the epidermal layers as well as receptor-specific regulatory mechanisms may contribute to distinct and potentially tumorigenic alterations of β-

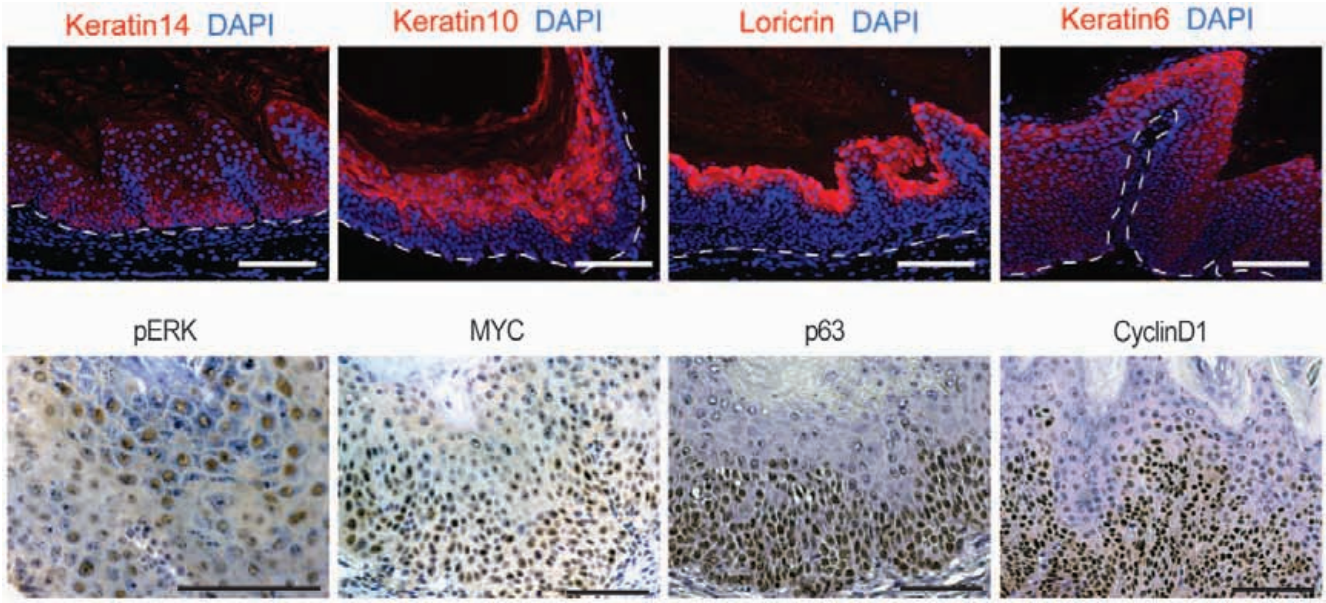

Figure 4. Characterization of papillomas developing in *Pdx1-Cre;Kras;N1ko* mice. Keratin14, Keratin10 and Loricrin expression show well-differentiated stratified squamous neoplasia. Keratin6 expression indicates pathological growth (upper panel). Immunohistochemical analysis of commonly activated pathways and markers expressed in *Pdx1-Cre;Kras;N1ko* papillomas (lower panel). The scale bars represent 50 μm.
doi:10.1371/journal.pone.0013578.g004

catenin activity. Therefore, we examined the capabilities of active Notch1 (N1IC) and Notch2 (N2IC) to inhibit β-catenin signaling activity in primary keratinocytes using a luciferase reporter assay. Both Notch receptors were able to inhibit β-catenin activity but N1IC was a significantly stronger inhibitor. Forced expression of N1IC represses β-catenin signaling by over 90% whereas N2IC overexpression leads only to a modest reduction of 30% (Fig. 6C). At the same time both Notch receptors showed a similar induction of *Hes1* promoter activity, serving as a read-out for similar activation of canonical Notch signaling (Fig.6 C).

Taken together, these results support a context- and cell-specific function in addition to a distinct expression pattern of Notch and Notch2 in keratinocytes.

Discussion

Neoplasms originating from cutaneous epithelial cells are the most common cancer-type in the United States with an annual incidence of over 1 million cases [44]. Developmental signaling pathways play a key role in the induction and progression of cancer. Our study reports a previously unrecognized epidermal expression of PDX1 and adds further evidence for a pivotal role of Notch1 but not Notch2 as a tumor suppressor in the skin, which may be particularly interesting in the light of new therapeutic approaches targeting single Notch receptors [45,46].

Epidermal PDX1 expression

As PDX1 is mainly expressed in the pancreas and duodenum, the *Pdx1* promoter is commonly utilized for pancreas-specific transgenic mouse lines. Surprisingly, we found conditional gene deletion in the skin using a *Pdx1-Cre* strain [2]. Further research provided strong evidence that PDX1 is physiologically expressed in the suprabasal layers of the skin (Fig. 2A and B; arrowheads) and rarely in basal keratinocytes (Fig. 2A and B; arrows). A similar pattern of *Pdx1* expression was observed in differentiation induced cultured keratinocytes (Fig. 2C). This hypothesis is supported by reports indicating a skin phenotype of *Pdx1* knockout mice, which survive 6.5 days postpartum and have, among other characteristic features, thin and cracking skin with little or no fur [7]. While these skin abnormalities may be due to indirect effects, they suggest a role of PDX1 during skin development, which should be addressed in further studies, e.g. by analyzing keratinocyte-specific *Pdx1* knockout mice, which however is beyond the scope of this report.

In contrast to the ubiquitous expression of Pdx1 in the suprabasal layers of the skin, *Pdx1-Cre;Kras;N1ko* mice developed skin papillomas and other cutaneous lesions only in preferred sites suggesting that Cre-mediated recombination may be mosaic and/or occurs in the cells resistant to neoplastic transformation. Notably, *Cre* expression in *Pdx1-Cre* mice is mosaic such that Cre-mediated recombination occurs far less frequently as would be suggested by the observed PDX1 expression. In addition, papillomas and most other skin tumors typically originate from the basal layer; in fact development from the suprabasal layer is a rather unlikely scenario (Fig. 7). Although PDX1 is mainly expressed in the suprabasal keratinocytes, we occasionally found PDX1 expression and Cre-mediated recombination in $K14^+$ cells (Fig. 3A, B and 7). These observations may be the reason for the relatively few tumors developing per animal. Interestingly, tumors of *Pdx1-Cre;Kras;N1ko* mice usually develop around exposed areas of the skin (Fig. 1D), possibly due to *Pdx1* activation in wound and scar associated basal layer keratinocytes (Fig. 3C). We speculate that cutaneous aggravation or micro-wounds due to grooming and scratching may trigger an inflammatory reaction and wound healing processes with upregulated Pdx1 and Notch expression [47], thus forming a tumor-prone environment in *Pdx1-Cre;Kras;N1ko* mice.

Intriguingly, other studies have reported skin phenotypes using *Pdx1-Cre* mice despite the fact that different transgenic strains were utilized [3,24]. These reports support our finding that *Pdx1* is expressed in the skin. However, only defined genetic alterations lead to a cutaneous phenotype. In the most often analyzed *Pdx1-Cre;Kras* mouse model, skin lesions were only rarely observed (below 5%, Fig.1B and [3,24]). In our study, *Pdx1-Cre;Kras;N1ko* but not *Pdx1-Cre;Kras;N2ko* or *Pdx1-Cre;Kras* developed skin lesions (Fig. 1A and B) which points to the importance of Notch1 but not Notch2 for skin tumor development.

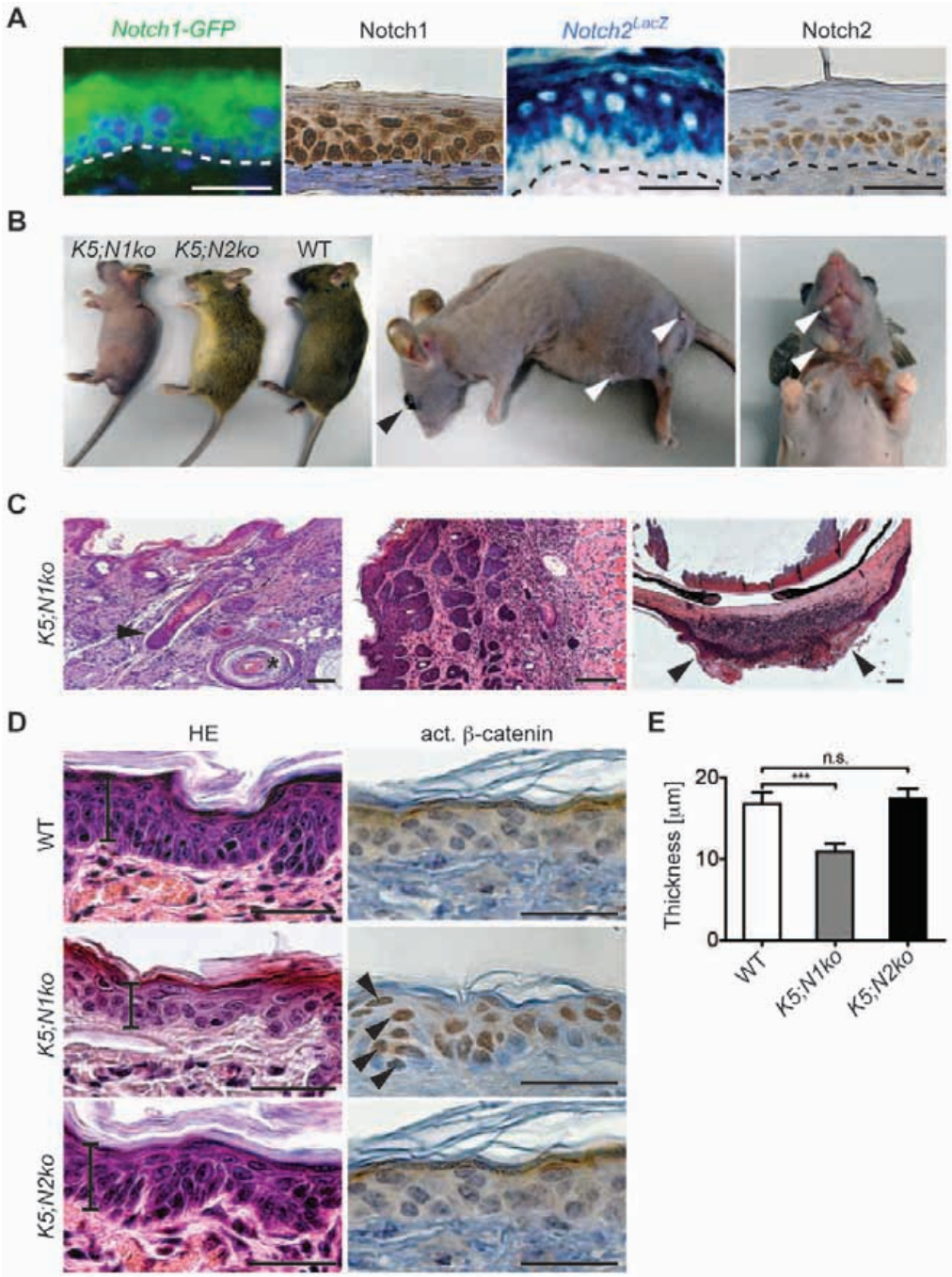

Figure 5. Phenotype of *K5;N1ko* and *K5;N2ko* mice. A: Notch1 is expressed in all layers of the adult skin whereas Notch2 is expressed only in the suprabasal layer as assessed using immunohistochemical staining and *Notch1-GFP* and *Notch2*^{LacZ} reporter mice. **B:** Gross phenotype of *K5;N1ko*, *K5;N2ko* and WT mice at 4 weeks of age (left). Spontaneous skin tumors (white arrows) and hyperplastic opaque corneas (black arrowhead) start to develop in 9 months old *K5;N1ko* mice (middle and right). **C:** Skin histopathologies of *K5;N1ko* mice include epidermal cyst (asterisk), hair follicle malformation (black arrowhead, left), skin tumors (middle), hyperplasia of the cornea (black arrows, right). **D:** HE stain shows morphology and thickness (indicated by scale lines) of WT, *K5;N1ko*, *K5;N2ko* epidermis (left panel). Immunohistochemical staining reveals ubiquitous expression of active β-catenin in *K5;N1ko* (black arrows) comparing to WT and *K5;N2ko* mice epidermis (right panel). **E:** The thickness of *K5;N1ko* epidermis is significantly reduced compared to *K5;N2ko* and WT. The scale bars represent 50 μm.
doi:10.1371/journal.pone.0013578.g005

Notch1 and Notch2 play different roles in skin tumorigenesis

Different Notch receptors have often distinct expression patterns, ligand preferences and discrete downstream signaling. Although different Notch receptors can compensate each other e.g. in pancreas development [48], individual Notch receptors commonly have distinct functions in development [49], tumorigenesis [46,50–52] or tissue regeneration [53]. The result of this study points to differences in expression pattern and distinctive cellular effectors as main cause of the diverse Notch1 and Notch2 knockout phenotypes. First, we found that Notch1 and Notch2

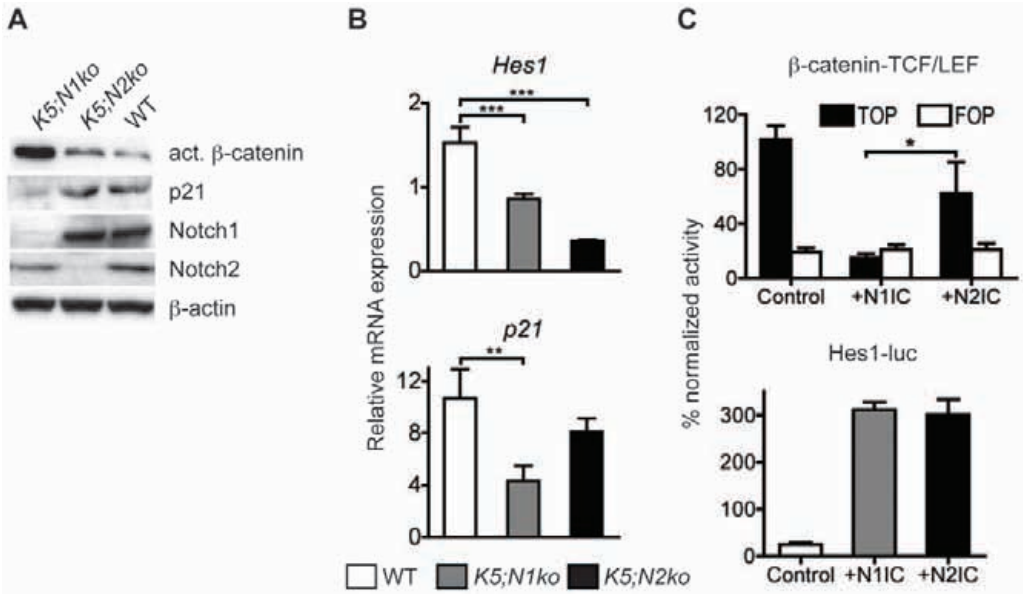

Figure 6. Biochemical analysis of *K5;N1ko* and *K5;N2ko* keratinocytes. A: Western blot analysis of primary keratinocytes isolated from different genotypes indicates correct *Notch1* and *Notch2* ablation and shows distinct modulation of β-catenin signaling and p21 expression. **B:** Quantitative RT-PCR show *Hes1* and *p21* transcripts levels in primary keratinocytes of the indicated genotypes. **C:** Luciferase reporter assay reveals that N1IC is a more potent inhibitor of β-catenin-LEF/TCF-sensitive TOP plasmid than N2IC. FOP plasmid is β-catenin-LEF/TCF-insensitive and serves as a specificity control. Both N1IC and N2IC induce Hes1 in a comparable manner as quantified using a Hes1-luc reporter.
doi:10.1371/journal.pone.0013578.g006

are present only in partially overlapping layers of the epidermis. Consistent with previous studies, Notch1 is present throughout all skin layers including the tumor-prone basal layer of the skin, whereas Notch2 is expressed exclusively in suprabasal keratinocytes [37]. These findings were confirmed using immunohistochemical staining as well as *Notch1-GFP* and *Notch2*^{LacZ} reporter mice (Fig. 5A). This divergent expression pattern is very likely at least partially responsible for the downregulation of p21 in *Notch1*- but not *Notch2*-deficient keratinocytes and in line with previous studies [37,40]. p21 is a cyclin-dependent kinase inhibitor that induces cell cycle arrest [35] and its loss is commonly associated with skin malignancies, particularly in an active Ras context [36]. In *Kras*^{G12D}-induced tumorigenesis inhibition of p21 *via* Myc activation, observed in *Pdx1-Cre;Kras;N1ko* papillomas (Fig. 4), is a critical step for malignant transformation [34]. Thus, the observed differences in p21 induction by Notch1 and 2 receptors (Fig. 6A and B) could partially explain the observed phenotypes.

The second notable difference between Notch1 and Notch2 was their ability to inhibit β-catenin-mediated signaling. β-catenin is responsible for hair-follicle morphogenesis and epidermal stem cell maintenance [54], whereas the disruption of the β-catenin signaling has been associated with several malignancies of the skin [18,42,43]. *Notch1* deficiency leading to accumulation of β-catenin in the nucleus has been associated with tumorigenesis [14]. Surprisingly, we did not observe a similar effect when the *Notch2*

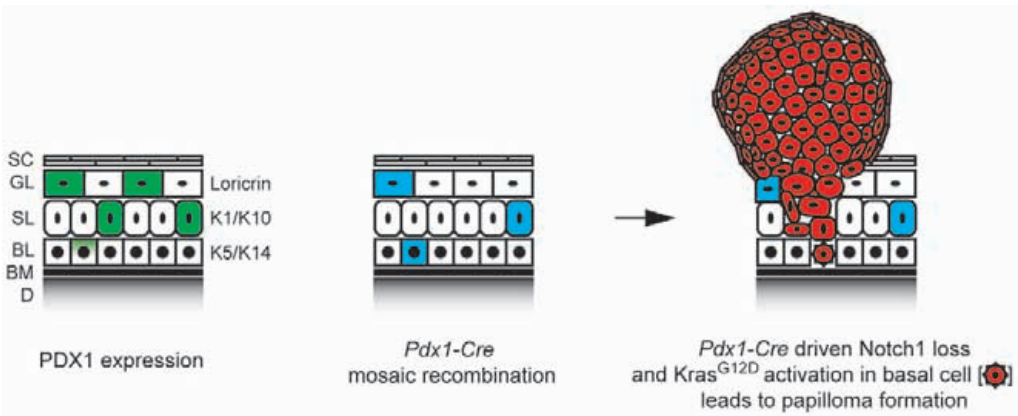

Figure 7. Model of epidermal Pdx1 expression and Cre-mediated epidermal recombination. Recombination rarely occurs in basal layer keratinocytes but leads to papilloma formation in *Pdx1-Cre;Kras;N1ko* mice: (SC) Stratum Corneum, (GL) Granular Layer, (SL) Spinous Layer, (BL) Basal Layer, (BM) Basement Membrane, (D) Dermis.
doi:10.1371/journal.pone.0013578.g007

receptor was abrogated (Fig. 5D and 6A). Additionally, we provide *in vitro* evidence of different inhibition capacities between both receptors (Fig. 6C) further supporting the postulate of distinct molecular functions of Notch1 and Notch2.

In line with the non-redundant roles of Notch1 and Notch2 in keratinocytes is the accelerated papilloma formation in double *Notch1/2*-deficient mice (Fig. 1A and B), suggesting that Notch2 cannot fully compensate for Notch1 loss. Besides different roles in regulation of p21 and β-catenin, Notch expression dosage may play a role as was recently shown [17]. In this study *Notch1* loss promoted skin tumorigenesis in a non-cell autonomous manner by impairing skin-barrier integrity and creating a wound-like microenvironment in the epidermis. Of note, *Notch2* ablation alone had no such capabilities unless combined with a *Notch3* knockout, suggesting that a certain threshold of Notch signaling is essential for skin homeostasis.

In conclusion, our results provide strong evidence for epidermal expression of *Pdx1* as of yet not identified function as well as distinctive roles of Notch1 and Notch2 in skin tumorigenesis potentially *via* different p21 and β-catenin pathway modulation.

Materials and Methods

Mouse strains

Kras$^{+/LSL\text{-}G12D}$, *Notch1*$^{fl/fl}$, *Notch2*$^{fl/fl}$, *Pdx1-Cre* and *Keratin5-Cre* transgenic mice have been described before [2,21,22,27,35]. Mice were interbred to obtain *Pdx1-Cre;Kras*$^{+/LSL\text{-}G12D}$ (*Pdx1-Cre;Kras*), *Pdx1-Cre;Kras*$^{+/LSL\text{-}G12D}$*;Notch1*$^{fl/fl}$ (*Pdx1-Cre;Kras;N1ko*), *Pdx1-Cre;Kras*$^{+/LSL\text{-}G12D}$*;Notch2*$^{fl/fl}$ (*Pdx1-Cre;Kras;N1ko*), Keratin5-Cre;*Notch1*$^{fl/fl}$ (*K5N1ko*) and Keratin5-Cre;*Notch2*$^{fl/fl}$ (*K5N2ko*) mice. Previously described reporter strains *LSL-ROSA26R-LacZ, Notch1-GFP* and *Notch2*^{lacZ} [23,38,39,55], were used as indicated in the text. All animals were of mixed C57BL/6J;129SV background. Animal care and experimental protocols were conducted in accordance with German animal protection laws and approved by the Institutional Animal Care and Use Committee at the Technical University of Munich.

Statistical Analyses

Kaplan-Meier curves were calculated using the tumor free survival time for each mouse from all littermate groups. The log-rank test was used to test for significant differences between the four groups. For gene expression analysis the unpaired two-tailed *Student's* t-test was used. For *P* values the following scale was used: * $p<0.05$, ** $p<0.01$, *** $p<0.001$.

Histology and Immunohistology

For morphologic, immunohistochemical, and immunofluorescence studies specimens were fixed in 4% buffered formalin then processed as described previously [56] and embedded in paraffin. Tissues were sectioned 4 mm and stained with hematoxylin and eosin (HE) or used for immunohistochemical studies with antibodies: CDK4 (Santa Cruz Biotechnology), K14, K10, K6, Loricrin (Covance), Notch1 (Abcam), Notch2 (The Developmental Studies Hybridoma Bank), pERK, (Cell Signaling), p63, CyclinD1 (BD), active-β-catenin (Upstate), PDX1 (gift of C.V. Wright). X-Gal staining of cryosections (10 mm) was carried out according to standard protocol, counterstained with nuclear fast red. Immunofluorescence was performed using Alexa 488 and 555 (Invitrogen). Nuclei were stained with DAPI. Pictures were taken using an Axiovert 200 M fluorescence inverse microscope equipped with the Axiovision software (Zeiss).

Histopathological Evaluation

HE stained sections were evaluated by a pathologist (B.S.) with expertise in human and mouse cancer pathology. The pathologist, where needed, also reviewed immunohistochemical stainings.

Western Blot Analysis

Protein extracts from freshly isolated primary keratinocyte cells were obtained using RIPA buffer containing proteinase inhibitors - Complete (Roche). Lysates were separated on standard SDS-PAGE electrophoresis, transferred to PDVF membranes as described previously [56] and incubated with antibodies: β-actin (Sigma), Notch1 (BD Pharmigen), Notch2 (The Developmental Studies Hybridoma Bank), p21 (LabVison), active β-catenin (Upstate). Antibody binding was visualized using horseradish peroxidase-labeled secondary antibodies and ECL reagent (Amersham).

Primary Keratinocytes Culture

Keratinocytes were isolated from 3 to 4 week old mice as described previously [57]. Briefly, mice in anlagen phase were sacrificed, trunk skin was removed disinfected and enzymatically treated to allow separation of epidermis from dermis. Detaching keratinocytes were collected, filtered through Teflon mesh (100 μm), washed and plated on Petri dish previously coated with collagen and fibronectin. Cells were maintained in DMEM Spiner modification media (Sigma) with addition of 8% FCS treated with Chelex (BioRad), 10 μg/ml Transferrin, 5 μg/ml Insulin, 10 μM Phosphoethyloamine, 10 μM Ethyloamine, 0.05 nM $CaCl_2$ (Sigma), 10 ng EGF, 0.36 μg/ml Hydrocortisone (Chemicon), 1% Glutathion, 1% Pen/Strep (Invitrogen).

Keratinocytes were plated and cultured for 3 to 5 days before use in luciferase and differentiation assays. Growth medium was changed every day. Induction of keratinocyte differentiation was achieved by addition of $CaCl_2$ to final concentration of 1.2–2 μM.

Fluorescent Activated Cell Sorting for Cre-mediated recombination analysis in Keratinocytes

Total isolated keratinocytes were stained with K14 or K10 antibodies (Covance) for 1 h at 4°C. Cells were washed in PBS +1% BSA and stained with the secondary antibody Alexa 488 (Invitrogen). Keratinocytes were washed and stained with propidium iodide followed by sorting using a FACS Aria 2 (BD Bioscience). DNA was isolated from the sorted cells utilizing DNeasy Blood & Tissue Kit (Qiagen) following the manufacturer's instructions. Recombination of genomic DNA was quantified by qPCR using the following program: 95°C for 10 min, 35 cycles of 95°C for 10 sec, 62°C for 10 sec and 72°C for 30 sec on a LightCycler 480 (Roche). All samples were analyzed in triplicate. β-globin genomic fragment was used for normalization. The following primers were used:

β-globin-F 5′-CCAATCTGCTCACACAGGATAGAGAGG-GCAGG-3′

β-globin-R 5′-CCTTGAGGCTGTCCAAGTGATTCAGGC-CATCG-3′

Del Notch1-F 5′-TGT GCT TTC ACA CTG GCA CAG-3′

Del Notch1-R 5′-CCA CTT AGA AGG AAT TCC ACC-3′

Luciferase assay

A luciferase reporter assay was performed with a pair of luciferase reporter constructs TOPFLASH, containing three copies of the TCF/LEF binding sites and FOP-FLASH, containing mutated binding sites (Upstate Biotechnology). Primary keratinocytes were cultured in 6-well plates and transiently

transfected in triplicates with Fugene 6 (Roche) and TOP/FOP or Hes1-luc plasmids with addition of forced expressing active Notch1 (N1IC) or Notch2 (N2IC) pcDNA3 plasmids and pRL-TK (Promega). Luciferase activity was measured with the Dual-luciferase reporter assay system (Promega), with the Renilla luciferase (pRL-TK) activity as an internal control, 48 h after transfection. The experiment was repeated three times, the mean of all results was taken and expressed as a percentage of induction over control (= 100%).

Wounding and preparation of wound tissue

Skin wound healing analysis was performed as described previously [58]. Briefly, full-thickness excisional skin wounds (6 mm in diameter) were made in WT mice. Animals were killed 5 days after wounding ($n = 4$), and an 8–10 mm area, including the complete epithelial margins, was collected and used for histopathological analysis. Three small areas (3×3 mm) of wounded and unaffected skin from the same animal were used to prepare RNA for expression analysis. Four mice were analyzed.

Quantitative RT-PCR

RNA was isolated from primary keratinocytes using Qiagen RNeasy Isolation Kit followed by cDNA synthesis (SuperScript II, Invitrogen). Real-Time PCR was performed with 800 nM primers diluted in a final volume of 20 µl in SYBR Green Reaction Mix (Applied Biosystems). RT-PCRs were performed as follows: 95°C for 10 min, 45 cycles of 95°C for 10 sec, 60°C for 10 sec and 72°C for 10 sec. using LightCycler 480 (Roche). All samples were analyzed in triplicate. Cyclophilin and HPRT were used for normalization. The following primers were used:

K6a-F 5′-GAGCTGGCTTTGGTGGTG-3′
K6a-R 5′-GTCCTCCACTGTGTCCTG-3′
K10-F 5′-GCCAGAACGCCGAGTACCAACAAC-3′
K10-R 5′-GTCACCTCCTCAATAATCGTCCTG-3′
Loricrin-F 5′-TCACTCACCCTTCCTGGTGC-3′
Loricrin-R 5′-CACCGCCGCCAGAGGTCTTC-3′
Hes1-F 5′-AAAATTCCTCCTCCCCGGTG-3′
Hes1-R 5′-TTTGGTTTGTCCGGTGTCG-3′
p21-F 5′-CACAGCGATATCCAGACATTCAG-3′
p21-R 5′-CGGAACAGGTCGGACATCA-3′
Pdx1-F 5′-TGCCACCATGAACAGTGAGG-3′
Pdx1-R 5′-GGAATGCGCACGGGTC-3′
Cyclophillin-F 5′-ATGGTCAACCCCACCGTGT-3′
Cyclophillin-R 5′-TTCTGCTGTCTTTGGAACTTTGTC-3′
Hprt-F 5′-GACCGGTCCCGTCATGC-3′
Hprt-R 5′-CATAACCTGGTTCATCATCGCTAA-3′

Acknowledgments

We thank Reinhard Fässler, Ramin Massoumi and Rudolf A. Rupec for helpful discussions and expertise help with mouse models as well as keratinocytes isolation and culture. The Notch2 antibody developed by S. Artavanis-Tsakonas was obtained from the Developmental Studies Hybridoma Bank. We thank W. Gao, Y. Hamada, C.A. Klug and J. Takeda for providing *Notch1-GFP*, *Notch2*^{LacZ} and *Keratin5-Cre* mice respectively. We are grateful to C.V. Wright for the PDX1 antibody. We thank M. Neuhofer and S. Ruberg for excellent technical assistance.

Author Contributions

Conceived and designed the experiments: PKM JTS. Performed the experiments: PKM. Analyzed the data: PKM BMG BS RS JTS. Contributed reagents/materials/analysis tools: HN UZS FR. Wrote the paper: PKM JTS.

References

1. Gannon M, Herrera PL, Wright CV (2000) Mosaic Cre-mediated recombination in pancreas using the pdx-1 enhancer/promoter. Genesis 26: 143–144.
2. Gu G, Dubauskaite J, Melton DA (2002) Direct evidence for the pancreatic lineage: NGN3+ cells are islet progenitors and are distinct from duct progenitors. Development 129: 2447–2457.
3. Hingorani SR, Petricoin EF, Maitra A, Rajapakse V, King C, et al. (2003) Preinvasive and invasive ductal pancreatic cancer and its early detection in the mouse. Cancer Cell 4: 437–450.
4. Gannon M, Gamer LW, Wright CV (2001) Regulatory regions driving developmental and tissue-specific expression of the essential pancreatic gene pdx1. Dev Biol 238: 185–201.
5. Brissova M, Shiota M, Nicholson WE, Gannon M, Knobel SM, et al. (2002) Reduction in pancreatic transcription factor PDX-1 impairs glucose-stimulated insulin secretion. J Biol Chem 277: 11225–11232.
6. Jonsson J, Carlsson L, Edlund T, Edlund H (1994) Insulin-promoter-factor 1 is required for pancreas development in mice. Nature 371: 606–609.
7. Offield MF, Jetton TL, Labosky PA, Ray M, Stein RW, et al. (1996) PDX-1 is required for pancreatic outgrowth and differentiation of the rostral duodenum. Development 122: 983–995.
8. Larsson LI, Madsen OD, Serup P, Jonsson J, Edlund H (1996) Pancreatic-duodenal homeobox 1 -role in gastric endocrine patterning. Mech Dev 60: 175–184.
9. Bray SJ (2006) Notch signalling: a simple pathway becomes complex. Nat Rev Mol Cell Biol 7: 678–689.
10. Lefort K, Dotto GP (2004) Notch signaling in the integrated control of keratinocyte growth/differentiation and tumor suppression. Semin Cancer Biol 14: 374–386.
11. Dotto GP (2008) Notch tumor suppressor function. Oncogene 27: 5115–5123.
12. Lin MH, Leimeister C, Gessler M, Kopan R (2000) Activation of the Notch pathway in the hair cortex leads to aberrant differentiation of the adjacent hair-shaft layers. Development 127: 2421–2432.
13. Uyttendaele H, Panteleyev AA, de Berker D, Tobin DT, Christiano AM (2004) Activation of Notch1 in the hair follicle leads to cell-fate switch and Mohawk alopecia. Differentiation 72: 396–409.
14. Nicolas M, Wolfer A, Raj K, Kummer JA, Mill P, et al. (2003) Notch1 functions as a tumor suppressor in mouse skin. Nat Genet 33: 416–421.
15. Pan Y, Lin MH, Tian X, Cheng HT, Gridley T, et al. (2004) gamma-secretase functions through Notch signaling to maintain skin appendages but is not required for their patterning or initial morphogenesis. Dev Cell 7: 731–743.
16. Vauclair S, Nicolas M, Barrandon Y, Radtke F (2005) Notch1 is essential for postnatal hair follicle development and homeostasis. Dev Biol 284: 184–193.
17. Demehri S, Turkoz A, Kopan R (2009) Epidermal Notch1 loss promotes skin tumorigenesis by impacting the stromal microenvironment. Cancer Cell 16: 55–66.
18. Xia X, Qian S, Soriano S, Wu Y, Fletcher AM, et al. (2001) Loss of presenilin 1 is associated with enhanced beta-catenin signaling and skin tumorigenesis. Proc Natl Acad Sci U S A 98: 10863–10868.
19. Blanpain C, Lowry WE, Pasolli HA, Fuchs E (2006) Canonical notch signaling functions as a commitment switch in the epidermal lineage. Genes Dev 20: 3022–3035.
20. Moriyama M, Durham AD, Moriyama H, Hasegawa K, Nishikawa S, et al. (2008) Multiple roles of Notch signaling in the regulation of epidermal development. Dev Cell 14: 594–604.
21. Radtke F, Wilson A, Stark G, Bauer M, van Meerwijk J, et al. (1999) Deficient T cell fate specification in mice with an induced inactivation of Notch1. Immunity 10: 547–558.
22. Besseyrias V, Fiorini E, Strobl LJ, Zimber-Strobl U, Dumortier A, et al. (2007) Hierarchy of Notch-Delta interactions promoting T cell lineage commitment and maturation. J Exp Med 204: 331–343.
23. Soriano P (1999) Generalized lacZ expression with the ROSA26 Cre reporter strain. Nat Genet 21: 70–71.
24. Hingorani SR, Wang L, Multani AS, Combs C, Deramaudt TB, et al. (2005) Trp53R172H and KrasG12D cooperate to promote chromosomal instability and widely metastatic pancreatic ductal adenocarcinoma in mice. Cancer Cell 7: 469–483.
25. Greenhalgh DA, Rothnagel JA, Quintanilla MI, Orengo CC, Gagne TA, et al. (1993) Induction of epidermal hyperplasia, hyperkeratosis, and papillomas in transgenic mice by a targeted v-Ha-ras oncogene. Mol Carcinog 7: 99–110.
26. Vitale-Cross L, Amornphimoltham P, Fisher G, Molinolo AA, Gutkind JS (2004) Conditional expression of K-ras in an epithelial compartment that includes the stem cells is sufficient to promote squamous cell carcinogenesis. Cancer Res 64: 8804–8807.
27. Tuveson DA, Shaw AT, Willis NA, Silver DP, Jackson EL, et al. (2004) Endogenous oncogenic K-ras(G12D) stimulates proliferation and widespread neoplastic and developmental defects. Cancer Cell 5: 375–387.
28. Hennings H, Michael D, Cheng C, Steinert P, Holbrook K, et al. (1980) Calcium regulation of growth and differentiation of mouse epidermal cells in culture. Cell 19: 245–254.

29. Wescott MP, Rovira M, Reichert M, von Burstin J, Means A, et al. (2009) Pancreatic ductal morphogenesis and the Pdx1 homeodomain transcription factor. Mol Biol Cell 20: 4838–4844.
30. Buettner M, Dimmler A, Magener A, Brabletz T, Stolte M, et al. (2004) Gastric PDX-1 expression in pancreatic metaplasia and endocrine cell hyperplasia in atrophic corpus gastritis. Mod Pathol 17: 56–61.
31. Kawamori D, Kajimoto Y, Kaneto H, Umayahara Y, Fujitani Y, et al. (2003) Oxidative stress induces nucleo-cytoplasmic translocation of pancreatic transcription factor PDX-1 through activation of c-Jun NH(2)-terminal kinase. Diabetes 52: 2896–2904.
32. Macfarlane WM, McKinnon CM, Felton-Edkins ZA, Cragg H, James RF, et al. (1999) Glucose stimulates translocation of the homeodomain transcription factor PDX1 from the cytoplasm to the nucleus in pancreatic beta-cells. J Biol Chem 274: 1011–1016.
33. Tarutani M, Cai T, Dajee M, Khavari PA (2003) Inducible activation of Ras and Raf in adult epidermis. Cancer Res 63: 319–323.
34. Oskarsson T, Essers MA, Dubois N, Offner S, Dubey C, et al. (2006) Skin epidermis lacking the c-Myc gene is resistant to Ras-driven tumorigenesis but can reacquire sensitivity upon additional loss of the p21Cip1 gene. Genes Dev 20: 2024–2029.
35. Tarutani M, Itami S, Okabe M, Ikawa M, Tezuka T, et al. (1997) Tissue-specific knockout of the mouse Pig-a gene reveals important roles for GPI-anchored proteins in skin development. Proc Natl Acad Sci U S A 94: 7400–7405.
36. Lowell S, Jones P, Le Roux I, Dunne J, Watt FM (2000) Stimulation of human epidermal differentiation by delta-notch signalling at the boundaries of stem-cell clusters. Curr Biol 10: 491–500.
37. Rangarajan A, Talora C, Okuyama R, Nicolas M, Mammucari C, et al. (2001) Notch signaling is a direct determinant of keratinocyte growth arrest and entry into differentiation. EMBO J 20: 3427–3436.
38. Lewis AK, Frantz GD, Carpenter DA, de Sauvage FJ, Gao WQ (1998) Distinct expression patterns of notch family receptors and ligands during development of the mammalian inner ear. Mech Dev 78: 159–163.
39. Hamada Y, Kadokawa Y, Okabe M, Ikawa M, Coleman JR, et al. (1999) Mutation in ankyrin repeats of the mouse Notch2 gene induces early embryonic lethality. Development 126: 3415–3424.
40. Mammucari C, Tommasi di Vignano A, Sharov AA, Neilson J, Havrda MC, et al. (2005) Integration of Notch 1 and calcineurin/NFAT signaling pathways in keratinocyte growth and differentiation control. Dev Cell 8: 665–676.
41. Di Cunto F, Topley G, Calautti E, Hsiao J, Ong L, et al. (1998) Inhibitory function of p21Cip1/WAF1 in differentiation of primary mouse keratinocytes independent of cell cycle control. Science 280: 1069–1072.
42. Chan EF, Gat U, McNiff JM, Fuchs E (1999) A common human skin tumour is caused by activating mutations in beta-catenin. Nat Genet 21: 410–413.
43. Reya T, Clevers H (2005) Wnt signalling in stem cells and cancer. Nature 434: 843–850.
44. Bagheri MM, Safai B (2001) Cutaneous malignancies of keratinocytic origin. Clin Dermatol 19: 244–252.
45. Moellering RE, Cornejo M, Davis TN, Del Bianco C, Aster JC, et al. (2009) Direct inhibition of the NOTCH transcription factor complex. Nature 462: 182–188.
46. Wu Y, Cain-Hom C, Choy L, Hagenbeek TJ, de Leon GP, et al. (2010) Therapeutic antibody targeting of individual Notch receptors. Nature 464: 1052–1057.
47. Chigurupati S, Arumugam TV, Son TG, Lathia JD, Jameel S, et al. (2007) Involvement of notch signaling in wound healing. PLoS One 2: e1167.
48. Nakhai H, Siveke JT, Klein B, Mendoza-Torres L, Mazur PK, et al. (2008) Conditional ablation of Notch signaling in pancreatic development. Development 135: 2757–2765.
49. Geisler F, Nagl F, Mazur PK, Lee M, Zimber-Strobl U, et al. (2008) Liver-specific inactivation of Notch2, but not Notch1, compromises intrahepatic bile duct development in mice. Hepatology 48: 607–616.
50. Kopan R, Ilagan MX (2009) The canonical Notch signaling pathway: unfolding the activation mechanism. Cell 137: 216–233.
51. Fan X, Mikolaenko I, Elhassan I, Ni X, Wang Y, et al. (2004) Notch1 and notch2 have opposite effects on embryonal brain tumor growth. Cancer Res 64: 7787–7793.
52. Mazur PK, Einwächter H, Lee M, Sipos B, Nakhai H, et al. (2010) Notch2 is required for PanIN progression and development of pancreatic ductal adenocarcinoma. Proc Natl Acad Sci U S A in press.
53. Siveke JT, Lubeseder-Martellato C, Lee M, Mazur PK, Nakhai H, et al. (2008) Notch signaling is required for exocrine regeneration after acute pancreatitis. Gastroenterology 134: 544–555.
54. Huelsken J, Vogel R, Erdmann B, Cotsarelis G, Birchmeier W (2001) beta-Catenin controls hair follicle morphogenesis and stem cell differentiation in the skin. Cell 105: 533–545.
55. Novak A, Guo C, Yang W, Nagy A, Lobe CG (2000) Z/EG, a double reporter mouse line that expresses enhanced green fluorescent protein upon Cre-mediated excision. Genesis 28: 147–155.
56. Siveke JT, Einwachter H, Sipos B, Lubeseder-Martellato C, Kloppel G, et al. (2007) Concomitant pancreatic activation of Kras(G12D) and Tgfa results in cystic papillary neoplasms reminiscent of human IPMN. Cancer Cell 12: 266–279.
57. Hakkinen L, Koivisto L, Larjava H (2001) An improved method for culture of epidermal keratinocytes from newborn mouse skin. Methods Cell Sci 23: 189–196.
58. Sakai T, Johnson KJ, Murozono M, Sakai K, Magnuson MA, et al. (2001) Plasma fibronectin supports neuronal survival and reduces brain injury following transient focal cerebral ischemia but is not essential for skin-wound healing and hemostasis. Nat Med 7: 324–330.

Appendix 3

Jens T. Siveke, Clara Lubeseder-Martellato, Marcel Lee, **Pawel K. Mazur**, Hassan Nakhai, Freddy Radtke, Roland M. Schmid.

Notch signaling is required for exocrine regeneration after acute pancreatitis

Gastroenterology. 2008 Feb;134(2):544-55.

BASIC–LIVER, PANCREAS, AND BILIARY TRACT

Notch Signaling Is Required for Exocrine Regeneration After Acute Pancreatitis

JENS T. SIVEKE,* CLARA LUBESEDER–MARTELLATO,* MARCEL LEE,* PAWEL K. MAZUR,* HASSAN NAKHAI,* FREDDY RADTKE,‡ and ROLAND M. SCHMID*

*Second Department of Internal Medicine, Klinikum rechts der Isar, Technical University of Munich, München, Germany; and ‡Swiss Institute for Experimental Cancer Research, Ecole Polytechnique Fédérale de Lausanne, Epalinges, Switzerland

Background & Aims: **The mechanisms for tissue regeneration and renewal after acute pancreatitis are not well understood but may involve activation of Notch signaling. To study the effect of Notch signaling ablation during acute experimental pancreatitis, we used a chemical and genetic approach to ablate Notch signaling in cerulein-induced pancreatitis in mice.** ***Methods:*** **Acute pancreatitis was induced by cerulein treatment in mice treated with the γ-secretase inhibitor dibenzazepine or in conditional Notch1 knockout mice. Mice were characterized using immunohistologic, biochemical, and molecular methods. To investigate Notch and β-catenin interaction, acinar 266-6 cells were analyzed using transfection and biochemical assays.** ***Results:*** **Loss of Notch signaling results in impaired regeneration after acute pancreatitis with fewer mature acinar cells in dibenzazepine-treated and Notch1-deficient mice in the regenerative phase 3 days after induction. β-catenin expression was increased and prolonged during exocrine regeneration. Crosstalk between Notch and β-catenin–mediated signaling was identified, with Notch1-IC inhibiting β-catenin–mediated transcriptional activity. This inhibition was dependent on a functional RAM domain.** ***Conclusions:*** **Inhibition of Notch signaling in vivo leads to impaired regeneration of the exocrine pancreas after acute pancreatitis. Our results suggest an interaction of Notch and Wnt signaling in pancreatic acinar cells, providing evidence for a role of these pathways in the regulation of the maturation process of acinar cells.**

Regenerative processes after organ injury are essential for tissue homeostasis and include the activation and proliferation of progenitor cells. Recently, acinar cell proliferation along with a dedifferentiation and redifferentiation process was described after cellular damage in a model of cerulein-induced acute pancreatitis. This process involved activation of embryonic pathways including Notch signaling,[1,2] for which an important role in organ regeneration and self-renewal is known.[3]

In mammals, 4 transmembrane Notch receptors (Notch1–4) and 5 ligands (Delta-like-1, -3, and -4 and Jagged-1 and -2) have been identified. Notch signaling activation is initiated by binding of a Notch ligand from one cell to a Notch receptor on a neighboring cell, leading to intracellular γ-secretase–dependent cleavage and release of the C-terminal intracellular domain (Notch-IC) followed by its nuclear translocation. Notch-IC then binds to RBP-Jκ, thereby converting RBP-Jκ from a transcriptional repressor into an activator by recruitment of coactivators, leading to transcription of Notch target genes such as members of the Hes and Hey family. Besides genetic inactivation of Notch signaling, γ-secretase inhibitors such as dibenzazepine (DBZ) or *N*-[*N*-(3,5-difluorophenacetyl)-L-alanyl]-*S*-phenylglycine t-butyl ester (DAPT) have been used for chemical inhibition of Notch processing. While the functional role of Notch signaling in vivo using genetic conditional loss-of-function models in various organs has been shown,[4–9] functional data defining the role of Notch signaling in the adult exocrine pancreas are lacking.

Notch function in the pancreas has been limited by early embryonic lethality of mice with Notch signaling deficiency, and thus most data exist for early pancreatic organogenesis. Specification and development of the pancreas are regulated by the transcriptional factors *Pdx1*

Abbreviations used in this paper: BrdU, bromodeoxyuridine; d1, day 1; d3, day 3; DAPT, *N*-[*N*-(3,5-difluorophenacetyl)-L-alanyl]-*S*-phenylglycine t-butyl ester; DBZ, dibenzazepine; qRT-PCR, quantitative reverse-transcription polymerase chain reaction; siRNA, small interfering RNA; TOP, TOP-FLASH.

0016-5085/08/$34.00
doi:10.1053/j.gastro.2007.11.003

and *Ptf1a*, both of which are expressed in pancreatic progenitor cells.[10] These cells give rise to all mature pancreatic cells, with glucagon-positive α cells appearing first. While this lineage was enriched in mice lacking *Delta-like1* and *Rbpj*, exocrine specification could not be analyzed due to early lethality or was not significantly altered in *Hes1* knockout mice.[11–13] More recently it was shown that conditional inactivation of *Rbpj* using *Pdx1*-Cre mice impaired but did not abolish acinar differentiation and proliferation,[12] while activation of Notch1 prevented exocrine and endocrine differentiation of pancreatic progenitor cells, leaving them in an undifferentiated state.[14–16] Thus, Notch signaling regulates cell fate decisions in both exocrine and endocrine lineages during organogenesis. However, its role during later embryonic stages and in adult tissue homeostasis is still largely unknown. In murine adult pancreata, *Notch1* messenger RNA (mRNA) has been shown to be weakly expressed in pancreatic exocrine cells while being strongly up-regulated in the acute and regenerative phase of acute pancreatitis.[1,2] During carcinogenesis, *Notch* mRNA is strongly up-regulated in precancerous and malignant lesions in mice and humans.[17]

In addition to Notch signaling, Wnt signaling has been implicated in cell fate decisions and proliferation in the embryonic and adult pancreas.[1,18–20] In the canonical branch of the Wnt pathway, Wnt activates one of several Frizzled or Lrp receptors, eventually leading to stabilization of cytosolic β-catenin by dissociation of a proteolytic complex. After entering the nucleus, β-catenin activates genes in collaboration with members of the Lef/Tcf transcription factor family.

In this study, we have investigated the effect of Notch inhibition in the adult pancreas and during cerulein-induced pancreatitis by either blocking Notch cleavage using the γ-secretase inhibitor DBZ or by generating conditional pancreas-specific Notch1 knockout mice. We show that Notch1 is an important regulator of pancreatic regeneration after acute pancreatitis and provide evidence for a close interaction of the Notch and β-catenin signaling pathways as a possible underlying cause.

Materials and Methods

Mouse Strains

For generation of *Notch1*-deficient mice, *Notch1*$^{f/f}$ mice[7] were bred with *Ptf1a*$^{+/Cre(ex1)}$ knockin mice[21] and then backcrossed to generate pancreas-specific *Ptf1a*$^{+/Cre(ex1)}$/*Notch1*$^{f/f}$ mice. Mice were of mixed 129SV/C57BL/6 genetic background and were backcrossed to C57BL/6 background. As control mice, littermates not expressing Cre recombinase as well as *Ptf1a*$^{+/Cre(ex1)}$ mice of the same age were used throughout the experiments. Genotyping was performed by polymerase chain reaction (sequences are shown in Supplementary Table 1; see supplemental material online at www.gastrojournal.org). For Notch1 expression studies, Notch1-GFP mice were used.[22]

DBZ and Cerulein Treatment

For DBZ experiments, C57BL/6 mice 8–12 weeks of age were used. DBZ (>99.9% purity) was custom synthesized by Syncom (Groningen, The Netherlands) and suspended in 0.5% hydroxypropyl methylcellulose (Methocel E4, Dow Chemical Co, Midland, MI), 1% ethanol, and 0.1% Tween 80 (Sigma-Aldrich, Steinheim, Germany) in water and injected intraperitoneally (10 μmol/kg, 0.2 mL/mouse) for indicated periods.

Pancreatitis was induced by administration of 8 hourly intraperitoneal injections of cerulein (10 μg/mL, 0.2 mL/mouse) over 2 consecutive days. At indicated time points, mice were killed and pancreata removed. All experiments were performed according to the guidelines of the local animal use and care committees.

Histology, Immunohistochemistry, and Immunofluorescence

For morphologic, immunohistochemical, and immunofluorescence studies, tissues were processed as described previously.[1,23] Antibodies and conditions used are listed in Supplementary Table 2 (see supplemental material online at www.gastrojournal.org).

Molecular, Biochemical, and Statistical Analyses

Detailed descriptions of procedures are provided in the Supplementary Methods (see supplemental material online at www.gastrojournal.org).

Results

DBZ Treatment in Adult Pancreas and Cerulein-Induced Acute Pancreatitis

To investigate the effect of Notch pathway inactivation in the adult pancreas, the γ-secretase inhibitor DBZ was utilized using the same protocol as previously reported to block Notch signaling in vivo.[4,24] C57BL/6 wild-type mice were treated with 10 μmol/kg DBZ for 5 consecutive days, after which pancreata were analyzed. As expected, DBZ treatment resulted in a massive conversion of crypt cells into goblet cells in the small intestine (Figure 1*A*, *insets*). While most of the exocrine pancreas consisted of normal-looking acinar tissue, we also noted decreased intercellular adhesion of acinar cells in some lobules (Figure 1*A*). These alterations were seen in all DBZ-treated mice but none of the vehicle-treated mice in 2 independent experiments (n = 5 and n = 3, respectively), suggesting a γ-secretase–dependent mechanism.

Because Notch signaling has been implicated in proliferation and apoptosis, we assessed proliferation by bromodeoxyuridine (BrdU) pulse experiments and the rate of apoptotic cells by immunohistochemical staining of cleaved caspase-3. Although we found a reduced pro-

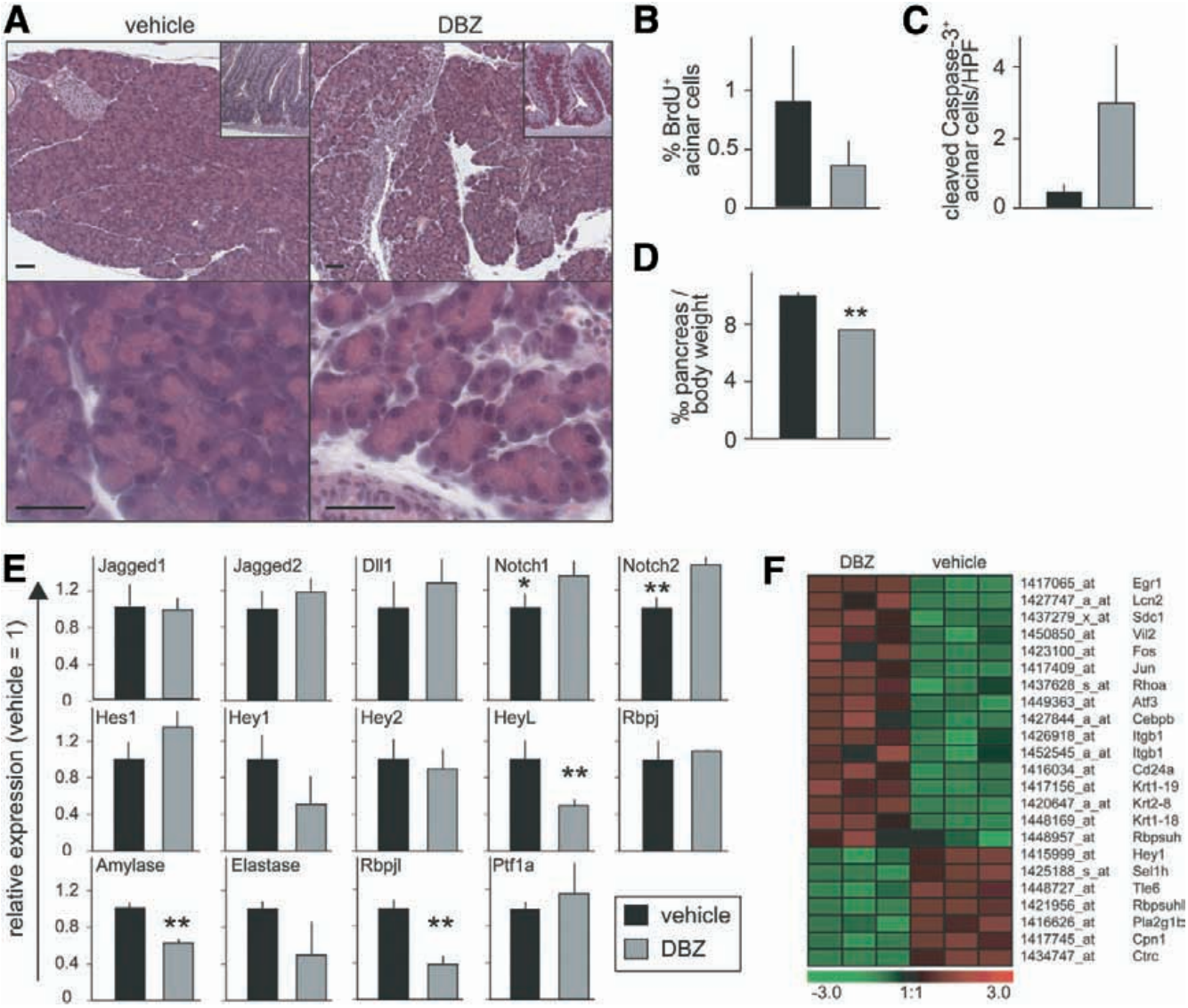

Figure 1. Effect of the γ-secretase inhibitor DBZ on the pancreas. (*A*) DBZ treatment alters pancreas morphology as shown by H&E staining. (*Inset*) DBZ-induced conversion of intestinal crypt cells into goblet cells as shown by periodic acid–Schiff staining. *Scale bar* = 50 μm. (*B* and *C*) Rate of BrdU-positive and cleaved caspase-3–positive acinar cells in DBZ- versus vehicle-treated mice ($P = .184$ for BrdU; $P = 0.059$ for cleaved caspase-3). (*D*) Reduced pancreas/body weight index in DBZ-treated mice (**$P = .002$). (*E*) Real-time qRT-PCR analysis of Notch signaling members, Notch target genes, and exocrine genes (*$P < .05$, **$P < .01$). (*F*) Image intensity display of expression levels of genes commonly activated during acute pancreatitis and of genes involved in Notch signaling.

liferation rate and an increased number of cleaved caspase-3–positive acinar cells in DBZ-treated mice compared with control mice, these alterations did not reach statistical significance. However, we found a significantly reduced pancreatic/body weight index and reduced absolute pancreatic weight after DBZ treatment (Figure 1*B–D* and data not shown).

To estimate the effect of γ-secretase inhibition on Notch-dependent signaling, real-time quantitative reverse-transcription polymerase chain reaction (qRT-PCR) of various Notch receptors, ligands, and target genes was performed. We found no reduction in expression levels of *Notch1* and *Notch2* and the Notch ligands *Jagged1*, -2, and *Dll1* between DBZ- and vehicle-treated mice (Figure 1*E*). However, we found a reduction in mRNA levels of the Notch target genes *Hey1* and *HeyL* but not *Hes1*, suggesting at least partial inhibition of active Notch signaling by DBZ treatment (Figure 1*E*).

We next performed genetic profiling of DBZ-treated versus control mice using Affymetrix microarrays, which showed down-regulation of the Notch target genes *Hey1*, *HeyL*, *Hes3*, *Sel1*, and *Tle6* (Figure 1*F*). In addition, genes activated during the acute course of cerulein-induced pancreatitis[25] and genes implicated in regulation of pancreatic differentiation, including *β1-integrin*, *cytokeratins 8, 18,* and *19*, and *clusterin*, were up-regulated in DBZ-treated mice. By contrast, genes expressed in differentiated acinar cells such as *chymotrypsin*, *carboxypep-*

tidase, and *Rbpjl*[26] were down-regulated (Figure 1*F*). This result was confirmed by qRT-PCR analysis showing reduced *amylase*, *elastase*, and *Rbpjl* levels, while *Ptf1a* and *Rbpj* were not altered by DBZ treatment (Figure 1*E*).

Based on these results, we hypothesized that DBZ treatment affects the differentiation status of the exocrine pancreas. Thus, we assessed protein expression of genes implicated in acinar differentiation. Western blot analysis showed decreased amylase and enhanced β-catenin expression in the pancreata of DBZ-treated mice (Figure 2*A*). Interestingly, we found cytoplasmic staining of β-catenin and E-cadherin in some acinar cells of DBZ-treated mice but not in vehicle-treated cells (Figure 2*B* and *C*). Immunohistochemical staining for clusterin, a marker of immature acinar cells, showed increased expression in DBZ-treated pancreata (Figure 2*D*). These results indicate that administration of DBZ induces moderate histologic alterations in the exocrine pancreas in vivo correlating with the molecular changes in genes defining exocrine differentiation.

Impaired Regeneration After Cerulein-Induced Pancreatitis in DBZ-Treated Mice

To test if Notch signaling affects pancreatic regeneration after cellular insult, we used the model of cerulein-induced acute pancreatitis. Using the same protocol as described previously,[1] we found up-regulation of Notch1 expression on day 3 (d3) after induction of pancreatitis, confirming previous results using transgenic Notch1-GFP mice,[22] while unstimulated and acutely injured pancreata showed no or very low expression (Figure 3*A* and data not shown). Thus, for further evaluation of Notch signaling ablation during acute pancreatitis, pancreata were analyzed on day 1 (d1) and d3 postinduction, receiving single daily doses of DBZ or vehicle beginning at the first day of cerulein treatment until the mice were killed (Figure 3*B*).

At d1, DBZ- and vehicle-treated mice showed similar acute tissue reactions with edema, acinar cell death, and an inflammatory cell reaction (Figure 3*C*). However, at d3, we noted substantial differences between the pancreata of DBZ- and vehicle-treated mice (Figure 3*D*). Histomorphologically, vehicle-treated mice revealed a mixed cellular picture with large areas of almost complete exocrine regeneration and only minor postinflammatory residues left. In some lobules, incomplete regeneration that slightly varied interindividually and between experiments occurred; in these areas, infiltrating cells and cells with round-shaped small acinar appearance were observed. In contrast, pancreata in DBZ-treated mice showed a

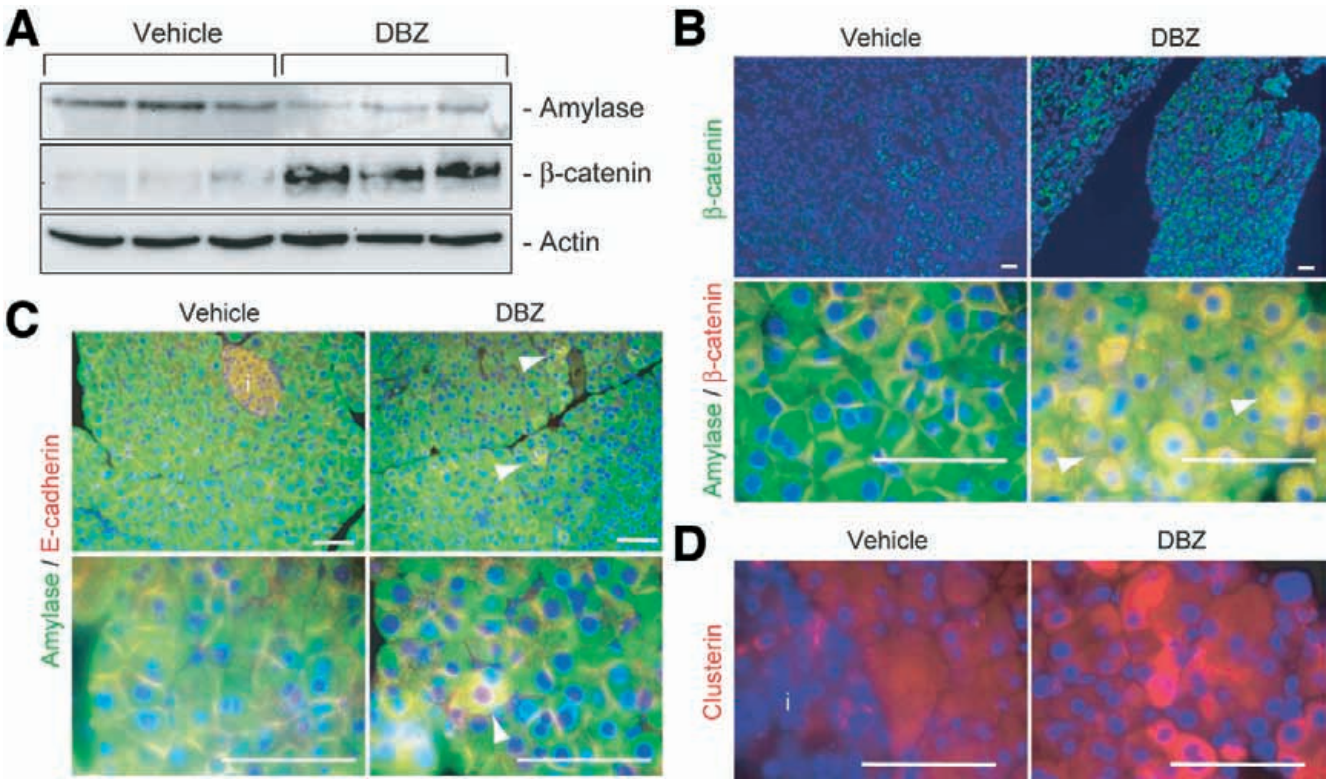

Figure 2. Analysis of exocrine cell differentiation in pancreata after DBZ treatment. (*A*) Western blot analysis of amylase, β-catenin, and actin (loading control) expression in DBZ- or vehicle-treated pancreatic whole cell lysates. (*B* and *C*) Immunofluorescence staining for β-catenin (*green*) and double immunofluorescence staining for amylase (*green*) and β-catenin (*B*, *red*) or E-cadherin (*C*, *red*) shows cytoplasmic localization of β-catenin in DBZ-treated acini. *Arrowheads* highlight cytoplasmic expression. (*D*) Immunofluorescence staining for clusterin shows higher expression levels in DBZ-treated acinar structures. Nuclei were counterstained with 4′,6-diamidino-2-phenylindole (*blue*); i = islet; *scale bar* = 50 μm.

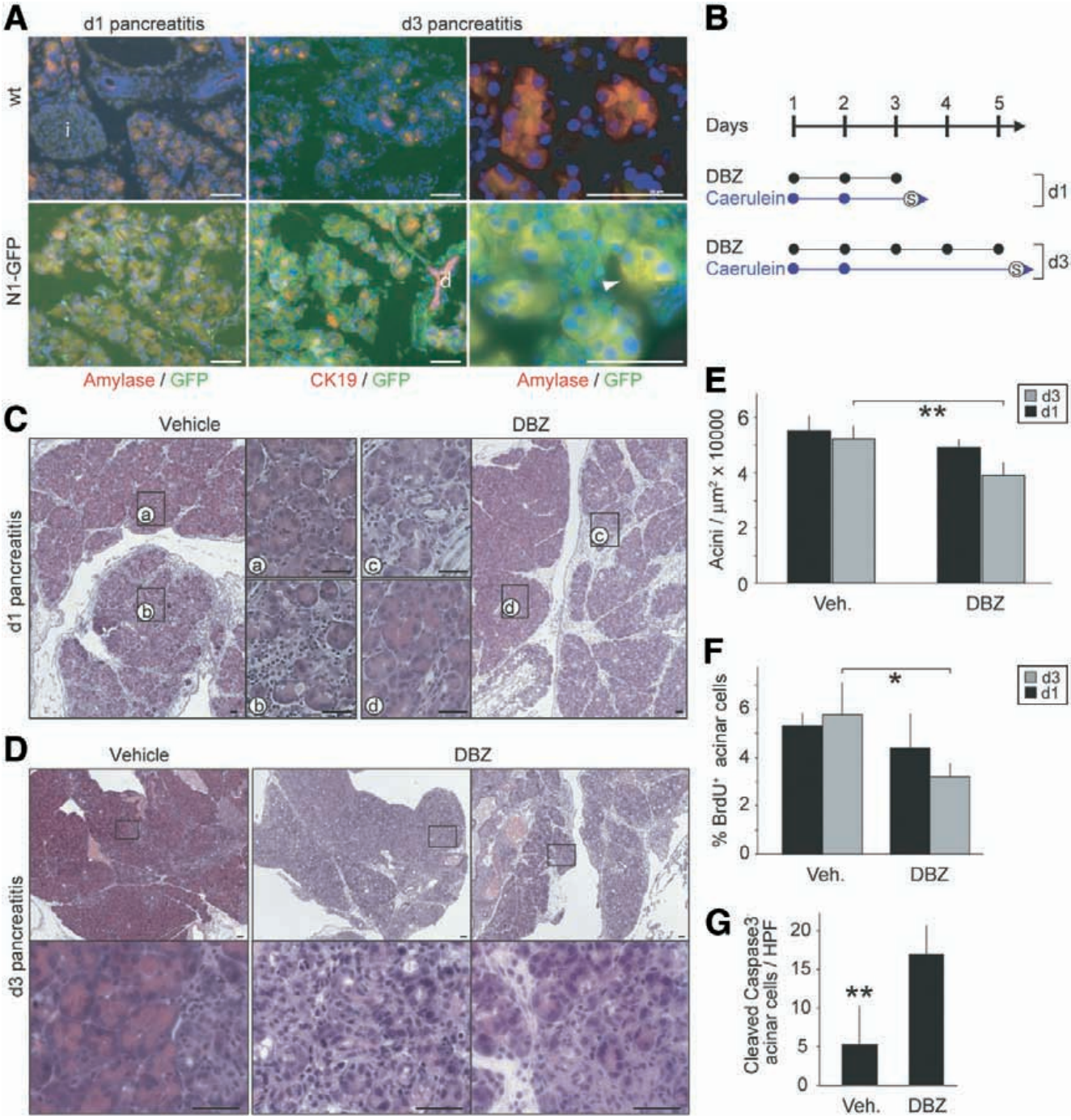

Figure 3. Cerulein-induced acute pancreatitis in DBZ- or vehicle-treated mice. (*A*) Notch1-GFP mice reveal increased expression of Notch1 on d3 postinduction of pancreatitis. *Arrowhead* indicates Notch1-positive acinar cells. (*B*) Experimental setup for the induction of cerulein-induced pancreatitis. Mice were injected with BrdU 2 hours before they were killed (s). (*C*) H&E staining at d1 pancreatitis shows acute tissue reaction of both vehicle- and DBZ-treated mice; *insets* show magnification with infiltrating cells between acini. (*D*) H&E staining at d3 pancreatitis shows impaired pancreas regeneration in mice treated with the γ-secretase inhibitor DBZ. *Insets* show magnifications with details of the regenerating acinar structures. (*E*) Morphometric assessment of acini shows a significant reduction in DBZ-treated mice at d3. (*F*) BrdU-positive acinar cells in DBZ- and vehicle-treated mice. *Black bars*, d1; *gray bars*, d3. At d3, DBZ induces a significant reduction of acinar cell proliferation (**P* = .032). (*G*) Significant increase in cleaved caspase-3–positive acinar cells in DBZ-treated mice 3 days after pancreatitis (***P* = .006). *Scale bar* = 50 μm.

marked reduction of differentiated acinar cells (Figure 3*D*). Quantification of acinar regeneration confirmed the morphologic findings, showing significantly less differentiated acini in DBZ-treated animals at d3 but not d1 (Figure 3*E*). Accompanied with this was a significantly reduced acinar cell proliferation and more apoptotic cells in DBZ-treated mice at d3 ($P = .032$ and $P = .006$, respectively; Figure 3*F* and *G*).

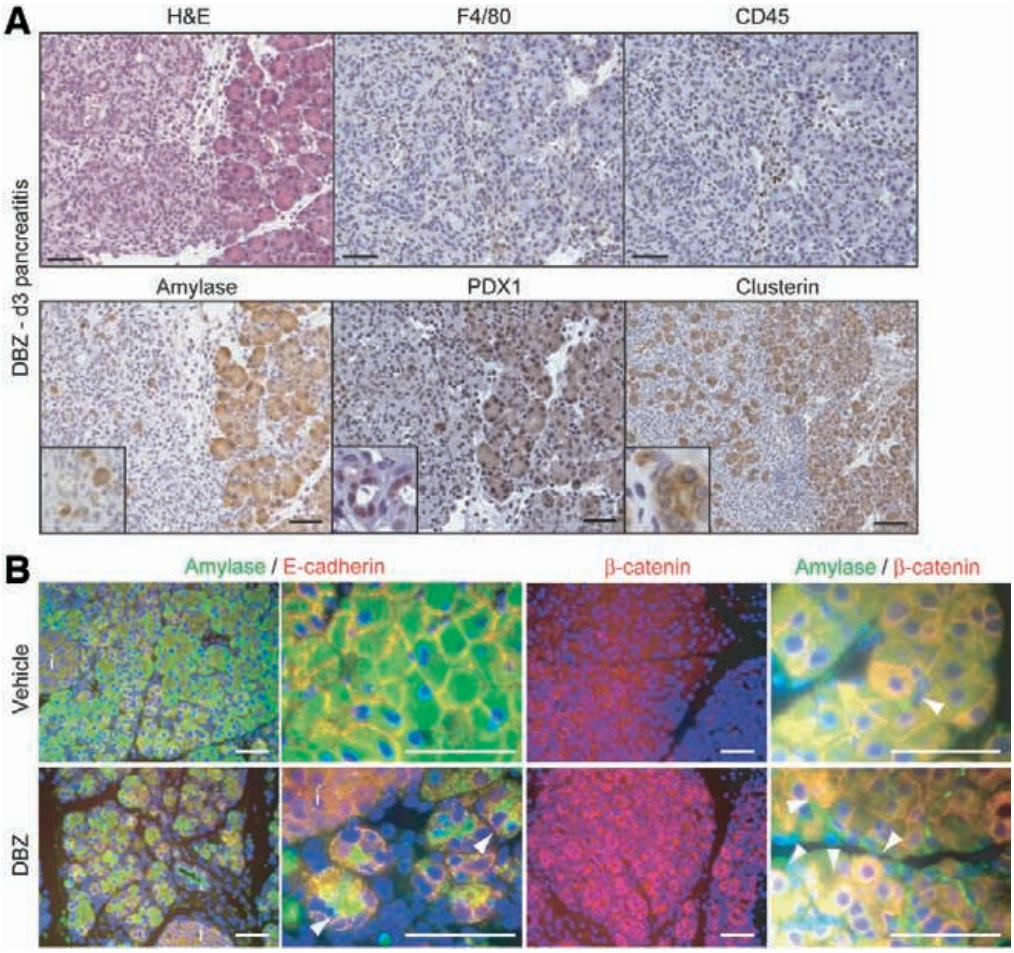

Figure 4. Effect of DBZ treatment in d3 pancreatitis. (*A*) H&E staining shows a pancreatic section containing an area with impaired tissue regeneration and neighboring regenerated acini. Immunohistochemical staining for CD45 and F4/80 shows infiltrating leukocytes and macrophages. Immunostaining for amylase, PDX1, and clusterin suggests that amylase-negative cells are immature acinar cells. *Insets* show higher magnification. (*B*) Double immunofluorescence staining for amylase (*green*) and E-cadherin or β-catenin (*red*) reveals higher and partially cytoplasmic expression (*arrowheads*) in DBZ-treated acinar cells. Nuclei were counterstained with 4′,6-diamidino-2-phenylindole (*blue*); i = islet; *scale bar* = 50 μm.

For further characterization, sequential sections were analyzed using different cell markers (Figure 4*A*; H&E). While some $CD45^+$ and $F4/80^+$ cells were found in the DBZ-treated pancreas at d3, there was no marked infiltration of inflammatory cells (Figure 4*A*). Cells within regions of impaired regeneration were mostly negative for exocrine (amylase, Figure 4*A*), ductal (DBA, not shown), and endocrine markers (insulin and glucagon, not shown) but expressed PDX1 and clusterin (Figure 4*A*), suggesting an immature acinus cell state. Because increased expression of E-cadherin and β-catenin has been described in dedifferentiated acinar cells, reflecting a transient progenitor status,[1] we next performed double immunofluorescence staining with amylase and either E-cadherin or β-catenin. In vehicle-treated mice, regenerated acinar cells showed a membrane-bound localization of E-cadherin and β-catenin, while in DBZ-treated acinar structures less amylase and increased E-cadherin and β-catenin expression was notable (Figure 4*B*).

Pancreas-Specific Inactivation of Notch1

Due to possible Notch-independent effects of γ-secretase inhibition, we next generated pancreas-specific *Notch1* knockout mice. Previously described *Notch1*$^{f/f}$ mice[7] were bred to *Ptf1a*$^{+/Cre(ex1)}$ mice generated in our group, in which Cre recombinase was inserted into exon 1.[21] Lineage tracing studies using *Ptf1a*$^{+/Cre(ex1)}$/*Rosa26r*^{lacZ} reporter mice revealed Cre-induced recombination in all pancreatic lineages (data not shown), similar to previously described *Ptf1a*-Cre mice.[10] For simplification, pancreas-specific *Ptf1a*$^{+/Cre(ex1)}$/*Notch1*$^{f/f}$ mice are termed *N1KO* mice, while *Ptf1a*$^{+/+}$/*Notch1*$^{f/f}$ and *Ptf1a*$^{+/Cre(ex1)}$/*Notch1*$^{+/+}$ littermates are referred to as wild-type (*N1WT*). X-gal staining in *N1KO/Rosa26r*^{lacZ} reporter mice revealed Cre-induced recombination in all pancreatic compartments of adult mice (Figure 5*A*). The efficiency of *Notch1* inactivation in the pancreas was shown by a reduction of *Notch1* mRNA levels to 20% and below protein detection levels compared with *N1WT* and *Ptf1a*$^{+/Cre(ex1)}$ mice at different ages, suggesting that no increase in Notch1-competent exocrine cells takes place over time (Figure 5*B* and *C*). *N1KO* mice were born at an expected Mendelian ratio and developed normally, showing no signs of disease up to an observation period of 18 months (data not shown). Thus, *Notch1* deficiency is dispensable for pancreatic development and organ function. Pancreata from 6- to 8-week-old *N1KO* mice were morphologically unremark-

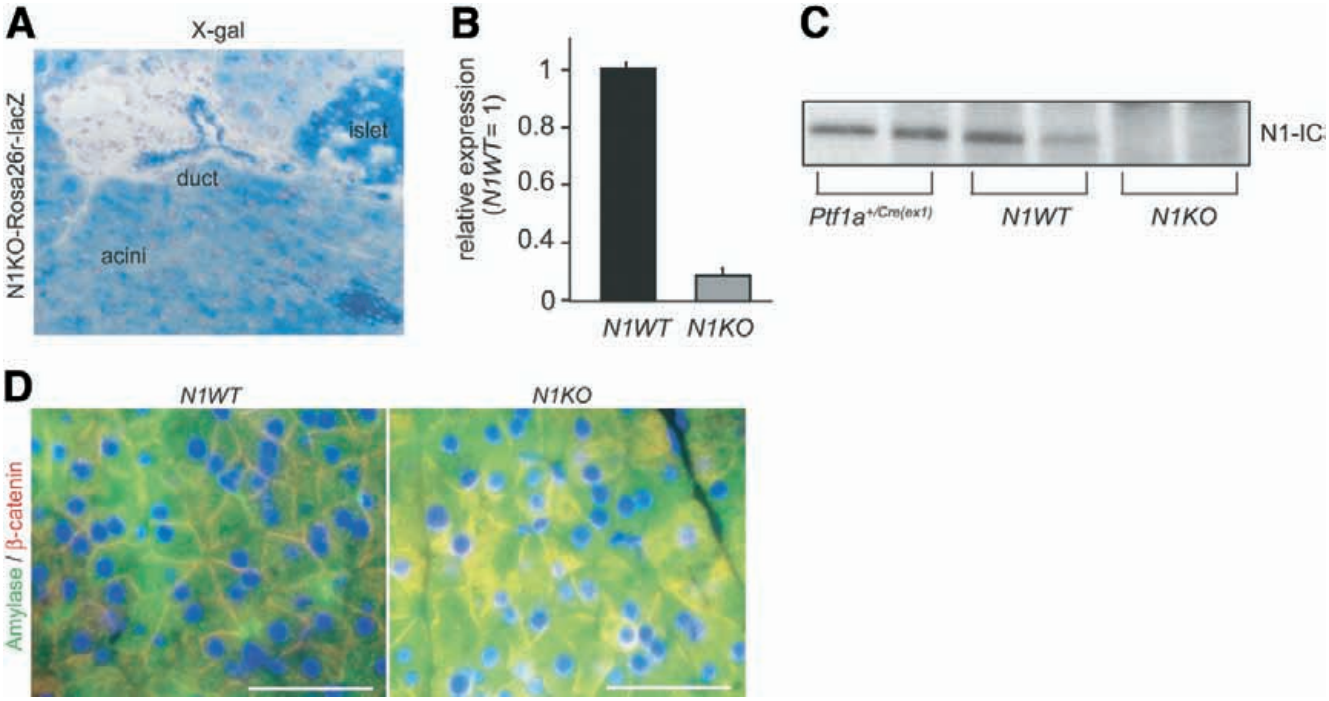

Figure 5. Characterization of Notch1-deficient exocrine pancreata. (*A*) X-gal staining shows Cre-induced recombination in all pancreatic compartments in 7-week-old *N1KO* mice. (*B*) Real-time qRT-PCR of *Notch1* mRNA in pancreata of *Ptf1a*$^{+/+}$, *Notch1*$^{f/f}$, and *Ptf1a*$^{+/Cre(ex1)}$; *Notch1*$^{f/f}$ mice. (*C*) Western blot analysis shows absence of Notch1-IC in *N1KO* pancreatic whole cell lysates. (*D*) Double immunofluorescence staining for amylase (*green*) and β-catenin (*red*) in *N1WT* and *N1KO* mice. Nuclei were counterstained with 4′,6-diamidino-2-phenylindole (*blue*); *scale bar* = 50 μm.

able and not distinguishable from *N1WT* mice; however, we observed a moderate increase in cytoplasmic β-catenin in some acinar cells, suggesting a potential alteration in the exocrine cell maturation status (Figure 5*D*). Pancreatic weight, acinar cell proliferation, and glucose tolerance were all normal (data not shown).

Notch1 Conditional Knockout Mice Show Impaired Regeneration After Cerulein-Mediated Pancreatitis

We next determined the role of Notch1 during regeneration after acute pancreatitis. During the early course of pancreatitis (d1) and similar to DBZ-treated mice, *N1KO* mice revealed similar morphologic alterations as seen in *N1WT* littermates (data not shown). However, at d3, we noted very similar tissue alterations in *N1KO* mice as found in DBZ-treated mice, with the fraction of impaired regenerated exocrine tissue being consistently higher compared with *N1WT* mice, albeit at varying levels between experiments (Figure 6*A* and *B*). Analysis of acinar regeneration showed significantly less acini in *N1KO* mice at d3 (Figure 6*B*). Opposite to the DBZ experiments, we found an increase in acinar cell proliferation and apoptosis (Figure 6*C* and *D*) in *N1KO* mice, suggesting that in the absence of Notch1 an increased turnover of acinar cells takes place. Similar to DBZ-treated mice, immature acinar cells of *Notch1*-deficient pancreata expressed PDX1 and clusterin and showed higher expression of E-cadherin and β-catenin (Figure 6*E* and *F* and data not shown). Moreover, we found increased protein expression of β-catenin in total pancreatic lysates of *N1KO* mice (Figure 6*G*). These data suggest that Notch1 has a direct or indirect influence on the β-catenin pathway during regeneration of the exocrine pancreas.

Inhibitory Effect of Notch1 on β-Catenin/Tcf Activity in the Acinar Tumor Cell Line 266-6

To analyze a possible interaction between β-catenin and Notch signaling in acinar cells, we sought to establish a cell culture system using the murine acinar cell tumor cell line 266-6.[27] Western blot analysis showed that 266-6 cells but not the mouse ductal pancreatic cancer cell line TD2[28] expressed amylase protein and *amylase* and *Ptf1a* mRNA (Figure 7*A* and data not shown). While we were able to detect Notch1 protein expression (Figure 7*B*), we were not able to inhibit Notch1 cleavage in 266-6 cells using DBZ (not shown). By contrast, the γ-secretase inhibitors L685,458 and DAPT reduced cleavage of Notch1-IC and expression levels of *Hes1* and *Hey1/L* mRNA (Figure 7*B* and *C* and data not shown). Thus, 266-6 cells show characteristics of acinar cells and display constitutive Notch1 activity, making this cell line suitable for further analysis of Notch and β-catenin interaction.

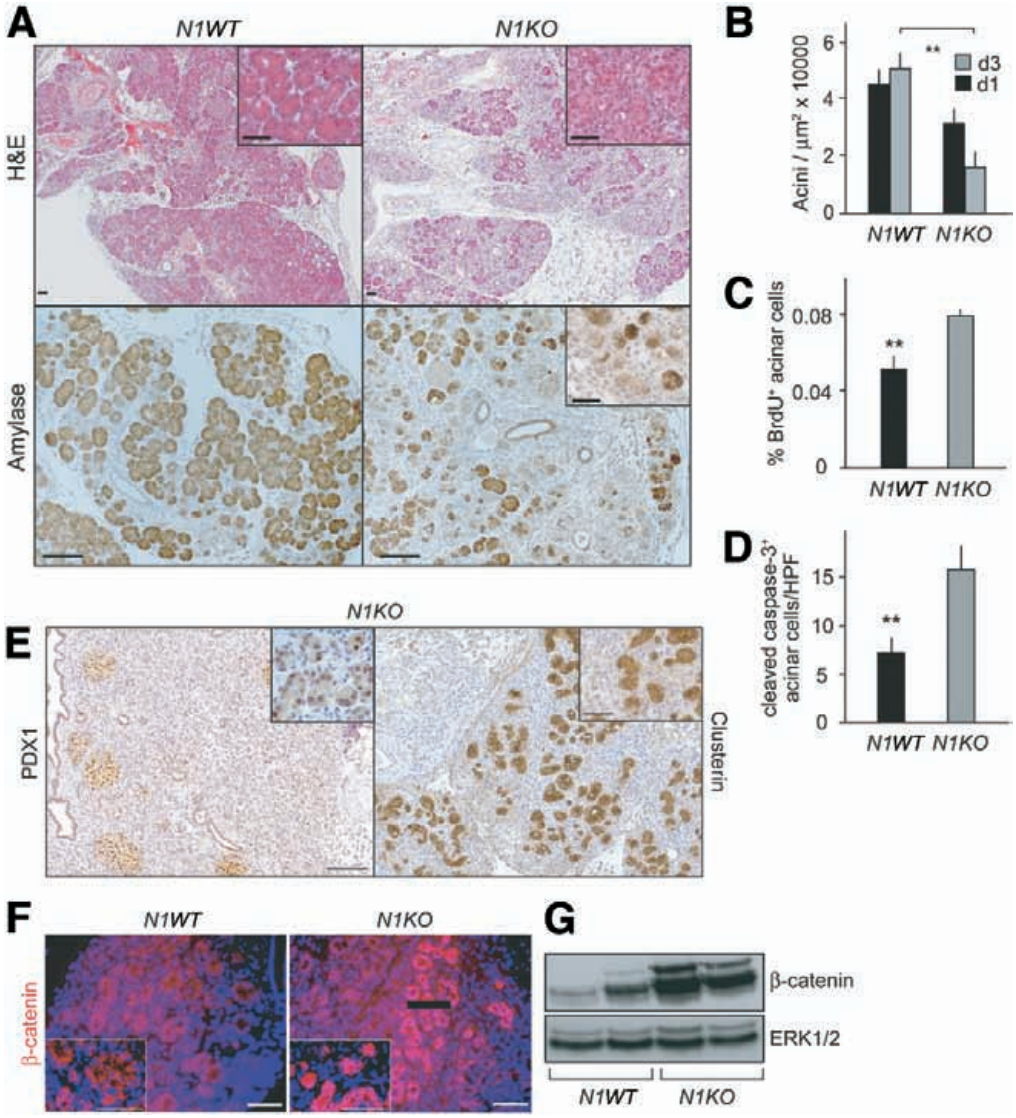

Figure 6. d3 pancreatitis in *N1WT* and *N1KO* mice. (*A*) H&E staining shows impaired tissue regeneration in *N1KO* pancreata. *Insets* show an area with regenerated acini. Immunohistochemistry for amylase shows fully differentiated acini in *N1WT* pancreas and many acinar cells with weak amylase staining in *N1KO* pancreas. (*B*) Morphometric assessment of acini shows a significant reduction in *N1KO* mice at d3. (*C*) BrdU-positive acinar cells are significantly increased in *N1KO* mice (**P = .0024). (*D*) Analysis of cleaved caspase-3–positive cells shows significantly more acinar cell apoptosis in *N1KO* mice (**P = .0016). (*E*) PDX1 and clusterin immunohistochemistry in *N1KO* mice shows expression in exocrine pancreatic cells. (*F*) Increased expression of β-catenin in *N1KO* compared with *N1WT* mice. Nuclei counterstained with 4′,6-diamidino-2-phenylindole (*blue*); *scale bar* = 50 μm. (*G*) Western blot analysis reveals increased expression of β-catenin in *N1KO* mice.

Measurement of the intrinsic transcriptional activity of β-catenin in 266-6 cells by using the β-catenin–responsive TCF reporter construct TOP-FLASH (TOP) and mutant control FOP-FLASH revealed a very low basal transcriptional activity of β-catenin (Figure 7*D*). To obtain higher β-catenin–induced TOP activation, 266-6 cells were transfected with Wnt1 or constitutively active S33/β-catenin, which resulted in high activity of TOP but not FOP-FLASH in a dose-dependent manner (Figure 7*D* and *E*).

To test if increased Notch signaling alters β-catenin activity, we cotransfected 266-6 cells with either S33 β-catenin or Wnt1 together with different Notch1 constructs. Notch1ΔE in contrast to Notch1-IC is integrated in the cell membrane and requires endogenous γ-secretase activity for cleavage to generate Notch1-IC. We found Notch1-IC and Notch1ΔE to inhibit both Wnt1 and S33β-catenin–induced TOP activity (Figure 8*A* and data not shown). The inhibitory effect of Notch1ΔE on S33 β-catenin-induced TOP activity was partially reversed in a dose-dependent manner by DAPT (Figure 8*B*). These data suggest an inhibitory role of Notch1 on the Wnt signaling pathway dependent on Notch1 intracellular cleavage.

We next tested the effect of Notch1 depletion on β-catenin activity by small interfering RNA (siRNA)-mediated knockdown. Notch1 but not control or Notch2 siRNA led to a significant reduction of Notch1-IC. In addition, Notch1 siRNA effectively inhibited Notch1 signaling, as shown using the artificial Rbpj responsive reporter construct pGa981-6 (Figure 8*C* and *D*). Cotransfection of TOP, S33 β-catenin, and control or Notch1 siRNA resulted in suppressed S33 β-catenin–mediated inhibition of TOP activity in Notch1 but not control siRNA-treated 266-6 cells, suggesting an inhibitory regulatory role of Notch1 on β-catenin activity (Figure 8*E*).

We next tested whether specific Notch domains are required for suppressing β-catenin–mediated transcrip-

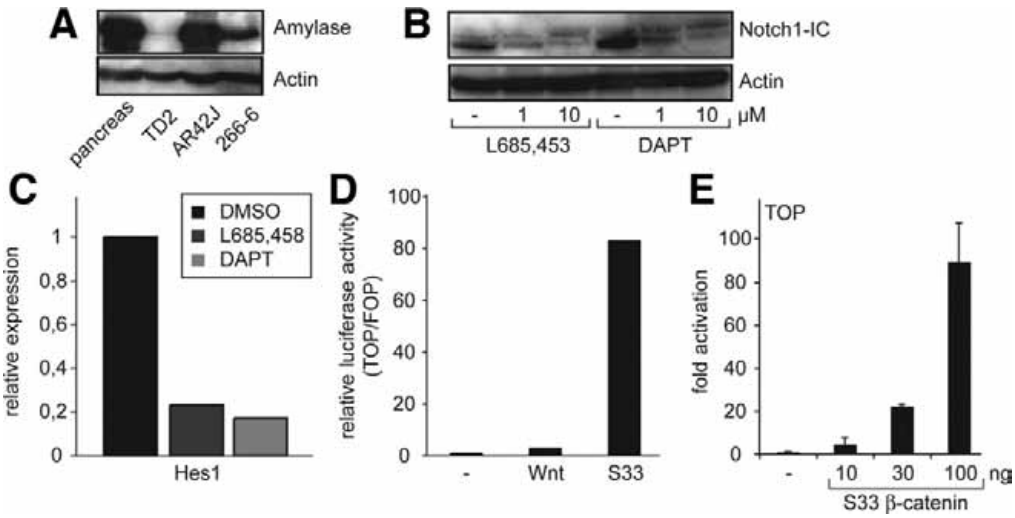

Figure 7. Notch and β-catenin signaling in 266-6 acinar cells. (*A*) Amylase protein expression in pancreatic whole cell lysates and different cell lines reveals expression in 266-6 cells demonstrating exocrine cell characteristics. (*B*) Analysis of Notch1-IC protein expression and inhibition in 266-6 cells. Notch1-IC is expressed in 266-6 cells and can be inhibited by treatment with γ-secretase inhibitors L685,458 and DAPT for 48 hours. (*C*) Treatment of 266-6 cells with γ-secretase inhibitors L685,458 and DAPT for 48 hours leads to down-regulation of *Hes1* mRNA. (*D*) Luciferase activity as measured by β-catenin/TCF TOP/FOP-FLASH ratio shows increased activity when transfected with Wnt1 or constitutively active S33 β-catenin for 48 hours in 266-6 cells. (*E*) Dose dependency of TOP activity by different amounts of S33 β-catenin. TOP and indicated amounts of S33 β-catenin were cotransfected and luciferase activity was measured after 48 hours. Results are the mean ± SD of triplicates and are representative of at least 3 independent experiments.

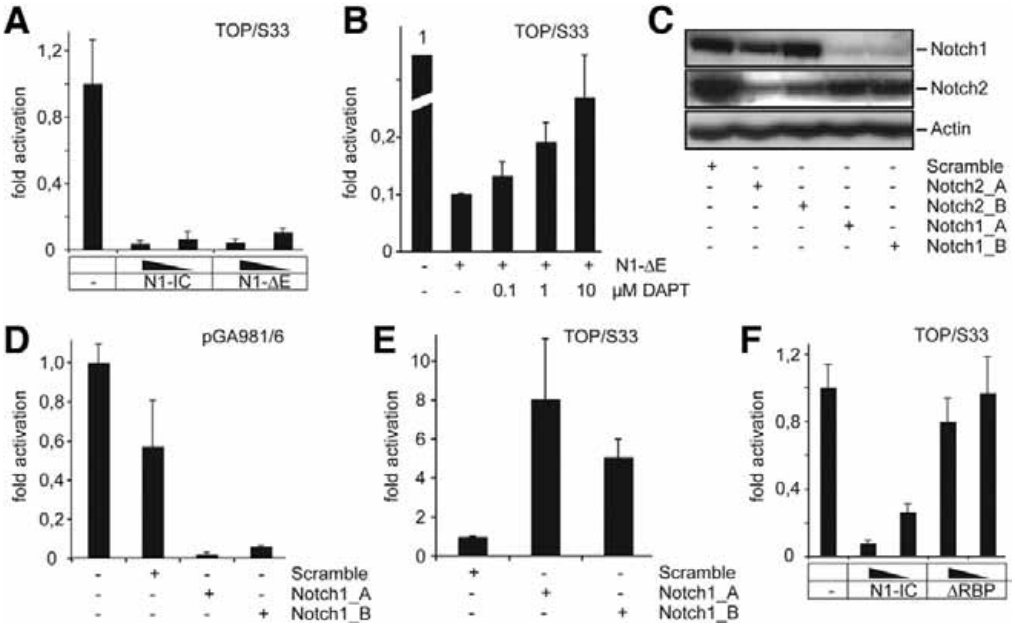

Figure 8. Notch1 regulates β-catenin–dependent transcriptional activity in 266-6 cells. (*A*) S33 β-catenin–induced TOP activity is inhibited in a dose-dependent manner by cotransfecting with either Notch1-IC or Notch1ΔE. (*B*) Inhibition of S33 β-catenin–induced TOP activity by Notch1ΔE can be modulated by DAPT treatment. 266-6 cells were treated with indicated amounts of DAPT. (*C*) Treatment of 266-6 cells with siRNA against either Notch1 or Notch2 leads to specific down-regulation of the respective Notch receptor. (*D*) RBP-Jκ–dependent transcriptional activity is suppressed after siRNA-mediated knockdown of Notch1. (*E*) S33 β-catenin–induced TOP activity is increased by siRNA-mediated knockdown of Notch1 using 2 different Notch1-specific siRNAs. (*F*) Notch1-IC is a stronger inhibitor of S33 β-catenin–induced TOP activity than Notch1-ICΔRBP, demonstrating the importance of a functional RAM domain. Results are the mean ± SD of triplicates measured at 48 or 72 hours for siRNA experiments and are representative of at least 4 independent experiments.

tional TOP activity. A Notch1-IC mutant lacking a functional RAM domain, Notch1-ICΔRBP, showed lower suppression of β-catenin–mediated activation (Figure 8*F*), suggesting that Notch1 signaling via Rbpj is required.

Discussion

In this study, we investigated the role of Notch signaling in pancreatic homeostasis and during acute pancreatitis using a chemical and genetic approach for ablation of Notch signaling. Several reports have shown an important role for Notch signaling in pancreatic organogenesis (overview in Cano et al[29]); however, and unexpectedly, unstimulated pancreata of *N1KO* mice did not reveal obvious abnormalities. The modest alterations in DBZ-treated but not *N1KO* pancreata regarding morphology, expression of acinar-expressed genes, and proliferation may thus possibly be due to DBZ-induced Notch inhibition in the pancreatic mesenchyme or Notch-independent effects of γ-secretase inhibition.[30] Other possible mechanisms include expression of other Notch receptors in acinar cells; however, we found no evidence for up-regulation of Notch2–4 in *N1KO* mice. In particular, Notch2 was not found to be up-regulated in acinar cells using heterozygous lacZ-knockin animals at the Notch2 locus (J.T.S., unpublished observation, May 2006).[31] Although the endocrine compartment was not the focus of this study, we found no striking abnormalities in *N1KO* mice, possibly due to the incomplete targeting of the endocrine compartment by *Ptf1a*$^{+/Cre(ex1)}$ mice (J.T.S., personal observation, March 2006).

Impaired recovery after acute pancreatitis in Notch-inhibited pancreata may be due to different mechanisms. Notch signaling inhibition in the pancreatic mesenchyme, such as in fibroblasts or blood vessels, would be a potential mechanism in DBZ-treated mice, yet these compartments are not targeted by *Ptf1a*$^{+/Cre(ex1)}$ in *N1KO* mice and can thus not sufficiently explain the very similar phenotype of chemically and genetically Notch-ablated mice. Another mechanism may be that inhibition of Notch signaling could increase the susceptibility of pancreatic cells to cerulein-induced damage. After cerulein-induced pancreatitis, acinar cell death and exocrine dedifferentiation peak at d1.[1] Using the same protocol of cerulein treatment, we observed similar tissue alterations at 8 hours (J.T.S., unpublished observations, March 2006) and d1 postinduction in wild-type, DBZ-treated, and *N1KO* mice, suggesting that Notch signaling is not involved in cerulein-induced acinar susceptibility to injury. In addition, our and other results regarding acinar expression of Notch1 showed low to absent expression in unstimulated pancreata while peaking on d3 postinduction of pancreatitis. This finding argues for a role of Notch1 in the regenerative phase of acute pancreatitis.[1] Another possibility would be exhaustion of the adult progenitor cell compartment by defective Notch signaling before or during injury. The cellular source of exocrine regeneration has not been decisively determined and may include differentiated acinar cells, centroacinar cells, or even other pancreatic cell compartments such as ductal or islet cells besides an adult progenitor cell. Recent evidence suggests that exocrine regeneration occurs primarily from preexisting acinar cells.[1,32] From our experiments and in the absence of cell lineage tracing experiments, we cannot conclude which cells are responsible for regeneration in our model. However, our results of impaired regeneration of the exocrine compartment support a model of Notch-regulated acinar cell regeneration. Because we do not find evidence for an essential role of Notch signaling in acinar proliferation, the role of Notch signaling may very well be regulating the differentiation status of acinar cells versus regulation of an adult progenitor compartment during acute pancreatitis, and both hypotheses should be addressed by lineage tracing experiments in future studies.

A potential mechanism for Notch1 regulating acinar differentiation is by interaction with β-catenin. Recent studies have found evidence for an interaction of both pathways in various organs, including skin and the hematopoietic system.[33–35] In the pancreas, β-catenin is essential for acinar specification during organogenesis, pointing to a central role of this pathway in acinar differentiation and cell integrity.[18–20] Loss-of-function studies in pancreatic organogenesis have shown the requirement for cell-autonomous β-catenin in acinar specification rather than survival.[18,20] The finding of increased acinar β-catenin mRNA expression early in acute pancreatitis and its decline later during regeneration[1] suggests that β-catenin may also be required during adult acinar maturation processes.

Our results of a prolonged and increased expression of β-catenin in Notch-ablated acini during acute pancreatitis suggest a modulatory function of Notch on the amount and activity of β-catenin. The fact that we found no alterations in the proliferative capacity in vivo in *N1KO* mice and in vitro in 266-6 cells after Notch1-IC transfection (J.T.S., personal observation, September 2006) suggests that both Notch and β-catenin may be involved in acinar differentiation rather than proliferation and is consistent with the role of β-catenin during embryonic exocrine development.[18] While the higher expression of β-catenin in Notch1-deficient acinar cells in vivo and the suppressed transcriptional activity of β-catenin by Notch1-IC in vitro may not be directly related, both results suggest that Notch signaling may interact with β-catenin in acinar cells. While the low basal activity of β-catenin in 266-6 cells may be due to an inhibitory effect of endogenous Notch, the strong TOP activity induced by constitutively active S33 β-catenin compared with Wnt1 suggests that the Notch/Wnt interaction may be at the level of β-catenin/Tcf transcriptional activity. Additional evidence for this hypothesis stems from the finding that the RBP-Jκ/RAM domain-dependent ef-

fect of Notch1 is critically important for inhibition, suggesting an RBP-Jκ–dependent effect such as induction of a yet unidentified protein or activation of a β-catenin–regulating protein.

In conclusion, we have identified Notch signaling to be important for regeneration of the adult murine pancreas during acute pancreatitis. We show that Notch1 is required for the exocrine regeneration of the pancreas in vivo. Molecular studies using a cell culture–based system provide evidence for an interaction of Notch1 with β-catenin. Given the potential application of γ-secretase or Notch signaling inhibitors in various diseases, it will be important to delineate which cellular compartment is affected by Notch inhibition by lineage tracing studies and to further characterize the mechanism of the Notch and β-catenin signaling interaction.

Supplementary Data

Supplementary data associated with this article can be found, in the online version, at doi:10.1053/j.gastro.2007.11.003 and www.gastrojournal.org.

References

1. Jensen JN, Cameron E, Garay MV, et al. Recapitulation of elements of embryonic development in adult mouse pancreatic regeneration. Gastroenterology 2005;128:728–741.
2. Gomez G, Englander EW, Wang G, et al. Increased expression of hypoxia-inducible factor-1alpha, p48, and the Notch signaling cascade during acute pancreatitis in mice. Pancreas 2004;28:58–64.
3. Wilson A, Radtke F. Multiple functions of Notch signaling in self-renewing organs and cancer. FEBS Lett 2006;580:2860–2868.
4. van Es JH, van Gijn ME, Riccio O, et al. Notch/gamma-secretase inhibition turns proliferative cells in intestinal crypts and adenomas into goblet cells. Nature 2005;435:959–963.
5. Jensen CH, Jauho EI, Santoni-Rugiu E, et al. Transit-amplifying ductular (oval) cells and their hepatocytic progeny are characterized by a novel and distinctive expression of delta-like protein/preadipocyte factor 1/fetal antigen 1. Am J Pathol 2004;164:1347–1359.
6. Croquelois A, Blindenbacher A, Terracciano L, et al. Inducible inactivation of Notch1 causes nodular regenerative hyperplasia in mice. Hepatology 2005;41:487–496.
7. Radtke F, Wilson A, Stark G, et al. Deficient T cell fate specification in mice with an induced inactivation of Notch1. Immunity 1999;10:547–558.
8. Schouwey K, Delmas V, Larue L, et al. Notch1 and Notch2 receptors influence progressive hair graying in a dose-dependent manner. Dev Dyn 2006;236:282–289.
9. Vauclair S, Nicolas M, Barrandon Y, et al. Notch1 is essential for postnatal hair follicle development and homeostasis. Dev Biol 2005;284:184–193.
10. Kawaguchi Y, Cooper B, Gannon M, et al. The role of the transcriptional regulator Ptf1a in converting intestinal to pancreatic progenitors. Nat Genet 2002;32:128–134.
11. Jensen J, Pedersen EE, Galante P, et al. Control of endodermal endocrine development by Hes-1. Nat Genet 2000;24:36–44.
12. Fujikura J, Hosoda K, Iwakura H, et al. Notch/Rbp-j signaling prevents premature endocrine and ductal cell differentiation in the pancreas. Cell Metab 2006;3:59–65.
13. Apelqvist A, Li H, Sommer L, et al. Notch signalling controls pancreatic cell differentiation. Nature 1999;400:877–881.
14. Hald J, Hjorth JP, German MS, et al. Activated Notch1 prevents differentiation of pancreatic acinar cells and attenuate endocrine development. Dev Biol 2003;260:426–437.
15. Murtaugh LC, Stanger BZ, Kwan KM, et al. Notch signaling controls multiple steps of pancreatic differentiation. Proc Natl Acad Sci U S A 2003;100:14920–14925.
16. Esni F, Ghosh B, Biankin AV, et al. Notch inhibits Ptf1 function and acinar cell differentiation in developing mouse and zebrafish pancreas. Development 2004;131:4213–4224.
17. Miyamoto Y, Maitra A, Ghosh B, et al. Notch mediates TGF alpha-induced changes in epithelial differentiation during pancreatic tumorigenesis. Cancer Cell 2003;3:565–576.
18. Murtaugh LC, Law AC, Dor Y, et al. Beta-catenin is essential for pancreatic acinar but not islet development. Development 2005;132:4663–4674.
19. Heiser PW, Lau J, Taketo MM, et al. Stabilization of beta-catenin impacts pancreas growth. Development 2006;133:2023–2032.
20. Dessimoz J, Bonnard C, Huelsken J, et al. Pancreas-specific deletion of beta-catenin reveals Wnt-dependent and Wnt-independent functions during development. Curr Biol 2005;15:1677–1683.
21. Nakhai H, Sel S, Favor J, et al. Ptf1a is essential for the differentiation of GABAergic and glycinergic amacrine cells and horizontal cells in the mouse retina. Development 2007;134:1151–1160.
22. Shou J, Ross S, Koeppen H, et al. Dynamics of notch expression during murine prostate development and tumorigenesis. Cancer Res 2001;61:7291–7297.
23. Siveke JT, Einwachter H, Sipos B, et al. Concomitant pancreatic activation of Kras(G12D) and Tgfa results in cystic papillary neoplasms reminiscent of human IPMN. Cancer Cell 2007;12:266–279.
24. Milano J, McKay J, Dagenais C, et al. Modulation of notch processing by gamma-secretase inhibitors causes intestinal goblet cell metaplasia and induction of genes known to specify gut secretory lineage differentiation. Toxicol Sci 2004;82:341–358.
25. Ji B, Chen XQ, Misek DE, et al. Pancreatic gene expression during the initiation of acute pancreatitis: identification of EGR-1 as a key regulator. Physiol Genomics 2003;14:59–72.
26. Beres TM, Masui T, Swift GH, et al. PTF1 Is an organ-specific and Notch-independent basic helix-loop-helix complex containing the mammalian suppressor of hairless (RBP-J) or its paralogue, RBP-L. Mol Cell Biol 2006;26:117–130.
27. Ornitz DM, Palmiter RD, Messing A, et al. Elastase I promoter directs expression of human growth hormone and SV40 T antigen genes to pancreatic acinar cells in transgenic mice. Cold Spring Harb Symp Quant Biol 1985;50:399–409.
28. Schreiner B, Greten FR, Baur DM, et al. Murine pancreatic tumor cell line TD2 bears the characteristic pattern of genetic changes with two independently amplified gene loci. Oncogene 2003;22:6802–6809.
29. Cano DA, Hebrok M, Zenker M. Pancreatic development and disease. Gastroenterology 2007;132:745–762.
30. Marambaud P, Shioi J, Serban G, et al. A presenilin-1/gamma-secretase cleavage releases the E-cadherin intracellular domain and regulates disassembly of adherens junctions. EMBO J 2002;21:1948–1956.
31. Hamada Y, Kadokawa Y, Okabe M, et al. Mutation in ankyrin repeats of the mouse Notch2 gene induces early embryonic lethality. Development 1999;126:3415–3424.
32. Desai BM, Oliver-Krasinski J, De Leon DD, et al. Preexisting pancreatic acinar cells contribute to acinar cell, but not islet beta cell, regeneration. J Clin Invest 2007;117:971–977.

33. Hayward P, Brennan K, Sanders P, et al. Notch modulates Wnt signalling by associating with Armadillo/beta-catenin and regulating its transcriptional activity. Development 2005;132:1819–1830.
34. Nicolas M, Wolfer A, Raj K, et al. Notch1 functions as a tumor suppressor in mouse skin. Nat Genet 2003;33:416–421.
35. Reya T, Duncan AW, Ailles L, et al. A role for Wnt signalling in self-renewal of haematopoietic stem cells. Nature 2003;423:409–414.

Received February 6, 2007. Accepted October 18, 2007.

Address requests for reprints to: Roland M. Schmid, MD, 2. Med. Department, Klinikum rechts der Isar, Ismaninger Str. 22, 81675 Munich, Germany. e-mail: roland.schmid@lrz.tum.de.; fax: (49) 8941404871.

Supported by grants from the Deutsche Krebshilfe (#107195) and the Lustgarten Foundation (RFP 05-014/06-012) (to J.T.S. and R.M.S.) and the Deutsche Forschungsgemeinschaft (R.M.S.).

Microarray data are available at ArrayExpress (accession no. E-MEXP-1276; http://www.ebi.ac.uk/arrayexpress).

The authors report that no conflict of interest exists.

The authors thank Dr Wei-Qiang Gao (Genentech, Inc) for providing transgenic Notch1-GFP mice, Dr M. van de Wetering and Dr H. Clevers for providing the β-catenin pathway expression and reporter plasmids, M. Gerhard for helpful discussions, and Mathilde Neuhofer and Christine Köhler for excellent technical assistance.

Appendix 4

Hassan Nakhai, Jens T. Siveke, Bettina Klein, Lidia Mendoza-Torres, **Pawel K. Mazur**, Hana Algül, Freddy Radtke, Lothar J. Strobl, Ursula Zimber-Strobl, Roland M. Schmid.

Conditional ablation of Notch signaling in pancreatic development.

Development. 2008 Aug;135(16):2757-65.

Development 135, 2757-2765 (2008) doi:10.1242/dev.013722

Conditional ablation of Notch signaling in pancreatic development

Hassan Nakhai[1,*], Jens T. Siveke[1,*], Bettina Klein[2], Lidia Mendoza-Torres[1], Pawel K. Mazur[1], Hana Algül[1], Freddy Radtke[3], Lothar Strobl[4], Ursula Zimber-Strobl[4] and Roland M. Schmid[1,†]

The role of the Notch signaling members *Notch1*, *Notch2* and *Rbpj* in exocrine pancreatic development is not well defined. We therefore analyzed conditional pancreas-specific *Rbpj* and combined *Notch1*/*Notch2* knockout mice using *Ptf1a*$^{+/Cre(ex1)}$ mice crossed with floxed *Rbpj* or *Notch1*/*Notch2* mice. Mice were analyzed at different embryonic stages for pancreatic exocrine and endocrine development. The absence of *Rbpj* in pancreatic progenitor cells impaired exocrine pancreas development up to embryonic day 18.5 and led to premature differentiation of pancreatic progenitors into endocrine cells. In *Rbpj*-deficient pancreata, amylase-expressing acini and islets formed during late embryonic and postnatal development, suggesting an essential role of *Rbpj* in early but not late development. Contrary to this severe phenotype, the concomitant inactivation of *Notch1* and *Notch2* only moderately disturbed the proliferation of pancreatic epithelial cells during early embryonic development, and did not inhibit pancreatic development. Our results show that, in contrast to *Rbpj*, *Notch1* and *Notch2* are not essential for pancreatogenesis. These data favor a Notch-independent role of *Rbpj* in the development of the exocrine pancreas. Furthermore, our findings suggest that in late stages of pancreatic development exocrine cell differentiation and maintenance are independent of *Rbpj*.

KEY WORDS: Notch, *Rbpj*, Conditional knockout mice, Pancreas, Development

INTRODUCTION

The Notch signaling pathway is a key regulator of developmental processes during organogenesis. Loss-of-function studies have proposed that Notch signaling regulates self-renewal leading to depletion of pancreatic progenitor cells and accelerated differentiation of endocrine cells (Apelqvist et al., 1999; Fujikura et al., 2006; Fujikura et al., 2007; Jensen et al., 2000). While these studies have provided evidence for an important role of Notch signaling in endocrine development, the dependence of the exocrine compartment on specific Notch signaling members is not well understood. Recently, RBPJκ, the transcriptional mediator of Notch signaling, was found to be a binding partner of PTF1A in the PTF1 complex, suggesting a Notch-independent function during pancreatic development (Beres et al., 2006; Masui et al., 2007). Moreover, because of the existence of multiple receptors, ligands and target genes, and because of the embryonic lethality of mice null for Notch signaling components, the precise role of individual Notch signaling components in early and late pancreatic organogenesis is not well defined. During pancreatic organogenesis, Notch1 and Notch2 expression has been described in the pancreatic epithelium, whereas Notch3 and Notch4 are expressed in mesenchymal and endothelial cells (Lammert et al., 2000).

In order to clarify the role of the epithelially expressed receptors Notch1 and Notch2 versus the abrogation of RBPJκ signaling, we analyzed conditional *Notch1/Notch2* double-knockout and *Rbpj* knockout mice by using *Ptf1a*$^{+/Cre(ex1)}$ mice for targeting pancreatic progenitor and exocrine cells.

[1]Department of Internal Medicine, Technical University of Munich, Ismaniger Strasse 22, 81675 Munich, Germany. [2]Institute of Immunology, Friedrich-Loeffler Institut, Paul-Ehrlich Strasse 28, 72076 Tuebingen, Germany. [3]ISREC, Chemin des Boveresses 155, 1066 Epalinges, Switzerland. [4]GSF-National Research Center for Environment and Health, Institute for Clinical Molecular Biology and Tumor Genetics, Marchioninistrasse 25, 81377 Munich, Germany.

*These authors contributed equally to this work
†Author for correspondence (e-mail: roland.schmid@lrz.tum.de)

Accepted 17 June 2008

MATERIALS AND METHODS

Generation of *Rbpj*$^{f/f}$ mice

In order to generate a conditional gene replacement vector for *Rbpj*, several genomic fragments of *Rbpj* were isolated from a λ-DASHII phage library (Stratagene) and subcloned into pBluescript SK+ (Stratagene). A neomycin resistance cassette, flanked by two *loxP* sites, was inserted into intron 7, and a single *loxP* site was integrated into intron 5. A herpes simplex virus thymidine kinase (HSV-tk) cassette was cloned at the 5′ end of the gene-targeting construct (Fig. 1A). The *Not*I-linearized vector was transfected into murine 129/SvJ ES cells, where it recombined with the host genome. The homologous recombination event occurred at a frequency of 1:602 and was verified by PCR and Southern blot analysis. The floxed *neo*-resistance cassette was removed by transient transfection of a vector expressing the Cre-recombinase. Blastocyst injection and germline transmission of the mutant allele were done as described previously (Tanigaki et al., 2002). Genotyping of mice was performed on DNA isolated from tail biopsies using a PCR kit (Qiagen). For the detection of floxed (0.55 kb fragment) and wild-type (0.5 kb) alleles of *Rbpj*, PCR amplification (1 minute at 94°C, 30 seconds at 58°C and 30 seconds at 72°C, for 40 cycles) was carried out using primers 5′-AGT TTA GGC TTT CCA AAA GGC-3′ (forward) and 5′-GTA TTG CTA AGA ACT TGT TGC-3′ (reverse). All mice were housed in pathogen-free conditions. All mouse protocols were approved by the Centre of Animals Research, the Faculty of Medicine, Technical University of Munich.

X-gal staining

β-gal activity was determined on whole-mount preparations as described previously (Kawaguchi et al., 2002).

BrdU labeling

In vivo pulse labeling with 5-bromo-2-deoxyuridine (BrdU) was used to mark newly synthesized DNA. BrdU (20 mmol/l, 5 ml/kg body weight) was injected intraperitoneally into pregnant mice 2 hours before sacrifice.

Histology and immunohistology

Dissected tissues were fixed in ice-cold 4% paraformaldehyde, paraffin-embedded and cut into 2-3 μm sections. Immunohistochemistry was performed using the following primary antibodies: rabbit anti-PTF1A (1:500, kind gift from Raymond J. Macdonald, University of Texas, USA); rabbit anti-PDX1 (1:10,000, kind gift from C. V. Wright, Vanderbilt University Medical

Center, Nashville, USA); guinea pig anti-insulin (1:1000, Linco); rabbit anti-glucagon (1:1000, Linco); guinea pig anti-glucagon (1:500, Linco); rabbit anti-β-galactosidase (1:500, ICN); rabbit anti-somatostatin (1:1000, ICN); rabbit anti-pancreatic polypeptide (1:500, BioTrend); rabbit anti-amylase (1:1000, Sigma) rabbit anti-phosphohistone H3 (1:500, Upstate); rabbit anti-carboxypeptidase A (1:500, BioTrend); mouse anti-CK19 [1:500, Developmental Studies Hybridoma Bank (DSHB), University of Iowa]; rabbit anti-HES1 (1:100, kind gift from T. Sudo, Toray Industries, Tokyo, Japan); rabbit anti-cyclin B1 (1:500, Millipore); rat anti-BrdU (1:250, Serotec); mouse anti-Neurogenin (1:500, DSHB). For immunoperoxidase detection, Vectastain ABC kit (Vector Labs) was used according to the manufacturer's instructions. For double immunofluorescence staining, the primary antibodies were followed by incubation with secondary antibodies conjugated with fluorescent Alexa 488 or Alex 568 (Molecular Probes). Sections were mounted with Vectashield mounting medium (Vector Laboratories) and examined using an Axiovert 200M (Zeiss) fluorescent inverse microscope equipped with the Axiovision version 4.4 software (Zeiss). The number of islets was calculated, with the definition of an islet being a group of β cells surrounded by α cells. For morphometric analyses, the pancreatic buds were immunostained with anti-PDX1 and analyzed using the AxioVision Image analysis software (Zeiss). To calculate the number of PHH3- and neurogenin 3-positive cells, whole pancreatic buds from three control and three knockout embryos were cut into 3 μm serial sections. Every fifth section was stained and the number of $PHH3^+$, neurogenin 3^+ and $insulin^+$ cells were counted and calculated relative to the whole area of $PDX1^+$ pancreatic epithelium in every section

Laser capture microscopy

Acini and pancreatic buds were dissected from 5- to 6-μm sections using a Leica and P.A.L.M microlaser system, respectively. Cells were incubated overnight at 37°C in 20 μl of TE buffer [1 mM EDTA, 20 mM Tris (pH 8)] containing 0.5 mg/ml proteinase K, after which the proteinase K was heat inactivated by incubation at 95°C for 15 minutes. For detection of the floxed (0.33 kb) and deleted (0.30 kb) alleles of *Notch1*, PCR amplification (94°C for 20 seconds, 55°C for 30 seconds, and 72°C for 30 seconds, for 40 cycles) was performed using primers P1 (5′-AAC TGA GGC CTA GAG CCT TGA AG-3′), P2 (5′-GTG GTC CAG GGT GTG AGT GTT C-3′) and P3 (5′-ACC TGT TCG CAG GCA TCT CCA G-3′). Floxed (0.29 kb) and deleted (0.37 kb) alleles of *Notch2* were detected using primers P4 (5′-GGA GAA GCA GAG ATG AGC AGA TGG-3′), P5 (5′-CAC ATG TGC GTG CGT GTG CAT G-3′), P6 (5′-CAG AGA TGA GCA GAT GGG CAT A-3′) and P7 (5′-GAG GCC AGA GGA CGA CTC TGT-3′). For *Rbpj*, a 2-kb (floxed) and a 0.75-kb (deleted) fragment were obtained using primers P8 (5′-TAT TGC TAA GAG CTT GTT GC-3′) and P9 (5′-ACT GAG TGT GTA TCT TAA GC-3′).

Western blot analysis

Whole-cell lysates were prepared and western blots were performed as previously described (Siveke et al., 2007).

RESULTS

Generation of pancreas-specific *Rbpj* and *Notch1/Notch2* knockout mice

$Ptf1a^{+/Cre(ex1)}$ mice were generated using a knock-in approach replacing exon 1 with Cre recombinase (Nakhai et al., 2007). For analysis of Cre recombinase expression, $Ptf1a^{+/Cre(ex1)}$ mice were crossed to $Rosa26R^{lacZ}$ (*R26R*) reporter mice (Soriano, 1999). In pancreata of newborn mice, Cre-induced recombination measured by X-gal staining occurred as expected from previous studies (Kawaguchi et al., 2002) (data not shown). To abrogate Notch receptor signaling, an approach generating either *Rbpj* or *Notch1/Notch2* double-knockout mice was chosen. For simplicity, $Ptf1a^{+/Cre(ex1)};Rbpj^{f/f}$ will be termed *RbpjKO* and $Ptf1a^{+/Cre(ex1)};Notch1^{f/f};Notch2^{f/f}$ will be termed *Notch1/2KO* mice; heterozygote littermates and littermates not expressing Cre recombinase will be termed $Rbpj^{+/-}$, $Notch1/2^{+/-}$ and *WT* mice, respectively.

To generate pancreas-specific, *Rbpj*-knockout mice, *loxP* sites were inserted flanking exons 6 and 7 of *Rbpj* in embryonic stem cells (ES) by homologous recombination (Fig. 1A). ES cell clones with a *floxed* (*f*) *Rbpj* locus were used to generate chimeric mice. The mutant mouse line ($Rbpj^{+/f}$) was established through germline transmission. Cre-recombinase-mediated deletion of exon 6 and 7 of *Rbpj* resulted in a mutant RBP-Jκ protein lacking a functional DNA-binding domain. By crossing $Rbpj^{f/f}$ mice with a Nestin-Cre deletor line, we were not able to obtain *Rbpj*-deficient newborns, and this provides strong evidence for a functionally null Rbpj transcript after Cre-induced recombination (data not shown). For pancreas-specific targeting, we next crossed $Rbpj^{f/f}$ mice with $Ptf1a^{+/Cre(ex1)}$ mice. $Ptf1a^{+/Cre(ex1)}$ mediated deletion of the *Rbpj* gene was verified by Southern blot analysis with DNA from different tissues of newborn $Ptf1a^{+/Cre(ex1)};Rbpj^{+/f}$ offspring (Fig. 1B). For conditional knockout of Notch1 and Notch2, previously described $Notch1^{f/f}$ and $Notch2^{f/f}$ mice were used (Radtke et al., 1999; Schouwey et al., 2006). As we did not find qualitative defects in pancreatic organogenesis, nor major abnormalities in the unstimulated adult pancreata of conditional *Notch1*, *Notch2* or combined *Notch1/Notch2* knockout mice over an observation period of 18 months (Siveke et al., 2008) (data not shown), combined *Notch1/2KO* were chosen for the analysis of pancreatic development. In *Notch1* and *Notch2* single receptor knockouts, as well as in double-knockout pancreata, Notch1 and Notch2 protein and transcripts were decreased to less than 10%, as analyzed by western blot and RT-PCR (data not shown). Both, *Rbpj* and *Notch1/Notch2* knockout lines were tested for the possibility of mosaic Cre-induced recombination using *Rosa26R* reporter mice as a surrogate for recombination-induced deletion of *Rbpj* or *Notch1/Notch2,* respectively. Using X-gal staining, we did not observe X-gal-negative exocrine cells in adult pancreata (Fig. 1G-I). Regarding recombination in the endocrine compartment, we found approximately 50% of endocrine cells to be X-gal positive, a recombination pattern that was very similar to that observed in $Ptf1a^{+/Cre(ex1)};Rosa26R^{lacZ}$ pancreata (Fig. 5M-U).

Although heterozygous $Rbpj^{+/-}$ and homozygous *Notch1KO*, *Notch2KO* and *Notch1/2KO* mice showed no gross abnormalities and developed normally, *RbpjKO* mice survived only until 4-5 days postpartum. Although moderate signs of growth retardation were observable at birth (Fig. 1C), the early death was caused by insufficient postnatal growth with impaired milk digestion. We were able to raise some *RbpjKO* mice to adulthood by feeding them with pancreatic enzyme-enriched animal food (data not shown). Examination of the *RbpjKO;R26R* mice at day 1 postpartum (dpp) revealed a small and severely altered pancreas (Fig. 1F,I). In the duodenal part of the mutant pancreas, weakly branched ducts were observable (Fig. 1F, arrowhead), whereas the splenic part of the pancreas showed no branching (Fig. 1F, arrows). Histological examination demonstrated a lack of acinar tissue with large duct-like structures being present in the splenic and duodenal portion of the pancreas (Fig. 1I, blue). Interestingly, *Notch1/2KO* mice did not reveal striking abnormalities in pancreatic tissue organization or cell lineage distribution, suggesting a non-essential role for Notch1 and Notch2 during pancreatic development. However, the mutant pancreas was noted to be slightly smaller than that of wild type when analyzed at 1 dpp (Fig. 1 E,H). To further clarify the role of ablated Notch signaling, early stages of pancreatogenesis were investigated.

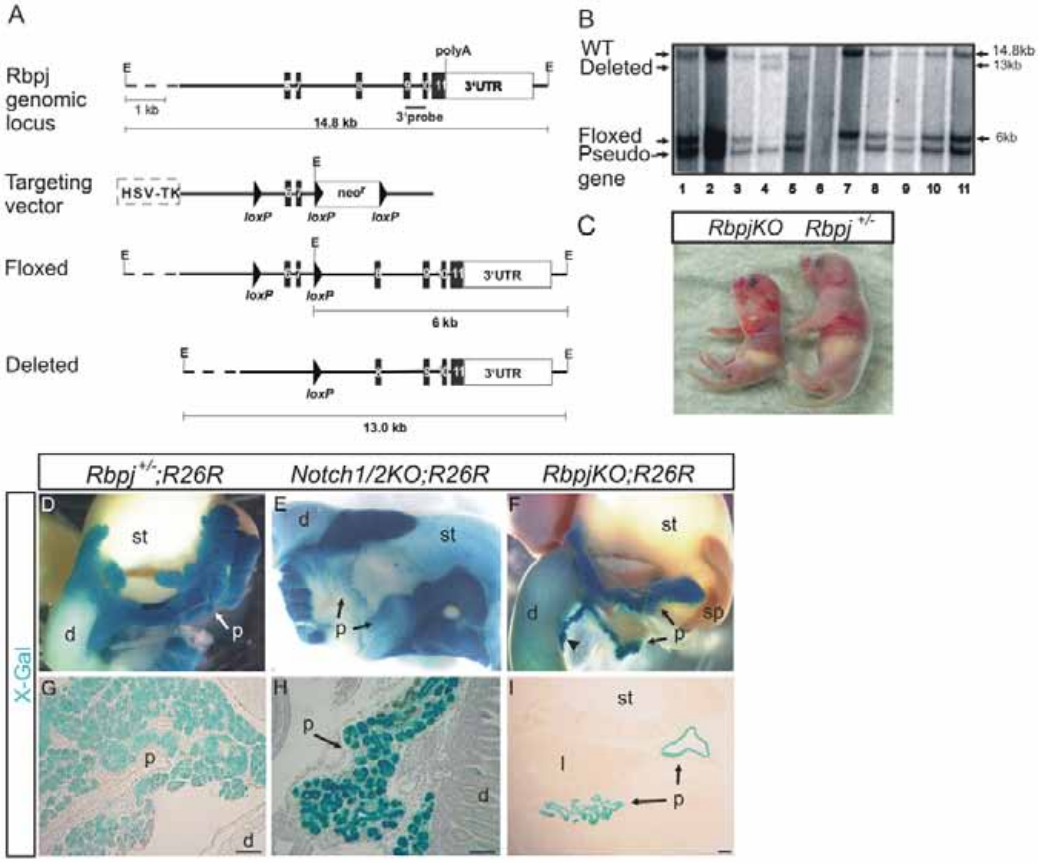

Fig. 1. Pancreas-specific *Rbpj* and *Notch1/2KO* mice. (**A**) Strategy for targeting the *Rbpj* locus to generate *Rbpj*$^{+/f}$ mice. The *loxP* sequences (arrowheads), exons (filled boxes), length of diagnostic restriction fragments and location of a 3′-probe (bar) used for Southern blotting are shown. *Eco*RI restriction enzyme sites (E) are indicated. (**B**) Southern blot analysis of Cre-mediated deletion in the following organs of an *Ptf1a*$^{+/Cre(ex1)}$;*Rbpj*$^{+/-}$ mouse: thymus (lane 1), spleen (2), liver (3), pancreas (4), kidney (5), head (6), lung (7), salivary gland (8), stomach (9), duodenum (10), and coecum (11). The positions and sizes of the fragments derived from the wild-type (WT), deleted, *floxed* and pseudogene alleles are indicated. (**C**) Newborn *RbpjKO* mice show increasing signs of growth retardation and die 4-5 days postpartum. (**D-I**) Macroscopic (D-F) and microscopic (G-I) X-gal staining analysis of intestinal tracts from newborn mice show X-gal^{+} pancreata (blue) from *RbpjKO;R26R*, *Notch1/2KO;R26R* and *Rbpj*$^{+/-}$;*R26R* pups. Arrowhead in F indicates weakly branched ducts in pancreatic rudiment. *neo*^{r}, neomycin-resistance gene; HSV-tk, herpes simplex virus thymidine kinase gene; d, duodenum; l, liver; p, pancreas; sp, spleen; st, stomach. Scale bar: 100 μm.

Early pancreatic development in *Rbpj*- and *Notch1/Notch2*-deficient pancreata

To analyze pancreatic development at defined stages of pancreatic organogenesis, we investigated pancreatic bud development at embryonic day 10 (E10) to E13.5 by immunohistochemistry and X-gal staining. The pancreatic buds of E13.5 *Rbpj*$^{+/-}$;*R26R* and *Notch1/2KO;R26R* embryos displayed the typical branching of the pancreatic epithelium. The *Notch1/2KO* buds appeared smaller and less branched than in control littermates (Fig. 2A,B,D). By contrast, *RbpjKO;R26R* embryos revealed a significantly reduced epithelial mass with weakly branched structures in both buds (Fig. 2C,D), suggesting that *Rbpj* is essential for the expansion of the pancreatic epithelium.

As *Hes1* is one of the target genes of *Rbpj*-dependent Notch signaling activation, we analyzed HES1 expression at E12.5. At this stage, HES1 protein was broadly detected within the nuclei of PDX1^{+} epithelial cells, as well as in PDX1^{-} mesenchymal elements (Fig. 2E). Compared with *Rbpj*$^{+/-}$;*R26R* littermate controls, *RbpjKO* and *Notch1/2KO* mice showed reduced, although not absent, HES1 expression in PDX1^{+} pancreatic cells, suggesting efficient ablation of Notch signaling (Fig. 2E-G). As the premature differentiation of pancreatic progenitor to endocrine cells has been suggested previously as a possible cause for the reduction of pancreatic epithelium in *Rbpj*-deficient buds (Fujikura et al., 2006), pancreatic sections at E11.5 were stained for X-gal and glucagon expression. In *Rbpj*$^{+/-}$;*R26R* embryos, glucagon-expressing cells formed small clusters peripheral to and dispersed within the dorsal bud (Fig. 2H, brown). Similar to *Rbpj*$^{+/-}$;*R26R* mice, *Notch1/2KO* mice showed no increased number of glucagon-positive cells (Fig. 2I, brown). By contrast, we observed an increased number of glucagon-positive cells in *RbpjKO;R26R* embryos at this time point, consistent with the premature differentiation of pancreatic progenitors to endocrine cells. These cells were found within and peripheral from the ventral and dorsal buds (Fig. 2J, brown).

As expression of the transcription factor neurogenin 3 (*Ngn3*) is a prerequisite for endocrine lineage development, E13.5 pancreata were analyzed for expression of NGN3. Consistent with previous results, we found decreased numbers of NGN3^{+} cells in *RbpjKO* mice at this stage (Fig. 2M,N), when compared with *Rbpj*$^{+/-}$;*R26R* embryos (Fig. 2K,N), suggesting an early commitment of these cells to endocrine cell lineages. We also found more insulin^{+} β cells per PDX1^{+} area in *RbpjKO* pancreata (Fig. 2Q,R). Regarding the differentiation of

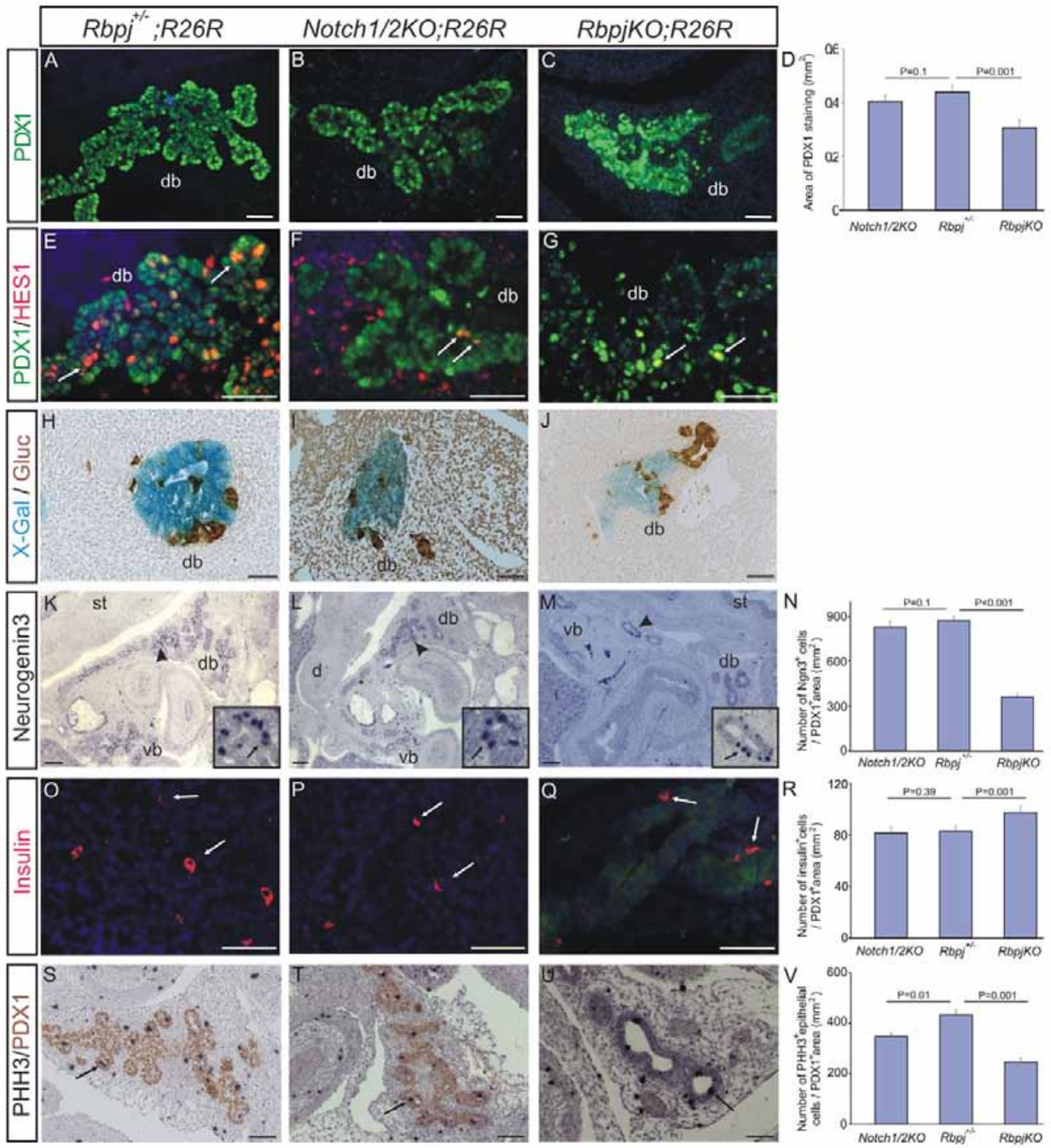

Fig. 2. Analysis of early pancreatic development in mutant embryos. (**A-C**) Pancreatic development of the respective mutant embryos at E13.5 as determined by PDX1 immunofluorescence (green). (**E-G**) Immunofluorescence for PDX1 (green) and HES1 (red) in pancreatic dorsal buds of mutant embryos at E12.5. (**H-J**) Double staining of pancreatic dorsal buds of mutant embryos for X-gal (blue) and glucagon (brown) at E11.5. (**K-M**) Nuclear expression of NGN3 in E13.5 mutant pancreata by immunohistochemistry. Arrowheads mark the areas in insets (enlarged 4×). Arrows in insets mark NGN3$^+$ cells (black). (**O-Q**) Insulin expression in mutant pancreata at E13.5 by immunofluorescence (red, arrows). (**S-U**) Double-immunostaining for phospho-histone H3 (PHH3, black, arrows) and PDX1 (brown) at E13.5. (**D**,**N**,**R**,**V**) Quantification of the number of NGN3$^+$, Insulin$^+$ and PHH3$^+$ cells, and size of area of PDX1$^+$ cells, in buds of E13.5 *Rbpj*$^{+/-}$*;R26R, Notch1/2KO;R26R* and *RbpjKO;R26R* embryos. Histograms show the mean size±s.d. for ventral and dorsal buds of three embryos each. Nuclei were counterstained with DAPI. Gluc, glucagon; vb, ventral bud; db, dorsal bud. Scale bar: 50 μm.

endocrine cells in *Notch1/Notch2*-deficient pancreata, no significant reduction of NGN3$^+$ cells (Fig. 2L,N) and no related β cell increase were notable at E13.5 (Fig. 2P,R). The reduced branching and epithelial mass in the *Notch1/2KO* and *RbpjKO* embryos was accompanied by a decrease in the number of proliferating cells in pancreatic epithelium, as detected by phospho-histone H3 (PHH3) and PDX1 double-immunostaining (Fig. 2S-U). While the relative number of the PHH3$^+$ cells to PDX1$^+$ cell area in *Notch1/2KO* buds was reduced by 25% in comparison with control mice (*Rbpj*$^{+/-}$*;R26R*; Fig. 2S,T,V), the relative number in *RbpjKO* buds was decreased to 40% (Fig. 2U,V).

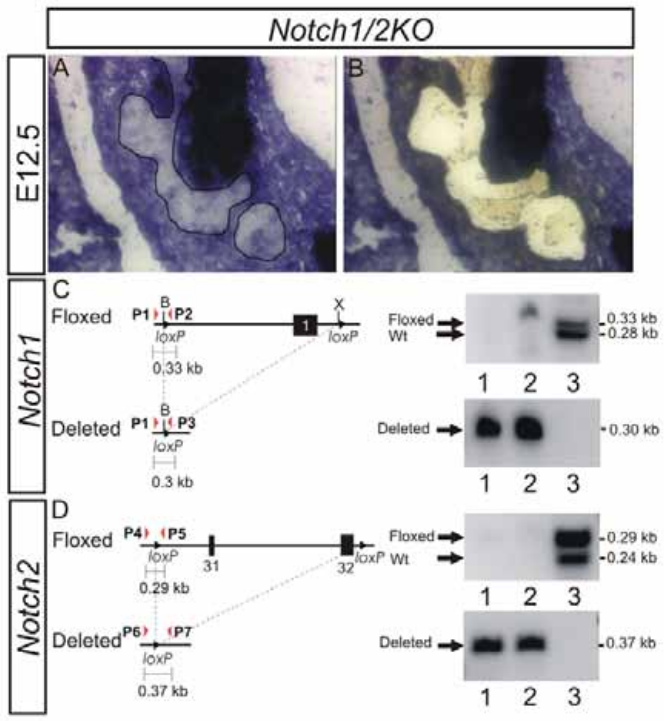

Fig. 3. Early Cre-induced recombination of *Notch1* and *Notch2* alleles in the pancreatic epithelium. (**A**,**B**) Detection of early α cells in the dorsal bud by immunostaining for glucagon at E12.5. (A) Microdissection of pancreatic epithelial cells. (B) Note that glucagon$^+$ cells (dark) are not dissected. (**C**,**D**) Schematic maps of the floxed *Notch1* (C) and *Notch2* (D) locus before and after Cre-induced recombination. The position and polarity of the primers used for amplification are represented by P1, P2 and P3 for *Notch1*, and P4, P5, P6 and P7 for *Notch2* (red arrowheads). DNA was isolated from pancreatic epithelial cells of two *Notch1/2KO* embryos (lane 1 and lane 2). As a control, DNA from heterozygous *Notch1/2*$^{+/f}$ mice was used (lane 3).

In contrast to the severe defects in pancreatic development observed in *RbpjKO* embryos, *Notch1/2KO* embryos showed only a marginal loss of the pancreatic mass, without defects in the development of the exocrine and endocrine compartments. One obvious explanation would be low expression, or inefficient recombination activity, of Cre recombinase during early pancreatic development, and, consequently, an inefficient inactivation of both *Notch1* and *Notch2* alleles. To determine the efficiency of Cre recombinase activity, we analyzed the recombination of the floxed *Notch1* and *Notch2* alleles by PCR analysis of microdissected epithelial cells of pancreatic buds from *Notch1/2KO* embryos at E12.5. The microdissection of early glucagon$^+$ cells not expressing *Ptf1a* was avoided by immunostaining the embryonic sections for glucagon. The epithelial cells from stained sections were isolated using a P.A.L.M. Microdissection system (Fig. 3A,B). The PCR was performed with DNA from two knockout embryos using specific primers for floxed and deleted *Notch1* and *Notch2* alleles, with DNA from heterozygous *Notch1/2*$^{f/+}$ embryos serving as a control for floxed and recombined alleles. For the detection of recombined DNA events, 4000 cells were used for each PCR reaction with a determined sensitivity to detect recombined alleles from DNA of about 200 cells. As shown in Fig. 3C,D, we could not detect any floxed *Notch1* and *Notch2* fragments in the DNA of double-knockout epithelial cells. Thus, *Notch1* and *Notch2* alleles were deleted in more than 95% of epithelial cells of *Notch1/2KO* pancreatic buds.

Appearance of acinar cells during late embryonic development in *Rbpj*-deficient pancreas

Exocrine cell differentiation in *Rbpj*$^{+/-}$ embryos was similar to that of *RbpjWT* and *Notch1/2WT* embryos, suggesting that heterozygosity for *Rbpj* and/or *Ptf1a* has no profound effect on exocrine lineage development. At E14.5, well-defined exocrine acini were observable in all of the littermate controls (Fig. 4A). However, in *RbpjKO* embryos neither amylase nor carboxypeptidase A expression was detectable at E14.5 (Fig. 4C, data not shown). In contrast to this, *Notch1/2KO* pancreata revealed amylase$^+$ cells, although the acinar compartment appeared smaller than in littermate controls (Fig. 4B). At E18.5, the exocrine pancreas showed no morphological differences in *Notch1/2KO*, when compared to control littermates (Fig. 4D,E). In *RbpjKO* at this stage, we surprisingly detected a few amylase$^+$ acini in the duodenal part and amylase$^+$ duct-like structures in the splenic portion of the rudimentary pancreas (Fig. 4F,J). These splenic amylase$^+$ duct-like structures contained amylase$^+$ cells (Fig. 4K, arrows), whereas most duodenal duct-like structures did not express amylase (Fig. 4L, arrow). In *RbpjKO* pups, the cells of both splenic and duodenal duct-like structures showed positive staining with CK19, a marker of differentiated ductal cells (Fig. 4I, black). These cells were also positive for X-gal staining, suggesting that all of them derived from *Rbpj*-deficient cells (Fig. 4I, arrows). In *Notch1/2KO* mice, ductal cells were CK19$^+$ and similar in appearance to in control littermates (Fig. 4G,H, arrows).

In *RbpjKO* mice at E18.5, co-immunostaining for PDX1 and amylase showed that the majority of amylase$^+$ cells were also PDX1$^+$, and were mitotically active, as determined by BrdU labeling (Fig. 4M,N). Because a functional PTF1 complex is required for the expression of acinar genes, such as amylase, we determined the expression of PTF1A in *RbpjKO* pancreata. Here, we detected PTF1A$^+$ cells surrounded by stromal cells outside the main duct and in the duodenal part of the rudimentary pancreas (Fig. 4O, arrows). To determine whether the *Rbpj* gene was actually deleted in amylase-expressing cells in the mutant pancreas, pancreatic sections from *RbpjKO* newborns were co-stained for X-gal and amylase, demonstrating the Cre-induced recombination of amylase$^+$ cells (Fig. 4P). In addition, PCR analysis of DNA isolated from amylase$^+$ cells by microdissection confirmed that the *Rbpj* gene was deleted in acinar cells from *RbpjKO* newborns (Fig. 4Q).

Endocrine cell development in *Rbpj*- and *Notch1*/*Notch2*-deficient pancreas

Most mature endocrine cells appeared after E14 in both *Notch1/2KO* and *RbpjKO* embryos, similar to in littermate controls. At E18.5, we could detect all endocrine cell lines, glucagon-producing α cells, insulin-containing β cells, somatostatin$^+$ δ cells, and pancreatic polypeptide$^+$ (PP) cells in both *Notch1/2KO* and *Rbpj*$^{+/-}$ embryos. In *RbpjKO* mice, these cells were detectable in the rudimentary pancreas within the tubular duct wall and in the protruding formations of the pancreatic tubule (Fig. 5A-L).

At E18.5, most endocrine cells of the *Rbpj*$^{+/-}$ control embryos aggregated with α cells starting to organize around core structures of β cells (Fig. 5P, arrowhead). Similar to control embryos, endocrine cells in both *Notch1/2KO* and *RbpjKO* embryos also started to aggregate; however, the number of formed islets was

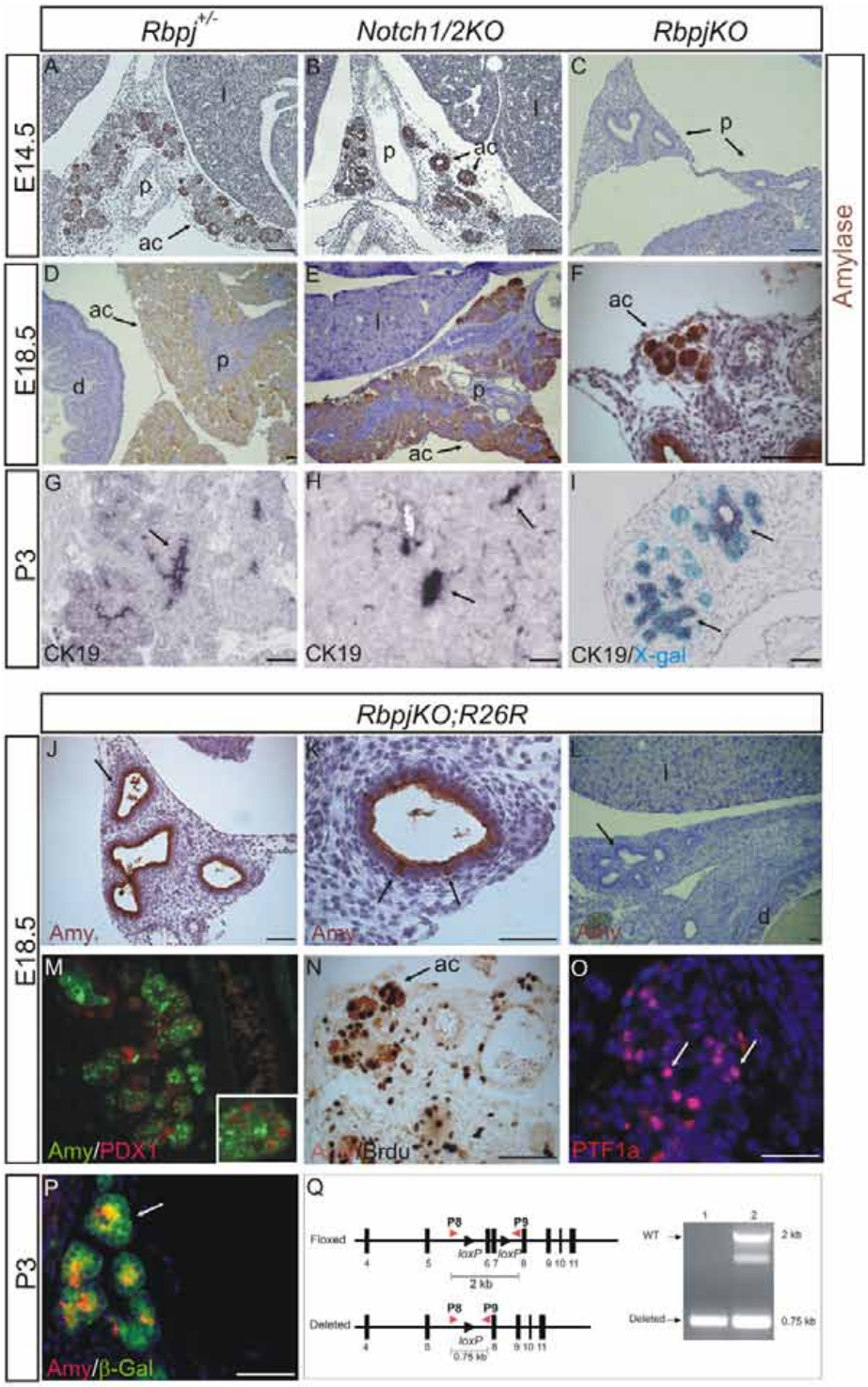

Fig. 4. Appearance of acinar cells in late stage of embryonic development of *RbpjKO* embryos. (**A-F**) Analysis of amylase expression at E14.5 (A-C) and E18.5 (D-F) in mutant pancreata. (**G-I**) Immunostaining of mutant pancreata with an antibody against the ductal marker CK19 (black, arrows) at day 3 postpartum (P3). (I) CK19 and X-gal (blue) co-staining of *RbpjKO* pancreas at P3. (**J-L**) Amylase staining (brown) of duct-like structures of *RbpjKO* pancreas at E18.5. In contrast to ventral bud (L), the most of dorsal duct-like structures are positive for amylase (J,K). (**M-O**) Amylase^{+} cells (green) from *RbpjKO* embryos express PDX1 (M, red) and PTF1A (O, red), detected by immunofluorescence, and are proliferating as determined by cytoplasmic amylase (brown) and nuclear BrdU (black) staining (N, arrow). Inset in M represents a 2.6× enlargement. (**P**) Double-immunofluorescence staining of acini from *RbpjKO;R26R* mice for amylase and β-galactosidase at P3. (**Q**) PCR analysis of DNA from microdissected acinar cells of *RbpjKO* (lane 1) and *Rbpj*$^{+/-}$ (lane 2) pancreata. Schematic maps of the *floxed Rbpj* locus before and after Cre recombination are shown. The position and polarity of the primers used for amplification are represented by P8 and P9 (red arrowheads). Nuclei were counterstained with DAPI. Amy, amylase; ac, acinar; m, mesentery. Scale bars: 50 μm (100 μm in D,E).

less than in control embryos (Fig. 5V). Regarding the morphological appearance of the formed islets, the endocrine epithelium in *Notch1/2KO* embryos, and more prominently in *RbpjKO* embryos, had a disturbed appearance. In most of the endocrine cell formations, α cells were not organized around β cells, and the morphology of these islet-like structures appeared to be long rather than circular like in the control mice (Fig. 5P,Q,R). In adult pancreata of *Notch1/2KO* mice, however, the islets appeared normal and were indistinguishable from wild-type controls (data not shown).

Because *Ptf1a*$^{+/Cre(ex1)}$*;R26R* mice show mosaic Cre-induced recombination in the endocrine compartment (data not shown), we sought to analyze whether this mosaicism was also present in the different knockout lines. Co-staining of islets from *Rbpj*$^{+/-}$*;R26R*, *Notch1/2KO;R26R* and *RbpjKO;R26R* mice with X-gal and the endocrine cell markers glucagon and insulin revealed that, in all three genetic backgrounds, some endocrine cells were not stained with X-gal, suggesting that these cells derived from epithelial cells that did not express, or only for a short time expressed, PTF1A (Fig. 5M-U, arrows). Conversely, we also found X-gal^{+} islets in all lines,

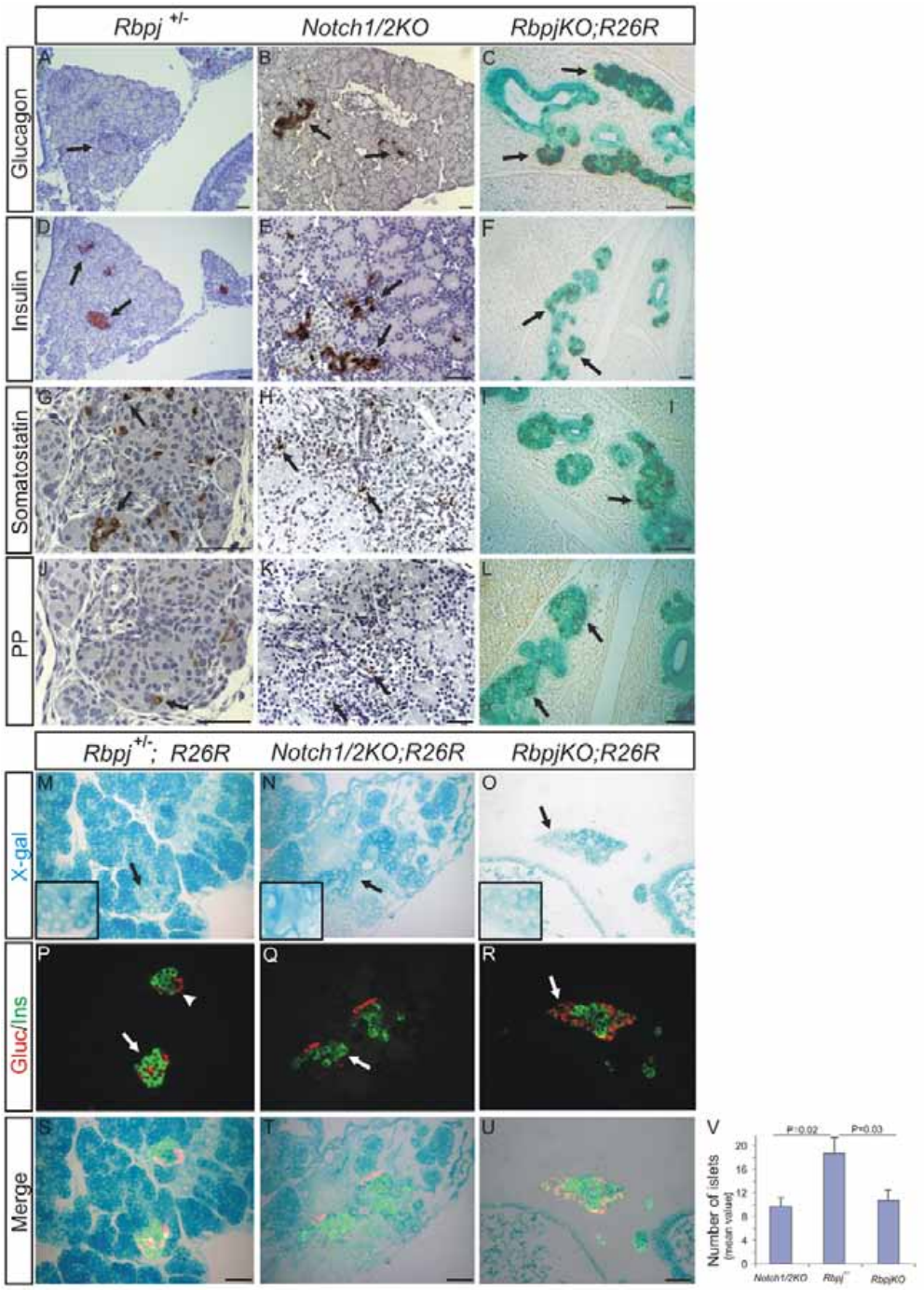

Fig. 5. Endocrine development in *RbpjKO*, *Notch1/2KO* and *Rbpj*$^{+/-}$ pancreata. (**A-L**) Transverse sections from E18.5 *Rbpj*$^{+/-}$, *Notch1/2KO* and *RbpjKO;R26R* embryos were analyzed for the expression of endocrine markers by immunohistochemistry. *RbpjKO* pancreas was stained by X-Gal (blue) in addition to the respective endocrine genes. l, liver. (**M-O**) X-gal staining of sections from *Rbpj*$^{+/-}$*;R26R*, *Notch1/2KO;R26R* and *RbpjKO;R26R* embryos at E18.5. Arrows mark the areas in insets (enlarged 2×). (**P-R**) Double-immunofluorescence staining of islets with anti-glucagon (red) and anti-insulin antibodies (green). (**S-U**) The merged images show co-expression of glucagon and insulin with β-galactosidase in islets of knockouts and control pancreata. (**V**) Histogram representing the number of islets±s.d. in pancreata of three embryos for the indicated genotype. Ins, insulin; Gluc, glucagon; PP, pancreatic polypeptide. Scale bar: 50 μm.

suggesting that incomplete deletion is not selected for in any genetic background (data not shown). Importantly, we found no difference in morphology or cellular composition between X-gal-negative and X-gal-positive islets in the different genetic backgrounds.

DISCUSSION

The regulation of organogenesis and proper cell fate determination in the pancreas has been found to involve the activation of Notch signaling. To elucidate the role of epithelially expressed Notch receptors and the specific role of the transcription factor *Rbpj* as a transducer of Notch signaling, we used a conditional gene-targeting approach to genetically inactivate either *Notch1* and *Notch2* or *Rbpj* in the pancreas.

Recently, two different mouse models for conditional genetic inactivation of *Rbpj* were described, using either transgenic *Pdx1-Cre* or *Ptf1a-Cre* knockin mice for the targeting of pancreatic progenitor cells (Fujikura et al., 2006; Fujikura et al., 2007). During early pancreatic development, both models, and our *RbpjKO* mice, revealed an essential role for *Rbpj* with premature glucagon^{+} cell development, a severe decrease in acinar cell differentiation and disturbed ductal branching in mutant mice. Differences in the phenotypical severity between these models during the early stages of organogenesis are possibly due to differences in the onset, timing and rate of Cre-induced genetic inactivation. In our *Ptf1a*$^{+/Cre(ex1)}$ mice, X-gal staining in the buds was observable at E10.5 in all pancreatic epithelial cells, similar

to that previously reported (Fujikura et al., 2007; Kawaguchi et al., 2002). However, even slight differences in targeting efficiency during early pancreatic organogenesis in transgenic *Pdx1-Cre* mice, and between different *Ptf1a*-knockin Cre lines, may have a large impact on the development of the respective cell compartments.

Of interest is the appearance of late exocrine cells in all models; however, phenotypical effects are notable. In our model, *RbpjKO* mice do not survive more than 4-5 days after birth, most probably as a result of the clinically apparent pancreatic insufficiency with impaired weight gain, a high content of milk in the stomach of animals and no apparent neurological phenotype. We favor this explanation over, for example, extra-pancreatic causes, as we could not detect any defects in other PTF1A-expressing organs, such as the retina or the CNS (data not shown). The reason why our *RbpjKO* mice are not able to show the same ability to develop an apparently normal adult exocrine compartment is not clear, but may possibly be explained by a more rigorous deletion of early progenitors in our mice. Nevertheless, the late appearance of acinar cells during organogenesis in our and other *Rbpj*-deficient pancreata (Fujikura et al., 2006; Fujikura et al., 2007) is surprising, and may occur through *Rbpj*-independent mechanisms involving a recently identified regulator of acinar cell development, the *Rbpj* homolog *Rbpjl* (Beres et al., 2006). These authors showed that the initiation of the acinar differentiation program by the PTF1 complex involves RBPJκ binding to PTF1A to form the PTF1-J complex. This complex then activates RBPJL, which itself binds to PTF1A to form the PTF1-L complex. PTF1-L has been shown to be the more active complex, activating acinar genes such as amylase and elastase (Beres et al., 2006). The finding of delayed expression of acinar genes such as amylase at E18.5 in *RbpjKO* mice may be explained by two mechanisms. First, Cre activation may not be complete in a few proacinar cells, which will eventually form the exocrine pancreas. However, our results showing Cre-induced recombination of both *Rbpj* alleles in microdissected acini and in adult pancreatic tissue (Fujikura et al., 2007) do not support this hypothesis. Secondly, spontaneous activation of *Rbpjl* in precursor cells expressing PTF1A may lead to the formation of PTF1-L and, thus, to a positive-feedback loop activating the *Rbpjl* promoter. The delayed appearance and the small initial population of acinar cells would be consistent with a stochastic activation of *Rbpjl*, a hypothesis as yet unproven however.

The defective ductal branching observed in our, as well as in other, models of Notch signaling ablation may be due to early reduction of the epithelial progenitor pool, as has been suggested previously (Fujikura et al., 2006; Fujikura et al., 2007). Interestingly, the ductal cells in *RbpjKO* and *Notch1/2KO* mice expressed CK19, suggesting that the differentiation of progenitor cells into ductal cells is not inhibited by inactivated *Rbpj*-dependent Notch signaling. Future studies may help to determine the factors regulating ductal differentiation in the pancreas.

Of unclear significance is our finding of amylase positivity in dorsal duct structures of *RbpjKO* pancreata. Although we detected amylase$^+$ cells within the ducts, we did not detect expression of PTF1A in these cells (data not shown); however, expression of these acinar transcription factors may be below detection limits. Other explanations include artificial staining of amylase produced by extraductal acinar cells; however, we did not observe acini in the dorsal part of the organ. Whether or not inactivated Notch signaling contributes to acinar cell fate determination from ductal cells or within ductal structures needs to be determined.

Interestingly, we found differences between *Notch1/Notch2* and *Rbpj* ablated mice regarding the severity of impaired pancreatic development. Whereas the buds of *Notch1/2KO* mice appeared smaller than those of wild-type littermates, this reduction did not reach the extent of that seen in *RbpjKO* mice. The reason for the reduced proliferation of pancreatic progenitors may be due to the requirement of Notch signals for the maintenance of actively proliferating pancreatic progenitor cells, as has recently been shown for the transcription factor *Sox9* (Seymour et al., 2007). In this regard, we also found reduced, but not completely abolished, expression of HES1 in *Notch1/2KO* and *RbpjKO* mice, as has been noted by others (Fujikura et al., 2006; Fujikura et al., 2007), possibly as a result of the expression of factors such as *Sox9*, which is necessary for the maintenance of HES1 expression. Studies with ectopic overexpression of Notch1 showed the prevention of exocrine and endocrine differentiation of pancreatic progenitor cells, leaving them in an undifferentiated state (Esni et al., 2004; Hald et al., 2003; Murtaugh et al., 2003). Despite technical issues, such as the transgenic expression and potentially non-physiological Notch1 levels, these results, as well as the aforementioned studies, point to a role for Notch in the regulation of pancreatic progenitor cells, with one of the main conclusions being a premature endocrine switch caused by insufficient Notch signaling. Interestingly however, we found such a switch in *RbpjKO* but not *Notch1/2KO* mice, possibly indicating the requirement of *Rbpj* but not *Notch1* or *Notch2* for the regulation of premature endocrine differentiation. However, we cannot rule out inefficient early Cre-induced inactivation of *Notch1* and *Notch2*. While we could determine successful recombination of both *Notch1* and *Notch2* alleles at E12.5 by PCR of microdissected epithelial cell, incomplete earlier inactivation of both Notch genes might indeed be responsible for the lack of effect in *Notch1/2KO* mice. The modest phenotype of *Notch1/2KO* mice was unexpected and is in contrast to the skin, where genetic inactivation of *Rbpj* and *Notch1*/*Notch2* leads to similar phenotypes (Schouwey et al., 2006). While early reports using mice null for Notch signaling family members, such as *Rbpj*, *Dll1* or *Hes1*, showed impaired growth and branching defects (Apelqvist et al., 1999; Jensen et al., 2000), differences between null mice and conditional genetic targeting approaches, such as the inactivation of targeted genes before pancreatic development is started and the additional targeting of extra-pancreatic cells in null mice, has a strong impact on the observable phenotype.

The different impact of pancreatic *Notch1/Notch2* and *Rbpj* inactivation in our study strongly suggests a Notch-independent role of *Rbpj* in pancreatic organogenesis. The near complete absence of acinar cells until late gestation suggests that RBPJκ is required for the formation of the acinar lineage. Recent studies have shown that RBPJκ is the binding partner of PTF1A for formation of the early PTF1-J complex (Beres et al., 2006; Masui et al., 2007; Obata et al., 2001). Our results are in line with a Notch-independent role of RBPJκ as an obligate partner of PTF1A to form a functional PTF1 complex, a pivotal event during early pancreatic development. Thus, RBPJκ in *Notch1/2KO* mice might still function as PTF1A-binding partner independently of its transducer role in the Notch signaling pathway.

As expected from previous reports (Apelqvist et al., 1999; Jensen et al., 2000), *RbpjKO* mice had earlier α cells underscoring the relevance of Notch signaling for the inhibition of premature differentiation of progenitor cells into early α cells. Our finding of less NGN3$^+$ cells in *RbpjKO* mice is similar to the results by Fujikura and colleagues (Fujikura et al., 2006; Fujikura et al., 2007), and suggests that these endocrine progenitor cells are also

compromised and forced into premature differentiation by *Rbpj* deficiency. Notably, *Notch1/2KO* mice revealed no significant decrease in NGN3$^+$ cells and several mechanisms may account for this finding. First, RBPJκ might be activated independently and might lead to the activation of target genes; second, the four *Notch1* and *Notch2* alleles might not be inactivated in a timely manner to preserve the progenitor pool; or third, the transition of the repressor into an activator state of RBPJκ may be, at least partially, Notch independent. Despite the premature differentiation of pancreatic progenitors in *Rbpj*-deficient mice, we found that all endocrine lineages develop in *RbpjKO* and *Notch1/2KO* mice, consistent with the hypothesis of a dispensable role of Notch signaling in late pancreatic development. However, we found fewer islets in both knockout lines, which, more prominently in *RbpjKO* mice, had a partially disturbed composition. One explanation for the development of endocrine cells despite the genetic inactivation of Notch signaling is the later expression of Cre recombinase in *Ptf1a*$^{+/Cre(ex1)}$ compared with in *Pdx1-Cre* mice at E10.5. However, development of the endocrine compartment and islet formation does not occur before E13.5, a time point at which *Rbpj* and both Notch genes are inactivated. Our finding of X-gal$^+$ islets composed of all endocrine lineages at E18.5 in both knockout lines is evidence for a non-essential role of Notch signaling in promoting endocrine cell fate determination and differentiation, whereas the lower amount of islets and the somewhat disturbed islet morphology, especially in *RbpjKO* mice, may be an at least partial result of the severe branching defect in these mice.

In conclusion, we demonstrate an essential role of *Rbpj*, but not of *Notch1* and *Notch2*, in pancreatic organogenesis. Using a concomitant approach of Notch signaling inactivation, we show that the epithelially expressed Notch receptors 1 and 2 are not essential for pancreatic development, whereas lack of *Rbpj* leads to premature differentiation of pancreatic progenitors and a decrease in endocrine progenitor cells. During late pancreatic development, however, differentiated exocrine and endocrine lineages mature in both knockout lines. Although *Rbpj* seems to be an important regulator of the early pancreatic progenitor pool, our findings strengthen the hypothesis of as yet unknown and potentially *Rbpj*-independent mechanisms regulating the cell fate of adult pancreatic cell lineages. As we can show successful inactivation of *Notch1* and *Notch2* alleles at E12.5, this finding strongly suggests that these receptors, but not *Rbpj*, are dispensable for exocrine and endocrine development. Thus, at least in the pancreas, a Notch-independent role of *Rbpj* during development seems to be a likely mechanism.

We are grateful to Jack Favor, Axel Walch and Andreas Voss for help with laser capture microscopy. We also thank Raymond J. MacDonald and Saadettin Sel for helpful discussions, and Christopher V. Wright and Tetsuo Sudo for their generous gift of PDX1 and HES1 antibodies, respectively. The CK19 antibody developed by Rolf Kemler and the Neurogenin antibody developed by O. D. Madsen were obtained from the Developmental Studies Hybridoma Bank, maintained by the University of Iowa. This work was supported in part by grants from the Deutsche Forschungsgemeinschaft to R.M.S. (SFB 4456 and SFB576), U.Z.-S. and L.S. (STR-461/3-2).

References

Apelqvist, A., Li, H., Sommer, L., Beatus, P., Anderson, D. J., Honjo, T., Hrabe de Angelis, M., Lendahl, U. and Edlund, H. (1999). Notch signalling controls pancreatic cell differentiation. *Nature* **400**, 877-881.

Beres, T. M., Masui, T., Swift, G. H., Shi, L., Henke, R. M. and Macdonald, R. J. (2006). PTF1 is an organ-specific and Notch-independent basic helix-loop-helix complex containing the mammalian Suppressor of Hairless (RBP-J) or its paralogue, RBP-L. *Mol. Cell. Biol.* **26**, 117-130.

Esni, F., Ghosh, B., Biankin, A. V., Lin, J. W., Albert, M. A., Yu, X., MacDonald, R. J., Civin, C. I., Real, F. X., Pack, M. A. et al. (2004). Notch inhibits Ptf1 function and acinar cell differentiation in developing mouse and zebrafish pancreas. *Development* **131**, 4213-4224.

Fujikura, J., Hosoda, K., Iwakura, H., Tomita, T., Noguchi, M., Masuzaki, H., Tanigaki, K., Yabe, D., Honjo, T. and Nakao, K. (2006). Notch/Rbp-j signaling prevents premature endocrine and ductal cell differentiation in the pancreas. *Cell Metab.* **3**, 59-65.

Fujikura, J., Hosoda, K., Kawaguchi, Y., Noguchi, M., Iwakura, H., Odori, S., Mori, E., Tomita, T., Hirata, M., Ebihara, K. et al. (2007). Rbp-j regulates expansion of pancreatic epithelial cells and their differentiation into exocrine cells during mouse development. *Dev. Dyn.* **236**, 2779-2791.

Hald, J., Hjorth, J. P., German, M. S., Madsen, O. D., Serup, P. and Jensen, J. (2003). Activated Notch1 prevents differentiation of pancreatic acinar cells and attenuate endocrine development. *Dev. Biol.* **260**, 426-437.

Jensen, J., Pedersen, E. E., Galante, P., Hald, J., Heller, R. S., Ishibashi, M., Kageyama, R., Guillemot, F., Serup, P. and Madsen, O. D. (2000). Control of endodermal endocrine development by Hes-1. *Nat. Genet.* **24**, 36-44.

Kawaguchi, Y., Cooper, B., Gannon, M., Ray, M., MacDonald, R. J. and Wright, C. V. (2002). The role of the transcriptional regulator Ptf1a in converting intestinal to pancreatic progenitors. *Nat. Genet.* **32**, 128-134.

Lammert, E., Brown, J. and Melton, D. A. (2000). Notch gene expression during pancreatic organogenesis. *Mech. Dev.* **94**, 199-203.

Masui, T., Long, Q., Beres, T. M., Magnuson, M. A. and MacDonald, R. J. (2007). Early pancreatic development requires the vertebrate Suppressor of Hairless (RBPJ) in the PTF1 bHLH complex. *Genes Dev.* **21**, 2629-2643.

Murtaugh, L. C., Stanger, B. Z., Kwan, K. M. and Melton, D. A. (2003). Notch signaling controls multiple steps of pancreatic differentiation. *Proc. Natl. Acad. Sci. USA* **100**, 14920-14925.

Nakhai, H., Sel, S., Favor, J., Mendoza-Torres, L., Paulsen, F., Duncker, G. I. and Schmid, R. M. (2007). Ptf1a is essential for the differentiation of GABAergic and glycinergic amacrine cells and horizontal cells in the mouse retina. *Development* **134**, 1151-1160.

Obata, J., Yano, M., Mimura, H., Goto, T., Nakayama, R., Mibu, Y., Oka, C. and Kawaichi, M. (2001). p48 subunit of mouse PTF1 binds to RBP-Jkappa/CBF-1, the intracellular mediator of Notch signalling, and is expressed in the neural tube of early stage embryos. *Genes Cells* **6**, 345-360.

Radtke, F., Wilson, A., Stark, G., Bauer, M., van Meerwijk, J., MacDonald, H. R. and Aguet, M. (1999). Deficient T cell fate specification in mice with an induced inactivation of Notch1. *Immunity* **10**, 547-558.

Schouwey, K., Delmas, V., Larue, L., Zimber-Strobl, U., Strobl, L. J., Radtke, F. and Beermann, F. (2006). Notch1 and Notch2 receptors influence progressive hair graying in a dose-dependent manner. *Dev. Dyn.* **236**, 282-289.

Seymour, P. A., Freude, K. K., Tran, M. N., Mayes, E. E., Jensen, J., Kist, R., Scherer, G. and Sander, M. (2007). SOX9 is required for maintenance of the pancreatic progenitor cell pool. *Proc. Natl. Acad. Sci. USA* **104**, 1865-1870.

Siveke, J. T., Einwachter, H., Sipos, B., Lubeseder-Martellato, C., Kloppel, G. and Schmid, R. M. (2007). Concomitant pancreatic activation of Kras(G12D) and Tgfa results in cystic papillary neoplasms reminiscent of human IPMN. *Cancer Cell* **12**, 266-279.

Siveke, J. T., Lubeseder-Martellato, C., Lee, M., Mazur, P. K., Nakhai, H., Radtke, F. and Schmid, R. M. (2008). Notch signaling is required for exocrine regeneration after acute pancreatitis. *Gastroenterology* **134**, 544-555.

Soriano, P. (1999). Generalized lacZ expression with the ROSA26 Cre reporter strain. *Nat. Genet.* **21**, 70-71.

Tanigaki, K., Han, H., Yamamoto, N., Tashiro, K., Ikegawa, M., Kuroda, K., Suzuki, A., Nakano, T. and Honjo, T. (2002). Notch-RBP-J signaling is involved in cell fate determination of marginal zone B cells. *Nat. Immunol.* **3**, 443-450.

Appendix 5

Fabian Geisler, Florian Nagl, **Pawel K. Mazur**, Marcel Lee, Ursula Zimber-Strobl, Lothar J. Strobl, Freddy Radtke, Roland M. Schmid, Jens T. Siveke.

Liver-specific inactivation of Notch2, but not Notch1, compromises intrahepatic bile duct development in mice.

Hepatology. 2008 Aug;48(2):607-16.

Liver-Specific Inactivation of *Notch2*, but not *Notch1*, Compromises Intrahepatic Bile Duct Development in Mice

Fabian Geisler,[1] Florian Nagl,[1] Pawel K. Mazur,[1] Marcel Lee,[1] Ursula Zimber-Strobl,[2] Lothar J. Strobl,[2] Freddy Radtke,[3] Roland M. Schmid,[1] and Jens T. Siveke[1]

The Notch pathway is an evolutionary conserved, intercellular signaling pathway that plays an important role in cell fate specification and the embryonic development of many organs, including the liver. In humans, mutations in the Notch receptor ligand *Jagged1* gene result in defective intrahepatic bile duct (IHBD) development in Alagille syndrome. Developmental abnormalities of IHBD in mice doubly heterozygous for *Jagged1* and *Notch2* mutations propose that interactions of Jagged1 and its receptor Notch2 are crucial for normal IHBD development. Because different cell types in the liver are involved in IHBD development and morphogenesis, the cell-specific role of Notch signaling is not entirely understood. We investigated the effect of combined or single targeted disruption of *Notch1* and *Notch2* specifically in hepatoblasts and hepatoblast-derived lineage cells on liver development using *AlbCre* transgenic mice. Hepatocyte differentiation and homeostasis were not impaired in mice after combined deletion of *Notch1* and *Notch2* (*N1N2*$^{F/F}$*AlbCre*). However, we detected irregular ductal plate structures in *N1N2*$^{F/F}$*AlbCre* newborns, and further postnatal development of IHBD was severely impaired characterized by disorganized ductular structures accompanied by portal inflammation, portal fibrosis, and foci of hepatocyte feathery degeneration in adulthood. Further characterization of mutant mice with single deletion of *Notch1* (*N1*$^{F/F}$*AlbCre*) or *Notch2* (*N2*$^{F/F}$*AlbCre*) showed that *Notch2* but not *Notch1* is indispensable for normal perinatal and postnatal IHBD development. Further reduction of *Notch2* gene dosage in *Notch2* conditional/mutant (*N2*$^{F/LacZ}$*AlbCre*) animals further enhanced IHBD abnormalities and concomitant liver pathology. *Conclusion:* Notch2 is required for proper IHBD development and morphogenesis. (HEPATOLOGY **2008;48:607-616.**)

See Editorial on Page 358

In humans and rodents, intrahepatic bile duct (IHBD) development begins with the condensation of hepatoblasts forming a single continuous cell layer around the larger portal veins called the ductal plate. Later, parts of the ductal plate reduplicate and dilate to form tubular structures that are subsequently incorporated in the portal mesenchyme. The remaining nontubular single-layered cells of the ductal plate are eliminated via apoptosis while the tubular structures further undergo a branching process to form the biliary tree. This process of ductal plate remodeling starts at the portal vein at ap-

Abbreviations: AGS, Alagille syndrome; IFN-α, interferon-α; IHBD, intrahepatic bile duct; P, postnatal day; WT, wild-type; X-gal, X-galactosidase.

From the [1]Second Department of Internal Medicine, Klinikum Rechts der Isar, Technical University of Munich, Munich, Germany; [2]Institute of Clinical Molecular Biology and Tumor Genetics, Hemholtz Zentrum Munich, German Research Center for Environment and Health (GmbH), Munich, Germany; and [3]Ludwig Institute for Cancer Research, Lausanne Branch, University of Lausanne, Epalinges, Switzerland.

Received January 4, 2008; accepted April 13, 2008.

Supported in part by grants from the Kommission für Klinische Forschung of the Technical University of Munich (KKF 33-04, to F. G.) and from the Deutsche Forschungsgemeinschaft (STR-461/3-2, to U. S. and L. J. S.).

Address reprint requests to: Fabian Geisler, Second Department of Internal Medicine, Klinikum Rechts der Isar, Technical University of Munich, Ismaninger Straße 22, 81675 Munich, Germany. E-mail: fabian.geisler@lrz.tum.de.

Published online in Wiley InterScience (www.interscience.wiley.com).

DOI 10.1002/hep.22381

Potential conflict of interest: Nothing to report.

Additional Supporting Information may be found in the online version of this article.

proximately embryonic week 8 and embryonic day 16.5 in humans and mice, respectively, progresses toward the periphery of the liver, and continues for the first weeks after birth.[1-3] In humans, abnormalities in physiological ductal plate remodeling can lead to a variety of diseases called ductal plate malformation, such as congenital hepatic fibrosis or Caroli's syndrome. Other congenital disorders of IHBD include Alagille syndrome (AGS), which is caused by mutations in the *Jagged1* gene encoding the Notch ligand Jagged1.[4,5] AGS is a multisystem disorder characterized by developmental abnormalities of the heart, eye, skeleton, and liver. Though progressive loss of interlobular bile ducts is the typical finding in liver biopsies,[6,7] bile duct proliferation may also be observed early in the course of AGS.[8,9]

The Notch signaling pathway plays an important role in cell fate specification and the embryonic development of many organs, including the hepatobiliary system. In mammals, four transmembrane Notch receptors (Notch1-4) and five ligands, including Dll1, Dll3, Dll4, Jagged1, and Jagged2, have been described.[10] Notch signaling activation is initiated by γ-secretase–dependent cleavage and release of cytoplasmic Notch-IC after ligand-receptor binding on neighboring cells. After translocation to the nucleus, Notch-IC binds and converts RBP-Jκ from a transcriptional repressor into an activator leading to transcription of Notch target genes such as *Hes* and *Hey* family genes. Expression analyses in human and mouse liver tissues have found Notch receptors and ligands to be expressed in embryonic and adult livers.[11-14] Whereas mice homozygous for null mutations in Notch pathway genes such as *Notch1*, *Notch2*, *Jagged1*, *Dll1*, or *Rbpj* could not be studied for proper organ development and homeostasis due to early embryonic lethal phenotypes,[10] recent studies using conditional inducible and developmental mouse models have shed light on the role of single Notch receptors and ligands in the hepatobiliary system. Postnatal inducible inactivation of *Notch1* using *MxCre* mice caused nodular regenerative hyperplasia by regulating hepatic proliferation but no biliary abnormalities.[12] In another study, mice heterozygous for a *Jagged1* null mutation and a hypomorphic *Notch2* allele showed features of human AGS, including bile duct paucity.[14] However, conditional hepatoblast-specific inactivation of *Jagged1* using *AlfpCre* mice had a normal bile duct development, as did the additional implementation of one hypomorphic *Notch2* allele.[15] Bile duct abnormalities were observed in 50% of mice only when a *Jagged1* null allele was introduced in combination with a conditional *Jagged1* allele.[15] An intricate network of different cell types including hepatoblasts, vascular epithelial cells, portal mesenchymal cells, and periportal connective tissue drives IHBD development and morphogenesis.[2,16] Thus, although Jagged1 has an important function during bile duct development, it may not act cell-autonomously in hepatoblasts but in adjacent cells to activate Notch signaling in hepatic progenitor cells and/or other cell compartments that are crucial for proper IHBD development. However, the cell-specific site of action of Notch2 has remained unclear and a possible contribution of other Notch receptors in tissue-specific knockout models has not been investigated. We investigated the effect of combined or single conditional ablation of *Notch1* and *Notch2* in hepatobiliary development and homeostasis using *AlbCre* mice and demonstrate that *Notch2* but not *Notch1* in hepatoblasts and hepatoblast-derived lineage cells is essential for normal IHBD development and morphogenesis in mice.

Materials and Methods

Mice. Mice carrying conditional knockout alleles for *Notch1* (*floxed Notch1, N1*$^{F/F}$ mice)[17] and *Notch2* (*floxed Notch2, N2*$^{F/F}$ mice)[18] were crossed with transgenic mice carrying a *Cre* gene under control of the albumin enhancer promoter (*AlbCre* mice).[19] After multiple rounds of crossing, we obtained the following genotypes that were used in this study: *N1N2*$^{F/F}$*AlbCre, N1*$^{F/F}$*N2*$^{F/+}$*AlbCre, N1*$^{F/+}$*N2*$^{F/F}$*AlbCre, N1*$^{F/F}$*AlbCre*, and *N2*$^{F/F}$*AlbCre*. For breeding of conditional *Notch1/Notch2* double-knockout animals, male *N1N2*$^{F/F}$*AlbCre* mice were mated with female *N1N2*$^{F/F}$ mice. All strains were maintained on a C57Bl6/Sv129 background. In all experiments *AlbCre*-negative littermates served as a control unless stated otherwise. Heterozygous *Rosa26-β-gal* reporter mice[20] were used to detect Cre-induced recombination events. For Notch1 expression studies, we used transgenic *Notch1-GFP* (*N1-GFP*) reporter mice[21]; for Notch2 expression studies, heterozygous mutant *Notch2* mice were used (*N2*$^{+/LacZ}$ mice, previously referred to by Hamada et al.[22] as *Notch2*$^{+/m}$). In these mice, 5 of the 6 ankyrin repeats and part of the downstream sequence of the *Notch2* gene are replaced with the *LacZ* gene.[22] For *Notch2* gene dosage studies, these mice were also used to create *Notch2* conditional/mutant mice (*N2*$^{F/LacZ}$*AlbCre*). Genotyping was performed via polymerase chain reaction or X-galactosidase (X-gal) staining of tails in heterozygous *Notch2* mutant mice (sequences shown in Supplementary Table 1). Mice were handled according to protocols that follow national guidelines for ethical animal treatment, and all experiments were performed according to the protocols approved by our Institutional Animal Care and veterinarian office.

Hepatocyte Isolation. Hepatocytes were isolated from 8-week-old animals by a standard in situ two-step

retrograde collagenase-perfusion technique (Liberase-Blendzyme-3, Roche, Germany) as described.[23] Seventy percent partial hepatectomy in 8-week-old C57Bl6 mice was performed as described.[24]

Protein Isolation and Western Blot Analysis. For preparation of whole-cell protein extracts, livers or primary hepatocytes were homogenized in Nonidet P-40 lysis buffer (50 mM Tris-HCl, 150 mM NaCl, 0.5% Nonidet P-40, 1 mM phenylmethylsulfonyl fluoride and protease- and phosphatase-inhibitor cocktail). The lysate was gently sonicated and clarified by centrifugation (14,000 rpm for 10 minutes at 4°C), snap-frozen in liquid nitrogen, and stored at −80°C until assayed. Protein extracts were analyzed via discontinuous sodium dodecyl sulfate–polyacrylamide gel electrophoresis as described.[23] Antibodies and conditions used are listed in Supplementary Table 2.

Histology and Immunohistochemical Analysis. For histological analysis, livers were removed, fixed in 4% neutral phosphate-buffered paraformaldehyde for 16 hours, embedded in paraffin, and sectioned. Serial 3.5-μm-thick sections were stained with hematoxylin-eosin or Sirius red using a standard protocol. Masson's trichrome staining was performed using a trichrome stain kit (Sigma, Germany). For immunohistochemical analyses and X-gal staining on frozen sections, tissues were processed as described[25] using antibodies as shown in Supplementary Table 2. For detection of mouse antibodies, a MOM kit (Vector Laboratories, UK) was used to block unspecific binding.

Results

Targeted Liver-Specific Disruption of Notch1 and Notch2. Constitutive knockout mice for *Notch1* or *Notch2* display embryonic lethality before embryonic day 11.5.[22,26] To study the function of Notch signaling in perinatal and postnatal liver development and homeostasis, we generated conditional knockout mice in which both *Notch1* and *Notch2* were inactivated, specifically in the liver (*N1N2*$^{F/F}$*AlbCre* mice). In the adult liver, albumin is expressed exclusively in hepatocytes. Consequently, Notch1 and Notch2 protein were not detectable in hepatocytes isolated from 8-week-old *N1N2*$^{F/F}$*AlbCre* mice (Fig. 1A). However, in the embryonic liver, albumin expression occurs in hepatoblasts as early as 13.5 days of gestation before intrahepatic bile ducts begin to differentiate from periportal hepatoblasts. In mice, the process of bile duct development and morphogenesis starts at around embryonic day 15 and extends until the first 2 weeks of age.[2] Thus, recombination of *floxed* alleles in mice carrying the *AlbCre* transgene can also be found in intrahepatic bile ducts in the adult mouse.[27,28] Consistently, when crossing *AlbCre* mice with a *Rosa26* reporter mouse,[20] liver parenchymal cells and the vast majority of bile ducts but not hematopoetic cells or portal vein mesenchyme were X-gal–positive when analyzed at postnatal day (P) 1 and P30, respectively (Fig. 1B). Because mature bile duct epithelial cells do not express albumin,[2] these data confirm that in *AlbCre* transgenic mice Cre expression occurs in hepatoblasts and/or precursors of intrahepatic bile duct cells before termination of bile duct development.

Liver-specific conditional double-mutant *N1N2*$^{F/F}$-*AlbCre* mice were born at Mendelian frequencies without apparent abnormalities. Because IHBD development in the mouse continues beyond the first weeks after birth we first analyzed the histological organization of the liver architecture after conclusion of postnatal bile duct development in 4-week-old *N1N2*$^{F/F}$*AlbCre* mice and control littermates. Livers of 4-week-old *N1N2*$^{F/F}$*AlbCre* mice were not distinguishable from controls on gross examination. For histological analysis we performed hematoxylin-eosin staining and pan-CK staining to identify the intrahepatic bile duct status in mutant and control mice.[2,29] *N1N2*$^{F/F}$ control mice had normal liver architecture and bile duct morphology (Fig. 2A,B). In contrast, combined deletion of *Notch1* and *Notch2* resulted in a disorganized biliary system. In all mice investigated at the age of 4 weeks (n = 12), portal and periportal areas and interlobular septs displayed multiple arborizing pan-CK–positive ductular structures that extended far into the hepatic lobe (Fig. 2C-F). Mature differentiated bile ducts, integrated into the portal mesenchyme, could be observed only in the hilar regions of the liver lobes around large portal veins (data not shown). In addition to these irregular ductular structures, which were abundant in all *N1N2*$^{F/F}$*AlbCre* mice analyzed, portal areas with proliferation and distortion of mature bile ducts accompanied by mild portal inflammation as assessed with anti-CD45 staining were also observed in 9 of 12 animals (Fig. 2G,H). Trichrome staining highlights enlarged portal tract expansion with mild deposits of collagen (Fig. 2I). These morphological changes were most pronounced in the periphery of the hepatic lobes and are suggestive of local cholestasis. In this context, small foci of hepatocyte feathery degeneration (bile infarcts) were also observed in 5 of 12 animals (Fig. 2J).

Early Postnatal IHBD Development Is Impaired in N1N2$^{F/F}$AlbCre Mice. Morphological findings in 4-week-old *N1N2*$^{F/F}$*AlbCre* mice suggest abnormal development of IHBD. To detect early differences in IHBD differentiation and morphogenesis between control and *N1N2*$^{F/F}$*AlbCre* mice, we analyzed mice at P1, P10, and

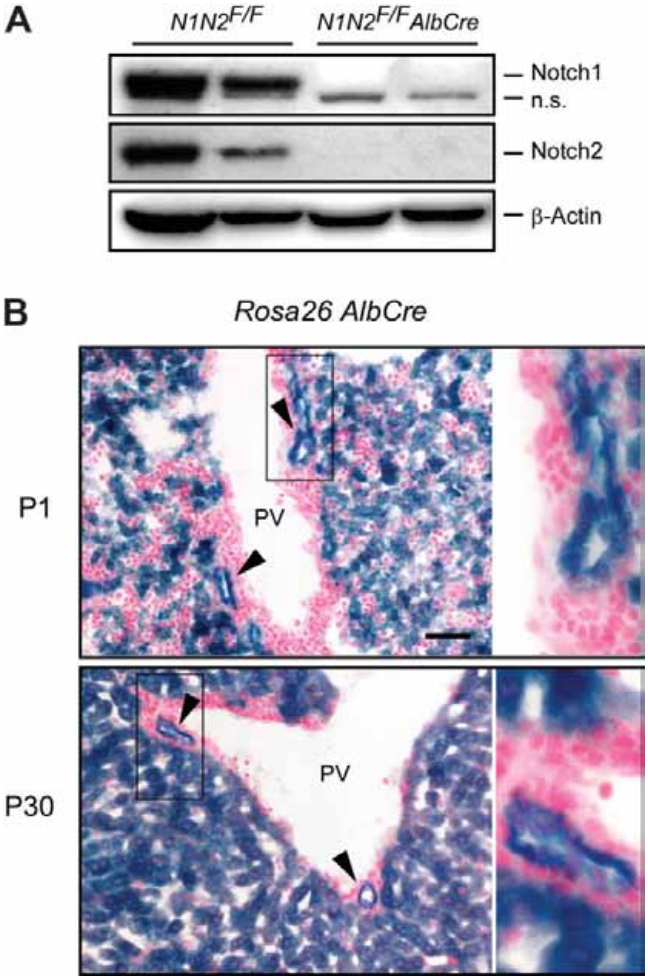

Fig. 1. Targeted liver-specific disruption of *Notch1* and *Notch2*. (A) Protein lysates were prepared from primary hepatocytes isolated from 8-week-old *N1N2*$^{F/F}$ mice and *N1N2*$^{F/F}$*AlbCre* littermates and subjected to western blot analysis using anti-Notch1, anti-Notch2, and anti-β-actin antibodies. n.s., nonspecific band. (B) Cre-induced recombination of *floxed* alleles occurs in both hepatocytes and biliary epithelial cells in livers from *Rosa26AlbCre* reporter animals at P1 and P30 as assessed with X-gal staining. Arrowheads indicate bile ducts. The outlined areas are magnified in the right panels. PV, portal vein. Scale bar = 50 μm.

P20. In control mice, typical ductal plate remodeling at P1 was apparent from the detection of pan-CK–positive epithelial cells forming tubular and nontubular structures around the larger portal veins (Fig. 3A). At P10 (Fig. 3C) and P20 (Fig. 3E), the tubular structures progressed further into mature differentiated bile ducts well integrated into the portal mesenchyme, whereas the nontubular part was largely eliminated, displaying only few pan-CK–positive ductal plate remnants. Ductal plate cells were also detected in *N1N2*$^{F/F}$*AlbCre* animals at P1; however, in contrast to control animals, these pan-CK–positive cells were mostly arranged irregularly around the portal veins and very rarely formed typical tubular structures (Fig. 3B). At P10 (Fig. 3D), the vast majority of portal tracts did not contain differentiated bile ducts. Instead, ductal plate remnants and abnormal CK-positive epithelial cells were abundant in the periportal area. Moreover, in 3 of 6 animals analyzed at P10, we observed small foci of feath-

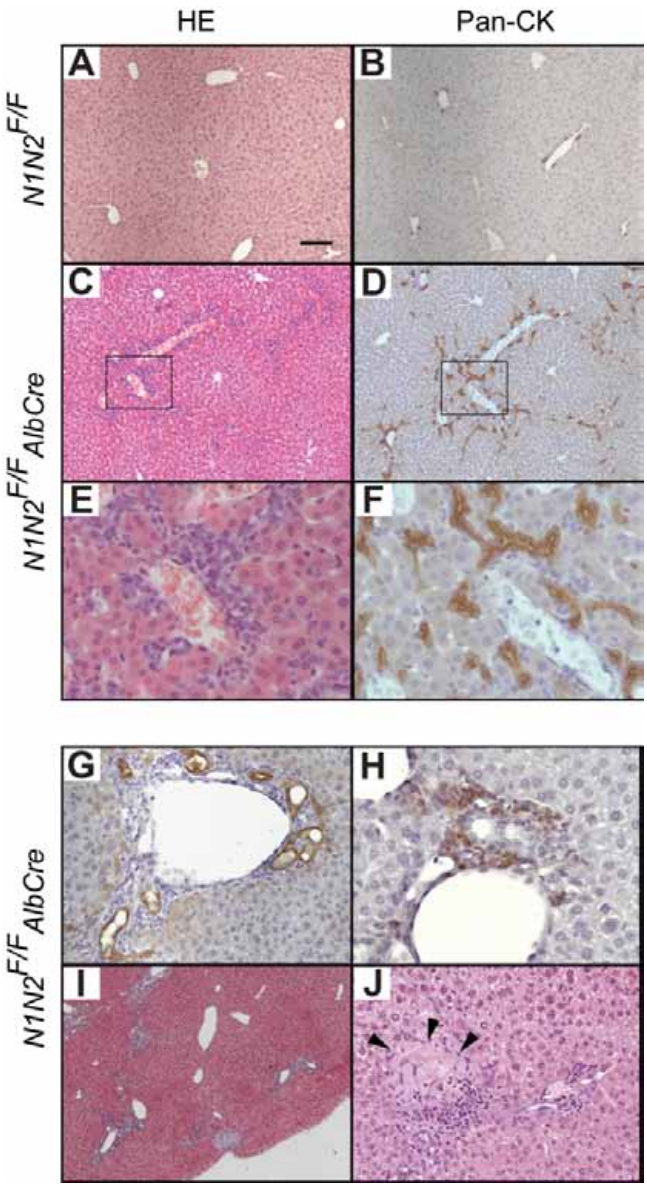

Fig. 2. Combined liver-specific disruption of *Notch1* and *Notch2* results in abnormal IHBD status. (A,B) Hematoxylin-eosin staining and pan-CK immunostaining of bile ducts of control livers at 4 weeks of age reveal normal parenchymal and portal tract architecture. (C-F) Serial sections of mutant livers display a disorganized biliary system characterized by multiple arborizing pan-CK–positive tubular structures. Insets in panels C and D are amplified in panels E and F. (G) Increased number of dilated and distorted bile ducts frequently surround larger portal veins as assessed with pan-CK staining. (H) Anti-CD45 immunostaining reveals periportal leukocyte infiltration. (I) Trichrome staining at low magnification demonstrates portal tract expansion with mild periportal and interlobular deposits of collagen. (J) Hematoxylin-eosin staining reveals a small focus of feathery hepatocyte degeneration (bile infarct, arrowheads). Scale bar in panel A = (E,F,H) 25, (G,J) 50, (A-D) 100, and (I) 200 μm.

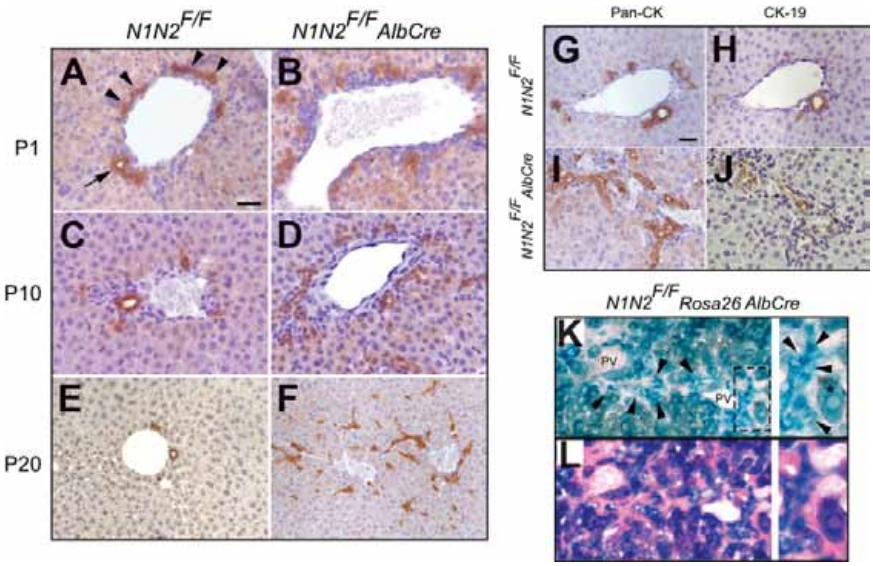

Fig. 3. Early postnatal IHBD development is impaired in *N1N2*$^{F/F}$*AlbCre* mice. Bile duct status in livers from (A,C,E) control and (B,D,F) *N1N2*$^{F/F}$*AlbCre* mice was analyzed at P1, P10, and P20 with pan-CK immunostaining. (A) In control livers, tubular (arrow) and nontubular (arrowheads) ductal plate structures can be observed at P1. The tubular portion further progressed into well-differentiated bile ducts, while the remaining ductal plate cells were progressively eliminated at (C) P10 and (E) P20. (B) In mutants, pan-CK–positive ductal plate cells are arranged irregularly and do not form typical tubular structures around most portal veins at P1. (D) At P10, abundant ductal plate remnants and abnormal pan-CK–positive cells are typically observed in mutant livers. (F) At P20, mutant livers largely lack regular bile ducts but display multiple disorganized ductular structures. (G-J) Adjacent sections of control and mutant livers at P20 were subjected to pan-CK and CK19 immunostaining. (H) In contrast to mature bile ducts in control sections, (J) CK19 staining is weak in irregular ductules of mutant livers. (K,L) X-gal staining of a liver section from a *N1N2*$^{F/F}$*Rosa26AlbCre* mouse at P20 reveals Cre-induced recombination events in both abnormal ductular structures (arrowheads) and hepatocytes (asterisk). The section in panel K was counterstained with nuclear fast red in panel L. The outlined area in panel K is amplified in the right panel. PV, portal vein. Scale bar in panel A = (A-D,K,L) 25 and (E,F) 50 μm. Scale bar in panel G = (G-J) 25 μm.

ery degeneration in the periphery of the liver lobes (data not shown). At P20 (Fig. 3F) the number of these pan-CK–positive epithelial cells further increased now forming strings of cells and tubular structures. However, these structures appeared disorganized and mostly not integrated into the portal mesenchyme.

Biliary epithelial cells become positive for polyclonal pan-CK antibodies early with ductal plate formation, while CK19 expression increases with maturation of bile ducts.[2] In this context, mature bile ducts of P20 control mice stained positive for both pan-CK and CK19 (Fig. 3G,H). In contrast, CK19 staining was weak in the pan-CK–positive duct-like structures observed in *N1N2*$^{F/F}$*AlbCre* animals (Fig. 3I,J). To analyze if these structures in *N1N2*$^{F/F}$*AlbCre* animals arise from cells in which *Notch1* and *Notch2* genes have been targeted by Cre-recombinase, we generated *N1N2*$^{F/F}$*Rosa26AlbCre* reporter mice and found X-gal staining of both hepatocytes and irregular ductular epithelial cells (Fig. 3K,L). Consequently, when analyzing livers from embryonic day 17.5 *N1N2*$^{F/F}$*Rosa26AlbCre* embryos, we detected Cre activity via X-gal staining in approximately 40% to 50% of liver cells (Supplementary Fig. 1A,B). In addition, polymerase chain reaction performed with DNA isolates from embryonic day 17.5 *N1N2*$^{F/F}$*AlbCre* livers using primers specific for deleted *Notch1* and *Notch2* alleles shows Cre-induced recombination of both alleles (Supplementary Fig. 1C).

In summary, cell-specific, combined disruption of *Notch1* and *Notch2* led to impaired IHBD development with the detection of multiple irregular duct-like structures, most likely because of impaired morphogenesis and maturation of the biliary tree.

Notch2, but Not Notch1, Is Indispensable for Normal IHBD Development. To elucidate whether both *Notch1* and *Notch2* are required for normal bile duct development and morphogenesis, we analyzed 4-week-old mutant mice that had at least one wild-type (WT) allele of *Notch1* or *Notch2*, respectively (*N1*$^{F/F}$*AlbCre*, *N1*$^{F/F}$-*N2*$^{F/+}$*AlbCre*, *N1*$^{F/+}$*N2*$^{F/F}$*AlbCre*, and *N2*$^{F/F}$*AlbCre*, [n = 5–8 each]). The phenotype observed in double-mutant *N1N2*$^{F/F}$*AlbCre* animals was completely rescued in mice carrying only one or two WT *Notch2* alleles. Bile duct structures and liver architecture observed in *N1*$^{F/F}$-*N2*$^{F/+}$*AlbCre* or *N1*$^{F/F}$*AlbCre* mice did not differ from *Cre*-negative littermates (Fig. 4A,B). Of note, we did not observe liver hyperplasia in mice lacking *Notch1* as reported for *N1*$^{F/F}$*MxCre* mice after postnatal inactivation of *Notch1*.[12] Neither an increased liver weight/body weight ratio at 4 weeks or 4 months of age nor enhanced

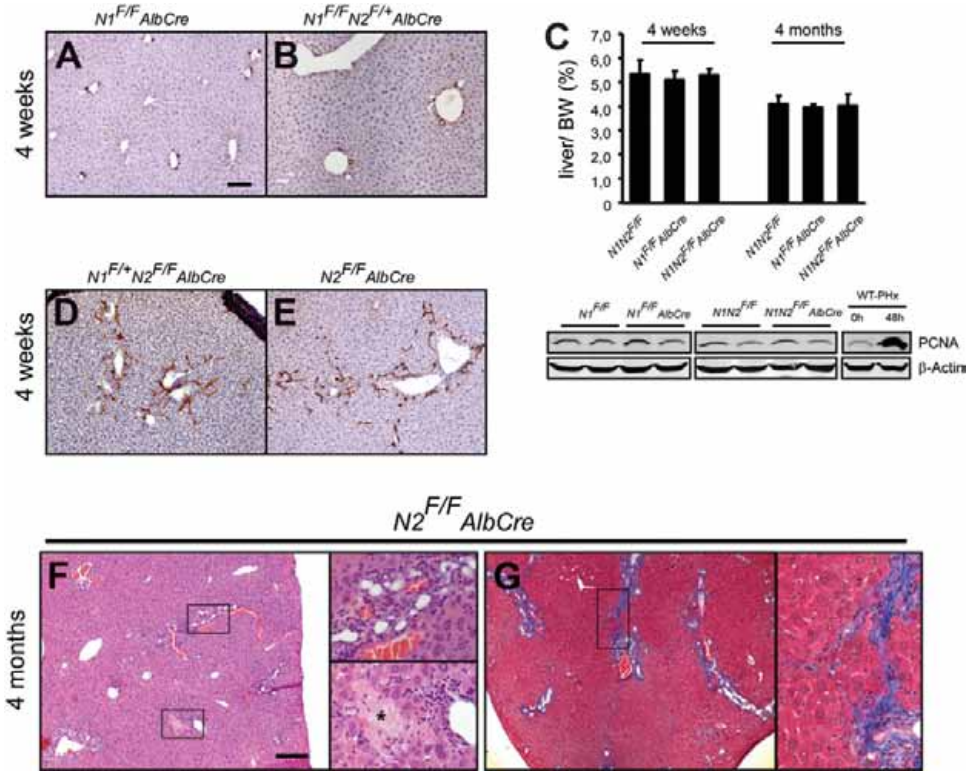

Fig. 4. Single conditional deletion of *Notch2*, but not *Notch1*, is sufficient to impair IHBD development. Normal bile duct status in livers from 4-week-old (A) $N1^{F/F}$*AlbCre* and (B) $N1^{F/F}N2^{F/+}$*AlbCre* mice as assessed with pan-CK immunostaining. (C) Conditional deletion of *Notch1* alone or in combination with *Notch2* did not alter organ size due to enhanced hepatocyte proliferation. Liver weight as a percentage of body weight was determined in mice of indicated genotype and age (upper panel), and western blot analysis of liver lysates from 4-week-old mice using anti–proliferating cell nuclear antigen and anti–β-actin antibodies (lower panel) were performed. Liver lysates from WT mice subjected to partial hepatectomy (PHx) at the time points 0 hours and 48 hours served as a control. Livers from 4-week-old (D) $N1^{F/+}N2^{F/F}$*AlbCre* or (E) $N2^{F/F}$*AlbCre* mice display IHBD abnormalities as observed in $N1N2^{F/F}$*AlbCre* animals as assessed by pan-CK immunostaining. (F) Hematoxylin-eosin staining of a liver section from a 4-month-old $N2^{F/F}$*AlbCre* mouse demonstrates abnormal liver architecture characterized by portal inflammation, fibrosis, bile duct dilation, proliferation (enlarged in right upper panel), and bile infarcts (asterisk in enlarged lower panel). The outlined areas in panel F are amplified in the right panels. (G) Trichrome staining illustrates portal tract expansion with portal and periportal fibrosis. The outlined area is amplified in the right panel. Scale bar in panel A = (A,B,D,E) 100 μm. Scale bar in panel F = (F,G) 200 μm.

proliferation of hepatocytes were detected in $N1^{F/F}$*AlbCre* or $N1N2^{F/F}$*AlbCre* animals as assessed by proliferating cell nuclear antigen western blot analysis (Fig. 4C) or bromodeoxyuridine immunostaining after adding bromodeoxyuridine to the drinking for 7 days (data not shown), indicating that liver-specific disruption of *Notch1* alone or in combination with *Notch2* does not alter organ size by enhanced spontaneous hepatocyte proliferation. When analyzing the bile duct status in livers of mutant mice carrying two *floxed* alleles of *Notch2* but one or two WT alleles of *Notch1* ($N1^{F/+}N2^{F/F}$*AlbCre* or $N2^{F/F}$*AlbCre*, respectively), we found the same morphological phenotype as in double-mutant $N1N2^{F/F}$*AlbCre* mice (Fig. 4D,E). Also, when analyzed at P1, $N2^{F/F}$*AlbCre* displayed irregular ductal plates with very few typical tubular structures (data not shown) indistinguishable from $N1N2^{F/F}$*AlbCre* mice. When analyzing $N2^{F/F}$*AlbCre* animals at 4 months of age, multiple irregularly shaped interlobular bile ducts of varying size frequently not integrated into the portal mesenchyme were the predominant findings. In 3 of 6 animals, these structural biliary abnormalities were accompanied by morphological alterations typically seen as a consequence of cholestasis, such as portal inflammation, bile duct proliferation, portal tract expansion, and portal fibrosis (Fig. 4F,G). These results suggest that Notch1 and Notch2 have nonredundant functions in IHBD development and that defective Notch2 signaling is responsible for structural abnormalities observed in $N1N2^{F/F}$*AlbCre* mice that cannot be compensated upon genetic reconstitution with WT *Notch1*. Of note, technically, we were not able to reliably demonstrate the expression profile of Notch proteins in control and mutant animals via immunohistochemistry using various antibodies under various conditions. Instead, we used transgenic *Notch1-GFP*[21] and heterozygous mutant $Notch2^{+/LacZ}$ reporter mice[22] to analyze hepatic Notch expression profile during IHBD development. Notch1 expression was notably absent in bile ducts but could be

detected in hepatocytes of *Notch1-GFP* mice both at P0 and P50. Notch1 expression was highest in a number of cells with small cytoplasm distributed throughout the liver at P0, most likely cells of the hematopoetic system such as lymphoid cells (Supplementary Fig. 2A-D). In contrast, when analyzing *Notch2*$^{+/LacZ}$ animals via X-gal staining, we found the strongest staining in both developing (Supplementary Fig. 2E) and mature (Supplementary Fig. 2F) bile ducts, whereas less intense staining could be observed in hepatocytes and other liver cells in newborns and in hepatocytes in P50 animals. This expression profile further supports our conclusions deduced from morphological findings in single mutant mice that Notch2, but not Notch1, plays a decisive role in IHBD development.

Severity of Bile Duct Malformations Is Further Enhanced in Notch2 Conditional/Mutant (N2$^{F/LacZ}$AlbCre) Animals. In *AlbCre* animals, Cre-mediated deletion of *floxed* alleles occurs progressively with age[30] and is most likely incomplete in hepatoblasts in *N2*$^{F/F}$*AlbCre* animals during embryogenesis when the first ductal plates form around the large central portal veins (see Supplementary Fig. 1). To test whether further putative reduction in *Notch2* gene dosage in hepatoblasts at earlier stages during embryonic development would further enhance biliary and concomitant structural abnormalities in central parts of the liver, we generated *Notch2* conditional/mutant mice (*N2*$^{F/LacZ}$*AlbCre*) and analyzed livers at 4 weeks of age (n = 9). Whereas livers of heterozygous *Notch2* mutant (*N2*$^{F/LacZ}$) control animals (n = 5) all displayed normal liver architecture and bile duct status (Fig. 5A,B), all *N2*$^{F/LacZ}$*AlbCre* animals showed an IHBD morphology similar to that observed in *N2*$^{F/F}$*AlbCre* mice (Fig. 5C). However, although IHBD abnormalities and concomitant pathology were detected predominantly in the liver periphery in *N2*$^{F/F}$*AlbCre* mice, central parts of the liver in the majority of *N2*$^{F/LacZ}$*AlbCre* animals were severely affected by bile duct abnormalities, characterized by abundant irregular biliary structures within inflamed and enlarged portal tracts (Fig. 5D). We also found large portal tracts with actual bile duct paucity containing only primitive non-remodeled, nontubular ductal plate structures (Fig. 5E). Consequently, in 5 of 9 *N2*$^{F/LacZ}$*AlbCre* animals, large areas of bile infarcts were detected in the central parts of the liver (Fig. 5F). Furthermore, we detected considerable fibrosis in these mice as assessed by Sirius red staining. (Fig. 5G,H).

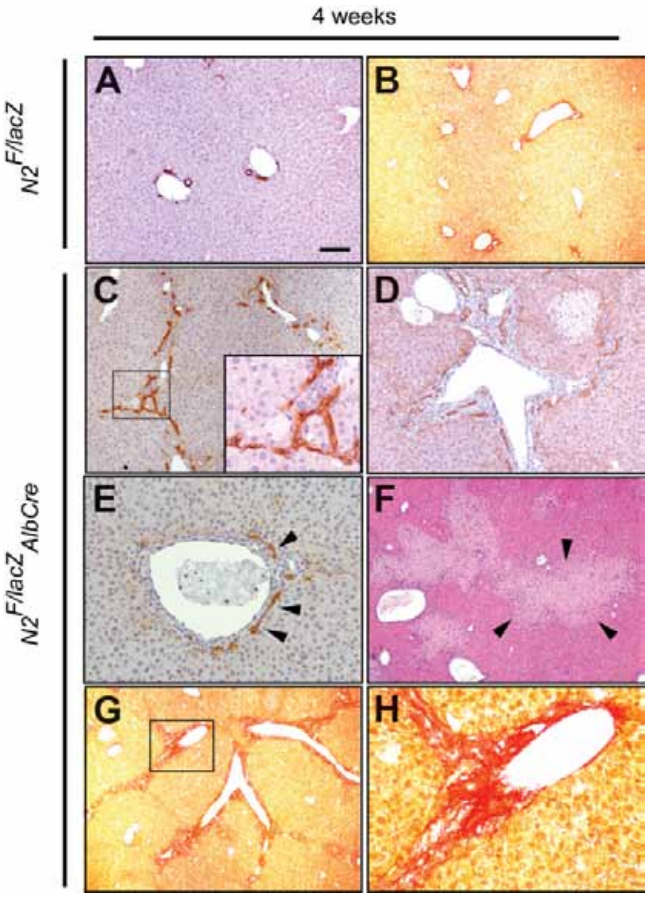

Fig. 5. Severity of the phenotype observed in *N2*$^{F/F}$*AlbCre* mice is enhanced in *Notch2* conditional/mutant (*N2*$^{F/LacZ}$*AlbCre*) animals. (A,B) Liver architecture and IHBD status in control heterozygous *Notch2*$^{F/LacZ}$ mutants are phenotypical WT as assessed with pan-CK immunostaining for detection of bile ducts and Sirius red staining to detect collagen content. (C) Four-week-old *Notch2* conditional/mutant (*N2*$^{F/LacZ}$*AlbCre*) animals show a similar IHBD status as observed in conditional *Notch2* (*N2*$^{F/F}$*AlbCre*) mice with the detection of multiple irregular ductules in pan-CK immunohistochemistry. The outlined area is magnified in the inset. (D-E) Large central portal tracts were also typically severely affected by IHBD malformations. (D) Pan-CK immunostaining reveals a large portal tract surrounded by severe inflammation and irregular bile ducts. (E) Frequently, large portal tracts did not contain any tubular biliary epithelial cells only displaying nonremodeled primitive ductal plate structures (arrowheads) as shown via pan-CK immunostaining. (F) Hematoxylin-eosin staining revealed large areas of central and peripheral bile infarcts (arrowheads) in *N2*$^{F/LacZ}$*AlbCre* animals. (G) Low-magnification view shows intense collagen deposits in portal and periportal areas of *N2*$^{F/LacZ}$*AlbCre* animals. The outlined area in panel G is magnified in panel H. Scale bar in panel A = (H) 25, (E) 50, (A,C,D) 100, and (B,F,G) 200 μm.

Discussion

In this study, we analyzed the role of liver-specific *Notch1* and *Notch2* ablation to hepatobiliary development and homeostasis. Encouraged by recent data that Notch1 might function as a tumor suppressor in hepatocytes,[12,31] we originally intended to study the role of Notch1 and Notch2 signaling in hepatocyte homeostasis using *AlbCre* mice. Because albumin expression is restricted to hepatocytes in the adult liver, and because the *AlbCre* mouse is widely used to "hepatocyte-specifically" induce Cre expression, we were surprised to detect normal hepatocytes but severe morphogenesis defects of the bile system in double-mutant *N1N2*$^{F/F}$*AlbCre* animals. How-

ever, because both hepatocytes and bile ducts originate from hepatoblasts, we found Cre-recombinase activity in hepatocytes and bile ducts but not in mesenchymal, endothelial, or hematopoetic cells when crossing *AlbCre* mice with the *Rosa26* reporter mouse. Thus, in agreement with previous reports,[27,28] the transgenic *AlbCre* mouse line is suitable for targeted disruption of *floxed* alleles in both hepatocytes and biliary epithelial cells.

In all our mouse strains lacking liver *Notch2* we detected a strong reduction of mature, regularly shaped bile ducts but observed abundant disorganized pan-CK–positive ductular structures along with impaired early postnatal remodeling and persistence of ductal plate structures. Biliary and structural abnormalities found were frequently accompanied by local cholestasis, feathery necrosis, portal inflammation, and enlarged portal tract expansion with collagen deposits. Because these findings were identical in $N1N2^{F/F}$*AlbCre* and $N2^{F/F}$*AlbCre* animals and further aggravated in $N2^{F/LacZ}$*AlbCre* mice, but were absent in $N1^{F/F}$*AlbCre* or $N1^{F/F}N2^{F/+}$*AlbCre* mice, we conclude that impaired Notch2 but not Notch1 signaling is responsible for the observed liver pathology. The pan-CK–positive duct-like structures were sometimes reminiscent of a ductular reaction, especially in the periphery of the portal area. Just like reactive ductular cells found in various states of the diseased liver,[32] these irregular structures found in mice lacking liver *Notch2* could possibly have arisen from preexisting cholangiocytes or their precursors, but also from progenitor cells such as oval cells. We detected Cre-induced recombination events in these abnormal ductular structures when analyzing $N1N2^{F/F}$*Rosa26AlbCre* mice, suggesting that they originate from albumin-expressing precursors, just like normal cholangiocytes. Together with the observation of ductal plate anomalies in *Notch2*-deficient mice, it is tempting to reason that these irregular pan-CK–positive ductules also originate from *Notch2*-deficient biliary epithelial cells or their precursors and are the result of impaired *Notch2*-dependent bile duct maturation and morphogenesis. However, we cannot fully rule out that an oval cell response contributes to the irregular duct-like structures observed, because albumin expression has been observed in rodent oval cells as well.[33,34]

Liver and bile duct development or maintenance of tissue integrity in the adult liver appeared perfectly normal in $Notch1^{F/F}$*AlbCre* mice. Interestingly, we did not find spontaneous hepatocyte proliferation or enlarged liver mass in the mouse strains lacking *Notch1*, specifically in the liver. This is somewhat surprising with respect to findings in mice with postnatal inactivation of *Notch1* ($N1^{F/F}$*MxCre* animals) using the interferon-α (IFN-α)–inducible *MxCre* promoter.[12] In that study, deletion of *Notch1* caused a striking eight-fold increase in hepatocellular proliferation accompanied by a 40% increase in liver mass.[12] One explanation for differences in hepatocyte proliferation as compared to transgenic *AlbCre* mice might be that IFN-α–induced activation of the *MxCre* promoter is not hepatocyte-specific. Rather, recombination of floxed alleles occurs in all tissues after IFN-α injection or likewise in all IFN-α–responsive tissues after polyl-ic injection most effectively in lymphatic tissues and the liver, including hepatocytes and nonparenchymal cells.[23,35] Because classic Notch signaling has been shown to inhibit hepatocyte growth factor (HGF) expression in vitro,[36] deletion of *Notch1* in cell compartments other than hepatocytes such as liver mesenchymal cells might alter expression of HGF within these cells and contribute to the enhanced proliferation of hepatocytes observed in $N1^{F/F}$*MxCre* animals.

In the conditional mouse strains investigated lacking a functional *Notch2* gene ($N1N2^{F/F}$*AlbCre* or $N2^{F/F}$*AlbCre* animals), the structural IHBD abnormalities were most pronounced in the periphery of the liver lobes, whereas in the central regions most portal tracts contained mature albeit frequently distorted bile ducts next to primitive pan-CK–positive ductular structures as well. Similar spatial disparities of IHBD morphology have also been described for human AGS, supporting the concept that Notch signaling is especially crucial for normal postnatal branching and elongation of IHBD.[37] However, it must be considered that in *AlbCre* animals, Cre-mediated deletion of *floxed* alleles occurs progressively with age[30] and bile duct development and morphogenesis around larger central portal veins starts at around embryonic day 15 before development of the finer branches of the biliary tree. Thus, it may well be the case that embryonic Notch2 levels using *AlbCre* mice still allow largely regular development and morphogenesis of functional IHBD in the central parts of the liver, thus preventing mice from severe generalized cholestasis and liver damage. Hence, progressive and cumulative *AlbCre*-driven recombination of *floxed* alleles may lead to Notch2 levels below a threshold that allows normal differentiation and morphogenesis of IHBD only later during bile duct development of the finer branches, thus leading to cholestasis-associated morphological changes, predominantly in the liver periphery. In this context, after further reduction of embryonic *Notch2* gene dosage in hepatoblasts in $N2^{F/LacZ}$*AlbCre* mice, we also found the central parts of the liver severely affected by structural bile duct malformation in the majority of mice, including bile duct paucity accompanied by profound portal inflammation and large areas of bile infarcts. However, though we did not find any structural abnormalities in livers of heterozygous $N2^{+/LacZ}$ mice,

we cannot rule out that loss of one functional *Notch2* allele in cells other than hepatoblasts and biliary precursors may contribute to the more severe phenotype observed in *N2*$^{F/LacZ}$*AlbCre* animals.

Although *Notch2*-deficient livers displayed a strong reduction of normally formed, well-maturated bile ducts, we observed an increase of disorganized primitive biliary-like structures together with portal inflammation, portal tract enlargement and fibrosis, and biliary necrosis. These morphological changes are typical for chronic cholestasis but are less common in AGS, which is characterized by actual bile duct paucity without a marked inflammatory response and development of fibrosis in the majority of cases, in contrast to other cholangiopathies such as biliary atresia.[3,6,38] Actual ductopenia has also been described in mice doubly heterozygous for *Jagged1* and *Notch2* mutations (*Jagged1Notch2*$^{+/-}$ mice) as assessed by DBA staining.[14] *Jagged1Notch2*$^{+/-}$ animals also displayed severe heart defects and only 50% survived beyond P7. Those animals reaching adulthood, though displaying ductopenia, showed only modest portal tract enlargement with an increased number of periportal epithelial cells that had not been further characterized but possibly resemble those pan-CK–positive biliary-like cells we observed in *Notch2*-deficient livers. Loomes et al.[15] also described a strongly increased number of disorganized biliary epithelial cells together with marked portal tract enlargement in 50% of *Jagged1*$^{F/-}$*AlfpCre* mice. Morphologically, these lesions equate those observed in our mouse model lacking liver *Notch2*. However, penetrance was lower, and expressivity of bile duct abnormalities and associated liver pathology seems less pronounced in *Jagged1*$^{F/-}$*AlfpCre* mice compared with our mouse strains lacking liver *Notch2*, presumably due to residual Jagged1 expression of liver endothelial cells.[15] It remains unclear whether the different phenotype in our mouse model compared with human AGS or *Jagged1Notch2*$^{+/-}$ animals are attributable to cell-specific disruption of Notch2 signaling in our model, while Notch signaling is affected in all cell types, including cells of the hepatic reparative complex[3,38] in *Jagged1Notch2*$^{+/-}$ animals and in AGS patients. Impaired Jagged1 signaling via Notch receptors other than Notch1 and Notch2 might also contribute to the different liver pathology in *Jagged1Notch2*$^{+/-}$ animals or in AGS patients. Nevertheless, the sporadic finding of *Notch2* mutations in *Jagged1* mutation negative AGS patients,[39] together with our findings that cell-specific disruption of *Notch2* in livers of mice with WT genetic *Jagged1* background leads to developmental IHBD abnormalities, underscore a central role for *Notch2* in bile duct development.

How does impaired Notch2 signaling in biliary precursor cells lead to impaired IHBD development? Two sequential steps are necessary for IHBD formation: lineage commitment of hepatoblasts to differentiate to biliary epithelial cells, and further morphogenesis and maturation to form the intrahepatic biliary tree. The detection of ductal plate cells and biliary epithelial structures in all conditional *Notch2*-deficient mouse strains—including *Notch2* conditional/mutant *N2*$^{F/LacZ}$*AlbCre* animals—suggests that Notch2 is not decisive for initial lineage commitment of hepatoblasts to biliary epithelial cells, although we cannot rule out that residual Notch2 even in *N2*$^{F/LacZ}$*AlbCre* animals might suffice for this process during embryogenesis. Nevertheless, Notch2 signaling seems especially important for normal ductal plate remodeling and further maturation of primitive biliary structures to mature bile ducts. We speculate that Jagged1 signals from adjacent portal vein and hepatic artery endothelial cells[13,14] are necessary to properly guide bile duct development along portal veins, thus leading to disorganized biliary structures once Notch2 signaling is impaired in biliary epithelial cells. *In vitro* data obtained from cultivated hepatoblasts showed that Notch signals down-regulate CCAAT-enhancer-binding protein-α expression in cultivated hepatoblasts,[40] providing a possible molecular link to the impaired IHBD development in *Notch2*-disrupted livers, because CCAAT-enhancer-binding protein-α has been suggested to negatively regulate expression of hepatocyte nuclear factor 1β[41] and hepatocyte nuclear factor 6,[42] both of which are essential for normal IHBD morphogenesis.[41,43]

In conclusion, we provide evidence that single targeted disruption of *Notch2*, but not *Notch1*, leads to impaired IHBD development, supporting a central role of Notch2 in biliary cell maturation and morphogenesis. Additional genetic and *in vitro* studies are required to further unravel the molecular mechanisms to define the role of Notch1 and Notch2 in hepatobiliary development and disease.

Acknowledgment: The authors thank Silvia Krutsch, Mathilde Neuhofer, and Silke Ruberg for excellent laboratory assistance. The CK19 antibody developed by Rolf Kemler was obtained from the Developmental Studies Hybridoma Bank and maintained by the Department of Bilological Sciences at the University of Iowa (Iowa City, IA). We thank Wei-Qiang Gao for providing *Notch1-GFP* reporter mice and Yoshio Hamada for providing heterozygous mutant *Notch2*$^{+/LacZ}$ mice.

References

1. Crawford JM. Development of the intrahepatic biliary tree. Semin Liver Dis 2002;22:213-226.
2. Shiojiri N. Development and differentiation of bile ducts in the mammalian liver. Microsc Res Tech 1997;39:328-335.

3. Lazaridis KN, Strazzabosco M, Larusso NF. The cholangiopathies: disorders of biliary epithelia. Gastroenterology 2004;127:1565-1577.
4. Li L, Krantz ID, Deng Y, Genin A, Banta AB, Collins CC, et al. Alagille syndrome is caused by mutations in human Jagged1, which encodes a ligand for Notch1. Nat Genet 1997;16:243-251.
5. Oda T, Elkahloun AG, Pike BL, Okajima K, Krantz ID, Genin A, et al. Mutations in the human Jagged1 gene are responsible for Alagille syndrome. Nat Genet 1997;16:235-242.
6. Emerick KM, Rand EB, Goldmuntz E, Krantz ID, Spinner NB, Piccoli DA. Features of Alagille syndrome in 92 patients: frequency and relation to prognosis. HEPATOLOGY 1999;29:822-829.
7. Hashida Y, Yunis EJ. Syndromatic paucity of interlobular bile ducts: hepatic histopathology of the early and endstage liver. Pediatr Pathol 1988; 8:1-15.
8. Deutsch GH, Sokol RJ, Stathos TH, Knisely AS. Proliferation to paucity: evolution of bile duct abnormalities in a case of Alagille syndrome. Pediatr Dev Pathol 2001;4:559-563.
9. Novotny NM, Zetterman RK, Antonson DL, Vanderhoof JA. Variation in liver histology in Alagille's syndrome. Am J Gastroenterol 1981;75:449-450.
10. Harper JA, Yuan JS, Tan JB, Visan I, Guidos CJ. Notch signaling in development and disease. Clin Genet 2003;64:461-472.
11. Nijjar SS, Crosby HA, Wallace L, Hubscher SG, Strain AJ. Notch receptor expression in adult human liver: a possible role in bile duct formation and hepatic neovascularization. HEPATOLOGY 2001;34:1184-1192.
12. Croquelois A, Blindenbacher A, Terracciano L, Wang X, Langer I, Radtke F, et al. Inducible inactivation of Notch1 causes nodular regenerative hyperplasia in mice. HEPATOLOGY 2005;41:487-496.
13. Kodama Y, Hijikata M, Kageyama R, Shimotohno K, Chiba T. The role of notch signaling in the development of intrahepatic bile ducts. Gastroenterology 2004;127:1775-1786.
14. McCright B, Lozier J, Gridley T. A mouse model of Alagille syndrome: Notch2 as a genetic modifier of Jag1 haploinsufficiency. Development 2002;129:1075-1082.
15. Loomes KM, Russo P, Ryan M, Nelson A, Underkoffler L, Glover C, et al. Bile duct proliferation in liver-specific Jag1 conditional knockout mice: effects of gene dosage. HEPATOLOGY 2007;45:323-330.
16. Shiojiri N, Nagai Y. Preferential differentiation of the bile ducts along the portal vein in the development of mouse liver. Anat Embryol (Berl) 1992; 185:17-24.
17. Radtke F, Wilson A, Stark G, Bauer M, van Meerwijk J, MacDonald HR, et al. Deficient T cell fate specification in mice with an induced inactivation of Notch1. Immunity 1999;10:547-558.
18. Besseyrias V, Fiorini E, Strobl LJ, Zimber-Strobl U, Dumortier A, Koch U, et al. Hierarchy of Notch-Delta interactions promoting T cell lineage commitment and maturation. J Exp Med 2007;204:331-343.
19. Postic C, Shiota M, Niswender KD, Jetton TL, Chen Y, Moates JM, et al. Dual roles for glucokinase in glucose homeostasis as determined by liver and pancreatic beta cell-specific gene knock-outs using Cre recombinase. J Biol Chem 1999;274:305-315.
20. Soriano P. Generalized lacZ expression with the ROSA26 Cre reporter strain. Nat Genet 1999;21:70-71.
21. Lewis AK, Frantz GD, Carpenter DA, de Sauvage FJ, Gao WQ. Distinct expression patterns of notch family receptors and ligands during development of the mammalian inner ear. Mech Dev 1998;78:159-163.
22. Hamada Y, Kadokawa Y, Okabe M, Ikawa M, Coleman JR, Tsujimoto Y. Mutation in ankyrin repeats of the mouse Notch2 gene induces early embryonic lethality. Development 1999;126:3415-3424.
23. Geisler F, Algul H, Paxian S, Schmid RM. Genetic inactivation of RelA/p65 sensitizes adult mouse hepatocytes to TNF-induced apoptosis in vivo and in vitro. Gastroenterology 2007;132:2489-2503.
24. Greene AK, Puder M. Partial hepatectomy in the mouse: technique and perioperative management. J Invest Surg 2003;16:99-102.
25. Siveke JT, Einwachter H, Sipos B, Lubeseder-Martellato C, Kloppel G, Schmid RM. Concomitant pancreatic activation of Kras(G12D) and Tgfa results in cystic papillary neoplasms reminiscent of human IPMN. Cancer Cell 2007;12:266-279.
26. Swiatek PJ, Lindsell CE, del Amo FF, Weinmaster G, Gridley T. Notch1 is essential for postimplantation development in mice. Genes Dev 1994;8: 707-719.
27. Xu X, Kobayashi S, Qiao W, Li C, Xiao C, Radaeva S, et al. Induction of intrahepatic cholangiocellular carcinoma by liver-specific disruption of Smad4 and Pten in mice. J Clin Invest 2006;116:1843-1852.
28. Dutton JR, Chillingworth NL, Eberhard D, Brannon CR, Hornsey MA, Tosh D, et al. Beta cells occur naturally in extrahepatic bile ducts of mice. J Cell Sci 2007;120:239-245.
29. Shiojiri N. Transient expression of bile-duct-specific cytokeratin in fetal mouse hepatocytes. Cell Tissue Res 1994;278:117-123.
30. Postic C, Magnuson MA. DNA excision in liver by an albumin-Cre transgene occurs progressively with age. Genesis 2000;26:149-150.
31. Hubscher SG, Strain AJ. Another Notch to be added to the list of hepatocellular growth regulatory factors? HEPATOLOGY 2005;41:439-442.
32. Roskams TA, Theise ND, Balabaud C, Bhagat G, Bhathal PS, Bioulac-Sage P, et al. Nomenclature of the finer branches of the biliary tree: canals, ductules, and ductular reactions in human livers. HEPATOLOGY 2004;39: 1739-1745.
33. Bird TG, Lorenzini S, Forbes SJ. Activation of stem cells in hepatic diseases. Cell Tissue Res 2008;331:283-300.
34. Wang X, Foster M, Al-Dhalimy M, Lagasse E, Finegold M, Grompe M. The origin and liver repopulating capacity of murine oval cells. Proc Natl Acad Sci U S A 2003;100(Suppl 1):11881-11888.
35. Kuhn R, Schwenk F, Aguet M, Rajewsky K. Inducible gene targeting in mice. Science 1995;269:1427-1429.
36. Yuan ZR, Kobayashi N, Kohsaka T. Human Jagged 1 mutants cause liver defect in Alagille syndrome by overexpression of hepatocyte growth factor. J Mol Biol 2006;356:559-568.
37. Libbrecht L, Spinner NB, Moore EC, Cassiman D, Van Damme-Lombaerts R, Roskams T. Peripheral bile duct paucity and cholestasis in the liver of a patient with Alagille syndrome: further evidence supporting a lack of postnatal bile duct branching and elongation. Am J Surg Pathol 2005; 29:820-826.
38. Fabris L, Cadamuro M, Guido M, Spirli C, Fiorotto R, Colledan M, et al. Analysis of liver repair mechanisms in Alagille syndrome and biliary atresia reveals a role for notch signaling. Am J Pathol 2007;171:641-653.
39. McDaniell R, Warthen DM, Sanchez-Lara PA, Pai A, Krantz ID, Piccoli DA, et al. NOTCH2 mutations cause Alagille syndrome, a heterogeneous disorder of the notch signaling pathway. Am J Hum Genet 2006;79:169-173.
40. Tanimizu N, Miyajima A. Notch signaling controls hepatoblast differentiation by altering the expression of liver-enriched transcription factors. J Cell Sci 2004;117:3165-3174.
41. Coffinier C, Gresh L, Fiette L, Tronche F, Schutz G, Babinet C, et al. Bile system morphogenesis defects and liver dysfunction upon targeted deletion of HNF1beta. Development 2002;129:1829-1838.
42. Yamasaki H, Sada A, Iwata T, Niwa T, Tomizawa M, Xanthopoulos KG, et al. Suppression of C/EBPalpha expression in periportal hepatoblasts may stimulate biliary cell differentiation through increased Hnf6 and Hnf1b expression. Development 2006;133:4233-4243.
43. Clotman F, Lannoy VJ, Reber M, Cereghini S, Cassiman D, Jacquemin P, et al. The onecut transcription factor HNF6 is required for normal development of the biliary tract. Development 2002;129:1819-1828.